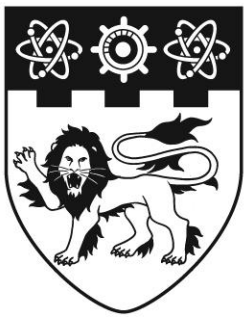

NANYANG TECHNOLOGICAL UNIVERSITY

# DESIGN AND SYNTHESIS OF CYCLOMETALLATED SULPHUR-*N*-HETEROCYCLIC CARBENE COMPLEXES AND THEIR APPLICATION IN CATALYSIS

**DEEPA KRISHNAN**

**SCHOOL OF PHYSICAL AND MATHEMATICAL SCIENCES**

**DEPARTMENT OF CHEMISTRY AND BIOLOGICAL CHEMISTRY**

**A thesis submitted to the Nanyang Technological University in partial fulfilment of the requirement for the degree of**

**Doctor of Philosophy**

**2011**

# ACKNOWLEDGEMENTS

I would like to express my sincere gratitude to my supervisor, Prof. Leung Pak Hing for his invaluable guidance, encouragement, support and enthusiasm throughout my degree candidature. His passion towards research was truly inspirational and it has been a great experience to work under his guidance.

I would like to thank Dr. Sumod and Dr. Li Yongxin for their valuable suggestions and ideas without which completion of my thesis would be impossible.

I would like to thank all my seinor colleagues Dr. Chen Shuli, Dr. Ma Mengto, Dr. Liu Fengli, Dr. Ding Yi, Dr. Minyi Chiang, Dr. Luo Ding, Dr. Mingjun for their valuable scientific and technical advice.

Next, I would like to extend my gratitude to all my fellow workers Cheow, Yinhua, Xu Chang, Chen Ke, Zang Na, Jeanette, Zhiyi and Melissa. Melissa was the one worked together with on my projects during her undergraduate studies. My appreciation is also extended to Ee Lingfor NMR spectroscopy, Wenwei for Mass spectroscopy, Shuqi for elemental analysis and Celine for helping me in regards with graduate stuffs.

I'm grateful to SPMS-NTU for my research scholarship.

I would like to thank all my friends especially, Magesh and Dr. Kalpana for cheering me up and providing suggestions during my good and bad times in Singapore. My Special thanks Suseela, for her love, support during my crucial times in Singapore. I also thank Aarti and Priya for their wonderful company and my stay with them was pleasant and memorable.

Last but not least, my deepest gratitude to my parents, Dhanalakshmi and Krishnan for their love and constant encouragement. The completion of my study would not be possible without my husband, Dr. Karthikeyan mainly for his patience, support and unconditional love during the pursuit of a PhD degree.

# TABLE OF CONTENTS

## *Chapter II: Synthesis of Cyclopalladated Sulphur-NHC Complexes And their Catalytic Potential Studies in Allylic Substitution Reaction.*

# LIST OF TABLES

# LIST OF FIGURES

## ABBREVIATION AND SYMBOLS

| | |
|---|---|
| ACN | acetonitrile |
| Ad | adamantyl |
| Ar | aryl |
| OAc | *O*-acetyl |
| BARF | tetrakis(3,5-bis(trifluoromethylphenyl))borate |
| br | broad |
| Bn | benzyl |
| $^{t}$Bu | *tert*-butyl |
| $^{i}$Bu | *iso*-butyl |
| $^{i}$Pr | *iso*-propyl |
| *c* | sample concentration for O.R.D analysis |
| *ca.* | Circa |
| calcd | calculated |
| Cbz | benzoyloxycarbonyl |
| COD | 1,5-cyclooctadiene |
| $CD_3CN$ | acetonitrile-$d_3$ |
| $CDCl_3$ | chloroform-$d_1$ |
| $^{13}C\{H^1\}$ | $^{13}$Carbon NMR Spectra |
| COSY | correlation spectroscopy |
| d | doublet (in NMR assignments) |
| dba | 1,3-dibenzylacetone |
| dd | doublet of doublet (in NMR assignments) |

| | |
|---|---|
| *de* | diastereomeric excess |
| DMA | N,N-Dimethylacetamide |
| DMT | dimethyltryptamine |
| dmiy | 1,3-dimethylimidazolin-2-ylidene |
| $(CD_3)_2SO$ | dimethyl sulphoxide-$d_6$ |
| ee | enantiomeric excess |
| *etal.* | and others (latin *alii*) |
| g | grams |
| h | hour(s) |
| HMBC | heteronuclear multiple bond coherence |
| HCl | hydrochloric acid |
| HMQC | heteronuclear multiple quantum coherence |
| Hz | hertz |
| m | multiplets (in NMR assignments) |
| Me | methyl |
| Mesityl | 2,4,6-trimethylphenyl |
| mg | milligram(s) |
| min | minute(s) |
| mmol | millimole(s) |
| M.p | melting point |
| MS | mass spectroscopy |
| NMR | Nuclear Magnetic Resonance |
| Ph | Phenyl |
| $^{31}P$ NMR | $^{31}P\{^{1}H\}$ NMR |

| | |
|---|---|
| ppm | parts per million |
| q | quartet (in NMR assignments) |
| *R* | rectus (Latin: right absolute configuration) |
| ROESY 2D | rotating frame nuclear overhauserenhancement two dimensional spectra |
| *S* | sinister (Latin: left absolute configuration) |
| s | singlet (in NMR assignment) |
| t | triplet (in NMR assignment) |
| *p*-tolyl | 4-methylphenyl |
| THF | tetrahydrofuran |
| TOFs | turnover frequency |
| TONs | turnover number |
| tpps | triphenylphosphine sulfide |
| VT | Variable temperature |
| XRD | X-ray diffraction |
| δ | NMR chemical shift in ppm |
| $[\alpha]_D$ | specific rotation measured at sodium D line (589nm) |

# SUMMARY

This thesis describes the design and development of new chiral cyclometallated sulphur functionalized *N*-Heterocyclic carbene complexes and their catalytic potential studies on C-N and C-O bond forming reactions.

In Chapter 1, a brief discussion on the history of *N*-Heterocyclic carbenes, its recent development of functionalized NHCs complexes and their catalytic potential activity in asymmetric catalysis is presented. Further, this chapter is concluded with describing the aim of this project.

Chapter 2, describes the synthesis of several S-functionalized cyclopalladated NHC racemic complexes with a potential chiral centre on the α-carbon. This in turn results in the formation of a five membered ring chelate. The ligands were easily obtained when the substituted thiolates react with the common intermediate namely, *1-(bromo(phenyl)methyl)-3-tert-butyl-1H-imidazol-3-ium bromide,* and *1-(bromo(phenyl)methyl)-3-mesityl-1H-imidazol-3-ium bromide* and their corresponding palladium(II) complexes were fully characterized. Analysis on ring rigidity of neutral and cationic sulphur-NHC palladacycles was carried out with the help of XRD, 2D-ROESY, VT NMR techniques. A detailed study on the role of the new cationic π-allylpalladium(II) sulphur-NHC complexes, as a catalyst, in allylic amination reaction was established.

Chapter 3, describes the new methodology which was developed to synthesize chiral five membered Sulphur-NHC bidentate metal complexes *via*

fractional crystallization method. The racemic ligands and its corresponding palladacycles synthesized in chapter 2 were unable to resolve either in the form of diastereomeric salt formation or amino acid method, therefore the diastereomeric sulphur ligands were achieved from the common intermediate *3-(bromo(phenyl)methyl)-1-((R)-1-phenylethyl)-1H-imidazol-3-ium* synthesized from *(R)-1-(1-phenylethyl)-1H-imidazole*. The rigidity of neutral chiral cyclometallated sulphur-NHC complexes obtained from the silver complexes were completely analysed by XRD, 2D-ROESY, VT NMR techniques. Evidently, the chiral cyclometallated sulphur-N-Heterocyclic carbene complexes with **(Rs*,S*,R*)** and **(Ss*,R*,R*)** remained locked in **λ** and latter in **δ** ring conformation in the solid as well as the solution state. The significant feature of these new complexes invariably display the Ph(α) substituent taking an axial position either above or below the coordinating plane, due to the relative *trans* disposition of the sulphur atom substituent. These complexes were found to be reactive in [2,3]-sigmatropic rearrangement of (E)-N,N-dibenzylbut-2-en-1-amine.

# CHAPTER 1

## *N*-Heterocyclic Metal Carbenes

## General Introduction

### 1.0 History of NHCs

In 1960's Wanzlick and Öfele discovered the *N*-Heterocyclic carbenes (NHCs) derived from heterocycles such as imidazole, dihydroimidazole and triazole which have attracted significant attention.[1] However, the first stable and shelf-able NHC was isolated by Arduengo in 1991,[2] which allowed for its better understanding in fundamental studies of chemical reactivity and their behaviour in organometallic chemistry over the past two decades.[3] The extraordinary catalytic properties of NHCs can be attributed to its strong σ- bond and weak π-bond between $C_2$ carbon and metal. Unlike other metal carbon bonds they do not undergo fast insertion or reductive elimination reactions and therefore they are referred as "spectator ligands", which in-turn account for their stability towards air and moisture.[4]

### 1.1 Synthesis of *N*-Heterocyclic Carbenes

#### *1.1.1 Preparation of Dissymmetrical NHCs*

A wide range of NHCs can be easily synthesized via one pot method as summarized by Herrmann in his review.[5] The straight forward synthesis of dissymmetrical N-substituted NHCs involves glyoxal, primary amine and formaldehyde as starting materials as seen in Scheme 1.1. The dissymmetrical N-substituted derivatives can be obtained through the addition of phosphoric acid, followed by its alkylation by reactive alkyl/aryl halides or triflates (Scheme 1.2).

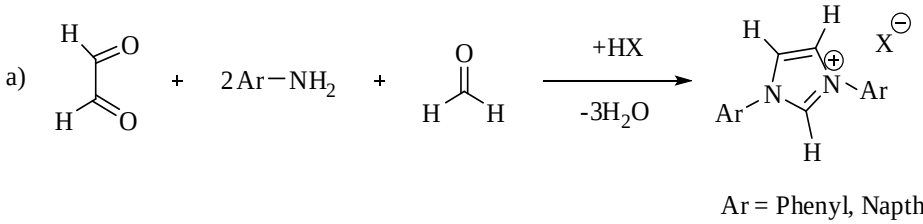


**Scheme 1.1**

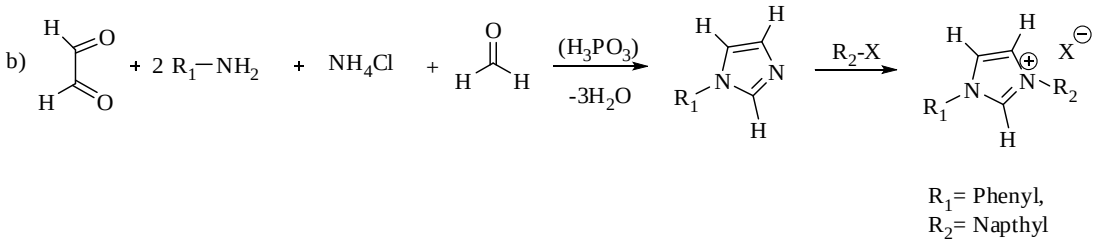


**Scheme 1.2**

Dissymmetrical NHC ligands have also been synthesized by Hermann *et al.*,[6] via a pot method using commercially available chiral amines as seen in Scheme 1.3.

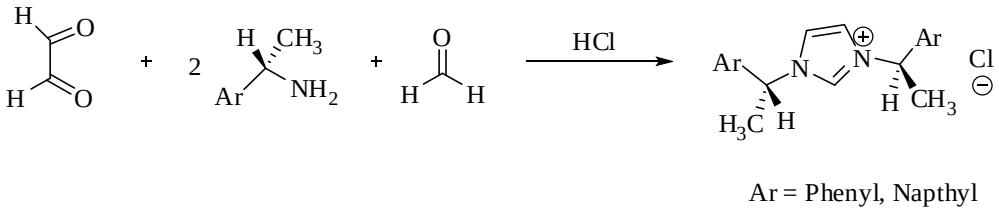


**Scheme 1.3**

Dissymmetrical imidazolinium and chiral imidazoliniums salts can also be synthesized from the commercially available amines and chiral diamines via the protocol shown in Scheme 1.4. Hartwig *et al.*,[7] and Grubbs *et al.*,[8] used these ligands as catalysts for asymmetric reactions such as alpha-arylation of amides and later for olefin metathesis in which they showed promising results.

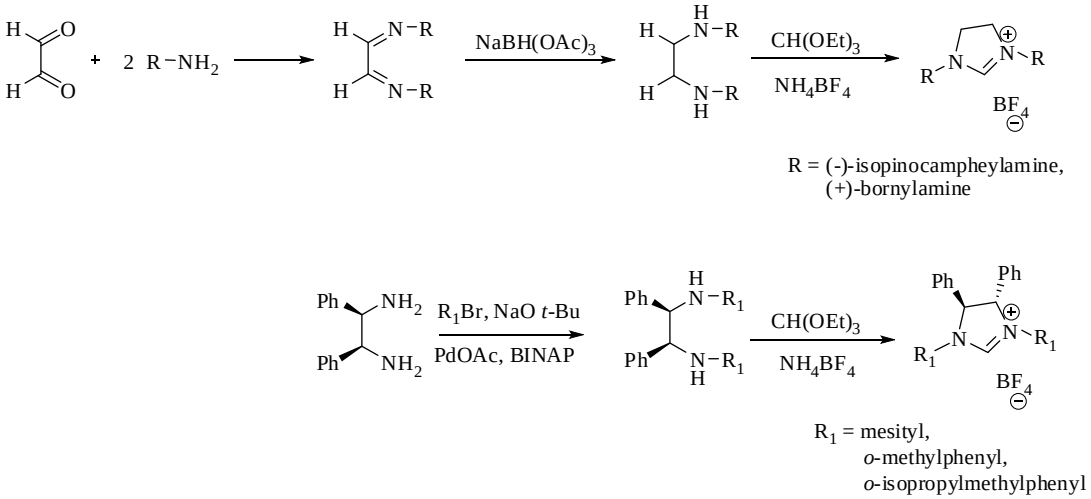


**Scheme 1.4**

### *1.1.2 Preparation of Asymmetrical chiral NHCs*

Assymmetrical chiral NHCs can by synthesized by reacting substituted imidazoles with oxazolines,[9] amino alcohols,[10] etc.; as shown in Scheme 1.5 & 1.6.

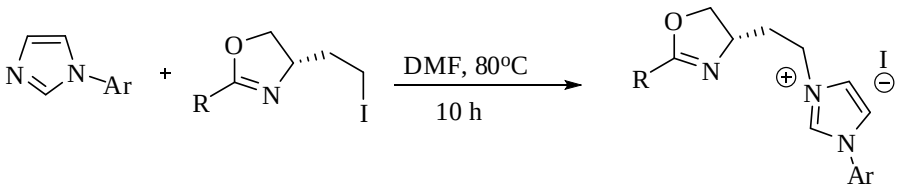


**Scheme 1.5**

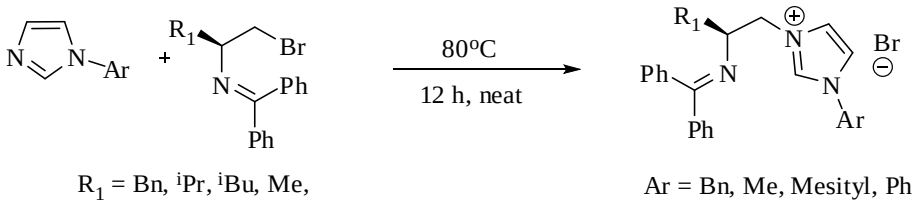


**Scheme 1.6**

### *1.1.3 Electronic and Steric Properties*

The electronic properties of NHCs are determined by measuring the CO vibrational frequencies[11] in low valent metal NHC carbonyl complexes where the π back donation of CO is directly related to the donor strength of the NHC. This is one of the most popular methods compared to other methods such as calorimetric studies[12] and cyclic voltammetric studies.[13]

However, $^{13}C$ NMR spectra are generally well accepted as it is more accurate and it also reduces the manipulation involved in the coordination of CO *trans* to the NHC system. The Figure 1.1 shows the donor ability of NHC in $^{13}C$ NMR,[14] where it describes that the saturated NHCs are strong donors compared to the corresponding unsaturated ones which in turn is in agreement with the calculated relative basicity of corresponding NHCs reported by Magill *et al.*[15]

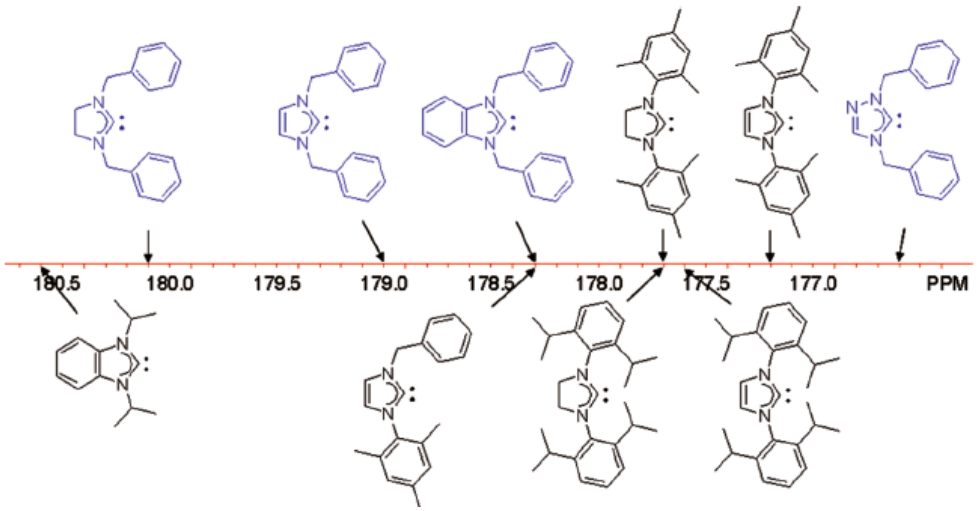


**Figure 1.1**

Nolan proposed a model to define the steric properties of NHC ligands that are measured in terms of buried volume $\%V_{Bur,}$[16] as shown in Figure 1.2, which is *"the amount of volume of a sphere centered on the metal, buried by*

*overlap with atoms of various NHC ligands"*. The volume is the space around the metal occupied by the ligand fragment and therefore, the $\%V_{Bur}$ increases as the functionality of the N-substituent is bulkier. Hence, for the saturated and unsaturated NHC ligands with bulkier group such as $^{t}$Bu group ($\%V_{Bur}$ = 37%) and adamantyl ($\%V_{Bur}$ = 37%) have greater $\%V_{Bur}$ than P$^{t}$Bu$_3$ ($\%V_{Bur}$ = 32%). Recently, Nolan in his review[17] explained that this influence is limited to two to three atoms around nitrogen and which is consistent with the data obtained from $^{i}$Pr NHC gold (I) complex [$\%V_{Bur}$ = 27.4%] and cyclohexyl NHC gold (I) complex [$\%V_{Bur}$ = 27.4%].

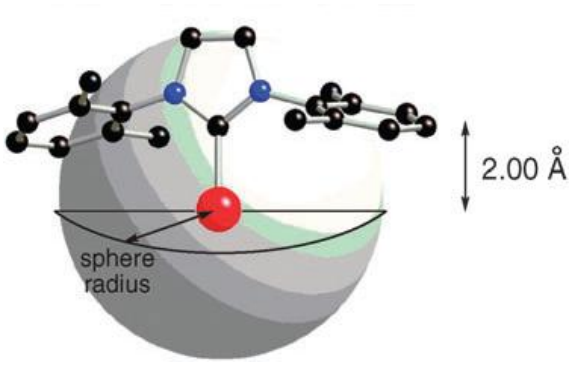


**Figure 1.2**

Therefore, the electronic and steric properties of NHCs can be determined accurately with the help of $^{13}C\{^{1}H\}$ NMR and buried volume ($\%V_{Bur}$).

## 1.2 Understanding of functionalized NHC complexes in asymmetric catalysis

One of the most active areas of research in chemistry is the hunt for new homogenous catalysts for organic transformations. The important goal in catalyst design study is to understand the mechanism by which the catalytic reaction

occurs and also to control deactivation of the catalyst during the course of reaction. The binding nature of NHCs to the metal is different from Fisher and Schorck carbenes as the electron density donated from the two nitrogen atoms to the carbene carbon act as a pure sigma donor towards the metal which in turn account for their high stability in catalysis compared to the corresponding phosphine analogue.

Decomposition of NHC-palladium complexes was first observed in $[PdMe(dmiy)(cod)]BF_4$ by Cavell *et al.*,[18] which brought attention on the serious drawbacks in the application of NHCs in catalysis reactions. However, further detailed studies on the dissociation of Metal-carbene bond in palladium complexes[19] reveals that the cause is due to the electronic and structural factors which tend to undergo reductive or *β*-hydride elimination as shown in Scheme 1.7.

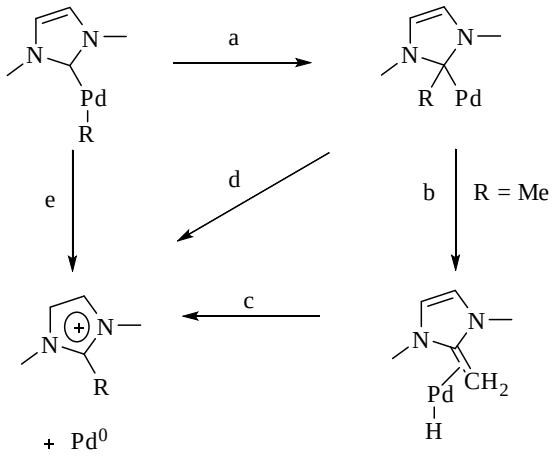


**Scheme 1.7**

a : migratory insertion; b : *β*-hydride elimination; c : reductive elimination; d : reductive elimination (where R is aryl or acyl group); e : concerted reductive elimination (where R is alkyl, aryl or acyl group).

Computational studies[20] established that, in the transition structure there is interaction between $C_{carbene}$ p-orbital, $C_{Me}$ orbital and Pd d-orbitals, as the angle of carbene plane (normally in the range of 65–80°) with respect to the coordination plane is in such a way that p-orbital of carbene is in correct orientation with the methyl orbital's which tends to mix-up and form $C_{carbene}$–$C_{Me}$ bond (as shown in Figure 1.3) and therefore, resulted in decomposition of the catalyst through reductive elimination process.

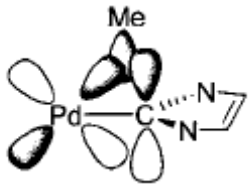


**Figure 1.3**

The effective overlapping of interacting orbitals can be reduced by (i) decreasing the dihedral angle between the carbene plane to that of coordinating plane; (ii) hindering the *cis* arrangement of alkyl group with respect to carbene. However, this can be achieved by introducing inflexible chelating NHC-based systems which were explained by Cavell *et al.*, in his review.[21]

### *1.2.1 Functionalized NHCs*

*N*-Heterocyclic carbenes that are synthesised from imidazole are functionalized by conventional synthetic methods. They have been reported in the literature, and these hybrid ligands which contain significantly different donor functions such as hard and soft donor groups have found increasing use in asymmetric catalysis.

Due to their hemilable behaviour, these hybrid ligands have the ability to provide vacant coordination sites on metals during the reaction that are "masked" in the ground state structure, and to stabilize the reactive intermediates. Therefore, these make an important class of ligands in organometallic catalysis.[22] The ease in preparation of functionalized NHC ligands by combining NHC moieties with wide range of classical donors such as P, N, O & S provides a gate way for construction of new chiral/achiral polydentate ligand with novel coordination chemistry. The NHC ligands functionalized with phosphine,[23] pyridine,[24] oxazoline,[25] amido,[26] ether[27] and their application in metal catalyzed reaction are reported in the literature. NHC functionalized with phosphines, pyridine, oxazoline and sulphur followed by its major applications in homogenous catalysis will be discussed briefly.

### *1.2.2 Functionalized NHC containing Phosphorus Donors*

#### *1.2.2.1 Bidentate Ligands and their catalytic applications*

Several groups have established that electron-rich phosphines with different source of palladium show high catalytic activity in cross-coupling reactions[28] and equal potential catalytic activity are also found in using monodentate *N*-heterocyclic carbene metal complexes.[29] With this background several bidentate phosphine NHC-ligands have been prepared to test their catalytic activity in cross-coupling reactions. In this combination, the carbene is strongly coordinated to the metal whereas phosphine acts as a hemiliable "arm" which is believed to coordinate/decoordinate from the metal to generate a vacant coordination site during the course of the reaction. This has not been proved experimentally under catalytic conditions, but the theoretical calculation proposed by Rösch *et al.*,[30] proven that during the course of Heck reactions, Pd-P bond was reversibly broken.

In 1996, Herrmann *et al.*,[31] reported the first study on a phosphine-imidazolium salt, followed by Nolan *et al.*,[32] with slight modification in ligand structure by introducing bulkier *N*-mesityl substituent on NHC. The latter was shown to be an efficient catalyst for Heck reaction using aryl bromides and n-butyl acrylate as substrates as shown in Scheme 1.8.

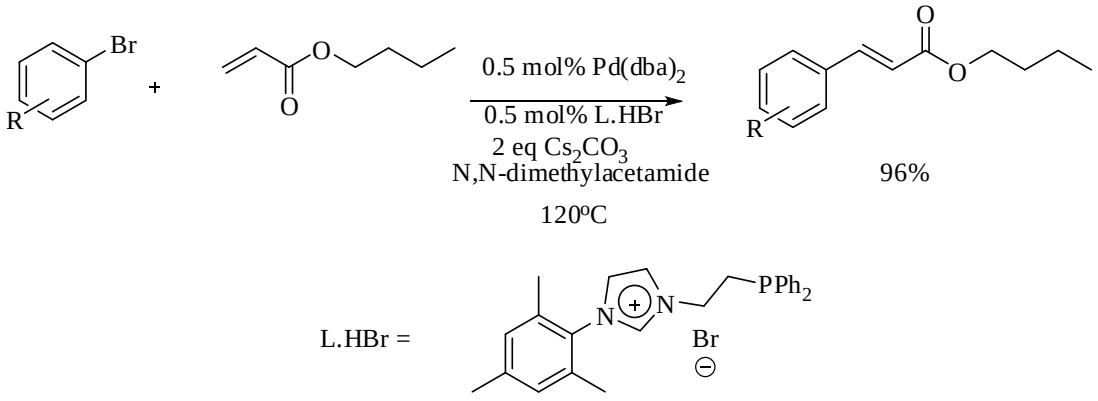


**1**

**Scheme 1.8**

Danopoulos *et al.*,[33] synthesized a series of phosphine-imidazolium analogues with ethylene and propylene linkage via a similar synthetic strategy to Herrmann. Lee *et al.*,[34] reported the improved method in which bis(imidazolium) salts can be significantly reduced by replacement of 1,2-dibromoethane with its chlorine analogue.

Zhou *et al.*, reported a new phosphine-imidazolium salt, in which the phosphine group is attached to a rigid phenyl ring, which leads to the formation of seven membered bidentate metal systems. Their catalytic activity in Heck coupling reactions were similar to that of Nolan system but, found high effectiveness in Suzuki coupling reactions of aryl halides with aryl boronic acids[35] as shown in Scheme 1.9.

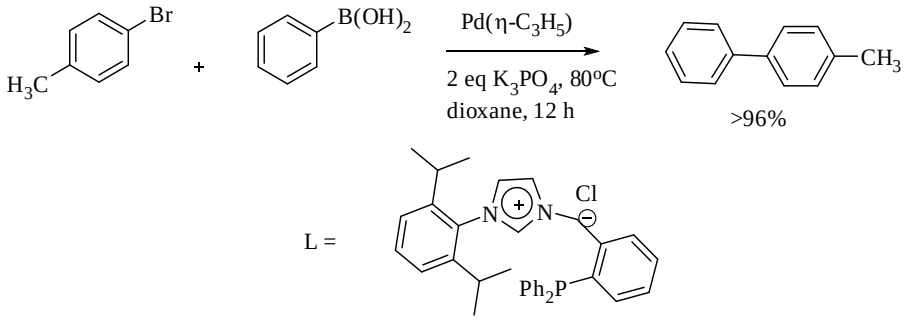


**2**

**Scheme 1.9**

Hydroarylation[36] of bicyclic alkenes with aryl iodides gave exclusively exo aryl norbornane products with high TONs upto 1.9 x $10^5$ and TOFs up to 6.3 x $10^4$ shown in Scheme 1.10.

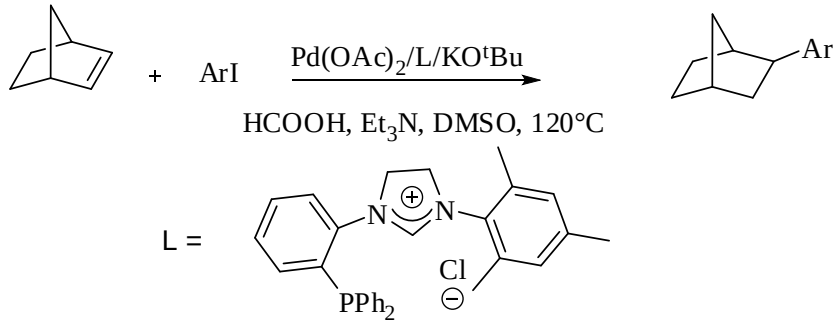


**3**

**Scheme 1.10**

Catalytic intramolecular hydroamination of 4-pentyn-1-amine as shown in scheme 1.11 was carried out effectively using [RhL(cod)]$BPh_4$ **4a**, [RhL$(CO)_2$]$BPh_4$ **4b**, and [IrL(cod)(CO)]$BPh_4$ **4c** as reported by Messerle *et al.*[37]

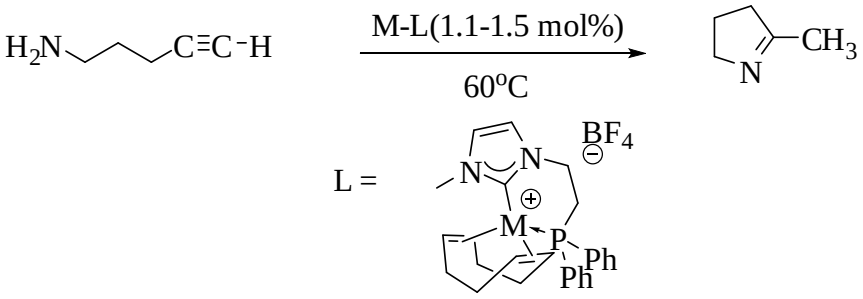


**4a-4c**

**Scheme 1.11**

Due to the requirement in asymmetric catalysis, Chung *et al.*,[38] reported the first chiral phosphine imidazolium iodide **5** synthesized from enantiopure ferrocenylamine. When this was tested against asymmetric hydrogenation of dimethyl itaconate using Rh(I) source in presence of KO$^t$Bu and $AgBF_4$, itafforded a low *ee* of 13%.

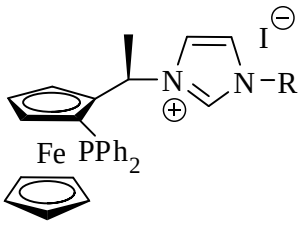


R = Ph, Me

**5a–5b**

The most effective asymmetric catalytic hydrogenation,[39] enantioselective conjugate addition[40] of aryl boronic acid to α,β-unsaturated esters and enones using rhodium complex **6** was reported by Helmchen *et al.*, as shown in Scheme 1.12.

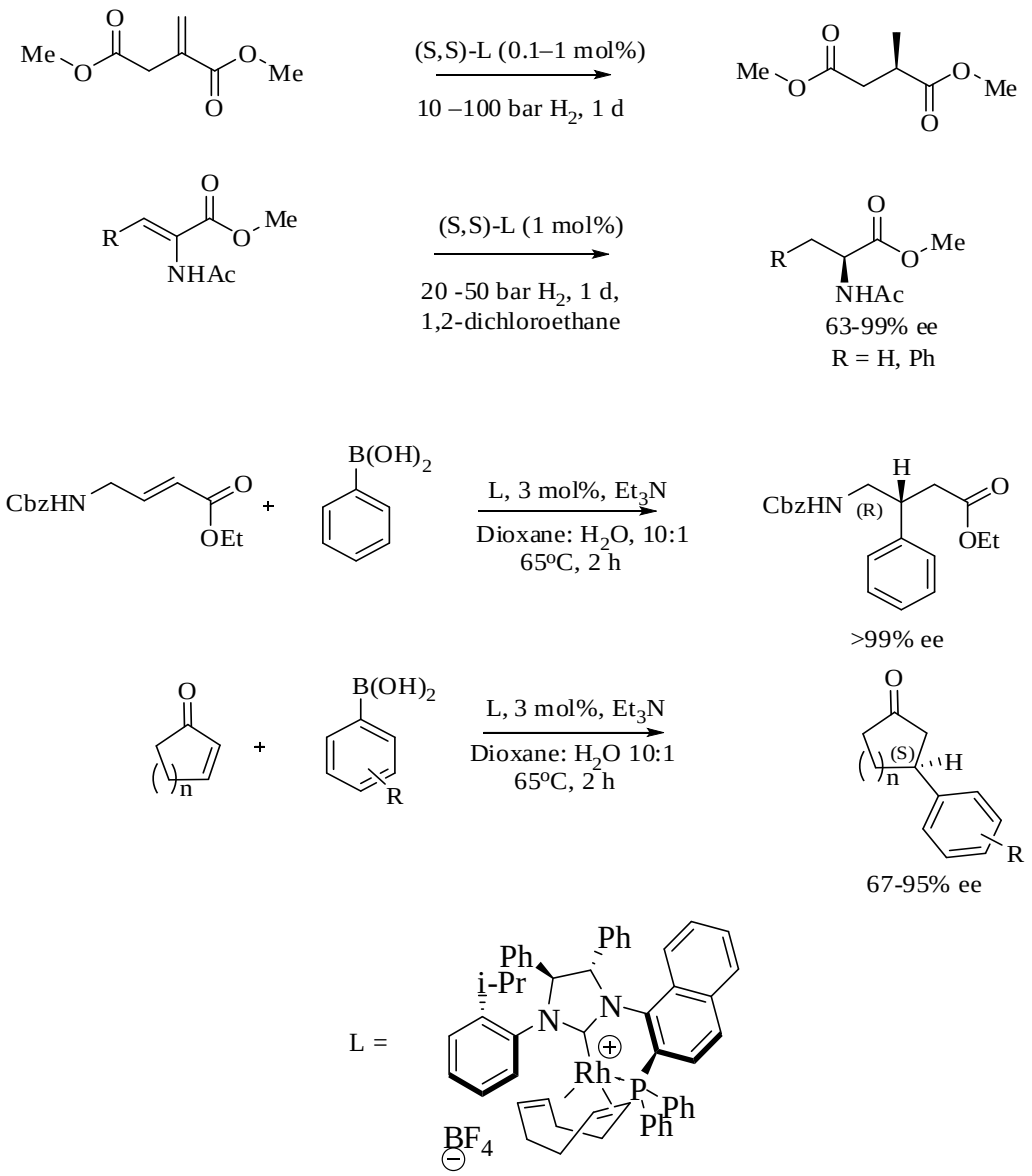


**6**

**Scheme 1.12**

Hahn *et al.*, synthesized phosphine-functionalized benzimidazolium salts,[41] similar to the method reported by Nolan. The use of benzimidazole is to enrich the electronic properties of the ligand precursor towards the catalytic reactions. The corresponding palladium complex **7** showed high activity in C–C coupling reactions of *para*-functionalized aryl bromides with styrene and *n*-butyl acrylate at 110°C as shown in Scheme 1.13.

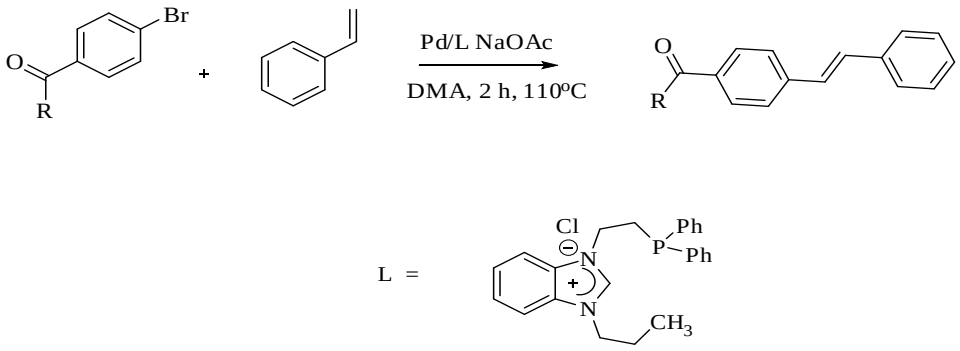


**7**

**Scheme 1.13**

*1.2.2.2 Tridentate ligands and its catalytic applications*

Togni *et al.*,[42] studied the coordination behaviour of palladium and rhodium complexes with NHC-based pincer-type chiral system which was synthesized using chiral ferrocenylamine as starting material, as similar to Chung's bidentate NHC ligand system.[32] This chiral tridentate ligand **8** with palladium source was tested for asymmetric addition of thiomorpholine to methacrylonitrileand gave selectivities up to 63–75% *ee* as shown in Scheme 1.14.

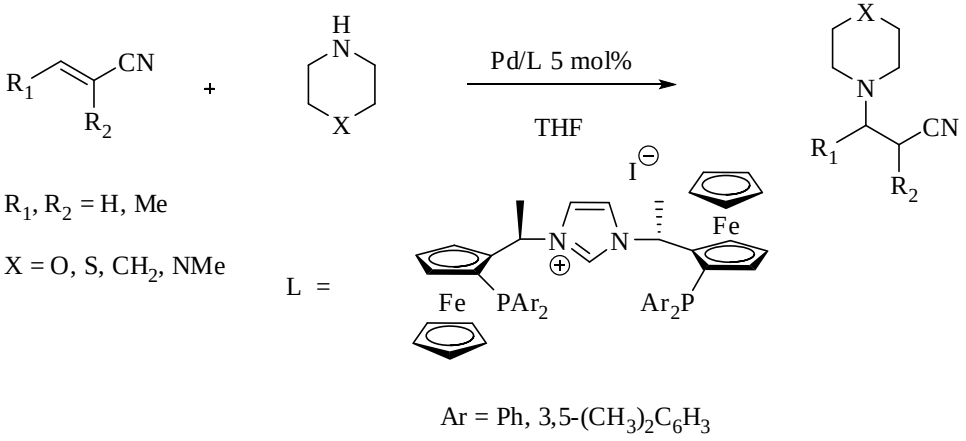


**8**

**Scheme 1.14**

Palladium(II) complex,[43] Ruthenium(II) complex[44] and Rhodium complexes[45] of achiral tridentate NHC system with two flanking phosphine side-arms were reported by Lee *et al.* These tridentate PCP ligand systems are flexible and capable of adopting either facial/meridional coordination modes in their ruthenium complexes similar to Togni's ferrocenyl-phosphine Ru-system.[43]

As shown in Scheme 1.15, Lee's tridentate PCP rhodium complex **9** gave *E*-isomer as major product when applied to chemoselective hydrosilylation of alkynes.

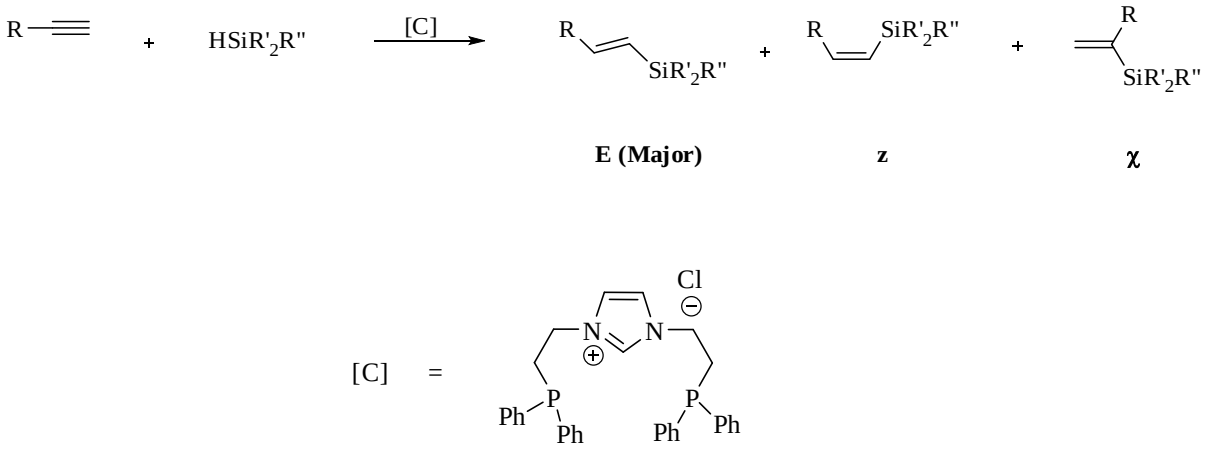


**9**

**Scheme 1.15**

Zhou *et al.*, synthesized tridentate ligand with central imidazolium moiety as a extension of their corresponding rigid bidentate phosphine-NHC system, but showed poor catalytic activity with $Pd(dba)_2$ towards Heck and Suzuki cross coupling reactions.[28]

Hahn *et al.*, also synthesized pincer type benzimidazole ligand precursor **10** and its corresponding palladium complex was shown to be less active towards C–C coupling reaction as compared to the bidentate phosphine-NHC system.

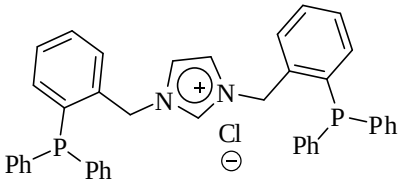

**10**

Lee *et al.*, also reported that unlike palladium, the coordination of phosphine-NHC ligand to Nickel(II) salts obtained air stable ionic complexes $[(Ni(L)_2]Cl_2$ **11**, which were found to be highly reactive towards Suzuki coupling reactions between phenylboronic acid and a range of aryl halides in a relatively short reaction time.[46]

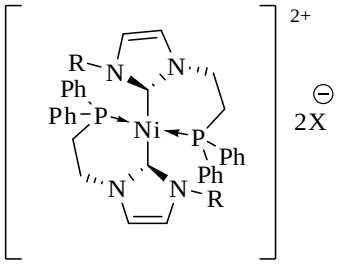

R =1-naphthylmethyl, benzyl, 4-fluorobenzyl,
3-methoxylbenzyl, X = Cl

**11**

### *1.2.3 Functionalized NHC containing Oxazoline Donors*

#### *1.2.3.1 Bidentate system and its catalytic applications*

The combination of an *N*-heterocyclic carbene with oxazoline units has also been developed among the other systems. The first example was reported by Herrmann *et al.*, in 1998 where, the NHC and oxazoline unit were linked by a methylene bridge. The corresponding Rh(I) complexes afforded low enantio selectivities (11% ee) when tested against hydrosilylation of ketones.[47]

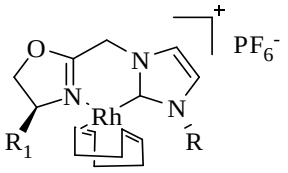


| | $R_1$ | R |
|---|---|---|
| **a** | Me | Bn |
| **b** | Me | $^i$Pr |
| **c** | $^t$Bu | Bn |
| **d** | $^t$Bu | $^i$Pr |

**12a–12d**

Shortly, Burgess *et al.*, reported the synthesis of iridium complexes[48] containing similar chiral bidentate phosphine-oxazoline ligands (*Phox*)[49] developed by Helmchen and Pfaltz. The complex **13** showed high catalytic activity and selectivity towards the asymmetric hydrogenation of *E*-1,2-diphenylpropene in 2 h with 50 bar $H_2$ at room temperature (Scheme 1.16)

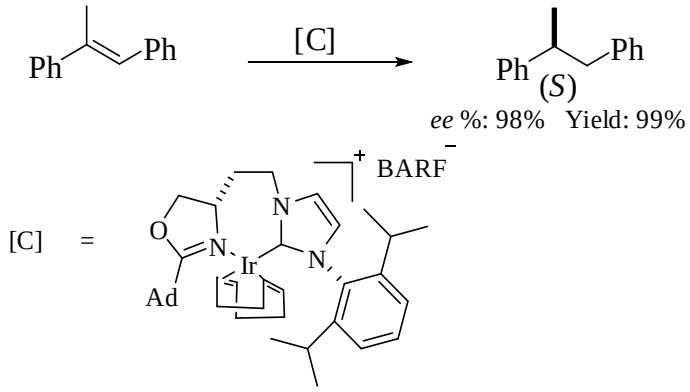


**13**

**Scheme 1.16**

Consequently, Gade expanded this area and synthesized a series of NHC-oxazoline Rh(I) complexes, in which the ligands were obtained by the direct condensation of an oxazoline and imidazole leading to five membered ring chelates. The corresponding Rh(I) complex **14** showed high enantioselectivity in asymmetric hydrosilylation of aryl alkyl ketones[50] ( Scheme 1.17).

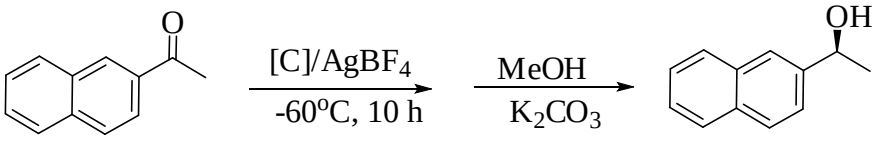


ee%: 98%Yield: 99%

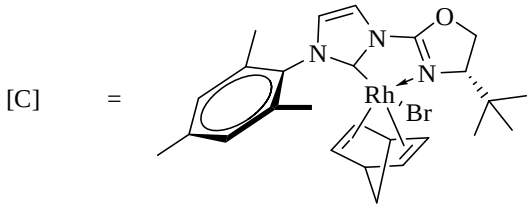


**14**

**Scheme 1.17**

Similar to oxazoline unit, Gade *et al.,* synthesized the robust benzoxazol[51] unit where by his platinum complex **15** was found to be active in hydrosilylation of alkenes with moderate activity and good selectivity with the formation of only linear products (scheme 1.18).

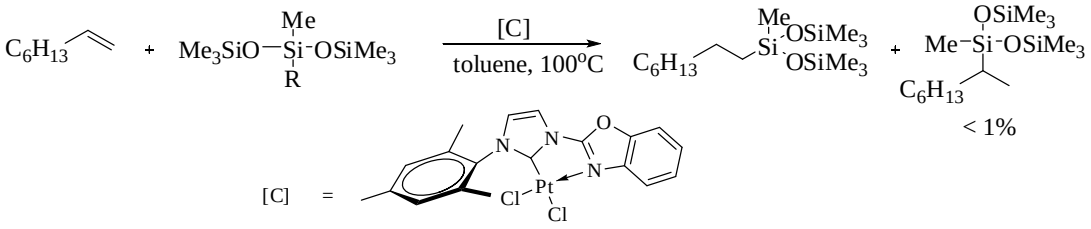


**15**

**Scheme 1.18**

Yuan *et al.,*[52] synthesized a string of Rh(I) complexes of **16a–16c** where by the complexes are able to successfully catalyse hydrosilylation of acetophenone to corresponding secondary alcohol in high yields but with very low enantioselectivity (<6% ee).

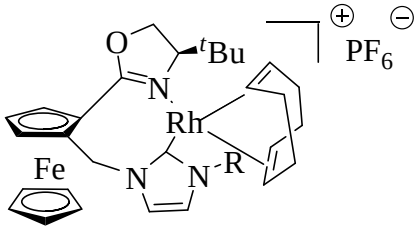


R = Me, $^{i}$Pr, Bn

**16a-16c**

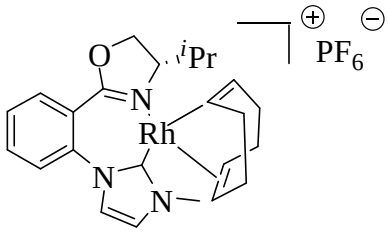


**17**

A chiral NHC oxazoline complex with rigid back bone was synthesized and its catalytic activity was studied by Crudden and his co-workers.[53] To their dismay, the complex **17** was not efficient to catalyze neither hydroboration nor hydrosilylation though their complex structure was highly rigid.

The planar chirality of the pseudo-*ortho*-paracyclophane combined with oxazoline and imidazolylidene ligands were studied by Bolm *et al.*, by which they obtained moderate yield with selectivity up to 46% ee in asymmetric hydrogenation of dimethylitaconate[54] using complex **18b.**

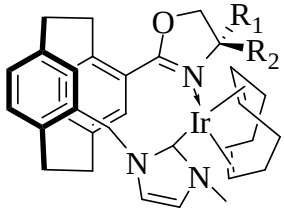


| | $R_1$ | $R_2$ | $R_3$ |
|---|---|---|---|
| a | Me | Me | Me |
| **b** | **Me** | **Me** | **Mesityl** |
| c | $^{t}$Bu | H | Me |

**18a-18c**

*1.2.3.2 Tridentate system and its catalytic applications*

The new bis(oxazoline) carbene ligands and their corresponding rhodium (III) and palladium (II) tridentate NCN complexes **19** and **20** were synthesized by Gade *et al.,* The modular strategies[55] of the new ancillary ligands were obtained from combination of Hermann's and Gade's bidentate systems.

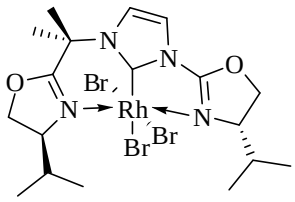


**19**

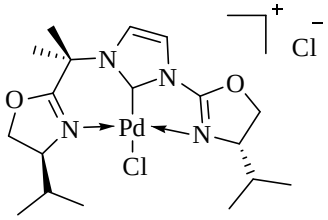


**20**

### 1.2.4 *Functionalized NHC containing Pyridine Donors*

1.2.4.1 *Bidentate system and its catalytic applications*

Pyridine functionalized NHC coordinate with different metals exhibited good reactivity in various catalytic reactions because of its inflexibility and chelating nature. Danopoulos and his co-workers[56] synthesized ligands in a bidentate fashion where pyridine and imidazolium units are linked by a methylene bridge similar to Hermann's complex **12**. The corresponding palladium complexes **21a** and **21b** were excellent pre-catalysts for the Heck coupling and amination reactions with highest TOFs being obtained with triethylamine as base.

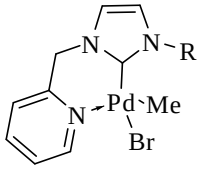


| | R |
|---|---|
| a | $^t$Bu |
| b | Mesityl |

**21a–21b**

Further, Danopoulos and his co workers reported in detail about the coordination behaviour and structural studies[57] of pyridine functionalized nickel complexes of **22, 23, 24, 25** which were developed from a series of different reaction conditions using $NiBr_2$(DME) as sole nickel source.

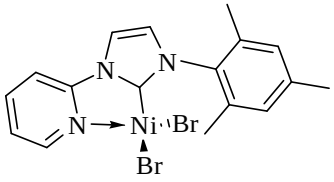

**22**

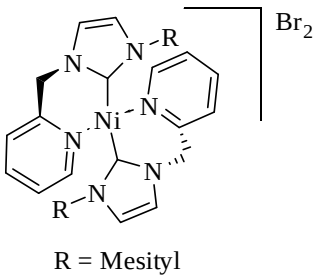

R = Mesityl

**23**

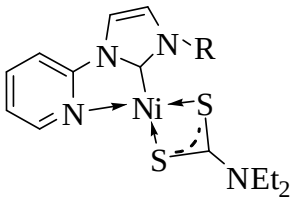

R = 2,6-$^{i}Pr_2C_6H_3$

**24**

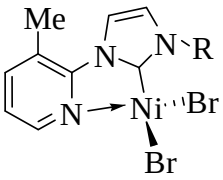

**25**

Recently, Chianese *et al.*,[58] widened this area to pyridine functionalized benzimidazolium bidentate system, where they accomplished high reactivity in allylic alkylation as well as allylic amination reactions using complex **26** as catalyst at ambient conditions (Scheme 1.19).

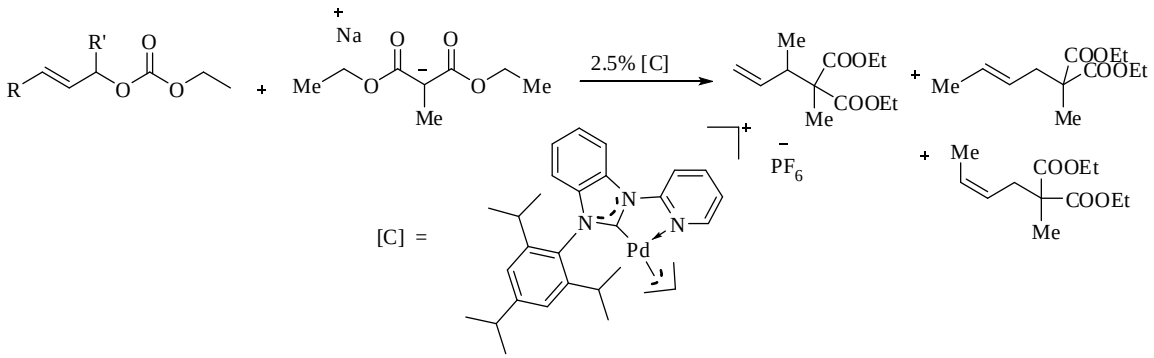

**26**

**Scheme 1.19**

*1.2.4.2 Tridentate system and its catalytic applications*

Crabtree *et al.*, synthesized a progression of tridentate complexes with various transition metal complexes. Complex **27** was one among them which showed excellent catalytic reactivity towards Heck coupling reaction.[59]

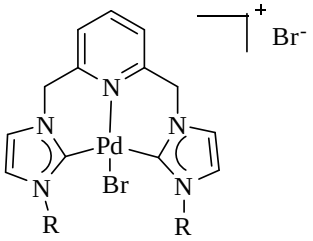


R = Me, $^{n}$Bu

**27**

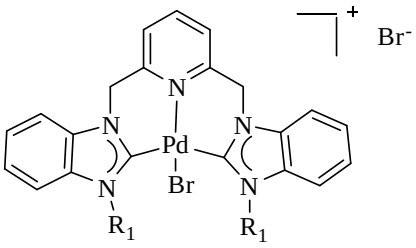


$R_1$ = Me, Et, $^{n}$Pr, $^{n}$Bu

**28**

Hahn *et al.*,[60] reported pyridine functionalized benzimidazolium tridentate palladium complex, and portrayed that complex **28** showed high catalytic activity towards Heck reaction.

### *1.2.5 Functionalized NHC containing Sulphur Donors*

*1.2.5.1 Bidentate Ligands and its catalytic applications*

Compared to other donor functionalized NHCs, the usage of sulphur-NHC complexes are quite rare, although their ability towards various catalytic transformations such as C–C, C–O, C–N bond formations have been proven. The sulphur-functionalized NHC compounds are categorized by functional groups such as thiolate, thioether, sulfoxide, thiophene, sulfonate and sulphonamide.

Complex **29** was documented as the first sulphur functionalized NHC complex reported by Sellmann *et al.*,[61] in 1992. This complex was claimed as an unexpected product obtained from the reaction of 1,2-ethanediamine-N,N-bis(2-

benzenethiolate) with nickel(II) chloride in DMF as solvent and their catalytic activity was not studied.

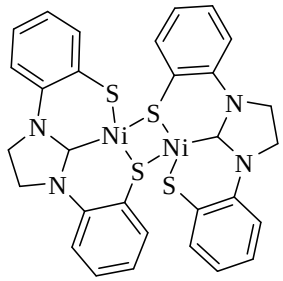


**29**

Chung *et al.,*[39] synthesized thioether functionalized NHC Rhodium (I) complexes which was similar to their corresponding phosphine analogues. The reactivity and selectivity of the complex **30** was lower as expected due to the fact that both do not really depends on the combination of several elements in skeletal structure of the catalyst and therefore gave 44% yield with 18% ee (R) on catalytic hydrogenation of dimethyl itaconate at 50°C under 10 atmospheric pressure of hydrogen.

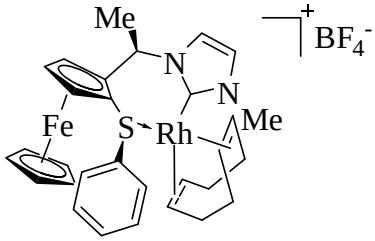


**30**

Huyhn *et al.,* studied in-depth on the dynamics and hemilabile behaviour of thioether functionalized bis(carbene)palladium(II) complexes and reported complex **31** with its superior catalytic reactivity in Suzuki-Miyauria and Mizoroki-Heck reactions with high TONs.

After exploring these studies on thioether tethered NHCs recently, Huynh *et al.* extended their research towards thiophene[62] functionalized palladium(II) bis carbene complexes which were closely similar to their thioether system.

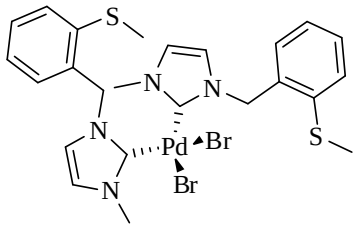

**31**

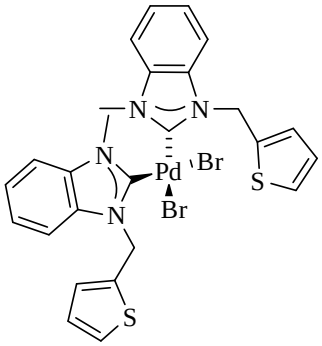

*cis-anti*

**32**

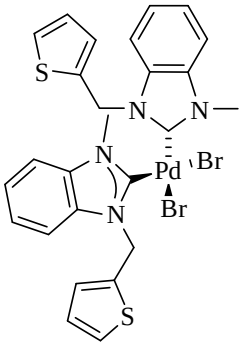

*cis-syn*

**33**

The complexes **32** and **33** were revealed to have high reactivity in Suzuki-Miyauria and Mizoroki-Heckreactions.

The hemilability of thioether functionalized NHC complexed to a palladium centre was reported by Huynh *et al.*,[63] on addition of triphenylphosphine, where the Pd–S bond cleaved and $PPh_3$ in turn will coordinated to the Pd metal centre as shown in Scheme 1.20.

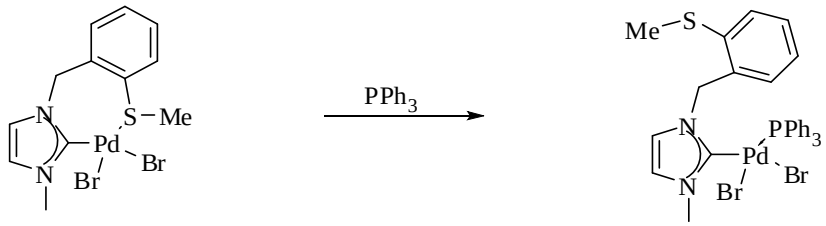

**34** **35**

**Scheme 1.20**

Fernandez *et al.,* and his co-workers synthesized a succession of chiral thioether functionalized imidazolium and benzimidazolium salts of NHC palladacycles[64] and recently reported that complex **36** showed remarkable reactivity and selectivity towards the allylic substitution of 1,3-diphenylpropenyl acetate with dimethyl malonate in which they achieved up to 91% *ee*[65] as compared to other sulphur donor functionalized NHCs.

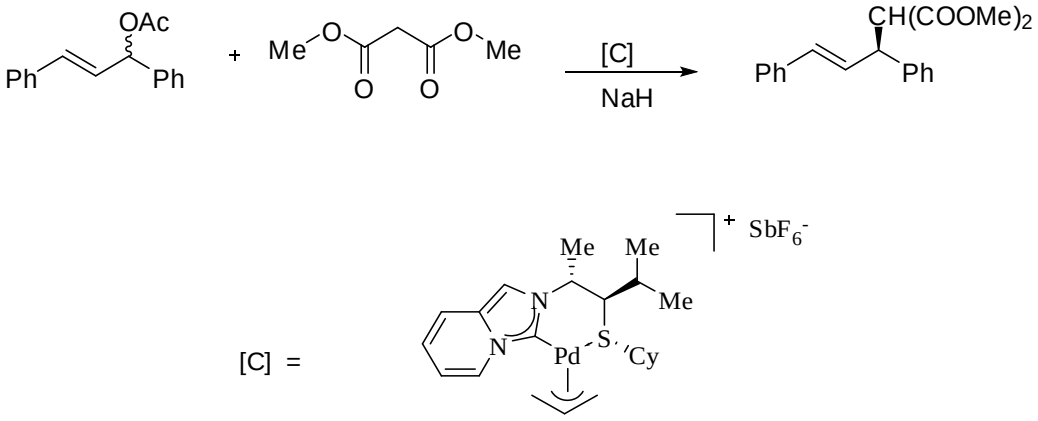


**36**

**Scheme 1.21**

*1.2.5.2 Tridentate ligands and its catalytic applications*

Tridentate benzimidazolium pincer type complexes **37 & 38** were synthesized by Huynh *et al.,*[66] using $Pd(OAc)_2$ in $(CH_3)_2SO$ at 80°C (KBr is required for formation of **37)**. Both the complexes demonstrated good catalytic activity towards the Mizoroki-Heck reaction; nevertheless complex **37** had the highest reactivity with 180,000 TONs in the reaction of *p*-bromobenzaldehyde and *t*-butylacrylate.

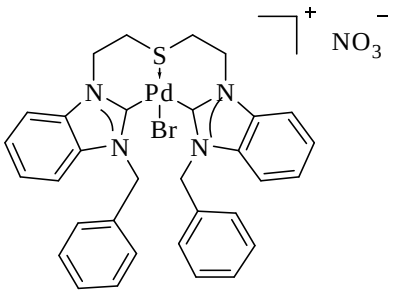

**37**

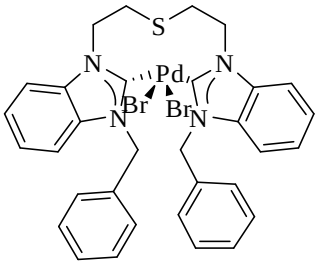

**38**

Based on $C_2$ symmetrical system, Fernandez and his co-workers[67] synthesized and characterized tridentate pincer type imidazolium **39** and benzimidazolium **40** palladium complexes. However, compared to palladium, silver complex of **39a** have shown to catalyze 1,3-dipolar addition reaction of imino esters and *t*-butyl acrylate in moderate yield with 55% enatioselectivity whereas silver complexes of corresponding benzimidazolium compounds indicate no reactivity.

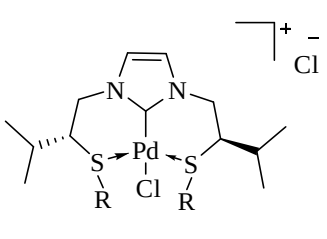

| | R |
|---|---|
| a | Cy |
| b | $^t$Bu |
| c | Ph |
| d | Bn |

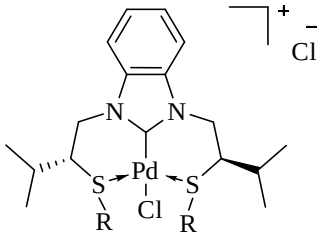

**39a–39d** **40a–40d**

## 1.3 ORGANOMETALLIC PALLADACYCLES

Organometallic palladacycles are generally formed by the coordination of organic substrates to the transition metal that comprises of Pd–C bond with the coordinating atom such as phosphorus, nitrogen, oxygen and sulphur.

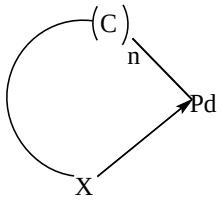


X = N, P, O, S ; $n \geq 1$

**Figure 1.4**

From early 1950's, organometallic palladacycles have found intensive application in catalytic/stoichiometric organic synthesis, as well as chiral resolving agents owing to the versatility in modification of steric and electronic properties in them. Result, to date, they are considered as one of the important classes of organometallic compounds.

The following discussion will spotlight only on organometallic palladacycles with sulphur as two electron donor atom. However, the number of cyclopalladated complexes containing sulphur atom as a part of the metallocyclic units are relatively limited compared to phosphorus or nitrogen donors due to their complicated synthesis.

### *1.3.1 Palladacycles containing Sulphur donor Ligand*

In 1972, Ishii *et al.*,[68] reported that metallation of benzyl methyl sulfide was not achieved using palladium(II) compounds, however, it can be easily done by manganese(I) using $[MnR(CO)_5]$ (R= Me/$CH_2Ph$) as they believed that the electrophilic substitution at the phenyl group was inhibited due to the strong coordination between sulphur and palladium.

Approximately 10 years later, Hiraki and co-workers acquired orthopalladated complex **41** with moderate yield from *t*-butybenzylsulfide and

$Pd(OAc)_2$ in methanol under reflux.[69] The dimeric complex **42** were obtained by metathetical reaction of complex **41** with LiCl in $THF/H_2O$ as solvent (Scheme1.22).

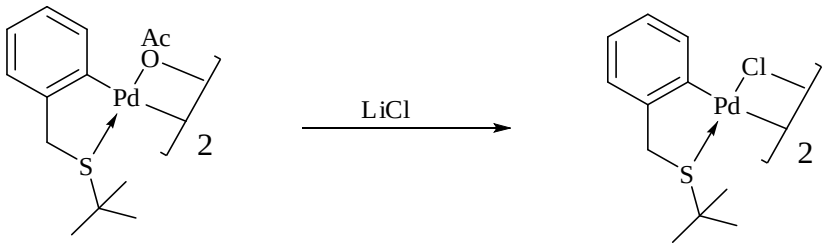


**41** **42**

**Scheme 1.22**

Furthermore, on treatment of dimer **42** with 3,5-lutidine established two set of mononuclear complexes **43a** and **43b** which was evident from the two sets of singlets for $^t$Bu protons in $^1$H-NMR spectrum (Scheme 1.23).

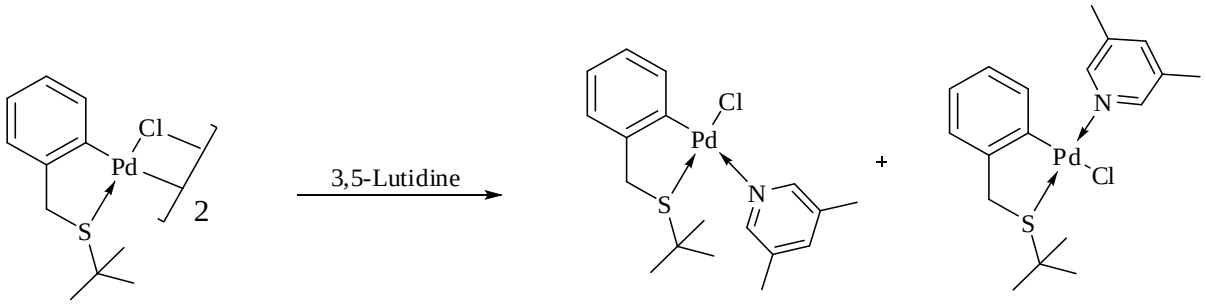


**42** **43a** **43b**

**Scheme 1.23**

Later in 1989, Dupont *et al.*,[70] established a series of orthopalladated complexes of various aryl sulphur moieties by his modified synthetic route; treatment of benzyl methyl sulfide with palladium acetate in acetic acid at reflux temperature produced cyclopalladated complex **44** in high yields. Similar bond

formation by palladium acetate was observed in its complexes with methyl-1-naphthyl sulfide and 2-biphenyl methyl sulfide to give corresponding complexes **46** and **47.**

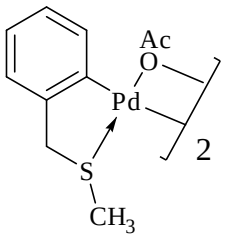


**44**

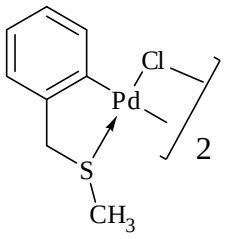


**45**

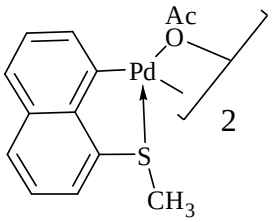


**46**

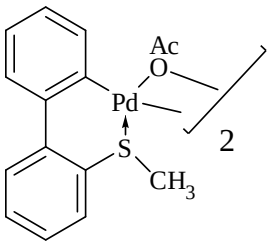


**47**

The $^{1}$H-NMR spectra of the cyclopalladated compounds **45** showed that they are fluxional in solution. However, after successive studies, the fluxionality of the molecules were assigned on two independent phenomena: (i) pyramidal inversion of the sulphur unit[71] (ii) and the inversion of the ring puckering of the palladacycles.[72]

In 1990, Dupont *et al.*,[73] reported the insertion reaction of CO and nitrile into the M–C bonds of cyclometallated compounds as shown in Scheme (1.24)

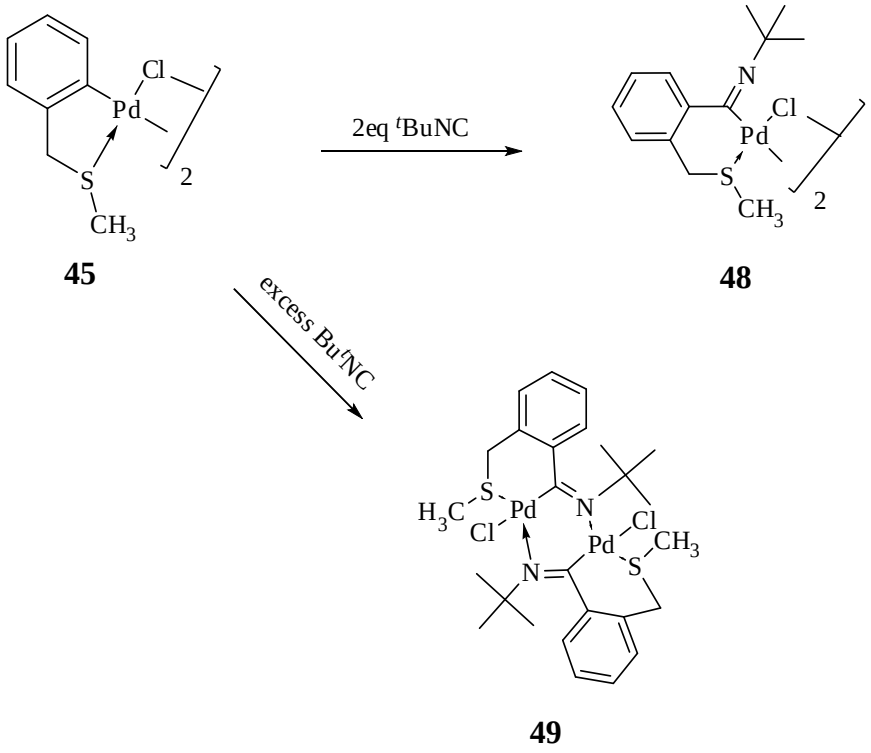


**45** **48** **49**

**Scheme 1.24**

The structure of complex **49** was determined by X-ray crystallographic study and found to be irreversible and inert to bridge-splitting reactions with pyridines or phosphines. Simultaneously, CO insertion was achieved when carbon monoxide was passed through a suspension of complex **50** in dichloromethane at room temperature to give complex **51** (Scheme 1.25). The rates of these reactions are much faster than the reactions of their nitrogen containing analogues.

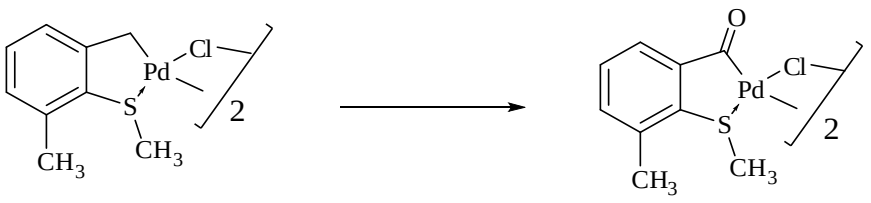


**50** **51**

**Scheme 1.25**

The first configurationally stable sulphur[74] containing palladacycles were synthesised by Dupont *et al.*, from optically active (1-alkylsulfanylethyl)benzenes and napthalenes. Among those complex **53** was highly active towards asymmetric Heck reaction at 90$^{o}$C with 1 mol% of catalyst using triethylamine as a base.

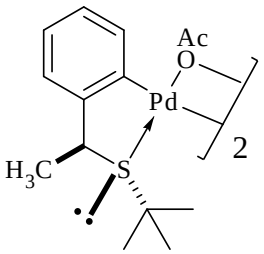


**52**

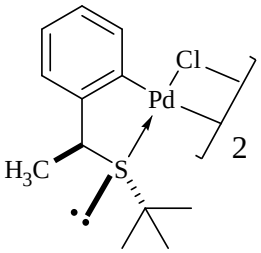


**53**

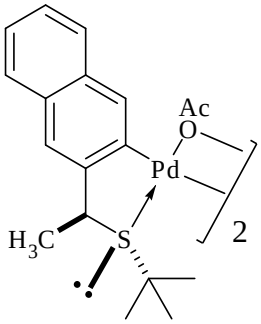


**54**

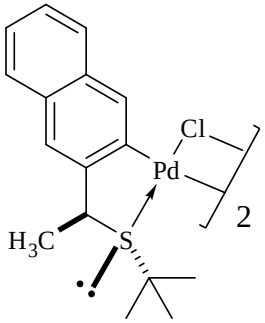


**55**

Derivative of ferrocene palladacycle **57** was obtained from the reaction of thiopivaloylferrocene **56** with sodium tetrachloropalladate in 62% yield[75] (Scheme 1.26).

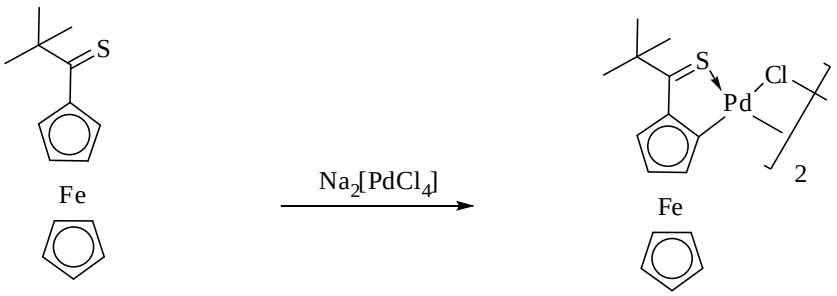


**56** **57**

**Scheme 1.26**

## 1.4 AIM OF THIS WORK

The aim of this project is to design, prepare and develop new chiral carbene metal coordination compounds in order to generate efficient asymmetric catalysts for a series of organic transformation reactions. Most of the existing chiral NHC ligands are monodentate and contain their stereogenic centres within the carbene ring itself, which leads to inefficient transmission of the chirality to the metal during the course of catalytic reactions.

Moreover, we are interested in developing a series of heterobidentate chiral NHC complexes with a potential chiral centre on the α-carbon that can form five membered chelate ringwith the metal ions and to study their catalytic activity in asymmetric reactions. The skeleton structures of these chiral complexes are as shown in the Figure 1.5

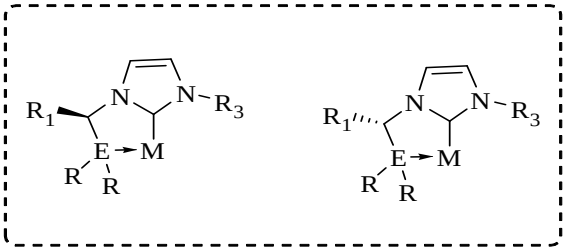


E = Hetero atom such as S, P, N

M = Pd

**Figure 1.5**

The stereochemical feature of these complexes is the transmission of chirality from the chiral carbon atom to the metal atom within the five member ring chelate. In general, steric crowding at the alpha chiral carbon will lead to a reduction in the bite angle and thus a stronger tendency to chelate with metal which leads to higher stereo- and enantio- selectivity in the course of catalytic reactions.

Henceforth, we are interested in synthesis of *N*-Heterocyclic carbene complexes with sulphur substituent on the α-carbon backbone, since such species will contain two chiral centres, (i) at the α-carbon and (ii) on sulphur coordination to metal.

The most important factors in the use of sulphur ligands are,

- Upon chelation to metal, the sulfur exhibits their stereogenicity which may induce to accelerate a reaction in a more stereoselective manner that results in a high degree of asymmetric induction.

- Due to their hemilable behaviour, these ligands have the ability to provide vacant coordination sites on the metal during the reactions.

- In contrast, catalytic reactions incorporating sulphur palladacycles as catalyst have by far been much less established.

In the second chapter, synthesis of a series of racemic five membered thioether tethered NHC palladacycles and their catalytic application towards allylic substitution reactions will be documented. In the final chapter resolution and reactivity of five chiral thioether tethered NHC palladacycles and their application towards [2,3] sigmatropic rearrangement reaction will be discussed.

# CHAPTER 2:

## Synthesis of Cyclopalladated Sulphur-N-Heterocyclic CarbeneComplexes and their Catalytic Potential Studies in Allylic Substitution Reactions

### 2.1 INTRODUCTION

Due to the lack of efficient synthetic methodologies, there are only a few reports on sulphur functionalized *N*-heterocyclic carbene ligands (NHCs) and their corresponding transition metal complexes as discussed in Chapter one. Furthermore, chiral complexes containing sulphur functionalized NHC are quite rare. Thus, we focused our attention on the synthesis of sulphur functionalized NHC five membered metal complexes.

In this chapter, we would like to discuss about the synthesis of a series of thioether tethered NHC ligand precursors with wide variability on the *N*-wing tip, along with their corresponding neutral and cationic palladium complexes in the first part, followed by their catalytic studies in allylic amination reactions in the latter part.

Transition metals have been successfully used as catalysts in various allylic substitution reactions and found to promote the reaction with varying regioselectivity. In addition to palladium other transition metal complexes such as Mo[76], Rh[77] and Pt[78] are used for catalytic allylic substitution reactions. The use of carbon, nitrogen, oxygen nucleophiles in allylic substitution enables the synthesis of C–C, C–N, and C–O bond formation which is the fundamental building blocks in organic chemistry.

As we focused only on palladium catalyzed allylic amination, the key intermediate is the formation of π-allyl palladium complexes by oxidative addition of allylic compounds to palladium followed by the nucleophilic attack of the amine at the allyl fragment leading to the formation of active $Pd^0$ species to give the desired products. The formation of active $Pd^0$ species can be achieved directly in the presence of phosphines and so far, a wide range of phosphine based metal complexes have profoundly demonstrated the high reactivity towards catalytic allylic amination reaction.

### *2.1.1 Possible pathway for allylic substitution reaction using palladium as catalyst*

The product distribution from the unsymmetrical substituted [Pd($\eta^3$-allyl)] intermediates is dependent on both the regio- and stereo-chemistry of the starting material. During the attack of the nucleophile on the monosubstituted [Pd($\eta^3$-allyl)] intermediates can lead to four possible diastereomeric (*syn* and *anti*) moieties are obtained that can equilibrate rapidly and in turn, can produce three isomeric products (branched, *cis, trans*). The Scheme 2.1 explicates the possible pathways for the origin of different products obtained from the allylic substitution reaction.

According to Trost,[79] factors that determine the regioselectivity of the reaction are,

(a) Steric factor: direct attack on the primary site i.e., less substituted carbon
(b) Electronic factor: where nucleophile tend to attack at the more electropositive carbon.

The product formation from either steric or electronic factors depends on the R group in the allyl substrate, the nucleophile, and the metal used.

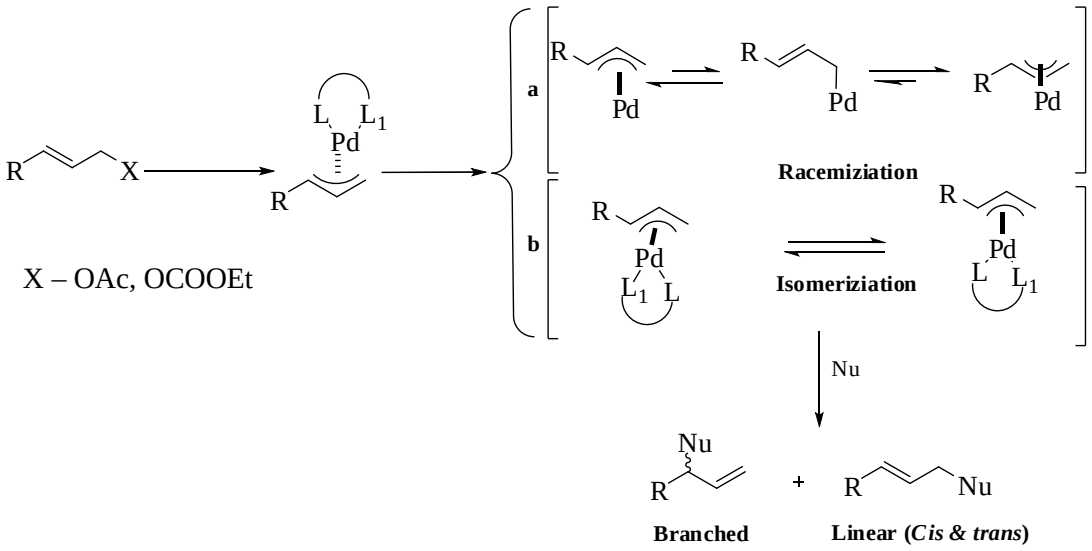


**Scheme 2.1**

### *2.1.2 Phosphines as catalyst*

Conversion of allylic alcohols directly into allylation product is highly desirable, especially from the perspective of atom economy. Ozawa *et al.*,[80] synthesized $sp^2$ hybridized diphosphinidenecyclobutene ligands precursors and its corresponding palladium complexes (**58a–58c**) where it was shown to be an effective catalyst in the direct conversion of allylic alcohols in the absence of activating agents at room temperature (Scheme 2.2).

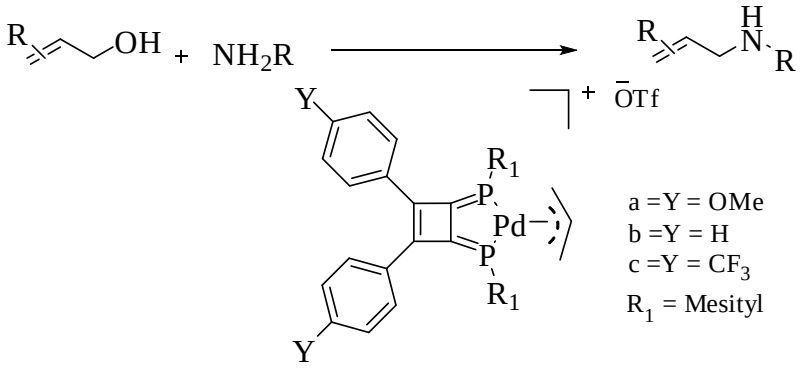


**58a–58c**

**Scheme 2.2**

Oshima *et al.,* used palladium acetate and a trisodium salt of tris(*m*-sulfonatophenyl)phosphine as a catalyst for allylation of amines with allylic alcohol in water as solvent medium as shown in (Scheme 2.3).[81]

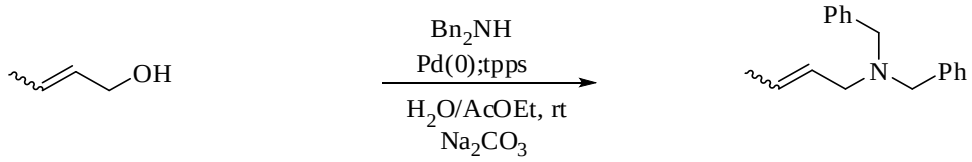


**Scheme 2.3**

In 2006, Yang *et al.,*[82] reported direct palladium catalyzed allylation of anilines (Scheme 2.4) in presence of 1-adamantane carboxylic acid in water as solvent medium with moderate yields.

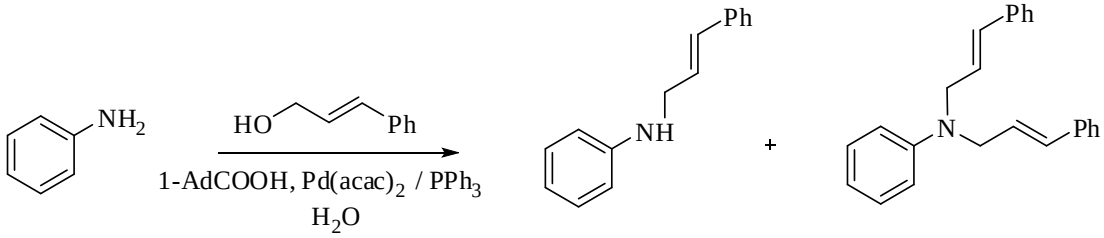


**Scheme 2.4**

Quite recently, Le Floch *et al.,*[83] synthesized xanthene-phosphole ligands, in which the phosphole group (strong π-accepting capacity) is attached to a rigid 9,9-dimethyl xanthane ring, which on treatment with $[Pd(allyl)Cl]_2$ dimer leads to the formation of eight membered bidentate palladium system **59** with larger bite angle (α = 116.08°). Their catalytic activity towards allylic amination reactions were found to be effective as the reaction gets completed in 1 h with high yield as shown in Scheme 2.5.

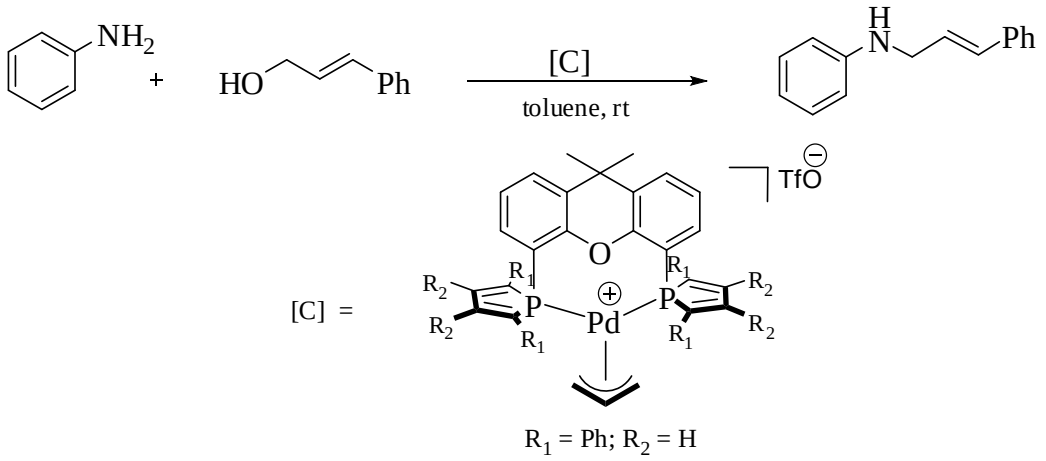


**59**

**Scheme 2.5**

### *2.1.3 N-Heterocyclic carbenes as catalyst*

Roland *et al.*,[84] succeeded in conducting allylic amination in a relatively short time under biphasic system using the combination of silver complex **60**, [(NHC)Pd(allyl)Cl] and $PPh_3$ (Scheme 2.6). The authors claimed that the reaction occured exclusively in the presence of $PPh_3$ which leads to the formation $[(NHC)Pd(allyl)(PPh_3)]^+$ complexes, during the course of cycle and they are found to be more electrophilic than [(NHC)Pd(allyl)Cl] which in turn explains its reactivity.

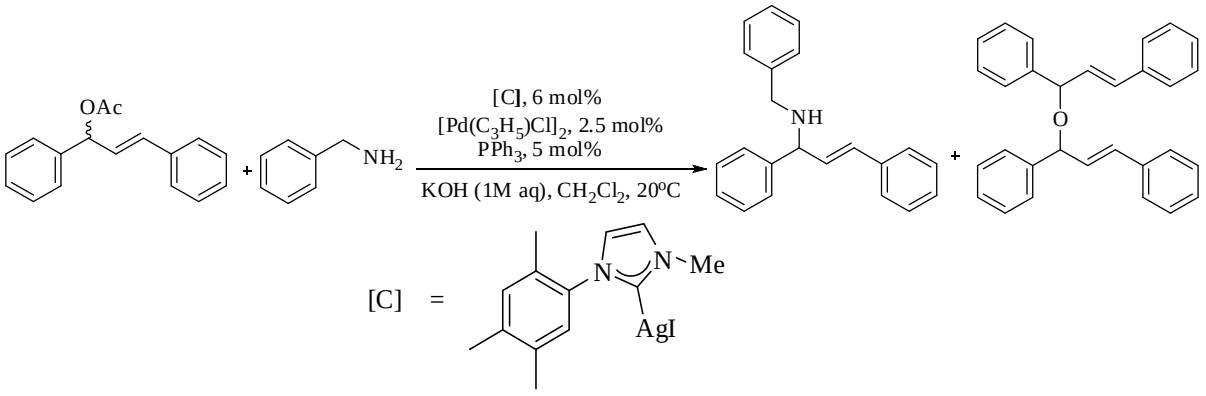


**60**

**Scheme 2.6**

The authors also concurred that the loss of enantioselectivity encountered when using NHC–$PPh_3$ ligands may be due to the *trans* influence of phosphine and carbene ligands which make the corresponding *trans* allyl carbons electronically equivalent.

Chianese *et al.*,[85] synthesized sterically rigid pyridine functionalized NHC bidentate palladacycles which were tested against the allylic amination reaction(Scheme 2.7). Two different substituted amines were identified along with amine (*trans*) which was the major product. The authors claimed that the catalytic regio-selectivity was not accomplished completely due to the reversibility of the amination reaction under their proposed conditions.

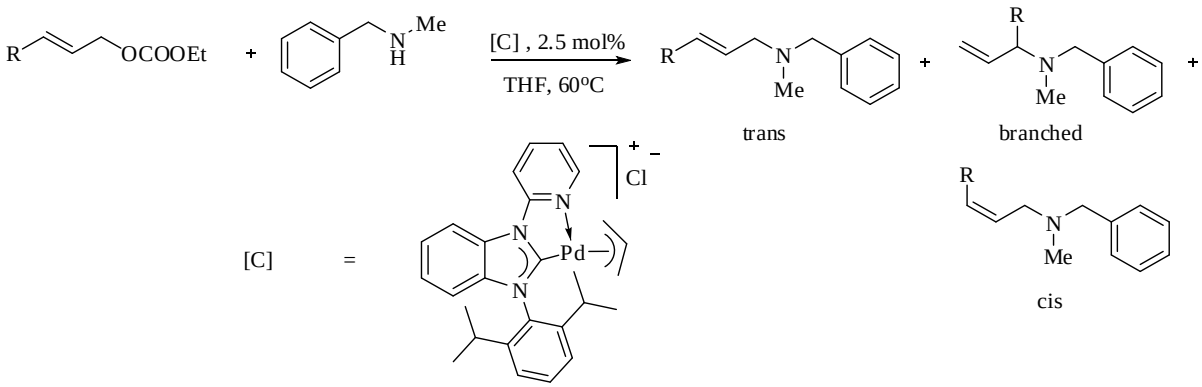


**61**

**Scheme 2.7**

To date, NHC-palladium catalysed reactions have found widespread utility in a number of reactions such as Stille couplings,[86] Heck reactions,[87] Suzuki couplings,[88] Hartwig-Buchwald,[89] Negishi reaction,[90] Kumada reaction,[91] Sonogashira reaction[92] and the key to their success in all these catalytic reactions is the ease with which they undergo oxidative addition and reductive elimination during the course of these catalytic reactions. Compared to allylic alkylation, the analogous amination reaction catalyzed by NHC–Pd complexes has been less

explored. Herein we describe our results with the expansion of this reaction, its scope, and limitations.

## 2.2 RESULT AND DISCUSSIONS

### *2.2.1 Synthesis and Characterization of Ligands*

The thioether-imidazolium bromides **(±)-64(a-b)** were prepared via a two-step procedure as shown in Scheme 2.8. The α-bromo compounds **(±)-63(a–b)** were readily available from the reaction of substituted imidazole and benzaldehyde with thionyl bromide in dichloromethane at -50°C under nitrogen atmosphere as reported in literature.[93] Subsequent, nucleophilic substitution reaction by sodium salt of substituted sulfides at -10°C under nitrogen atmosphere gave the desired ligands in high yield.

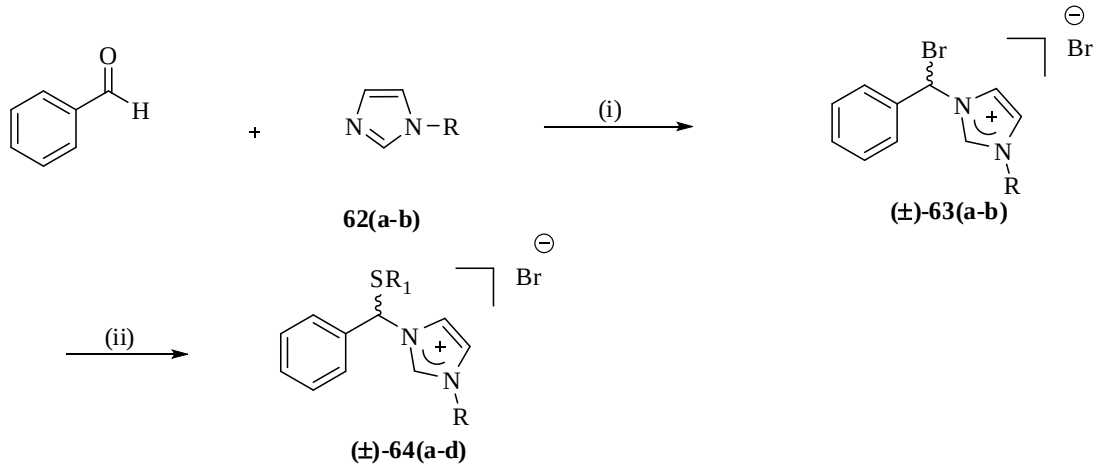


**Reagents and conditions:** (i) $SOBr_2$ (2M), DCM, –50°C, yield: 60-65%; (ii) $R_1SNa$, DCM/ACN, –10°C, yield: 70-80%.

**62a:** R = 2,4,6-trimethylbenzene ; **62b:** R = $^t$Bu; **63a:** R = 2,4,6-trimethylbenzene;
**63b:** R = $^t$Bu; **64a:** R = 2,4,6-trimethylbenzene, $R_1$= Ph; **64b:** R = $^t$Bu, $R_1$= Ph;
**64c:** R = $^t$Bu, $R_1$= *p*-tolyl; **64d:** R = $^t$Bu, $R_1$= $^t$Bu.

**Scheme 2.8**

### *2.2.2 Synthesis and Characterization of Racemic Palladium Complexes [66(a–d)] and [67(a–c)]*

To extend further the properties of carbene ligands derived from **(±)-64(a–d)**, the silver carbene complexes **65(a–d)** were efficiently prepared by reaction of **(±)-64(a–d)** with $Ag_2O$. According to the procedure reported by Wang and Lin,[94] this silver carbene complexes was used as a carbene transfer agent in the reactions with $[(\eta^3\text{-allyl})Pd(COD)]BF_4$ and $PdCl_2(CH_3CN)_2$ which proceeded at room temperature in the dark to afford cationic **(±)-66(a–d)** and neutral **(±)-67(a–c)** palladium(II) complexes in 90% and 55% yield, respectively, as shown in Scheme 2.9.

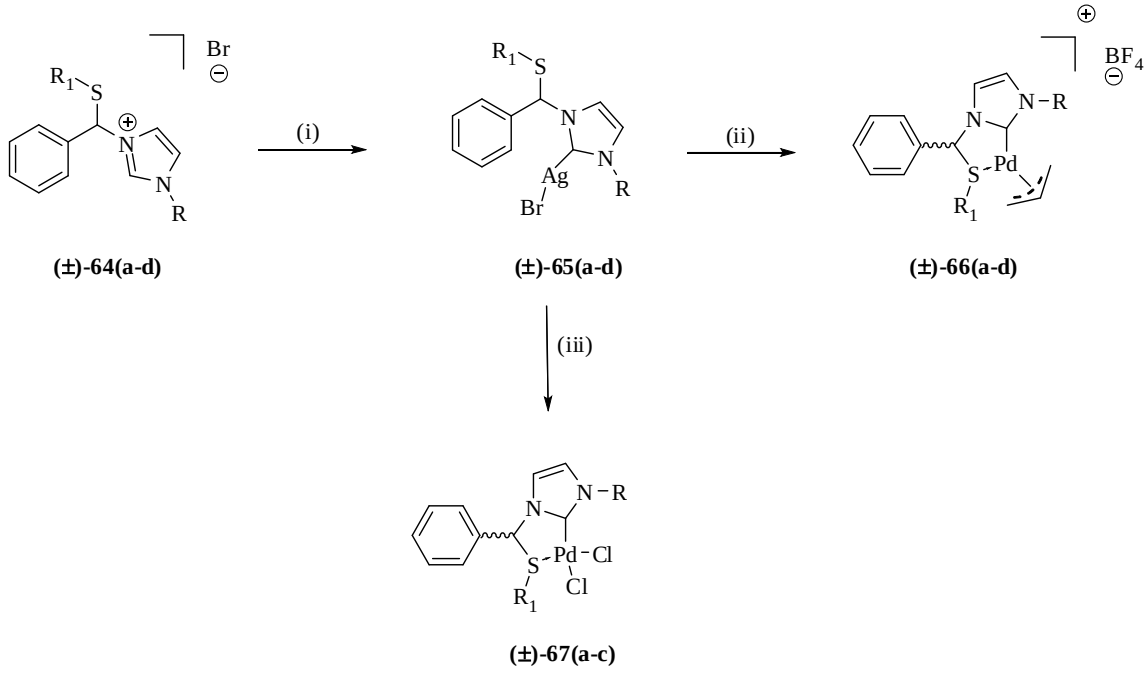


**(±)-64(a-d)** **(±)-65(a-d)** **(±)-66(a-d)**

**(±)-67(a-c)**

**Reagents and conditions:** (i) $Ag_2O$(0.55eq); DCM, rt , 3 h , 85-90% , in dark; (ii) $(\eta^3\text{-allyl})Pd^+(COD)BF_4^-$(1eq), DCM, rt, 4 h, 85-90%; (iii) $PdCl_2(CH_3CN)_2$ (1eq), $CH_3CN$, rt, 6 h, 55-60%.

**65a:** R = 2,4,6-trimethylbenzene, $R_1$ = Ph ;**65b:** R = $^t$Bu, $R_1$ = Ph; **65c:** R = $^t$Bu, $R_1$ = *p*-tolyl; **65d:** R = $^t$Bu, $R_1$ = $^t$Bu; **66a:** R = 2,4,6-trimethylbenzene, $R_1$= Ph; **66b:** R = $^t$Bu, $R_1$ = Ph ; **66c:** R = $^t$Bu, $R_1$ = *p*-tolyl; **66d:** R = $^t$Bu, $R_1$ = $^t$Bu; **67a:** R = $^t$Bu, $R_1$ = Ph ; **67b:** R = $^t$Bu, $R_1$ = *p*-tolyl; **67c:** R = $^t$Bu, $R_1$ = $^t$Bu.

**Scheme 2.9**

## List of New Ligands and Palladium(II) complexes

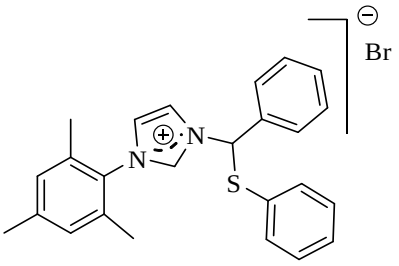


**(±)-64a**

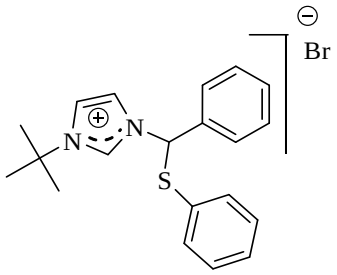


**(±)-64b**

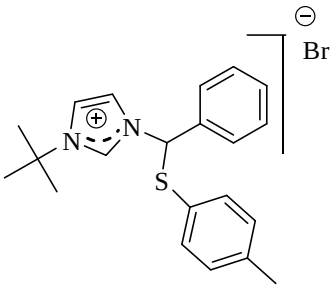


**(±)-64c**

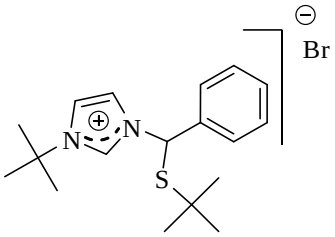


**(±)-64d**

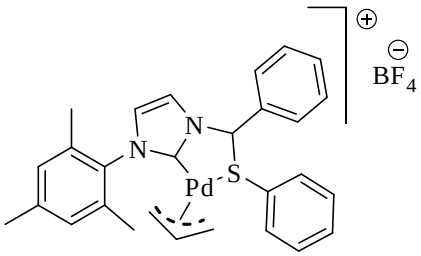


**(±)-66a**

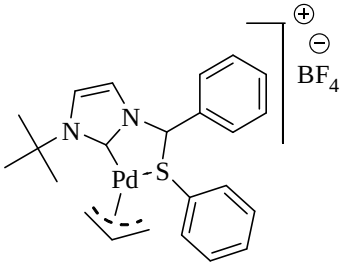


**(±)-66b**

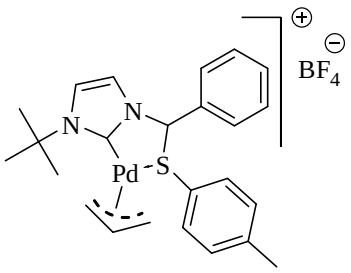


**(±)-66c**

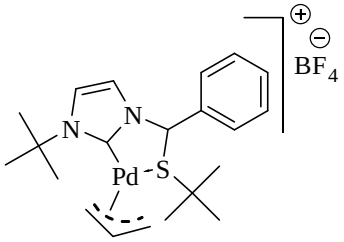


**(±)-66d**

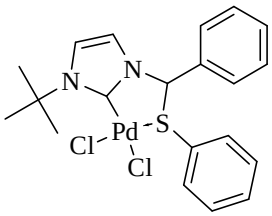


**(±)-67a**

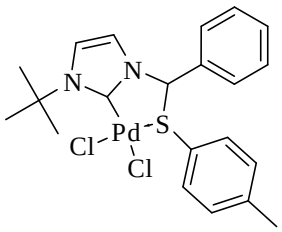


**(±)-67b**

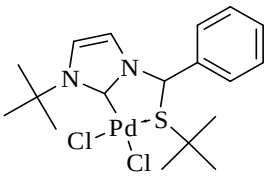


**(±)-67c**

We constantly observed low yields for the neutral S-NHC palladium complexes **(±)-67(a–c)** and the reason behind this was the formation of dimeric complexes which are consistent with dynamic/hemiliable studies reported by Huynh *et al.*[62] The existence of the dimeric complex (Figure 2.1) was confirmed by its molecular ion peak in LCMS and additional proton peaks in $^{1}$H-NMR spectrum along with its monomeric unit. However, we failed to obtain the pure

form of dimeric complex as it readily decomposed in an array of solvents during the crystallization process. The neutral complexes **(±)-67(a–c)** are solvent dependent; and from our observation through LCMS and $^{1}$HNMR spectroscopy, it was clear that they get transformed to dimeric complexes when dissolved in acidic solvents such as dichloromethane or chloroform at elevated temperatures.

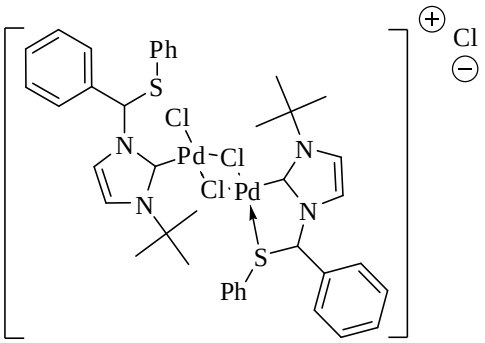


**Figure 2.1**

Notably, the formation of dicarbenesilver(II) bromide for **(±)-65a, [(±)-85a** and **(±)-85b** in **chapter 3],** compared to that of bromo(carbene)silver(I) complexes of **(±)-65(b-d)**, were presumably due the steric bulky nature of N-substituents for the former substrates, i.e., mesityl and Phenylethyl groups.

### *2.2.3 Structural Studies of Racemic Cyclopalladated Complexes*

#### *2.2.3.1 Molecular Structure of Cyclopalladated Complex* (**Rs*,S*)-66a**

The molecular structure of complex (**Rs*,S*)-66a** was determined by a single crystal X-ray diffraction study. The colorless needle type crystals with a size of 0.30 x 0.08 x 0.02 mm$^3$ of complex (**Rs*,S*)-66a** were grown by slow diffusion of diethyl ether into an acetone solution of the complex at –20$^{o}$C. The molecular structure with the numbering scheme is presented in Figure 2.2. Selected bond lengths and bond angles are listed in Table 2.1.

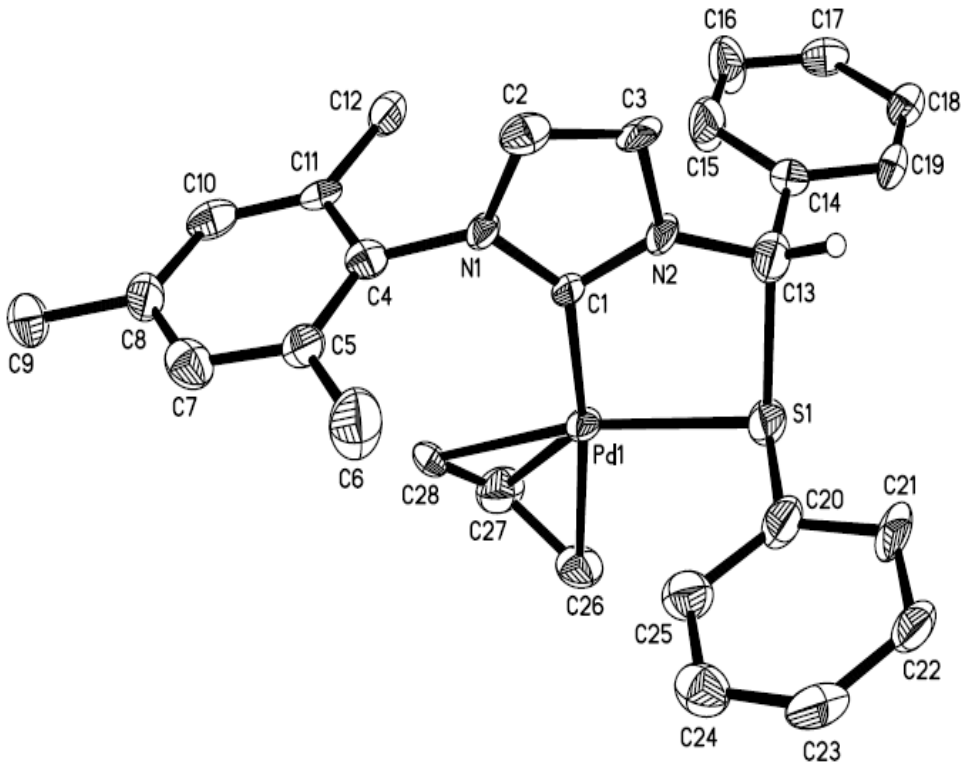


**Figure 2.2** Molecular structure of complex (**Rs*,S*)-66a**; Thermal ellipsoids are drawn at the 50% probability level. Hydrogen atoms except **H (13)** and the $BF_4^-$ counter anion are omitted for clarity.

In the solid state, the structure of the complex **66a** contains two stereogenic centres, α-carbon and the S atom with the (**Rs*,S*)** configuration. The complex **66a** is a racemic compound in which the metal chelate rings in **(Rs,S)-66a** and **(Ss,R)-66a** with opposite ring chiralities as they are enantiomers. The eight possible ring conformations with two stereogenic centres are shown in Figure 2.3**.**

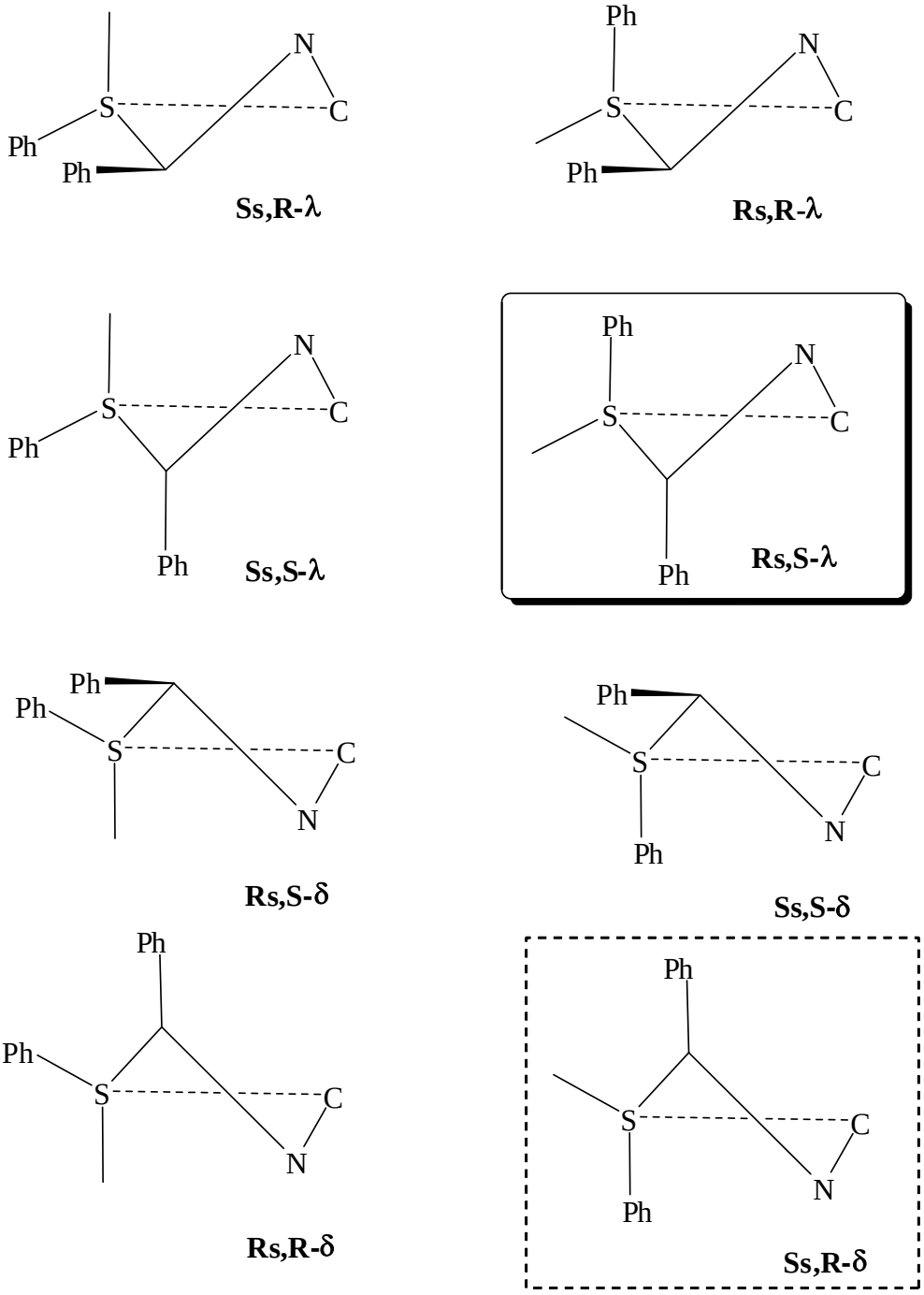
N
S
C
Ph
Ph
Ss,R-λ
Ph
N
S
C
Ph
Rs,R-λ
N
S
C
Ph
Ph
Ss,S-λ
Ph
N
S
C
Ph
Rs,S-λ
Ph
Ph
S
C
N
Rs,S-δ
Ph
S
C
N
Ph
Ss,S-δ
Ph
Ph
S
C
N
Rs,R-δ
Ph
S
C
N
Ph
Ss,R-δ

**Figure 2.3**

.

Generally, upon chelation, the sulphur atom exhibits a stereogenic center that was formed with ***R*** configuration. The significant feature of this complex is that the phenyl substituent at α-carbon (**C13**) adopts axial position below the coordinating PdCS ring and this can be explain based on lower steric interactions contributed by a relative *trans* disposition of the phenyl group at sulphur. The ring conformation in **(Rs*,S*)-66a** is a consequence of the **S** configuration at **C13** and the preference for the attached Ph group to adopt an axial disposition which lead to the arrangement of **λ** conformation.

Furthermore, the **δ**-conformation of **(Rs,S)-66a** has both substituents in equatorial positions (shown in Figure 2.3) and its enantiomer [**(Ss,R)-66a** in the box with dashed border] apparently has the **δ** conformation as a consequence of the **R** configuration at **C13** and the phenyl substituent adopt an axial *trans* disposition.

Due to the high steric nature of mesityl group, it forces itself in a perpendicular arrangement with respect to the imidazole-2-ylidene plane which blocks the upper face of the heterocyclic plane and consequently the allyl group positioned at the lower face. The C(20)–S(1)-C(13)-C(14) torsion angle between the phenyl substituent at α-carbon and the phenyl substituent at sulphur is 101.4$^{o}$. The monocationic complex exhibit the usual distorted square-planar geometry through coordination of palladium(II) ion, with a $C_{carbene}$–Pd bond distance of 2.030 Å and with a bite angle of C(1)–Pd(1)–S(1) 82.7$^{o}$. The longer Pd–C bond *trans* to the carbene carbon (Pd–C26 = 2.167Å) compared to the Pd–C bond *trans* to the sulphur atom (Pd–C28= 2.123Å) reflects the strong *trans* influence of the carbene. In all these five membered complexes, the sulfur form dative

bond with palladium and the bond angles about sulfur, is distorted tetrahedral, due to the presence of one lone pair of electrons in $sp^3$orbital. Hence, for a bidentate complex (**Rs*,S*)-66a**, the M-S-C bond angles of C(20)–S(1)–Pd(1) and C(13)–S(1)–Pd(1) were found to be 105.2$^o$ and 96.8$^o$ which is lesser than the observed angle for tetrahedral geometry and this presumably, due to the large steric influence of the lone pair.

**Table 2.1: Selected bond lengths (Å) and angles ($^o$) of palladium complex (Rs*,S*)-66a:**

| | | | |
|---|---|---|---|
| Pd(1)–C(1) | 2.030(9) | N(2)–C(1)–Pd(1) | 118.2(6) |
| Pd(1)–S(1) | 2.366(2) | N(1)–C(1)–N(2) | 104.0(7) |
| Pd(1)–C(28) | 2.123(8) | N(2)–C(13)–H(13) | 109.7 |
| Pd(1)–C(27) | 2.177(10) | C(1)–Pd(1)–S(1) | 82.7(2) |
| Pd(1)–C(26) | 2.167(9) | C(13)–S(1)–Pd(1) | 96.8(3) |
| C(1)–N(1) | 1.368(11) | C(20)–S(1)–C(13) | 101.4(4) |
| C(1)–N(2) | 1.339(10) | C(20)–S(1)–Pd(1) | 105.2(3) |
| N(1)–C(1)–Pd(1) | 137.6(6) | N(2)–C(13)–S(1) | 106.2(6) |
| N(2)–C(13)–C(14) | 115.3(8) | C(14)–C(13)–S(1) | 105.9(6) |
| C(1)–Pd(1)–C(28) | 105.1(3) | C(1)–Pd(1)–C(26) | 172.0(3) |

*2.2.3.2 Ring Conformation of Cyclopalladated Complex (±)-66a in Solution*

It is well evident that in solid state the five-membered palladacycle adopts **λ**-ring conformation where the prochiral sulphur atom is locked into stereochemically axial(Ph) and equatorial(lonepair) position due to the axial *trans* disposition of the phenyl group at **C13**. The rigidity of the CS ring chelate in solution were determined using the 2D $^{1}H$–$^{1}H$ rotating frame nuclear overhauser enhancement (ROESY) and variable temperature NMR spectroscopic techniques. Figure 2.3 represents the 2D $^{1}H$–$^{1}H$ ROESY NMR spectrum for **(±)-66a** in $CD_3OD$.

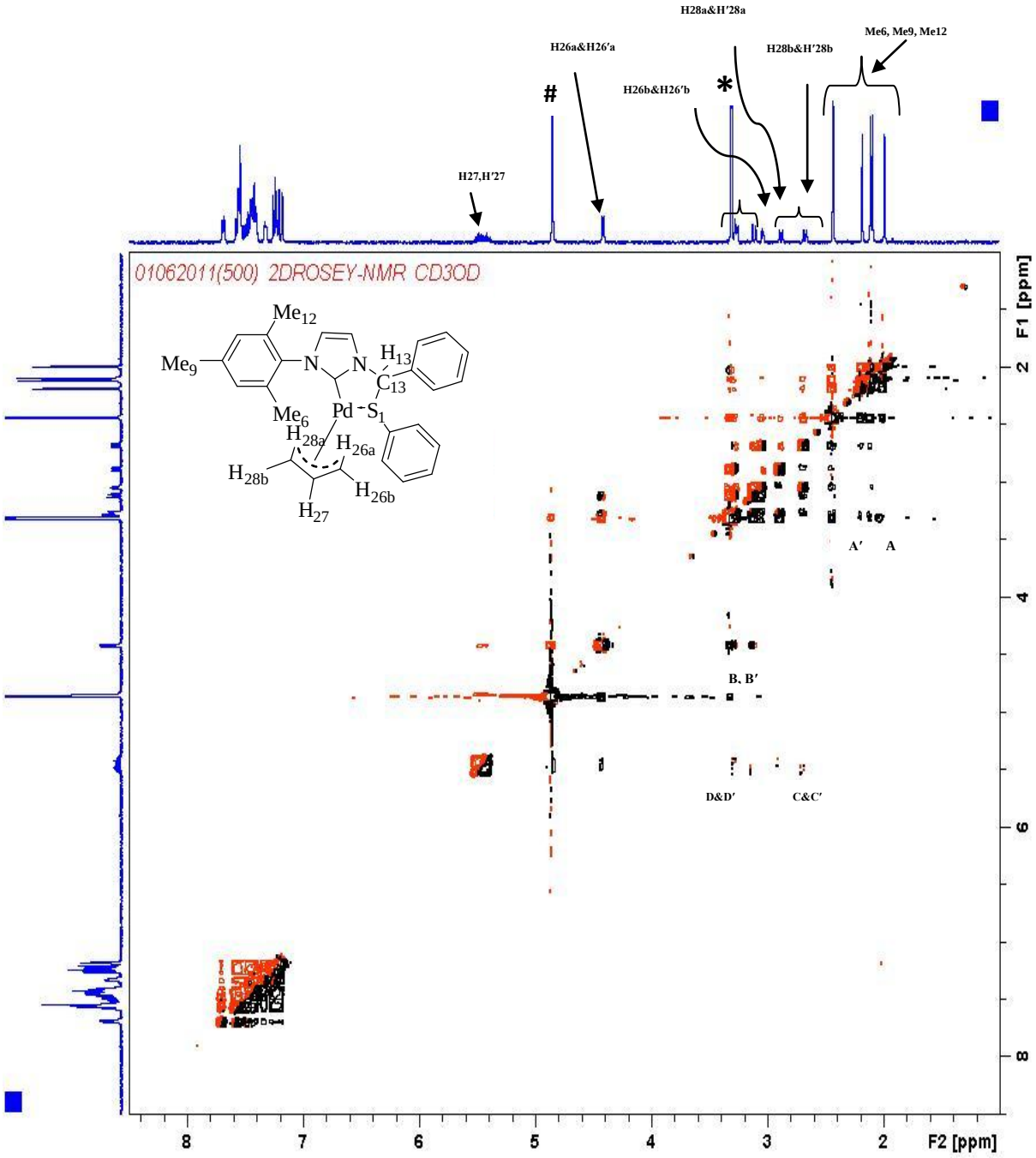


**Figure 2.4:** 2D $^{1}$H-$^{1}$H ROESY NMR spectrum of **(±)-66a** in $CD_3OD$.

**Selected NOE signals: (A&A′)**: Me6–H28b; Me'6–H′28b; **(B&B′)**: H26a–H26b; H′26a–H′26b; **(C&C′)**: H28b–H27; H′28b–H′27; **(D&D′)**: H26b–H27; H′26b–H′27; ***** $CD_3OD$ solvent peak; # - $H_2O$ peak.

The NMR data for **(±)-66a**, suggest the existence of two diastereomers (or stable rotamers) in solution as there were two sets of methyl resonances for the mesityl group. This suggest the presence of both **(Rs*,S*)-66a** and **(Rs*,R*)-66a** in solution [or two stable rotamers of **(Rs*,S*)-66a**].

Key correlations between the allyl protons **H26(a/b) or H′26(a/b**) and the aromatic proton of the sulphur substituent were not observed in 2D $^{1}H$–$^{1}H$ ROESY, however, the exchange cross-peaks between the allyl protons are detected in the spectrum, indicating the occurrence of a dynamic process which interconvert's these protons in solution. Moreover, due to the existence of two diastereomers (or stable rotamers) in solution at room temperature, there are considerable interactions observed in the aromatic region of 2D $^{1}H$–$^{1}H$ ROESY NMR spectrum and those NOE signals are inconclusive as they merged with each other.

The chemical exchange of *syn* and *anti* hydrogens on the same carbon via a $\eta^3$-$\eta^1$-$\eta^3$ process are well known dynamic behaviour observed for π-allyl ligands.[95] In $^{1}H$-NMR spectrum for the complex **(±)-66a**, the allylic proton *trans* to S appear as broad doublets [3.12-3.15, 3.03-3.06 ppm] where as sharp and distinct signals appear for the allylic protons *trans* to NHC [4.30-4.28, 3.18-3.15 ppm] were recorded at room temperature in $CDCl_3$. Hence, the terminal allylic hydrogens [C28–Pd1 = 2.123 Å] *trans* to the sulphur fragment are broadened which illuminates the process of *syn-anti* isomeriziation were proceeding through an $\eta^1$-allyl fragment, where dechelation occurs *trans* NHC fragment [C26–Pd1 = 2.167 Å] owing to their higher trans-effect compared to sulphur.

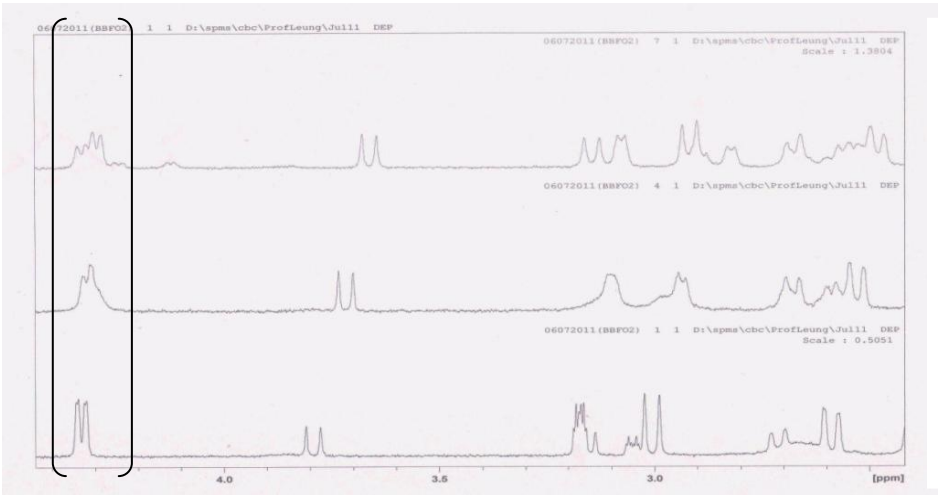


**(I)**

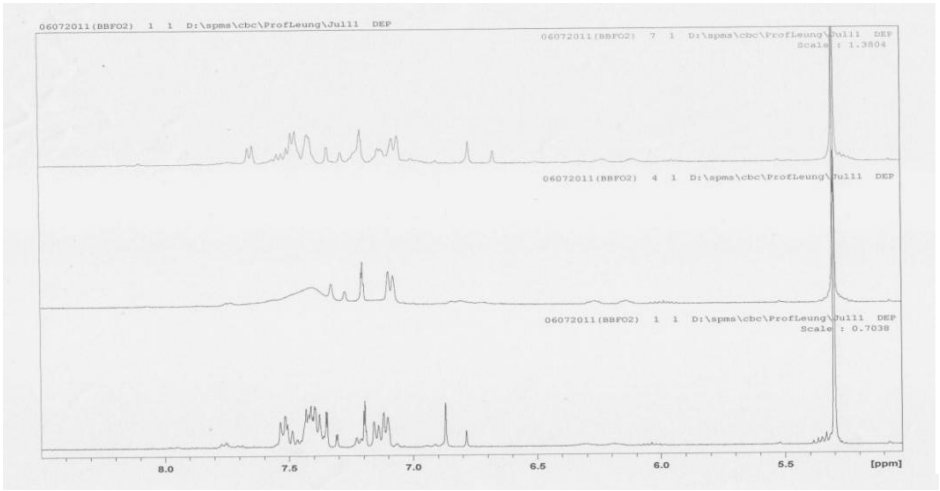


**(II)**

**Figure 2.5(I&II):** Variable temperature $^{1}$H-NMR spectra of the complex **(±)-66a** in $CD_2Cl_2$ solution.

Figure 2.5 (I&II), depicts the characteristic variable-temperature of $^{1}$H-NMR spectra at low temperatures. At temperature 296K, the $^{1}$H-NMR spectra

complex **(±)-66a** were simple. As the temperature is lowered each resonance tends to broaden and finally get collapses as the temperature reaches 256K. This temperature was considered as coalescence point where the signal is at its broadest, and before any splitting was observed. The resonances of the allyl protons [H26(a,b) & H28(a,b)] and aromatic protons provides evidence for the reduced rate of dynamic process at lower temperatures.

The low temperature spectra displaying the chemical exchange of the *syn* and *anti* protons of the allyl group validates the retention of **λ** ring conformation on palladacycle with *cis* disposition of the Ph substituents on **C13** and **S1** [**(Ss,S-λ)** shown in Figure 2.3] and inturn suggest the pyramidal inversion of configuration of the sulfur atom in **(±)-66a**.

### 2.2.3.3 Ring Conformation of Cyclopalladated Complex (±)-66b in Solution:

Suitable crystals for X-ray crystallography were not able to be achieved for the complex in a wide range of solvents. Figure 2.6 presents the 2D $^{1}$H-$^{1}$H ROESY NMR spectrum for **(±)-66b** in $CD_3OD$. The $^{l}$H-NMR data for **(±)-66b**, suggest the existence of two diastereomers (or stable rotamers) in solution as there appears two singlet resonances for the $^{t}$Bu group one for each of the two diastereomers. Therefore, suggests the presence of both **(Rs*,S*)-66b** and **(Rs*,R*)-66b** in solution [or two stable rotamers of **(Rs*,S*)-66b**].

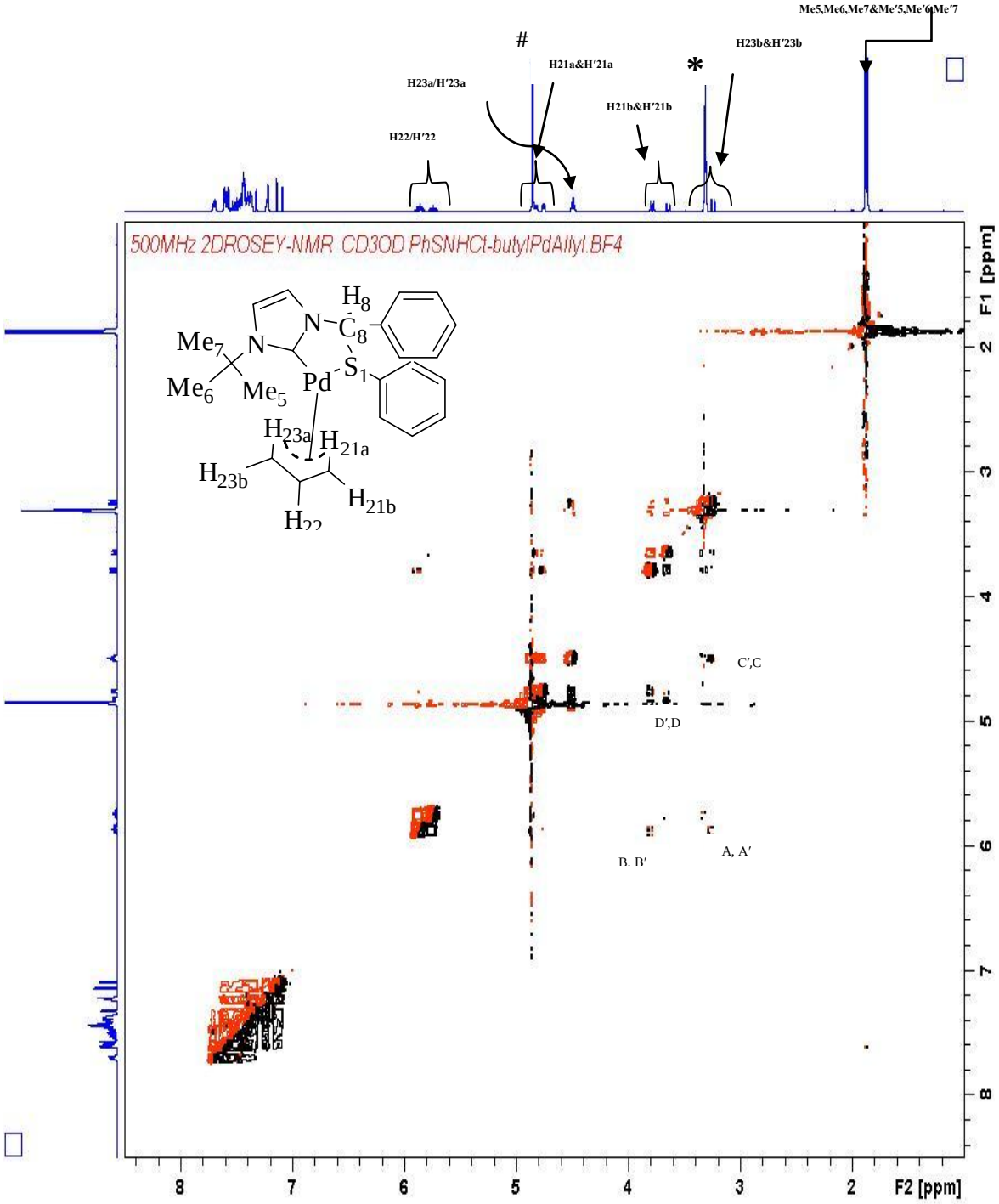


**Figure 2.6** 2D $^{1}$H-$^{1}$H ROESY NMR spectrum of **(±)-66b** in **$CD_3OD$**.

**Selected NOE signals:** * $CD_3OD$ solvent peak; # $H_2O$ peak. **(A&A′)**: H22-H23b; H′22-H′23b; **(B&B′)**: H22-H21b; H′22-H′21b; **(C&C′)**: H23b-H23a; H′23b-H′23a; **(D&D′)**: H21b-H21a; H′21b-H′21a.

In a 2D $^{1}H$-$^{1}H$ ROESY NMR spectroscopy experiment carried out on a $CD_3OD$ solution of complex **(±)-66b** room temperature, no interligand NOEs between the allyl protons and the aromatic protons of the substituent at the sulphur are observed, whilst exchange of cross-peaks between the allyl protons are detected in the spectrum indicating the occurrence of a *syn-anti* dynamic process which interconverts these protons.

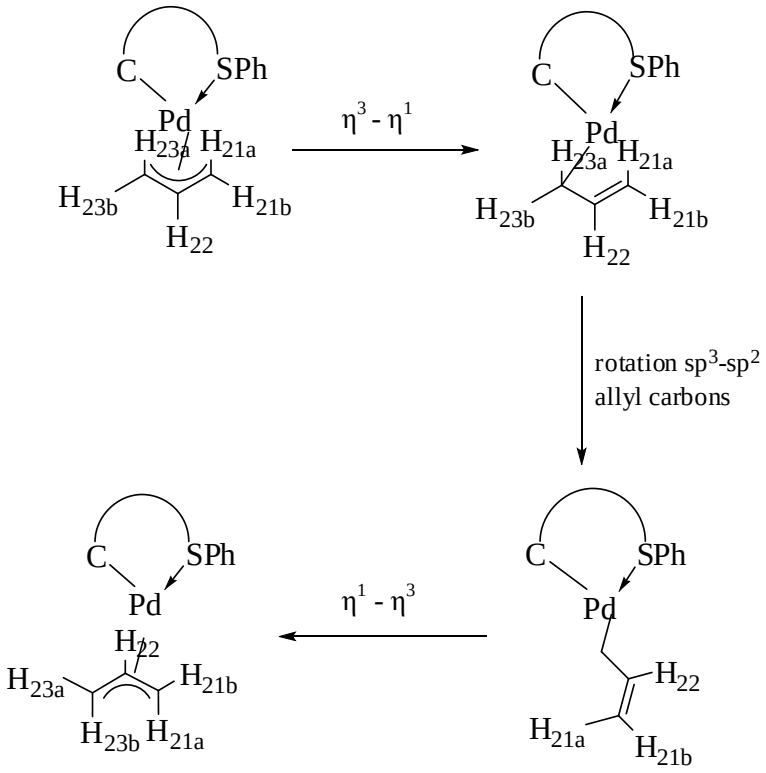


**Figure 2.7** The dynamic behaviour of the complex **(±)-66b** in solution.

As similar to **(±)-66a,** the rigidity of the complex **(±)-66b** were also determined with VT-NMR spectroscopic technique. The Figure 2.8 represents the VT-NMR spectra at low temperatures. The coalescence temperature for complex **(±)-66b** was found to be 263K, where each resonance at this temperature was broaden before any splitting was observed.

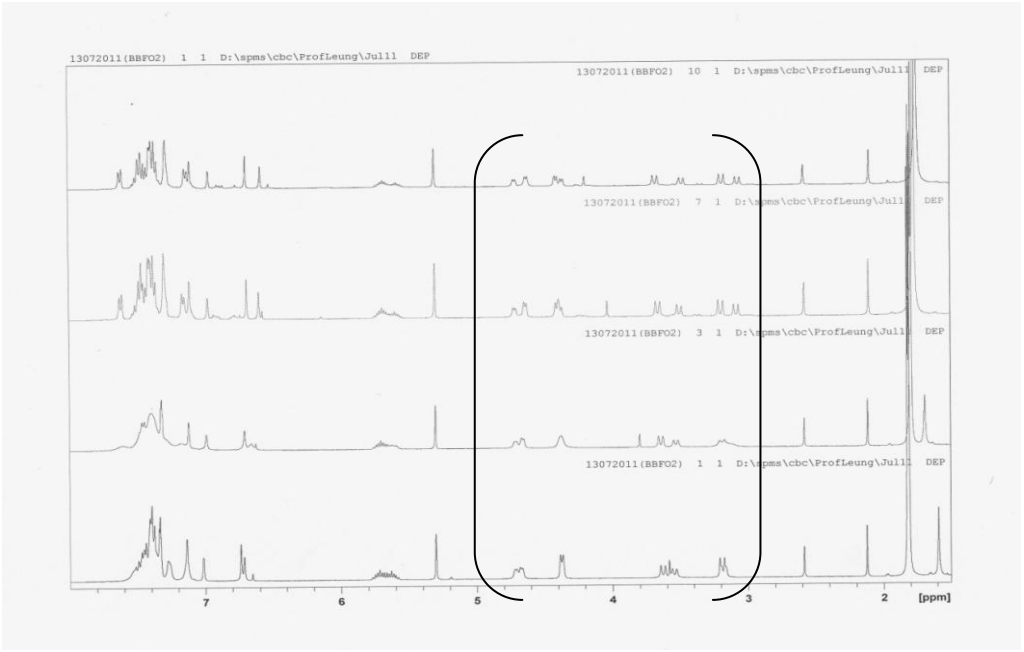


**Figure 2.8** VT NMR of complex **(±)-66b in $CD_2Cl_2$**

Therefore, at lower temperatures the rigidity in CS ring chelate of complex **(±)-66b** was presumably retained during the dynamic process with the inversion of configuration of the sulphur atom.

*2.2.3.4 Ring Conformation of Cyclopalladated Complex **(±)-66c** in Solution*

Unfortunately, suitable crystals for X-ray crystallography were not able to be isolated for this complex in wide range of solvents. Figure 2.9 presents the 2D $^1$H-$^1$H ROESY NMR of complex **(±)-66c** in $CD_3OD$. As similar to **(±)-66b,** the $^1$H NMR data for **(±)-66c**, suggest the existence of two diastereomers (or stable rotamers) in solution as there were two singlet resonances for the $^t$Bu group one for each of the two diastereomers. This indicates the presence of both **(Rs*,S*)-** and **(Rs*,R*)-66c** in solution (or two stable rotamers of **(Rs*,S*)-66c**).

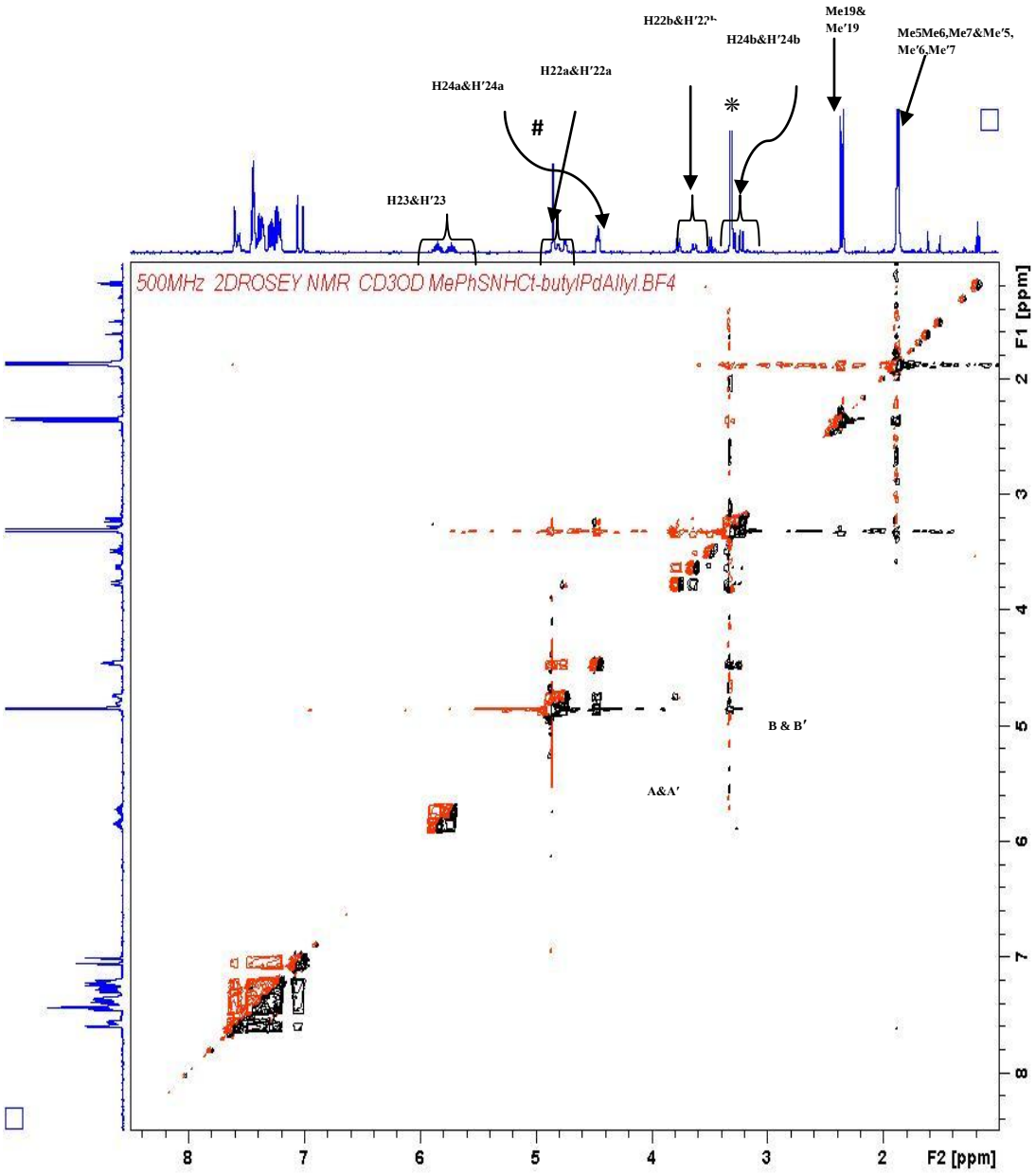


**Figure 2.9** 2D $^{1}$H-$^{1}$H ROESY NMR spectrum of **(±)-66c** in $CD_3OD$.

**Selected NOE signals: (A&A′)**: H22a-H22b; H′22a-H′22b; **(B&B′)**: H24a-H24b; H′24a-H′24b; * $CD_3OD$ solvent peak**; # -** $H_2O$ peak.

From the 2D $^{1}$H-$^{1}$H ROESY NMR spectrum it was not possible to identify the NOE signals in the aromatic region due to the overlap of signals that are attributed by the presence of rotamers. Again, the expected key correlations

between the allyl protons *trans* to NHC with the *p*-tolyl protons on the sulphur substituent were not observed. However, the exchange cross-peaks between the allyl protons were detected. As similar to the previous complexes**,** complex **(±)-66b** undergo fast and selective *syn-anti* exchange of allyl protons (at room temperature) which are *cis* to carbene. In $^{1}$H-NMR spectrum for the complex **(±)-66c,** the allylic proton(H24) *trans* to S appear at 3.2 ppm and signals appear for the allylic protons *trans* to NHC at 4.47 ppm were monitored at various low temperatures in **$CD_2Cl_2$.**

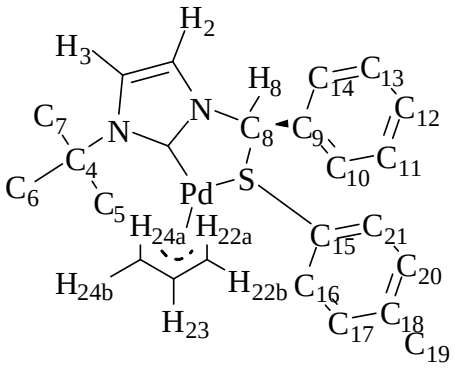


**Figure 2.10**

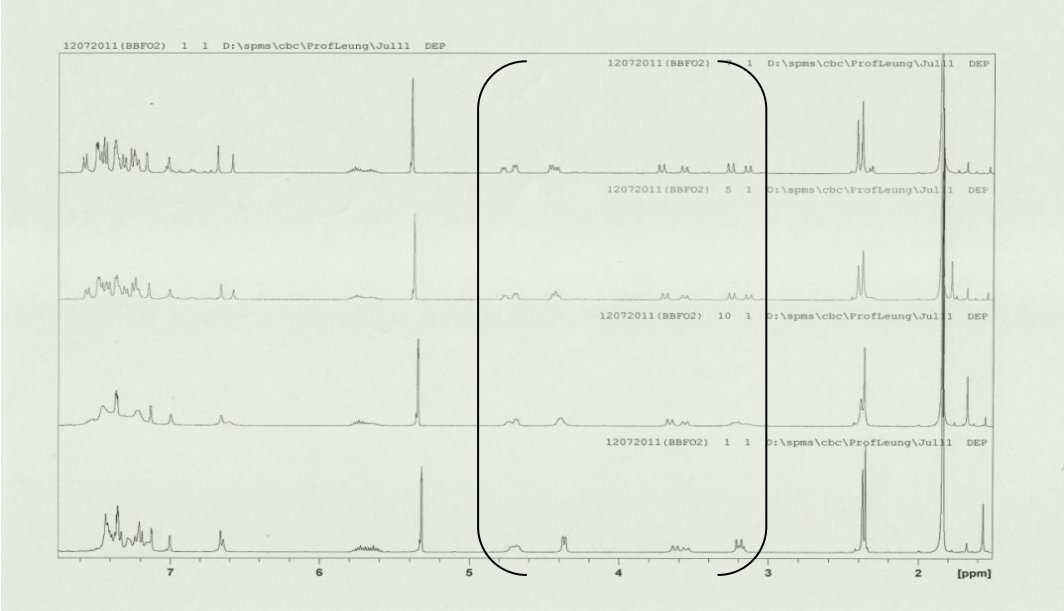


**Figure 2.11** VT $^{1}$H-NMR spectra of complex **(±)-66c in $CD_2Cl_2$**

Figure 2.11 represents the temperature dependence shown by the VT NMR spectra of the complex **(±)-66c** in $CD_2Cl_2$ which are due to configurational exchange. The signals are broaden at coalescence temperature 258K and reforms to other isomer at 193K. Thus the interconversion of isomers which proceed through the process of initial breaking of C22–Pd1 bond with the formation of $\eta^1$-allyl fragment, rotation around the C24–C23 single bond and reformation of the $\eta^3$-allyl complex.

Here again we presume that the rigid of complex **(±)-66c** were retained (either **λ** or **δ**) in solution and the inversion of configuration of sulphur atom that leads to the *cis* disposition of phenyl and *p*-tolyl substituents on the two stereogenic centres i.e., C8 and S1.

*2.2.3.5 Molecular Structure of Cyclopalladated Complex (Ss*,R*)-67b*

The racemic complex **67b** contains the metal chelate ring in **(Rs,S)-67b** and **(Ss,R)-67b** with opposite ring chirality as they are enantiomers. The solid structure of was determined by an X-ray single crystal diffraction study. The yellow coloured single crystals of complex **(Ss*,R*)-67b** were grown by slow diffusion of diethyl ether into an acetonitrile solution at room temperature. The solubility of the complex **(±)-67b** was quite poor and it is soluble only in acetonitrile at elevated temperatures. The molecular structure of **(Ss*,R*)-67b** with the numbering scheme is presented in Figure 2.12. Selected bond lengths and bond angles are listed in Table 2.2.

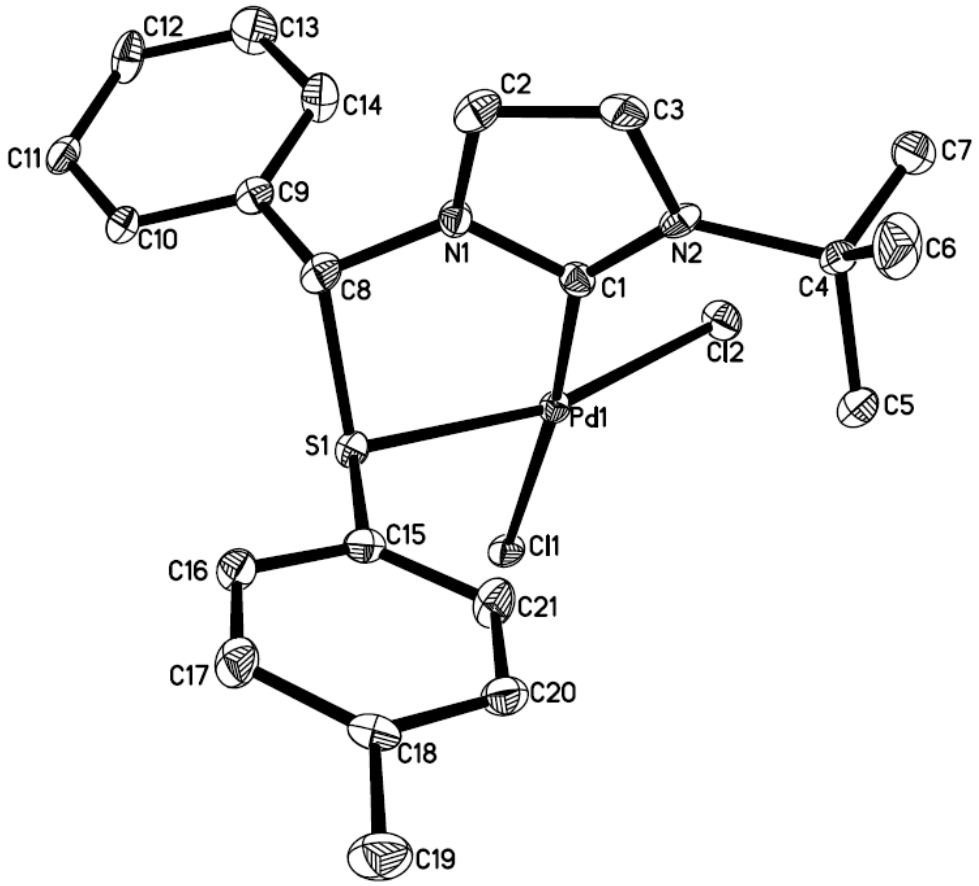


**Figure 2.12** Molecular structure of complex **(Ss*,R*)-67b**; Thermal ellipsoids are drawn at the 50% probability level and hydrogen atoms are omitted for clarity.

In the solid state, the complex **(Ss*,R*)-67b** is arranged in a **δ**-envelope conformation, where the sulphur atom is placed on the lower face of the heterocyclic plane (Figure 2.12). Mostly in the series of sulphur NHC five membered palladacycles obtained so far, the phenyl substituted at α-carbon invariably adopts axial position on account of the lower steric interactions originated by a relative *trans* disposition of the phenyl group at sulphur. The **S** configuration at S as the substituens on sulphur and the α-C adopt the preferred *trans* disposition with **δ** ring conformation. The C(15)–S(1)–C(8)–C(9) torsion angle between the phenyl substituted at the α-carbon and phenyl at the sulphur is 100.6$^{o}$.

The coordination geometry of palladium(II) complex exhibits the square-planar geometry, with a $C_{carbene}$-Pd bond distance of 2.030 Å along with a bite angle of C(1)–Pd(1)–S(1) 82.55$^{o}$. The stronger *trans* influence of the carbene compared to the sulphur donor is illustrated by a Pd(1)–Cl(1) [2.3608 Å] bond longer than Pd(1)–Cl(2) [2.3385 Å]. Selected bond lengths and bond angles of palladium complex **(Ss*,R*)-67b** are listed in Table 2.2 as shown below.

**Table 2.2 Selected bond lengths (Å) and angles ($^{o}$) of Palladium complex (Ss*,R*)-67b:**

| | | | |
|---|---|---|---|
| Pd(1)–C(1) | 1.995(4) | N(2)–C(1)–Pd(1) | 140.6(3) |
| Pd(1)–S(1) | 2.2678(12) | Cl(1)–Pd(1)–Cl(2) | 92.12(4) |
| Pd(1)–Cl(1) | 2.3608(11) | N(1)–C(8)–S(1) | 106.5(3) |
| Pd(1)–Cl(2) | 2.3385(12) | C(9)–C(8)–N(1) | 115.3(4) |
| S(1)–C(8) | 1.847(5) | C(1)–Pd(1)–S(1) | 82.55(13) |
| N(1)–C(8) | 1.455(6) | C(8)–S(1)–Pd(1) | 95.73(16) |
| C(1)–N(1) | 1.368(6) | C(9)–C(8)–S(1) | 110.3(3) |
| C(1)–N(2) | 1.349(6) | C(15)–S(1)–Pd(1) | 111.19(16) |
| N(1)–C(1)–N(2) | 104.9(4) | S(1)–C(8)–H(8) | 108.2 |

*2.2.3.6 Ring Conformation of Cyclopalladated Complex (±)-67b in Solution*

The conformation of the complex **(±)-67b** in solution was examined by 2D $^{1}$H–$^{1}$H ROESY NMR techniques. The assignment of proton peaks was obtained from the combination of COSY, HMQC and HMBC NMR spectra.

Figure 2.13 presents the 2D $^{1}H–^{1}H$ ROESY NMR spectrum for **(±)-67b** in $CD_3CN$.

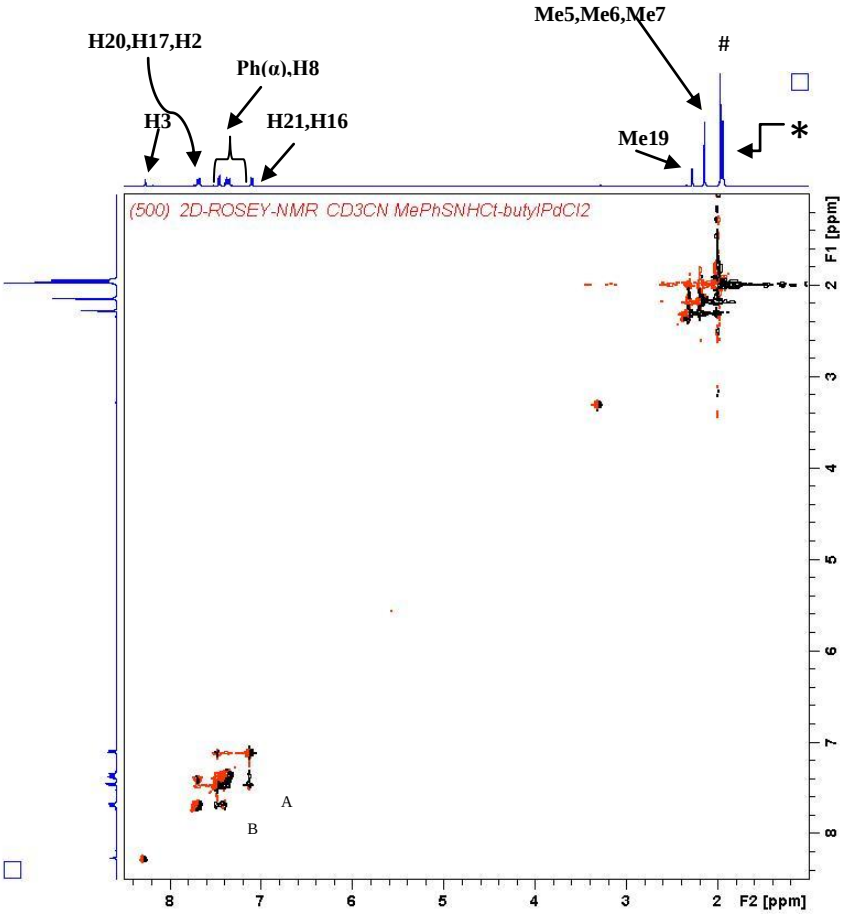


**Figure 2.13** 2D $^{1}H–^{1}H$ ROESY NMR spectrum of **(±)-67b** in $CD_3CN$.

**Selected NOE signals: (A)**: H16–H8; **(B)**: H8–H2; * $CD_3CN$ solvent peak; # $H_2O$ peak;

In 2D $^{1}H–^{1}H$ ROESY NMR spectrum of complex **(Ss,R)-67b**, two strong NOE signals (A, B) were clearly recorded; (A) the interactions between H8 and H16, (B) the interactions of H8 with H2. These interactions confirm the existence of **δ**-ring conformation of complex **(Ss,R)-67b** with the phenyl at the axial position.

On the other hand, the non-existence of **(Ss,S,λ)-67b** ring conformer was confirmed with the absence of NOE signals of Ph(α) with *p*-tolyl. As a result the

existence of the five membered CS chelate in the **δ** ring conformation with a *trans* disposition of the phenyl and *p*-tolyl substituents on the two stereogenic centres C8 and S1, respectively, a single diastereomer **(Ss,R,δ)-67b** exists in solution.


**Figure 2.14** Absolute conformation of the PdCS ring

*2.2.3.7 Molecular Structure of Cyclopalladated Complex (Rs*,S*)-67c*

The molecular structure of the complex **(Rs*,S*)-67c** was determined by single crystal X-ray diffraction study. The yellow coloured crystals with a size of 0.36 x 0.34 x 0.12 $mm^3$ of complex **(Rs*,S*)-67c** were grown from a mixture of acetonitrile/diethyl ether solution at room temperature. The molecular structure with the numbering scheme is presented in Figure 2.15. Selected bond lengths and bond angles are listed in Table 2.3.

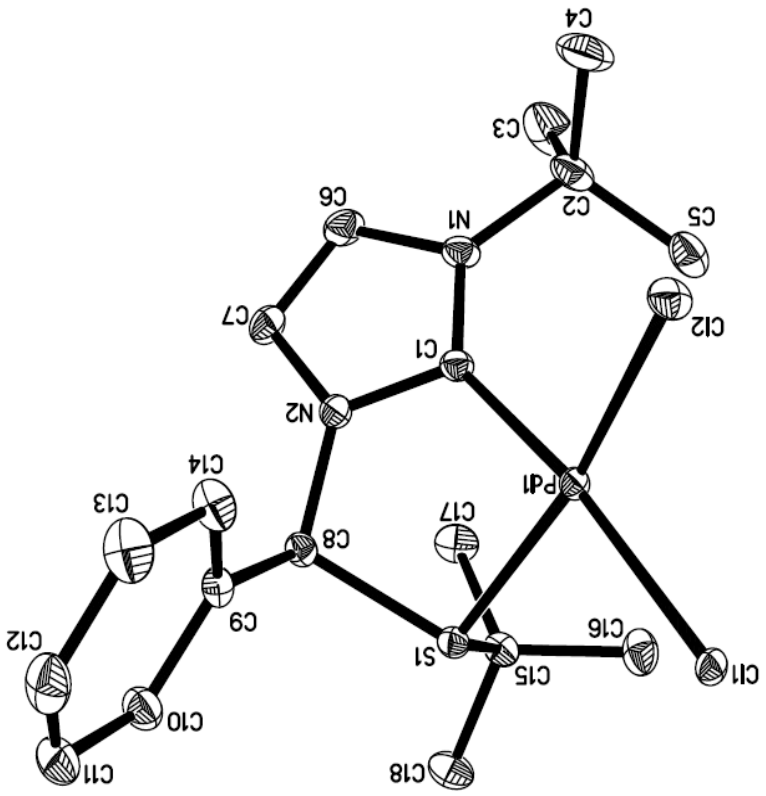


**Figure 2.15** Molecular structure of complex **(Rs*,S*)-67c**; Thermal ellipsoids are drawn at the 50% probability level and hydrogen atoms are omitted for clarity.

In solid state, the phenyl substituted at C8 and $^{t}$Bu group at sulphur are placed in axial positions with the $^{t}$Bu substituent projecting above the heterocyclic plane because of relative *trans* disposition, resulting in a five-membered chelate ring, with an **λ**-envelope conformation (Figure 2.15). Upon coordination to the palladium(II) centre, the **R** configuration at sulphur atom is a consequence of the high steric bulk of this group forces a perpendicular arrangement with respect to the coordinating PdCS plane in order to minimize steric interactions. The C(9)–C(8)–S(1)–C(15) torsion angle between the phenyl substituted at α-carbon and $^{t}$Bu is 106.04$^{o}$. The longer Pd–Cl(1) bond [2.3842 Å] *trans* to the carbene compared to Pd–Cl(2) [2.3513 Å] reflects its strong trans-

influence effect of NHC compared to sulphur. The complex exhibits the expected square-planar geometry, with a $C_{carbene}$-Pd bond distance of 1.9776 Å.

**Table 2.3 Selected bond lengths (Å) and angles (°) of Palladium complex (Rs*,S*)-67c:**

| | | | |
|---|---|---|---|
| Pd(1)–C(1) | 1.9776(13) | N(1)–C(1)–N(2) | 105.32(11) |
| Pd(1)–S(1) | 2.2573(3) | N(2)–C(8)–C(9) | 115.77(11) |
| Pd(1)–Cl(1) | 2.3842(3) | C(1)–Pd(1)–S(1) | 82.32(4) |
| Pd(1)–Cl(2) | 2.3513(3) | C(15)–S(1)–Pd(1) | 110.38(4) |
| C(1)–N(1) | 1.3528(17) | C(1)–N(2)–C(8) | 122.07(11) |
| C(1)–N(2) | 1.3668(17) | C(1)–Pd(1)–Cl(2) | 94.96(4) |
| C(8)–S(1) | 1.8416(13) | C(9)–C(8)–S(1) | 107.96(9) |
| C(8)–N(2) | 1.4547(17) | S(1)–Pd(1)–Cl(1) | 89.244(12) |
| N(2)–C(1)–Pd(1) | 115.18(9) | C(15)–S(1)–C(8) | 106.04(6) |

*2.2.3.8 Ring Conformation of Cyclopalladated Complex (±)-67c in Solution*

From a single crystal X-ray analysis it is well established that in solid, state the five membered palladacycle **(Rs*,S*)-67c** adopts **λ** ring conformation. The rigidity of the CS ring chelate in solution state was determined by 2D $^1$H–$^1$H ROESY NMR technique. The assignment of proton peaks was obtained by a combination of COSY, HMQC and HMBC NMR spectra. Figure 2.16 presents the 2D $^1$H–$^1$H ROESY NMR spectrum for **(±)-67c** in $(CD_3)_2SO$. Figure 2.17

presents the absolute conformation of the cyclopalladated complex **(±)-67c** and selected chemical shifts of the complex are given in Table 2.4.

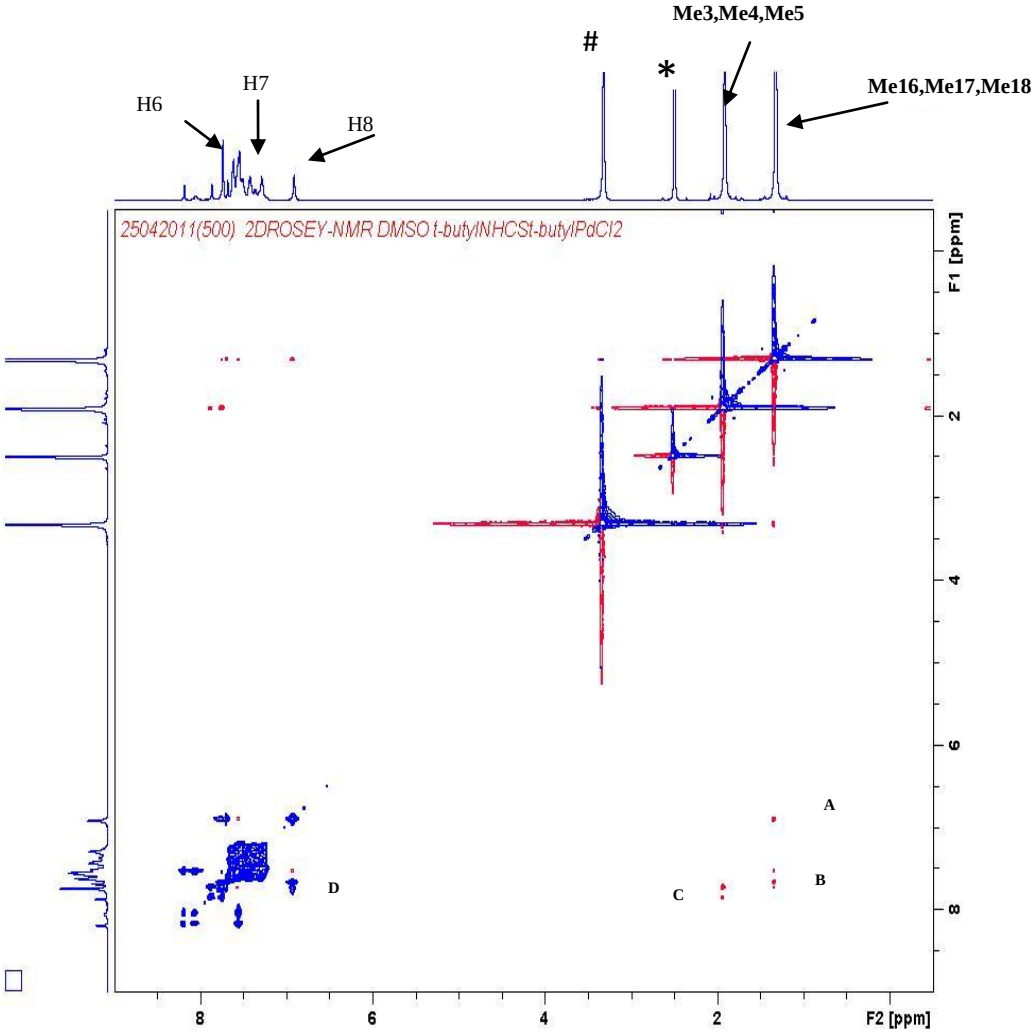


**Figure 2.16** 2D $^{1}H$–$^{1}H$ ROESY NMR spectrum of **(±)-67c** in $(CD_3)_2SO$.

**Selected NOE signals**: **(A)**: Me16/Me17/Me18 – H8; **(B)**: Me16/Me17/Me18 – H7; **(C)**: Me2/ Me3/ Me4– H6; (**D)**: H8 – Ph(α); ***** $(CD_3)_2SO$ solvent peak; **#** $H_2O$ peak.

In solution state the five membered thioether NHC palladacycle adopts **λ** ring conformation. Here in the phenyl group on the α-carbon takes up the axial position below the plane of the PdCS ring. The *trans* axial disposition of the phenyl substituent is due to the repulsive interaction with $^{t}$Bu substituent on the

sulphur. In 2D $^{1}H–^{1}H$ ROESY NMR spectrum, a strong NOE signal (C) was observed for the interactions between Me2/Me3/Me4 – H6 and signals (A) & (B) seen are due to the NOE interaction between Me16/Me17/Me18 with H8 as well as H7. Moreover, the absence of NOE signals of the phenyl substituent on the α-carbon with Me16/Me17/Me18 of sulphur atom completely rules out a **(Rs,R,δ)-67c** ring conformation.

As a result the sulphur atom were locked stereochemically in **R** configuration with non-equivalent axial ($^{t}$Bu group) and equatorial (lone pair) positions and hence in agreement with the **λ** ring conformation. Consequently, the existence of the five membered CS chelate in the **λ** ring conformation with a trans disposition of the phenyl and $^{t}$Bu substituents on the two stereogenic centers C8 and S1, respectively, as a single diastereomer in solution.

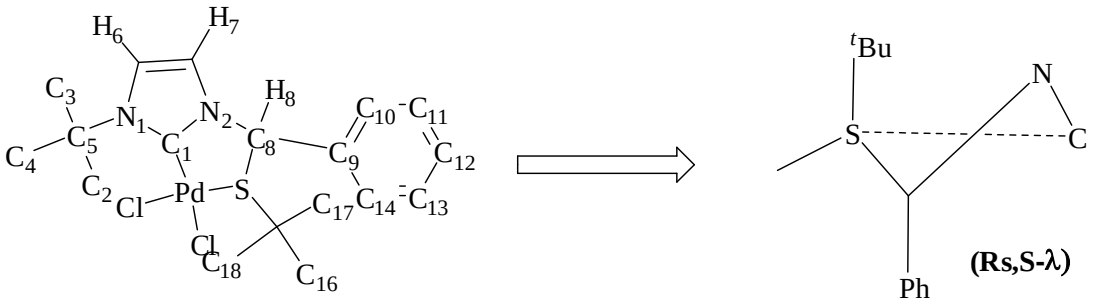


**Figure 2.17** Absolute conformation of the PdCS ring.

**Table 2.4** Selected chemical shifts for **(±)-67c** in $(CD_3)_2SO$

| **Proton** | **δ(ppm)** |
|---|---|
| Me3/Me4/Me5 | 1.92(s) |
| Me16/Me17/Me18 | 1.32(s) |
| H7 | 7.74(s) |
| H8 | 6.91(s) |
| Ph | 7.27–7.68(m) |

## 2.3 CATALYTIC STUDIES ON ALLYLIC AMINATION REACTION

After obtaining insights into the coordination behaviour of sulphur in palladium(II) complexes from the aforementioned solid and solution state structural studies, an investigation was undertaken to access their performances in catalytic allylic amination. The allylation of 1-phenylethanamine was chosen as a model reaction (Scheme 2.10). All the experiments were carried out under the same experimental conditions, in dry THF with 1 equivalent of allylic alcohol and 3 equivalent of amine using 5 mol% of catalyst.

In the first series of experiments, catalytic amounts (5 mol %) of complexes **67b** and **67c**, in the reaction of cinnamyl alcohol (1 equiv) with (±) 1-phenylethanamine (3 equiv) were used in acetonitrile (1 mL) at room temperature. Presumably the racemic amine was used in these preliminary studies. After 15 h, there were no significant spots on the TLC, therefore the reaction temperature was raised to 50$^{o}$C for 6 h, and subsequently to 80$^{o}$C for 5 h, but there was no product formation detected by TLC. Hence, the substrate was changed from the allylic alcohol to the corresponding carbonate, as the latter was expected to be the superior leaving group. As a result, the new model reaction was performed with cinnamyl ethylcarbonate (1 equiv) and 1-phenylethanamine (3 equiv) in acetonitrile (1 mL) using (5 mol %) of complexes (±)-**67b** and (±)-**67c** at 50$^{o}$C followed by 80$^{o}$C, however, once again no product was detected.

Zhang *et al.*[96] had observed that the catalytic reactivity of the NHC based palladacycles was greatly improved by replacing the two coordinating halides with weakly coordinating ligands such as acetate groups. The use of silver salts

in the model reaction (Scheme 2.10) was subsequently investigated where the dichloro groups in complex **67c** and **67b** were substituted with weakly coordinating ligands in the presence of different silver salts. The newly formed catalysts were generated in situ by treating the dichloropalladium complex **(±)-67b** and **67c** (entries 1 to 8) with 2 molar equivalents of different silver salts so as to replace the chlorides with the corresponding weakly coordinating ligands for an hour prior to the addition of the catalysis substrates. However, after screening through different silver salts and at different temperatures as seen in Table 2.5, the reactivity of the catalysts remained unchanged and no product spots was observed by TLC, rather they gave rise to an intractable dark reaction mixture at higher temperature that may arise due to decomposition induced by AgX-promoted thioether cleavage.[97]

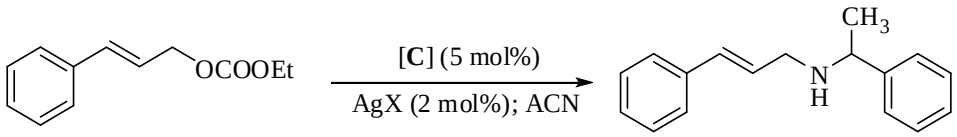


**Scheme 2.10**

**Table 2.5** Screening of neutral palladium(II) complexes

| Entry | [C] | Additive | Time(h) | Temp.($^{o}$C) | Conv. (%) |
|---|---|---|---|---|---|
| 1 | 67b | $AgBF_4$ | >24 | 50–80 | No rxn[b] |
| 2 | 67b | $AgPF_6$ | >24 | 50–80 | No rxn[b] |
| 3 | 67b | $AgSbF_6$ | >24 | 50–80 | No rxn[b] |
| 4 | 67b | $AgOOCCF_3$ | >24 | 50–80 | No rxn[b] |

| | | | | | |
|---|---|---|---|---|---|
| 5 | 67c | $AgBF_4$ | >24 | 50–80 | No rxn[b] |
| 6 | 67c | $AgPF_6$ | >24 | 50–80 | No rxn[b] |
| 7 | 67c | $AgSbF_6$ | >24 | 50–80 | No rxn[b] |
| 8 | 67c | $AgOOCCF_3$ | >24 | 50–80 | No rxn[b] |

[b]Determined by TLC. [c]Reaction condition: 0.242 mmol of cinnamyl ethyl carbonate, 0.727 mmol of (±)-1-phenyl ethanamine, 0.012 mmol of [C], 0.024 mmol of Ag salts[entries 3 to 10], acetonitrile (2 mL).

In a second series of experiments, the model reaction was attempted with racemic complex **66a** in dry THF at room temperature. A new spot on the TLC plate was observed along with starting material. Hence, the temperature of the reaction was raised to 50$^{o}$C, where the reaction proceeded smoothly with full conversion in 15 h without the need for any additives.

**Screening of catalysts:**

With the optimized conditions in hand, the investigation on racemic substituted thioether functionalized NHC cationic palladium complexes **66a, 66c, 66d** catalyzed allylic amination was initiated using the cinnamyl ethyl carbonate (1 equiv) and (±)-1-phenylethanamine (3 equiv) in THF (2 mL). The results are summarized in Table 2.6.

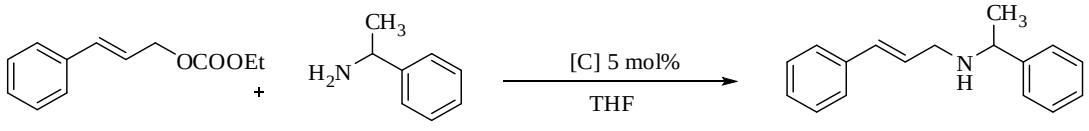


**Scheme 2.11**

**Table 2.6** Screening of cationic palladium(II) complexes

| Entry | [C] | Additive | Time(h) | Temp($^o$C) | Conv. (%)[d] |
|---|---|---|---|---|---|
| **1** | **66a** | **NIL** | **15** | **50** | **96[a]** |
| 2 | 66c | NIL | 15 | 50 | 79[a] |
| 3 | 66d | NIL | 15 | 50 | 75[a] |

[a]Determined by $^1$H-NMR spectroscopy, contains both the bis(allyl) and mono(allyl) products [c]Reaction condition: 0.242 mmol of cinnamyl ethyl carbonate, 0.727 mmol of (±)-1-phenylethanamine, 0.012 mmol of [**C**], at 50$^o$C. [d]After the reaction time indicated, compounds were worked-up and conversions were determined after isolation through silica gel column chromatography.

It was established from these studies that the racemic complexes **66a, 66c, 66d** all promoted the allylic amination reaction giving products in moderate to high yields. The best yields were obtained using (±)-**66a** and it also proved to the most stable to air and moisture and in array of solvents. The NMR spectral characteristics of the complex (±)-**66a** are in agreement with those reported in the literature for similar complexes with sulphur bidentate NHC ligands.[63, 64]

**Scope of the leaving group:**

In the preliminary reaction screening, cinnamyl ethyl carbonate was used as it is proved to be good leaving group. We further investigated the reactivity of complex **(±)-66a** using the alternative leaving groups such as OH, OMe, OAc and the results are summarized in Table 2.7.

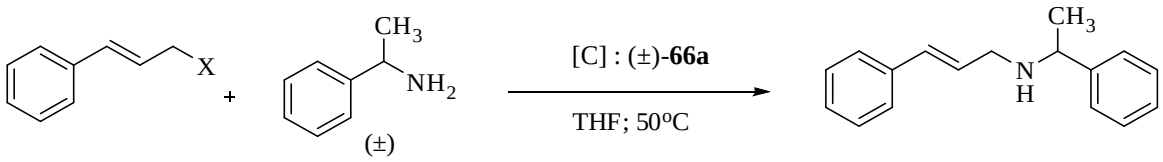


**Scheme 2.12**

**Table 2.7** Screening of leaving group

| Entry | X | [C] mol% | Time(h) | Conv. (%)[a] |
|---|---|---|---|---|
| 1 | OH | 5 | >24 | No rxn |
| 2 | OMe | 5 | >24 | 28 |
| 3 | OAc | 5 | 15 | 86 |
| **4** | **OCOOEt** | **5** | **15** | **96** |

[a]Determined by 1H-NMR spectroscopy; contains both the bis(allyl) and mono(allyl) products [c]Reaction condition:0.242 mmol of [X], 0.727 mmol of (±)-1-phenylethanamine, 0.012 mmol of [**C**], at 50$^{o}$C.

No conversion was observed with the hydroxyl leaving group (entry 1) and up to 30% for OMe (entry 2) with longer reaction time. Conversely, OAc (entry 3) was found to be as good as carbonate only with slight difference in yield. Therefore, it was concluded that the ethyl carbonate group would be a suitable leaving group for a wide range of allylation reactions involving amines.

**Optimization of catalyst loading:**

Having confirmed from our model reaction study that 5 mol% of catalyst loading leads to the complete conversion of allylation within 15 h and the next goal was to lower the catalyst loadings to levels comparable with the pyridine-NHC complex **61** as reported by Chianese *et al.*[98] (2.5 mol%, 24 h at 60$^{o}$C). Investigations were therefore performed to evaluate the efficiency of the amination reaction using catalyst loadings of 5, 2, 1, and 0.5 mol% (Scheme 2.13).

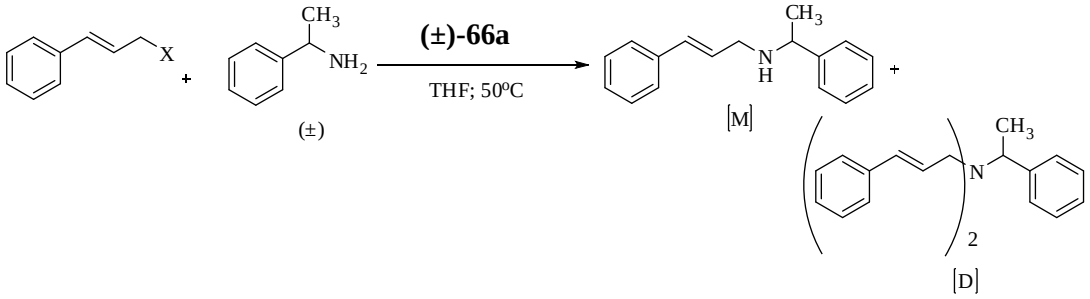


**Scheme 2.13**

**Table 2.8** Optimization of catalyst loading

| Entry | [C][b]mol% | Time (h) | Conv.(%)[a] [M+D] |
|---|---|---|---|
| 1 | 5 | 15 | 96 |
| **2** | **2** | **24** | **95** |
| 3 | 1 | 24 | 83 |
| 4 | 0.5 | >24 | 37 |

[a]Isolated yield[M+D] products.{M= monoallylation; D= bis-allylation}.[b]Reaction condition: 0.242 mmol of cinnamyl ethyl carbonate, 0.727 mmol of (±)-1-phenylethanamine, **(±)-66a** (5 mol%, 0.012 mmol; 2 mol%, 0.005 mmol; 1 mol%, 0.002 mmol; 0.5 mol%, 0.001 mmol), THF (2 mL) at 50°C. After the reaction time indicated, compounds wereworked-up and conversions were determinedafter isolation through silica gel column chromatography.

From the results obtained and summarized in Table 2.8, the best loading factor was found to be with 2 mol% of catalyst and in terms of yield when compared with 1 mol% and 0.5 mol%, although the reaction time was quite long compared to 5 mol%. The reaction was incomplete for 0.5 mol% loading, giving only 37% conversion of the amine product.

**Regioselectivity of the reaction:**

For the regioselective allylic amination reactions, pioneering work has been done by Hayashi and Ito with butenyl acetate as the single substrate.[99]

However, the origin of the regioselectivity of monosubstituted substrates in palladium catalyzed reaction remains to be unravelled.

In order to determine the regioselectivity of allylic amination reaction using the catalyst (±)-**66a**, a model study was undertaken with γ- methyl and γ- phenyl substituted carbonates such as (*E*)-but-2-enyl ethyl and cinnamyl ethyl carbonates (entries 1 and 2 in Table 2.9) and optimized catalytic conditions.

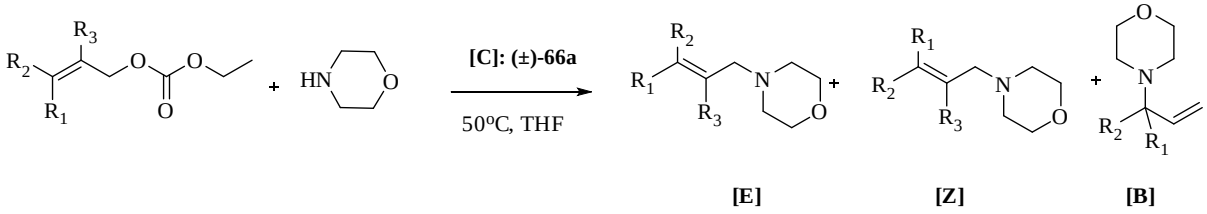


**Scheme 2.14**

**Table 2.9** Reaction of γ-substituted allyl carbonates with morpholine

| Entry | $R_1$ | $R_2$ | $R_3$ | Time (h) | Conv.(%)[a] [E/Z/B] | [Yield][b] |
|---|---|---|---|---|---|---|
| 1 | Me | H | H | 15 | 82/17/0(99%) | 98% |
| 2 | Ph | H | H | 15 | 99/0/0(99%) | 98% |

[a]Determined by $^1$H-NMR spectroscopy; **E**: trans isomer; **Z**:cis isomer; **B**: branched isomer. Reaction condition: 0.242 mmol of cinnamyl ethyl carbonate, 0.727 mmol of primary/secondary amines, 0.0048 mmol of (±)-**66a**, THF (2 mL) at 50°C. After the reaction time indicated, compounds were worked-up and [b]yield conversions were determined through silica gel column chromatography.

The (*E*)-but-2-enyl ethyl carbonate (entry 1) on amination gave exclusively linear products with 80:20 *trans:cis* isomers without any trace of the branched isomer. However, in the case of cinnamyl ethyl carbonate (entry 2) isomerisation of *trans/cis* was not observed, along with absence of the branched isomer and both were confirmed from the $^1$H-NMR spectrum; for entry 2 a

doublet with a coupling of 16 Hz appeared in range of 6.5–6.55 ppm for Ha (trans coupling); and a sextuplet with a coupling of 6 Hz in range of 6.2-6.3 ppm; followed by a doublet with a coupling of 6 Hz in range of 3.14–3.16 ppm contributing from the two Hc (Figure 2.18).

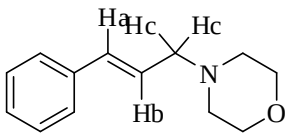


**Figure 2.18** (E)-cinnamylmorpholine

The product obtained from the above two γ- methyl and γ- phenyl carbonates (entries 1 & 2), proved that the $\eta^3$-allyl palladium intermediate retains the memory of a leaving group position and gave exclusively linear product.

The regioselectivity is determined by the attack of nucleophile on the π-allyl intermediate amongst of all four diastereomers which equilibrates rapidly under the catalytic conditions as described in Figure 2.19.

Hence, during the catalytic cycle, it is apparent that the orientation of the $R_1$ (Me/Ph) substituted π-allyl intermediate ought to be strongly controlled by the thioether functionalized NHC ligand in a bidentate fashion and consequently, they should be positioned away from the sulphur moiety which leads to the formation of linear product over branched one.

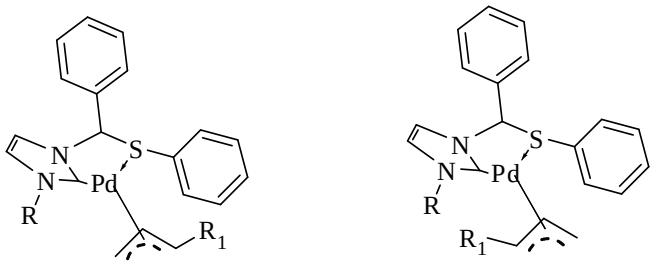


**syn isomer**

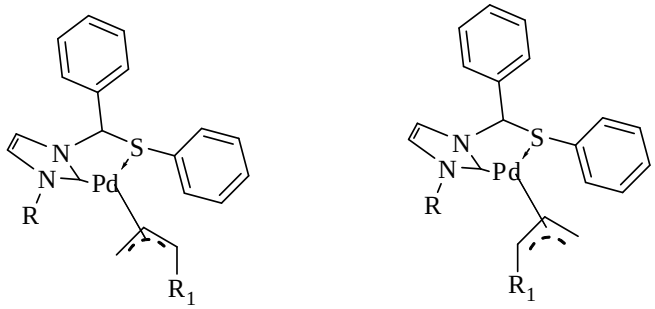


**anti isomer**

**Figure 2.19**

Generally, in allylic substitution reaction catalyzed by heterobidentate palladium species, the nucleophile attacks the Pd-$\eta^3$-allyl species in *trans* position to the higher trans-effect substituent,[100] and in our case, the NHC carbene imposes a higher trans effect when compared to sulphur.

Hence, from our observations and results obtained we wish to put-forward that the regioselectivity of our reaction is possibly due to the following factors,

a) Thioether functionalized NHC ligand slow down the rate of racemization of substituted π-allyl intermediate which leads to favored linear product.
b) Higher *trans* effect of N-heterocyclic carbenes as compared to sulphur favored linear product.

**Substrate scope of aliphatic amines:**

A wide range of both primary and secondary aliphatic amines with cinnamyl carbonate substrate were investigated (Scheme 2.15) and all reactions provided the linear products in a highly regioselective manner by means of 2 mol% of catalyst **(±)-66a** at 50$^{o}$C and the results are summarized in **Table 2.10**

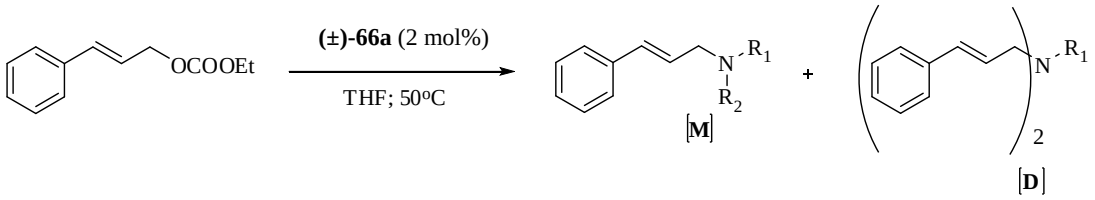


**Scheme 2.15**

**Table 2.10** Reaction of amines with (E)-cinnamyl carbonate

| Entry | Amine | Time(h) | Conv.(%)[a] [M/D] |
|---|---|---|---|
| 1 | 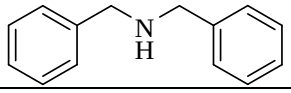 | 24 | 93/nil |
| 2 | 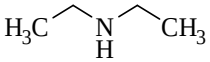 | 15 | 82/nil |
| 3 | 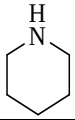 | 20 | 98/nil |
| 4 | 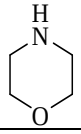 | 15 | 98/nil |

| | | | |
|---|---|---|---|
| 5 | 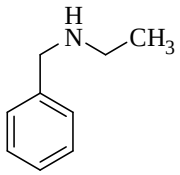 | 15 | 92/nil |
| 6 | 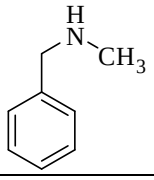 | 20 | 80/nil |
| 7 | 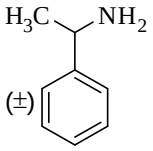 | 24 | 88/7(95) |
| 8 | 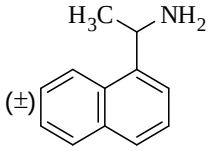 | 24 | 69/5(74) |
| 9 | 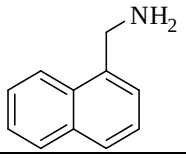 | 20 | 50/18(68) |
| 10 | 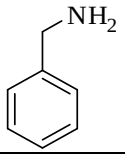 | 24 | 42/28(70) |

M = monoallylation; D = bisallylation**.**Reaction condition: 0.242 mmol of cinnamyl ethyl carbonate, 0.727 mmol of primary/secondary amines, 0.0048 mmol of (±)-**66a**, THF (2 mL) at 50$^{o}$C. After the reaction time indicated, compounds were worked-up and [a]yield conversions were determined through silica gel column chromatography.

From the results summarized in Table 2.10, moderate to high yields were obtained for allylation of secondary amines (entries 1, 2, 3, 4, 5, 6) compared to that of primary amines. Owing to longer reaction time for amines (entries 7, 8, 9, 10), the cinnamyl ethyl carbonate tends to hydrolyze to the corresponding alcohol which was subsequently recovered after column purification. This may be one of the reasons for the lower yield and another possible reason may be due to poor solubility of amines (entries 8, 9) in THF.

The scope and limitations of aliphatic primary amines (Entries 7-10) in these allylic amination reactions were also investigated in this work. The reaction of naphthalen-1-ylmethanamine and phenylmethanamine (entries 9 & 10) under optimized conditions gave higher percentage of bis-allylation product when compared to 1-phenylethanamine and its 1-(napththalene-1-yl)ethanamine counterparts (entries 7 and 8), and thus, explained the effect of basicity of amines.

Furthermore, all (*E*)-cinnamyl allyl amines gave a similar $^{1}$H-NMR spectrum; a doublet with a coupling range of 16 Hz appeared in range of 6.5 ppm for Ha (trans coupling); and a sextuplet with a coupling of 6 Hz in range of 6.2–6.3 ppm; followed by a doublet with a coupling of 6 Hz in range of 3.14–3.16 ppm contributing from the two Hc (Figure 2.18) pointing out that *trans* linear product was obtained from *trans* substrate, with full stereoretention.

The achiral allylic amination method described here using catalyst **(±)-66a** without any activator is restricted to aliphatic primary/secondary amines and on the other hand not suitable for aromatic amines owing to their low nucleophilicity.

**Substrate scope of allylic carbonates:**

After results obtained from studies on the substrate scope of primary and secondary aliphatic amines towards allylic amination reaction, the same reaction under optimized conditions was performed using various α/γ mono and di substituted carbonates with morpholine (Scheme 2.16). Morpholine was used as a standard amine during the entire course of substrate studies on allylic carbonates in order to attain a clear picture of regio selective mechanism and

thereby avoiding the bis-allylation. As to our expected, the reaction proceeded smoothly and allowed for complete conversion (except entry 6) with the formation of regioisomers which again agreed with the controlled racemiziation of π-allyl intermediate species by the NHC-sulphur bidentate chelate.

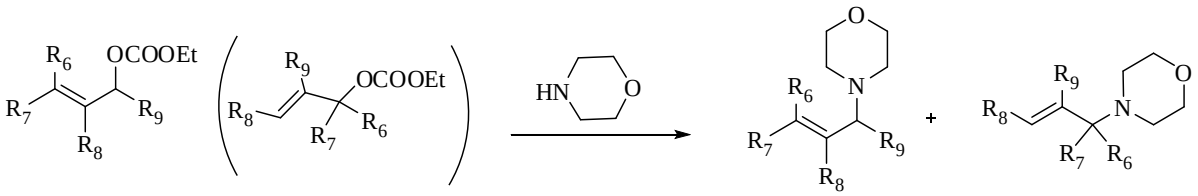

**Scheme 2.16**

**Table 2.11** Reaction of morpholine with various allylic carbonates

| Entry | Allylic carbonates | Linear Product (*trans*) | Linear Product (*cis*) | Branch Product | Time (h) | Conv. (%)[a] [E/Z/B] | Yield (%) |
|---|---|---|---|---|---|---|---|
| 1 | 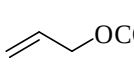 | 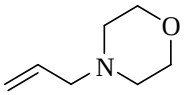 | NIL | NIL | 15 | 99/0/0 | 98[b] |
| 2 | 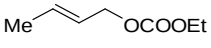 | 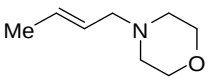 | 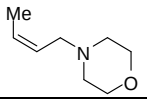 | NIL | 15 | 82/17/0 | 98[b] |
| 3 | 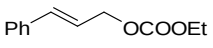 | 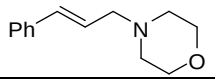 | NIL | NIL | 15 | 99/0/0 | 98[b] |
| 4 | 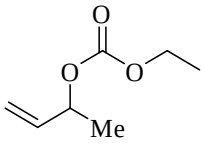 | 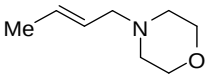 | 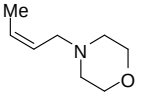 | 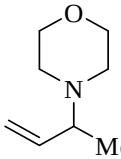 | 15 | 47/20/32 | 90[a] |

| | | | | | | | |
|---|---|---|---|---|---|---|---|
| 5 | 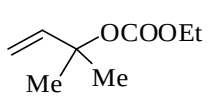 | 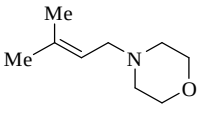 | NIL | 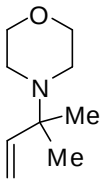 | 96 | 70/0/29 | 68[a] |
| 6 | 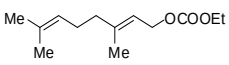 | 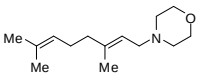 | NIL | NIL | 24 | 50/0/0 | 50[c] |
| 7 | 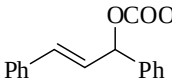 | 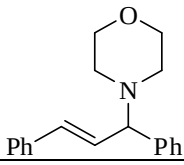 | NIL | NIL | 15 | 99/0/0 | 95[a] |

[a]Determined by $^1$H-NMR spectroscopy; **E**: trans isomer; **Z**:cis isomer; **B**: branched isomer. Reaction condition: 0.242mmol of α/γ substituted carbonates 0.727 mmol of primary/secondary amines, 0.0048 mmol of (±)-**66a**, THF (2 mL) at 50$^o$C. After the reaction time indicated, compounds were worked-up and [b]yield conversions were determined through silica gel column chromatography. [c]0.012 mmol of (±)-**66a** were used.

From the results summarized in Table 2.11, the reaction of allyl ethyl carbonate (entry 1) proceeded in similar manner to that of γ-phenyl substituted carbonate (entry 3) with full conversion under optimized conditions (2 mol%, cat **(±)-66a**, 50$^o$C, THF). The γ-methyl substituted carbonate (entry 2) (contains 20% of cis isomer) also allowed full conversion to allylated products with *trans*/*cis* ratio (4:1) devoid of any branched isomer. From this result, we conclude that the *trans* substrate ionized initially to a syn-[Pd($\eta^3$-alkenyl)] complex which then preferentially leads to the formation of *trans* linear product. Similarly the formation of *cis* linear product should be ideally obtained from the anti-[Pd($\eta^3$-alkenyl)] complex.

However, when α-substituted allylic carbonate (entry 4) and highly branched α,α-disubstituted (entry 5) were used, two sets of allylated products were obtained with moderate regioselectivity. Unlike γ-methyl substituted carbonate

(entry 2)**,** the regioselectivity for these two carbonates was not good yielding linear/branched isomer almost in the ratio 7:3. To explicate the result showed on table 2.11 (entry 4 & 5), the ratios of the product distribution conclude that the branched substrate is expected to ionize partially to an anti-[Pd($\eta^3$-alkenyl)] and syn-[Pd($\eta^3$-alkenyl)] complex which leads to the formation *cis* and *trans* linear products. Notably, branched product arises primarily from anti-[Pd($\eta^3$-alkenyl)] intermediate, with a moderate regioretention, i.e., intermediate Pd–allyl complex retains a "memory" of the position of the leaving group for the nucleophile to attack the carbon that originally carried the leaving group, beyond the inherent reactivity difference between *syn* and *anti* complexes as explained in Figure 2.20.

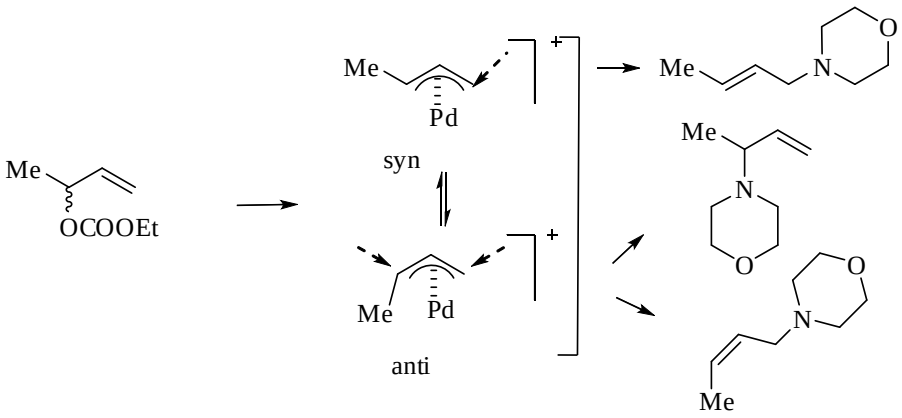


**Figure 2.20** Memory effect of $\eta^3$–allylPd complex

The reaction time for highly branched α,α-disubstituted allylic carbonate (entry 5) was longer compared to α-substituted allylic carbonate (entry 4) and this can be explained in terms of steric factors. Allylation of morpholine with (E)-1,3-diphenylallyl ethyl carbonate (entry 7) proceeded smoothly under standard optimized conditions.

The γ,γ-disubstituted allylic carbonate (entry 6) gave exclusively linear product with 5 mol% of catalyst **(±)-66a** with lower yield. Initially, we carried out the reactions (entry 6) with usual 2 mol% of catalyst, however, even after 72 h, on examination using $^{1}$H-NMR spectroscopy; the product formation did not exceed more than 40%. Moreover, the change of mole percent from 2 to 5 does not have much effect on $^{1}$H-NMR spectroscopy. In general, the catalyst **(±)-66a** was not successful to producing complete conversion for the compounds multiple C=C bond along with longer chains due to the difficulty in the formation of π-allyl intermediate at ambient temperature.

Moreover, from the above Table 2.11, it is significant that all the reactions of various allylic carbonates proceeded with complete conversion, except entry 6. Hence, the catalyst **(±)-66a** was successful in producing good regioselectivity for a wide range of substrates with aliphatic amines (primary and secondary alkyl substituted amines) and moderate regioselectivity in various α/γ substituted allylic carbonates towards allylic amination under mild and simple conditions and without the aid of activators such as triphenylphosphine, carboxylic acids, etc.

From the investigations and the results obtained, it was rationalized that **(±)-66a** is the catalyst precursor, and the reaction proceeded with active catalyst Pd(0). The reaction mechanism follows the usual pathway as reported in literature[101] as shown below Scheme 2.17.

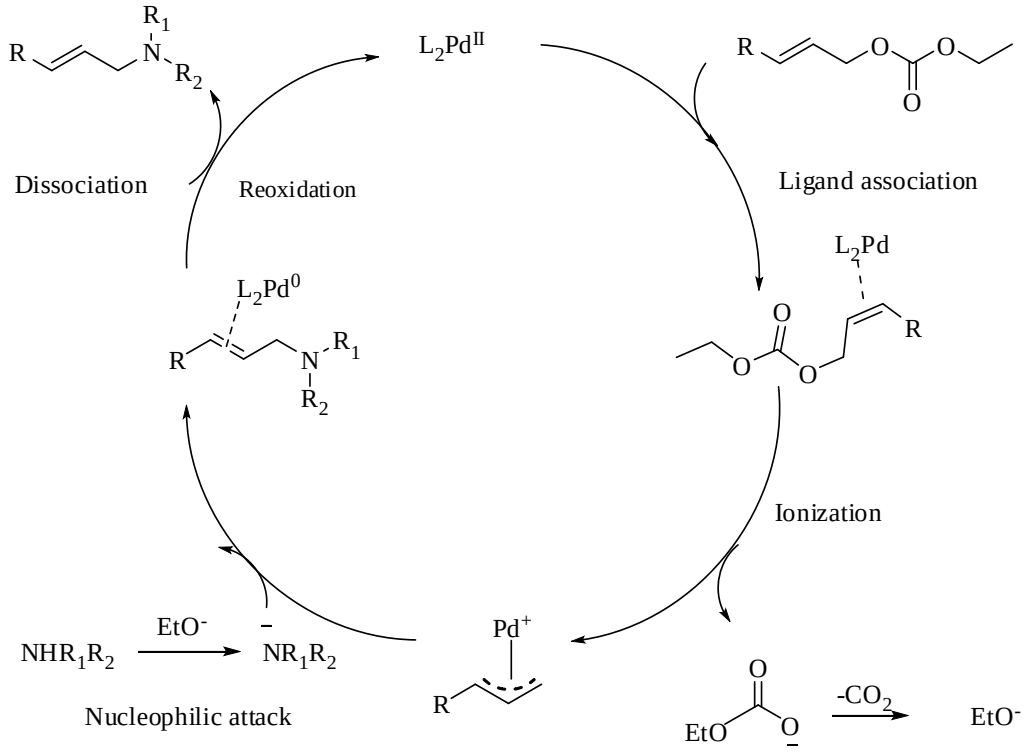


**Scheme 2.17**

## 2.4 CONCLUSION

In summary, heterobidentate C/S ligands and their corresponding neutral/cationic palladium complexes were successfully designed, developed and completely characterized with studies revealing that the sulphur containing metal chelate ring adopts the **λ-** and **δ-**envelope conformation. An efficient and convenient catalytic system has been successfully developed for allylic amination reaction. Among these cationic complexes, **(±)-66a** was found to be the most effective catalyst, for a wide range of allyl carbonates as well as aliphatic amines, for the production of allylamines in a highly regioselective

manner and in moderate to high yields. One significant point is that no phosphines were employed in this reaction. It is generally and substitution reactions and many phosphine ligands have been employed[102] previously. A limitation of the catalytic system designed in this work was that the reaction failed when performed with aromatic amines and cyclic carbonates.

# Chapter 3

## Synthesis of Chiral Cyclopalladated Sulphur-NHC Complexes and their Catalytic Studies in [2,3]-Sigmatropic Rearrangement Reaction

### 3.1 INTRODUCTION

As discussed in chapter two, complex **(±)-66a** was found to be an effective catalyst for allylic amination reaction under mild conditions without any additives. The reaction proceeded smoothly in tetrahydrofuran to afford the expected substitution product in high yields. These encouraging results suggested that an investigation into the design and synthesis of related optically active catalysts was warranted and a study of the key stereochemical features of these complexes that are likely to be of importance in asymmetric catalysis. Resolution of the carbene ligand precursors **(±)-64(a-d)** (followed by complexation) or their palladium(II) complexes was seen as an appropriate way of obtaining an optically pure catalyst that could be subsequently trialed in asymmetric catalysis.

Hence, we decided to begin our study with the resolution of racemic ligands by incorporating with metal centres and finally proceed with its application in asymmetric catalysis.

#### *3.1.1 Optical Resolution*

The preparation of enantiomerically pure compounds is important in areas such as pharmaceutical and food industries. Optical resolution via crystallization is whole or partial separation into its components of a racemic mixture. The first

diastereomeric salt formation of (R,R)-tartaric acid from the racemate via its salt formation with (R,R)-quinotoxine was observed by Louis Pasteur in 1848.

Later in 1899, Marckwald and McKenzie discovered non-enzymatic kinetic resolution.[103] Unfortunately this approach did not acquire much practical importance; this was followed by Pope and Peachey by their half equivalent method.[104]

### *3.1.2 Resolution of diastereomeric salt formation*

To date, amongst the various techniques available, optical resolution via diastereomeric salt formation is still a useful technique on an industrial scale. It is a direct, simple and clean method to reproduce from laboratory to industrial scale. From the literature reports, more than half of the chiral drugs on the pharmaceutical market are produced by the diastereomeric salt formation method using enantiomerically pure resolving agents.[105]

#### *3.1.2.1 Resolution of racemic bases*

This is one of the most popular methods for resolution of bases amongst other resolution techniques. Commonly, (R,R)-tartaric acid (R,R-TA), (R,R)-dibenzoyl tartaric acid (R,R-DBTA), (R,R)-di-*p*-toluoyl tartaric acid (R,R-DPTA), (S)-mandelic acid (S-MA), or (1S)-camphorsulfonic acid (S-CSA) have been used as resolving agent to form a pair of diastereomeric salts.

(R,R)-DBTA was used successfully to resolve Flavopyridol,[106] which is a potent anticancer intermediate. An intermediate for indinavir, *cis*-1-amino-2-indanol was resolved with (S)-phenylpropionic acid.[107] (S)-mandelic acid was

used to resolve 3-methylamino-1-(2-thienyl)propan-1-ol which is an intermediate for duloxetine[108] as shown in Scheme 3.1

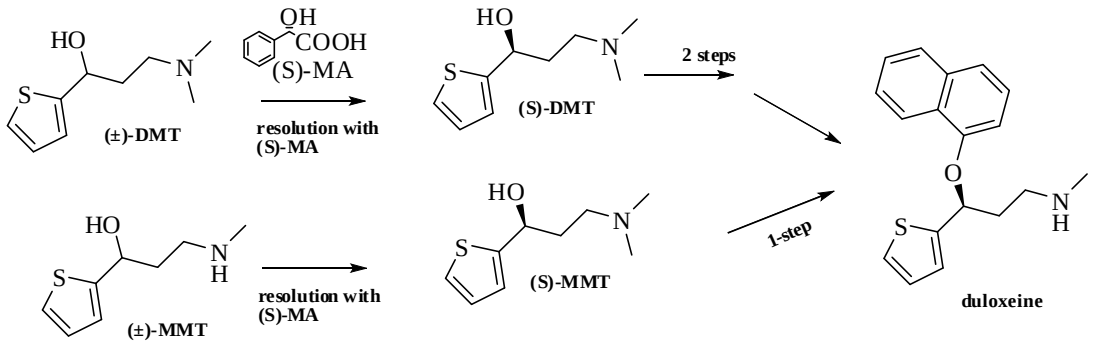


**Scheme 3.1**

Camphorsulphonic acid was used as the resolving agent for a metabolite [1-(3-hydroxy-4-methylphenyl)-2-methyl-3-(1-piperidyl)-propan-1-one]of tolperisone[109] as shown in Scheme 3.2 below.

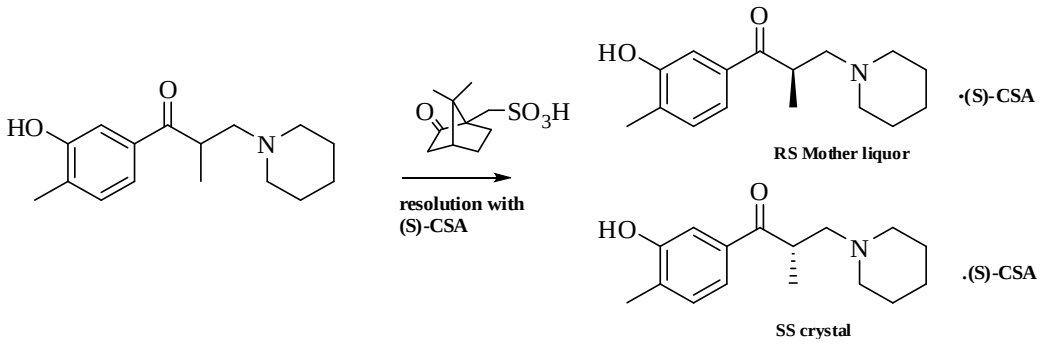


**Scheme 3.2**

(1*R*)-3-Bromocamphor-8-sulfonic acid[110] [(R)-BRCS] was the resolving agent for a tetrahydroquinoline intermediate of the antibacterial agent

flumequine, and *N*-acetyl-phenylalanine was found to be an effective resolving agent for benzodiazepins.[111]

*3.1.2.2 Resolution of racemic acids*

Alkaloids such as quinine, cinchonine (CH), cinchonidine (CD), and brucine were often used to resolve racemic acids. Among these (R)- or (S)-1-phenylethlamine (PEA) is an efficient and standard resolving agent for acids such as 3-phenyl-1-methyallenecarboxylic acid,[112] *tert*-butyl(phenyl)phosphanylthioic acid[113] and a ferrocenecarboxylic acid.[114] (R)-1-cyclohexyl-ethylamine was used as resolving agent for 1, 1-binaphthyl-2,2-dicarboxylic acid.[115] (1R,2S)-ephedrine was used for the resolution of a racemic cyclopentene dicarboxylic acid.[116]

### 3.1.3 *Resolution of palladacycles*

Optical resolutions of palladacycles using chiral auxiliaries are well established by many groups.[117] However the resolution towards donor functionalized NHC based palladacycles has been much less explored.

Chauvin *et al.,*[118] reported the synthesis of chiral NHC palladacycles via resolution using an optically active ortho-metallated amine, the resulting diastereomers being separated by fractional crystallization followed by the treatment with HCl to remove the resolving agent (shown in Scheme 3.3).

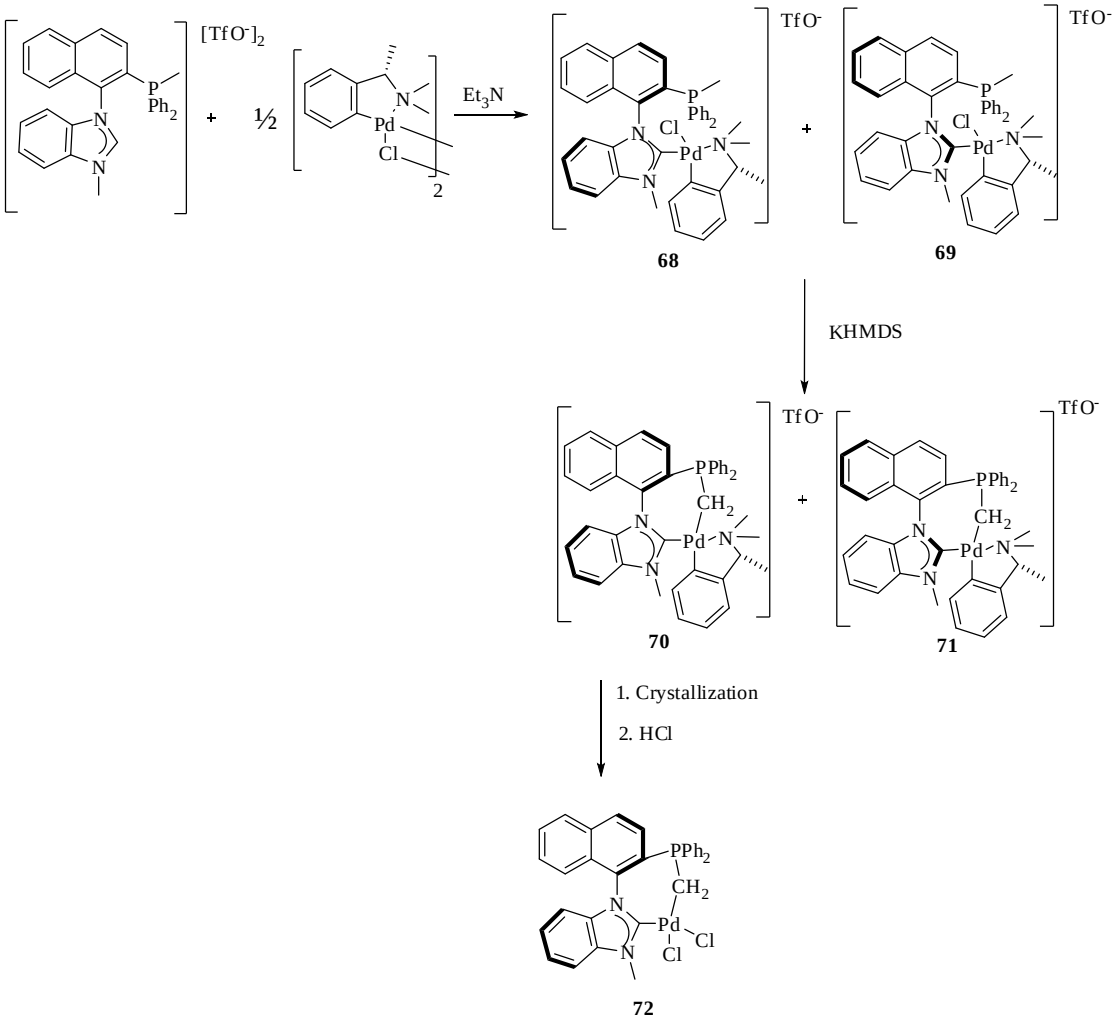


**Scheme 3.3**

However Leung *et al.*, have recently, reported and way of resolving various pyridine based NHC palladacycles[119] through their diastereomeric adducts with naturally occurring amino acids (Scheme 3.4). The rigid pyridine functionalized chiral NHC palladacycles were found to show moderate reactivity but unable to provide a steric environment for selectivity towards asymmetric allylic alkylation reaction.

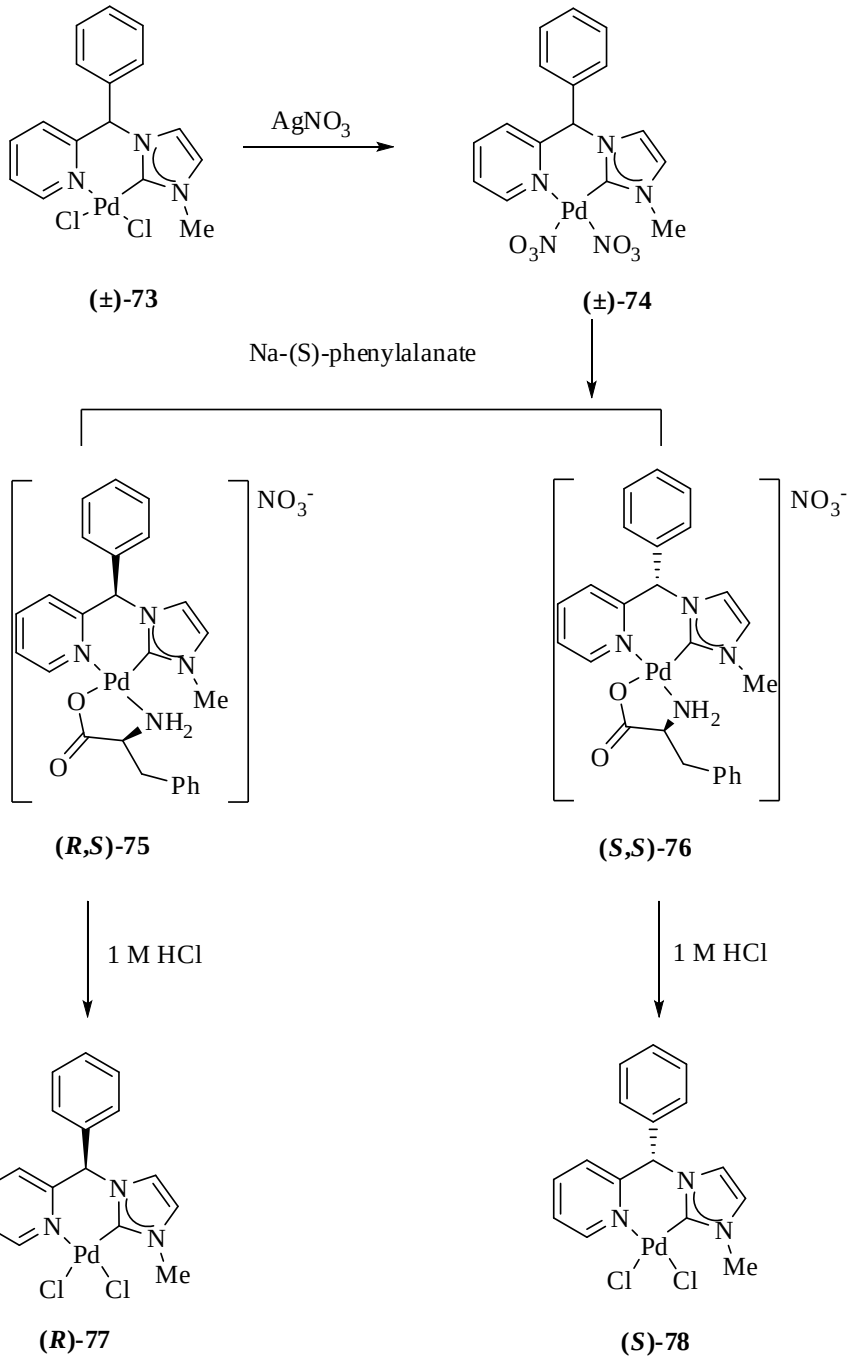
AgNO3
(±)-73
(±)-74
Na-(S)-phenylalanate
NO3-
(R,S)-75
(S,S)-76
1 M HCl
1 M HCl
(R)-77
(S)-78

**Scheme 3.4**

## 3.2 RESULT AND DISCUSSION

Initially, resolution of racemic ligand **64a** was attempted with sodium salt of L-(+) tartaric acid which was synthesised from commercially available L-(+) tartaric acid dissolved in 1.05 equivalent of sodium hydroxide in methanol (5 mL) for 15 h at room temperature. This was followed, by the addition of racemic ligand **64a** in 1:1 ratio and stirred for another 15 h at room temperature. However, on evaporation of methanol to half volume, it did not end up with the expected resolution. Subsequently, sodium salts of other chiral acids such as DBTA, DPTA, MA, and CSA were screened but the formation of diastereomeric salt was not achieved with all above chiral acids. From the experimental observations and proton in the $^{1}$H-NMR spectrum it was concluded that sodium was not an efficient metal to abstract the counter bromide ion from the *N*-heterocyclic carbene ligands to form diastereomeric salt mixture. And therefore, silver salts of corresponding chiral acids were used as silver is a better scavenger to abstract bromide to form the corresponding diastereomeric salts.

Consequently, the formation of diastereomeric salt of chiral acids with racemic ligand **64a** as seen from the change of the chemical shift value of the carbene proton from $^{1}$H NMR spectrum from $\delta$ = 10.87 to 10.20 ppm.

However, the crystallization of diastereomeric salts was not achieved with subsequent screening using various chiral acids such as DBTA, DPTA, MA, CSA and solvents such as methanol, ethanol, acetone, and chloroform.

Therefore attempts to resolve the racemic ligand **64a** by using various silver salts of enantiopure acids as resolving agents were unsuccessful as the resulting diastereomers could not be separated via crystallization. The attempted resolution of the carbene ligand precursor **(±)-64a** was subsequently suspended and resolution of the analogous palladium(II) complexes investigated instead.

We started the resolution on palladium(II) complex **(±)-67b** was initially investigate during sodium salt of a amino acids as chiral resolving agents. After screening through series of sodium salts of amino acids, such as (*S*)-phenyl alanine, (*S*)-proline, (*S*)-leucine, (*S*)-valine and (*S*)-aspartic acid; (*S*)-valinate showed the best results in terms of the formation of diastereomers with palladium complex (±)-**67b.** Treatment of complex (±)-**67b** with one molar equivalent of sodium valinate in methanol (5 mL) stirred at room temperature for 15 h gave a 1:1 mixture of diastereomers as shown in the Scheme 3.5.

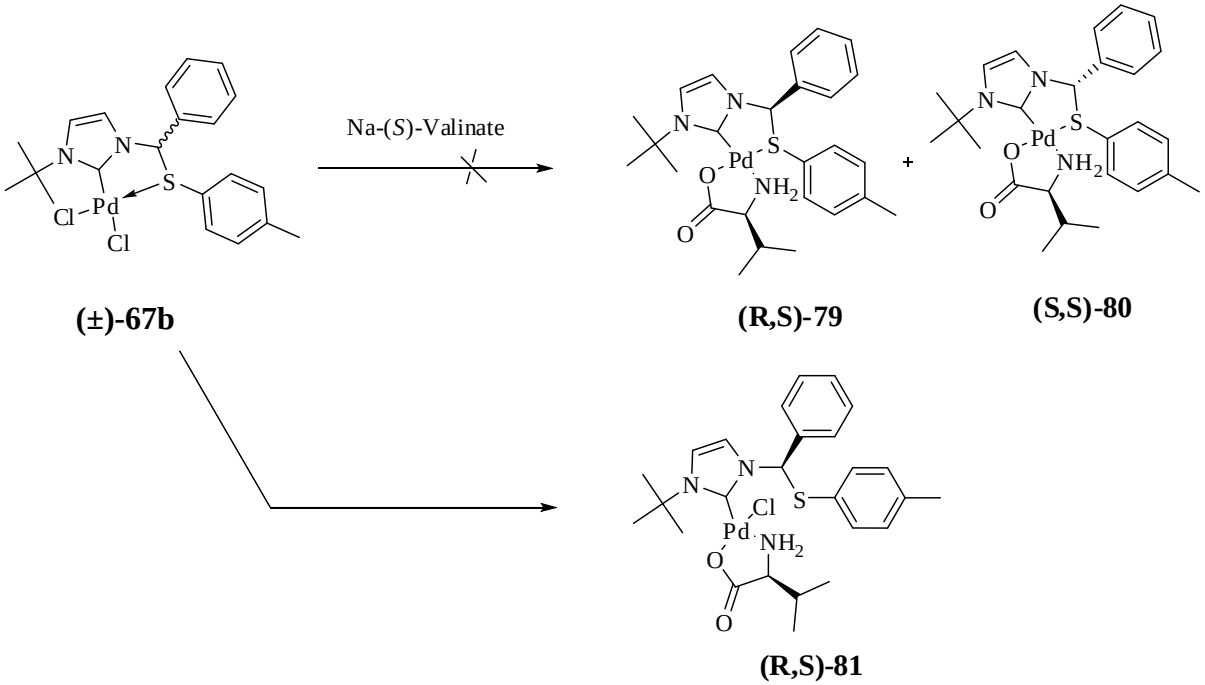


**Scheme 3.5**

This was confirmed from two sets of diastereomeric peaks seen in the $^{1}$H-NMR spectrum. Separation of these two isomers was based on their solubility difference; hence the less soluble diastereomer was crystallized from methanol which was then separated and analyzed by X-ray single crystal diffraction studies.

From investigations through the X-ray single crystal diffraction, it was seen that, the sulphur was not coordinated to the palladium during the diastereomer formation with (*S*)-valinate and it shows its hemi labile behaviour. As a result, palladium complex **(R,S)-81** was obtained as the amino acid adduct. The Figure 3.1 shows the molecular structure with numbering scheme of complex **(R,S)-81**. The quality of crystal obtained was not good enough for the estimation of bond lengths and angles at the required accuracy. However, it is well established that sulphur was not coordinated to the palladium complex during course of diastereomeric formation with (*S*)-valinate. Besides that, the geometry around the palladium centre is square planar with the chloride ion occupying *cis* position to the carbene and amino acid occupying the other two coordination sites on palladium.

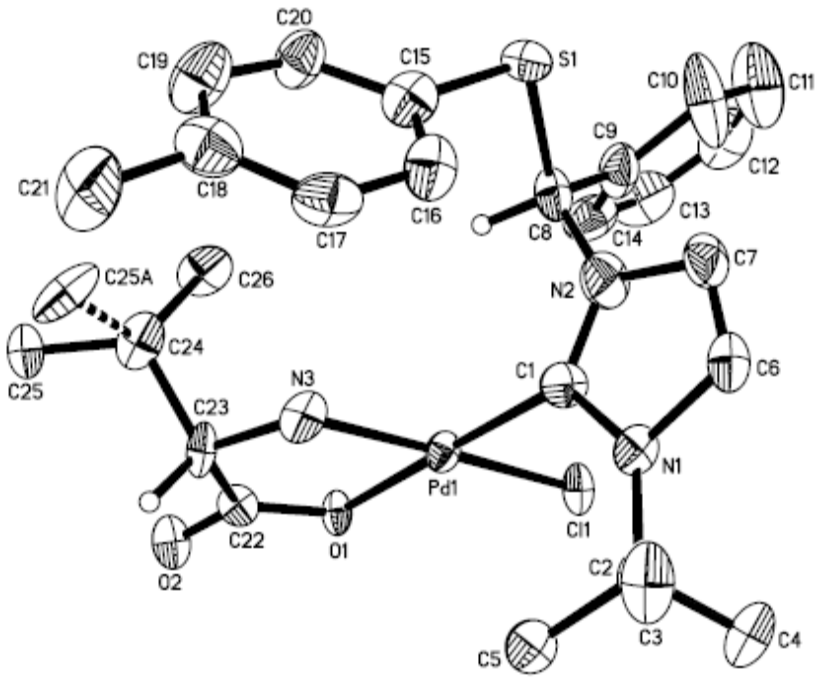


**Figure 3.1** Molecular structure of complex **(R,S)-81**; Thermal ellipsoids are drawn at the 50% probability level. Hydrogen atoms except for H **(C8)** and H **(C23)** are omitted for clarity.

The lability of S→Pd bond in the neutral palladium complex was further confirmed by the addition of one equivalent of $PPh_3$ to the racemic complex **(±)-67b** which gave a clean $^1H$ NMR spectrum corroborating the formation of the NHC–phosphine complex **(±)-82** as the sole product in 95% yield (Scheme 3.6).

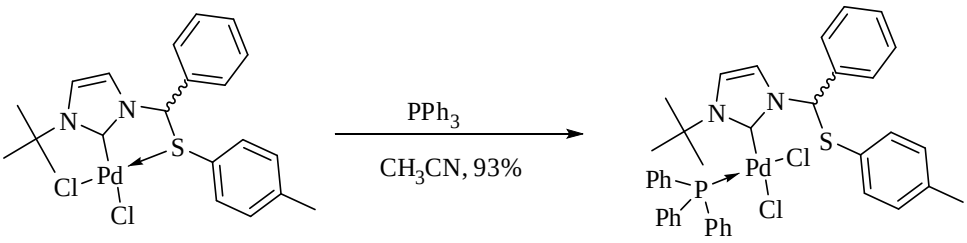


**(±)-67b** **(±)-82**

**Scheme 3.6**

Due to the steric bulk of the phosphine ligand, the Pd–$C_{carbene}$ bond rotation was hindered which in turn resulted in the *cis* arrangement of NHC and $PPh_3$. The NMR spectrum of **(±)-82** contained a signal and carbon at 156.2 ppm and the phosphine donor resonates at 23.37 ppm in the $^{31}P\{^1H\}$ NMR spectrum. Single crystals of complex **(±)-82** were obtained by slow diffusion of diethyl ether into an acetonitrile solution of the complex at room temperature. Figure 3.2 shows the molecular structure with numbering scheme of complex **(±)-82** and Table 3.1 lists the selected bond lengths and angles.

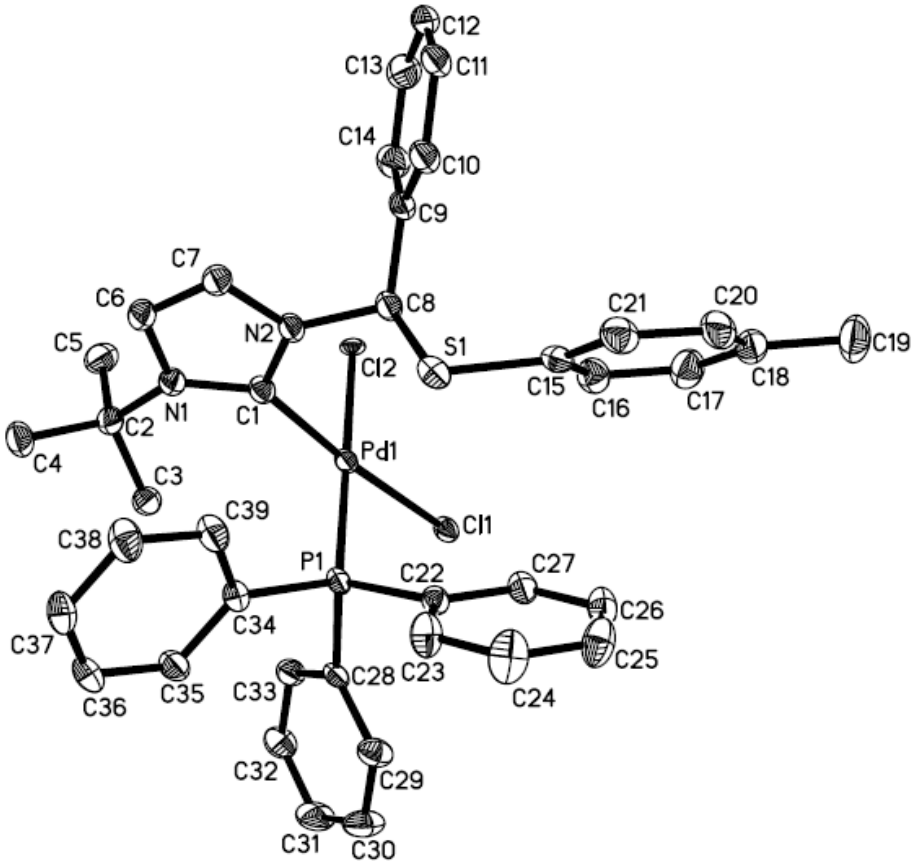


**Figure 3.2** Molecular structure of complex **(±)-82**; Thermal ellipsoids are drawn at the 50% probability level. Hydrogen atoms are omitted for clarity.

The palladium atom is located in a distorted square planar coordination sphere with one NHC, one $PPh_3$ and two chloride ions. The stronger *trans* influence of the $PPh_3$ donor compared to the NHC was illustrated by a Pd(1)–Cl(2) [2.3973 Å] bond which was longer than Pd(1)–Cl(1) [2.3393 Å] and by the C(1)–Pd(1)–P(1) angle of 95.80$^o$.

**Table 3.1 Selected bond lengths (Å) and angles (°) of racemic palladium complex (±)-82:**

| | | | |
|---|---|---|---|
| Pd(1)–C(1) | 1.997(3) | C(1)–Pd(1)–P(1) | 95.80(9) |
| Pd(1)–P(1) | 2.2744(8) | C(1)–Pd(1)– Cl(2) | 85.96(9) |
| Pd(1)–Cl(1) | 2.3393(7) | P(1)–Pd(1)– Cl(1) | 87.99(3) |
| Pd(1)–Cl(2) | 2.3973(7) | N(2)–C(1)–Pd(1) | 121.20(2) |
| C(1)–N(1) | 1.347(4) | N(1)–C(1)–N(2) | 105.6(3) |
| C(1)–N(2) | 1.357(4) | C(1)–Pd(1)–P(1) | 95.80(9) |
| C(2)–N(1) | 1.508(4) | C(22)–P(1)–Pd(1) | 115.52(11) |
| C(8)–N(2) | 1.473(4) | C(28)–P(1)–Pd(1) | 111.95(10) |
| Cl(1)–Pd(1)–Cl(2) | 90.36(3) | C(34)–P(1)–Pd(1) | 116.94(11) |

It is well established from the X-ray crystallographic studies of the complex **(±)-67b,** that S–Pd bond cleavage was observed when coordinating with a tertiary phosphine or a hard donor ligand such as carboxylato. Therefore, the S–Pd bond in complex **(±)-67b** exhibits the highest degree of hemilability. Due to the hemiliable behaviour, the complex **(±)-67b** and its analogues are not possible to be resolved as pure enantiomers.

Ultimately, no promising results were found for the resolution of either the racemic ligand **(±)-64a** or its corresponding palladacycle; This difficulty was addressed by introducing an existing chiral moiety in to the backbone of the carbene ligand (at N-1 see figure 3.3) resulting in the formation of diastereomers

that can be separated readily by crystallization due to their difference in chemical and physical properties.

The chiral moiety attached to $N_1$ of the carbene ligand acts as an external chiral source to resolve the complex as diastereomers as shown in Figure 3.3. This appears to be the only possible way that is available to study the chirality and the ring conformation of novel five membered S-NHC chelates. The ring conformation study was restricted to only two different substituents on sulphur (i.e. R = $^t$Bu or *p*-tolyl).

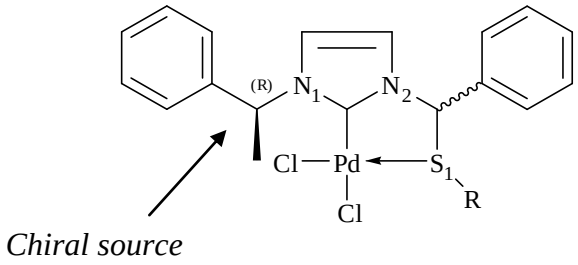


**Figure 3.3** Basic structure for diastereomeric S-NHC palladacycle

### *3.2.1 Synthesis and characterization of diastereomeric ligands*

The thioether-imidazolium bromides **(±)-84(a–b)** were prepared in a two-step procedure as shown in Scheme 3.7. The α-bromo compound **83** was readily available from the reaction of substituted chiral imidazole and benzaldehyde with thionyl bromide in dichloromethane at -50$^{o}$C under nitrogen atmosphere followed by subsequent, nucleophilic substitution reaction by sodium salt of substituted sulfides at -10$^{o}$C.

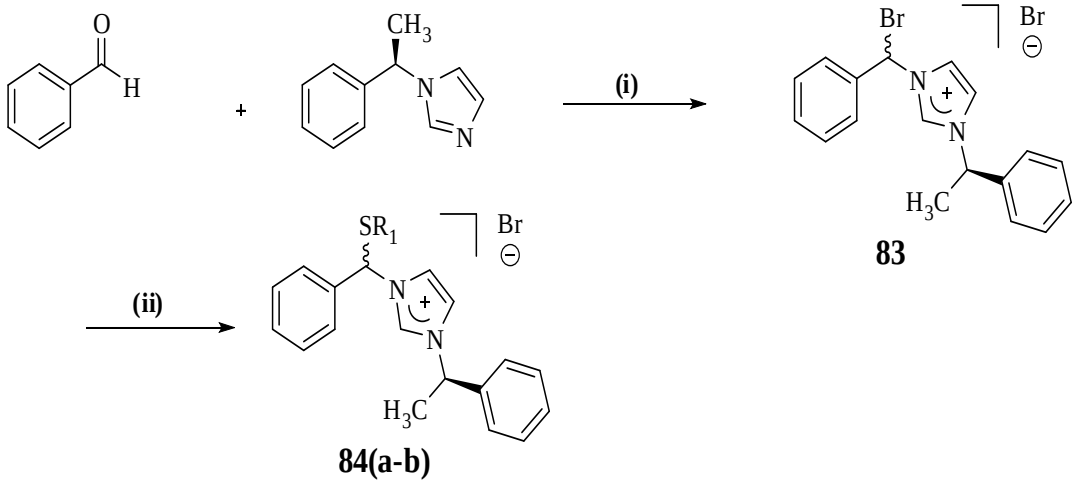


**Reagents and conditions:** (i) $SOBr_2$ (2M), DCM, –50$^{o}$C, 75% yield; (ii) $R_1SNa$, DCM, –10$^{o}$C, 80-85%yield.

**84a:** $R_1$ = $^{t}$Bu; **84b:** $R_1$ = *p*-tolyl.

**Scheme 3.7**

### *3.2.2 Synthesis and characterization of palladium complexes*

The silver carbene complexes **85a** and **85b** were efficiently prepared by treating 0.55 equivalent of $Ag_2O$ with **84a** and **84b.** Subsequent reaction with **[**$PdCl_2(CH_3CN)_2$] and [$PtCl_2COD$] which gave the neutral complexes, **86** and **87, 88** and **89** in moderate to high yields.

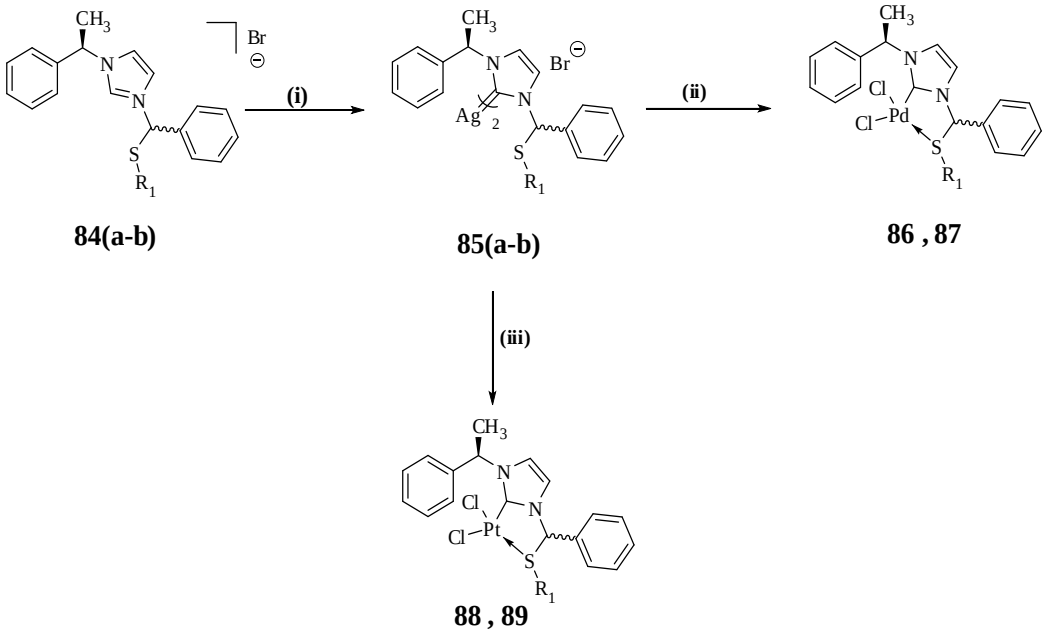


**84(a-b)** **85(a-b)** **86 , 87**

**88 , 89**

**Reagents and conditions:** (i) $Ag_2O$ (0.55eq), DCM, rt , 3 h , 85-90% , in dark, (ii) $PdCl_2(CH_3CN)_2$, $CH_3CN$, rt, 6 h, 50-52%. (iii) $PtCl_2COD$, $CH_3CN$, rt, 87-90%.

**84a:** $R_1$ = $^t$Bu, **84b:** $R_1$ = *p*-tolyl , **85a:** $R_1$ = $^t$Bu, **85b:** $R_1$ = *p*-tolyl , **86:** R = $^t$Bu, **87:** R = *p*-tolyl ,**88:** R = $^t$Bu**, 89:** R = *p*-tolyl.

**Scheme 3.8**

## List of New Complexes:

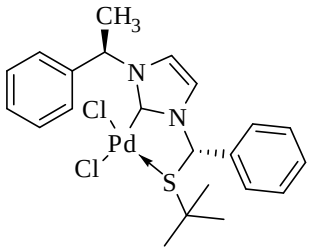


**($R_S$*,S*,R*)-86**

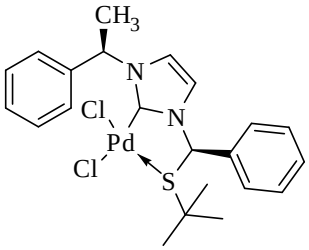


**($S_S$*,R*,R*)-86**

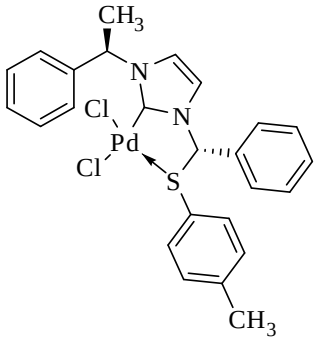


**($R_S$*,S*,R*)-87**

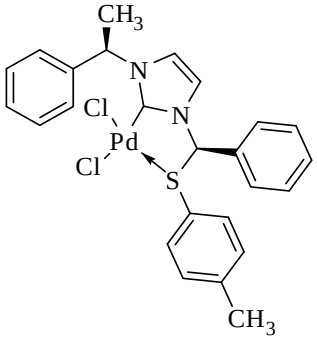


**($S_S$*,R*,R*)-87**

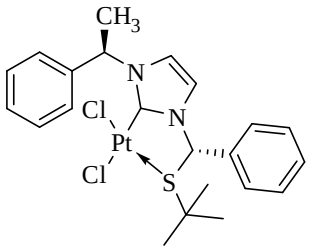


**($R_S$*,S*,R*)-88**

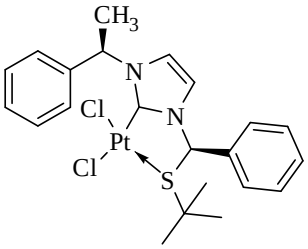


**($S_S$*,R*,R*)-88**

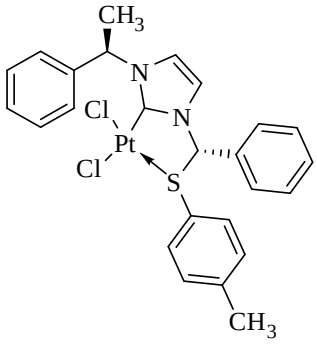


**($R_S$*,S*,R*)-89**

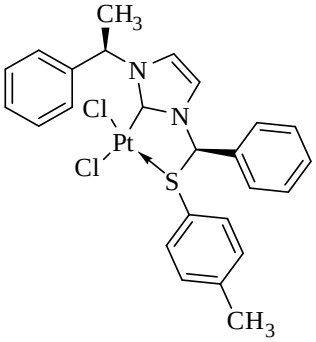


**($S_S$*,R*,R*)-89**

### *3.2.3 Separation of diastereomers of palladium complex 86*

The corresponding palladium complex **86** contains 1:1 mixture of two diastereomers **($R_S$*,S*,R*)-86** and **($S_S$*,R*,R*)-86**. The separation of these two isomers was based on their difference in solubility. A single crystallization of the diastereomeric mixture from acetonitrile/diethyl ether afforded the less soluble diastereomeric complex **($R_S$*,S*,R*)-86** as yellow crystals in 85% yield and >98% d*e* (according to the $^1$H-NMR data) with $[\alpha]_D$ = **+100** (*c* 0.2, $CH_3CN$).

The remaining diastereomeric mixture in the mother liquor of **($S_S$*,R*,R*)-86** complex did not crystallize in most of the organic solvents tested. Hence, suitable single crystals for XRD were not obtained. However according to $^1$H-NMR data, the d*e* of **($S_S$*,R*,R*)-86** complex was >98% with $[\alpha]_D$ = **+214** (*c* 0.2, $CH_3CN$).

The absolute configuration of **($R_S$*,S*,R*)-86** complex was determined by X-ray single crystal diffraction study. Their solution structures of **($R_S$*,S*,R*)-86** and **($S_S$*,R*,R*)-86** were established by 2D $^1$H-$^1$H ROESY NMR spectroscopy studies.

*3.2.3.1 Molecular Structure of the ($R_S$*,S*,R*)-86*

The molecular structure of the chiral complex was determined by an X-ray single crystal diffraction study. The yellow coloured crystals with a size of 0.38 x 0.26 x 0.24 $mm^3$ of complex **($R_S$*,S*,R*)-86** were grown by slow diffusion of diethyl ether into acetonitrile solution of the complex at room temperature. The molecular structure with the numbering scheme is presented in Figure 3.4. Selected bond lengths and bond angles are listed in Table 3.2.

In solid state, the complex **($R_S$*,S*,R*)-86** exhibits **λ**-conformation, where the phenyl substituent at the α-carbon invariably adopts axial position below the coordinating PdCS plane (Figure 3.4). The axial position of the phenyl on the stereogenic centre is attributed to the repulsive interaction between the $^t$Bu substituent on the sulphur and the phenyl group at C12. Upon chelation, the sulfur atom becomes a stereogenic center that was formed with the ***R***-configuration, in which the selectivity can be explained by the lower steric interactions due to the relative *trans* disposition of the phenyl(α) and $^t$Bu groups.

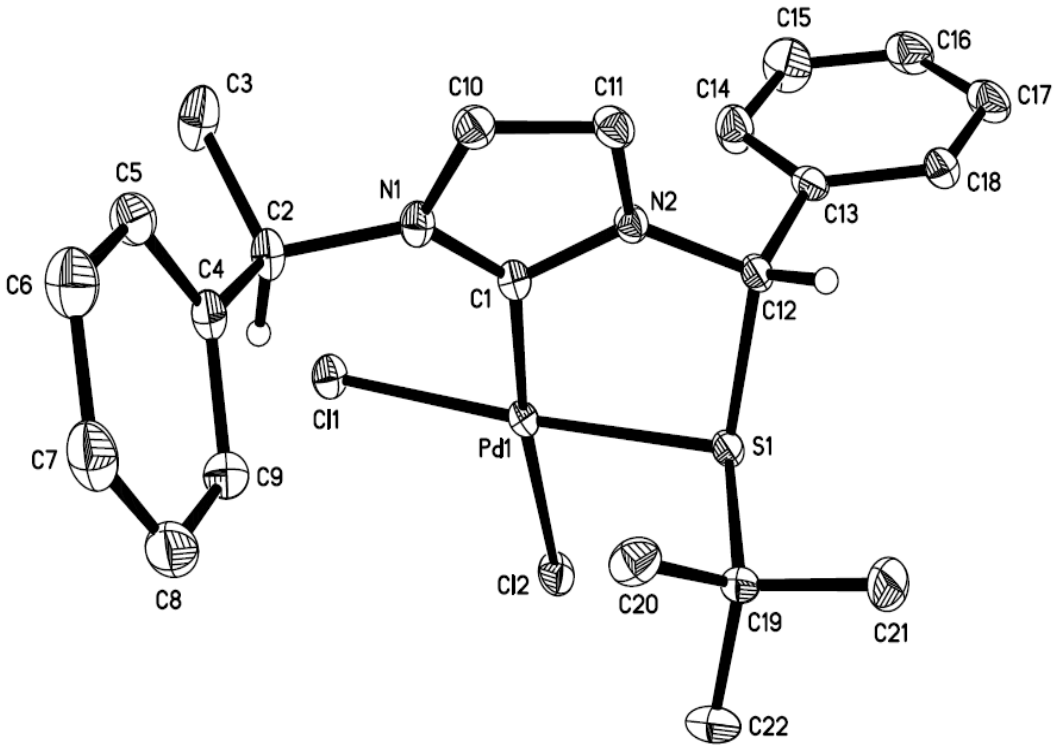


**Figure 3.4** Molecular structure of complex **($R_S$*,S*,R*)-86**; Thermal ellipsoids are drawn at the 50% probability level. Hydrogen atoms except for H **(C12)** andH **(C2)** are omitted for clarity.

The C(13)–C(12)–S(1)–C(19) torsion angle between the phenyl substituent at α-carbon and $^{t}$Bu substituent on sulphur is 112.24$^{o}$. The longer Pd–Cl(1) bond [2.3842 Å] *trans* to the carbene compared to Pd–Cl(2) [2.3513 Å] reflects its strong trans-influence effect. The complex exhibits the distorted square-planar geometry, with a $C_{carbene}$–Pd bond distance of 1.9776 Å along with the bite angle of 84.40$^{o}$.

**Table 3.2 Selected bond lengths (Å) and angles (°) of chiral palladium complex ($R_S$*,S*,R*)-86:**

| | | | |
|---|---|---|---|
| Pd(1)–C(1) | 1.984(13) | C(1)–Pd(1)–S(1) | 84.40(4) |
| Pd(1)–S(1) | 2.266(4) | N(2)–C(12)–S(1) | 107.37(9) |
| Pd(1)–Cl(1) | 2.317(4) | S(1)–C(12)–H(12) | 180.10 |
| Pd(1)–Cl(2) | 2.362(4) | N(2)–C(12)–H(12) | 180.10 |
| C(1)–N(1) | 1.355(19) | C(12)–S(1)–Pd(1) | 99.21(5) |
| C(1)–N(2) | 1.360(19) | C(12)–S(1)–C(19) | 102.32(7) |
| N(1)–C(1)–N(2) | 104.68(12) | C(13)–C(12)–S(1) | 112.24(9) |
| C(1)–N(2)–C(12) | 124.53(12) | Cl(1)–Pd(1)–S(1) | 170.913(14) |
| N(2)–C(12)–C(13) | 112.73(12) | Cl(1)–Pd(1)–Cl(2) | 172.83(4) |
| N(2)–C(1)–Pd(1) | 117.06(10) | C (1)–Pd(1)–Cl(1) | 95.71(4) |

*3.2.3.2 Solution Structure of complex ($R_S$*,S*,R*)-86*

For the ***S*** absolute configuration at the α-carbon chiral center, the five membered palladacycle can adopt a **δ** or **λ** conformation as illustrated in Figure 3.6. The assignment of proton peaks was obtained from the combination of COSY, HMQC and HMBC spectra's. Figure 3.5 presents the 2D $^{1}$H-$^{1}$H ROESY NMR spectrum for **($R_S$*,S*,R*)-86** in $(CD_3)_2SO$. Selected chemical shifts of the complex are given in Table 3.3.

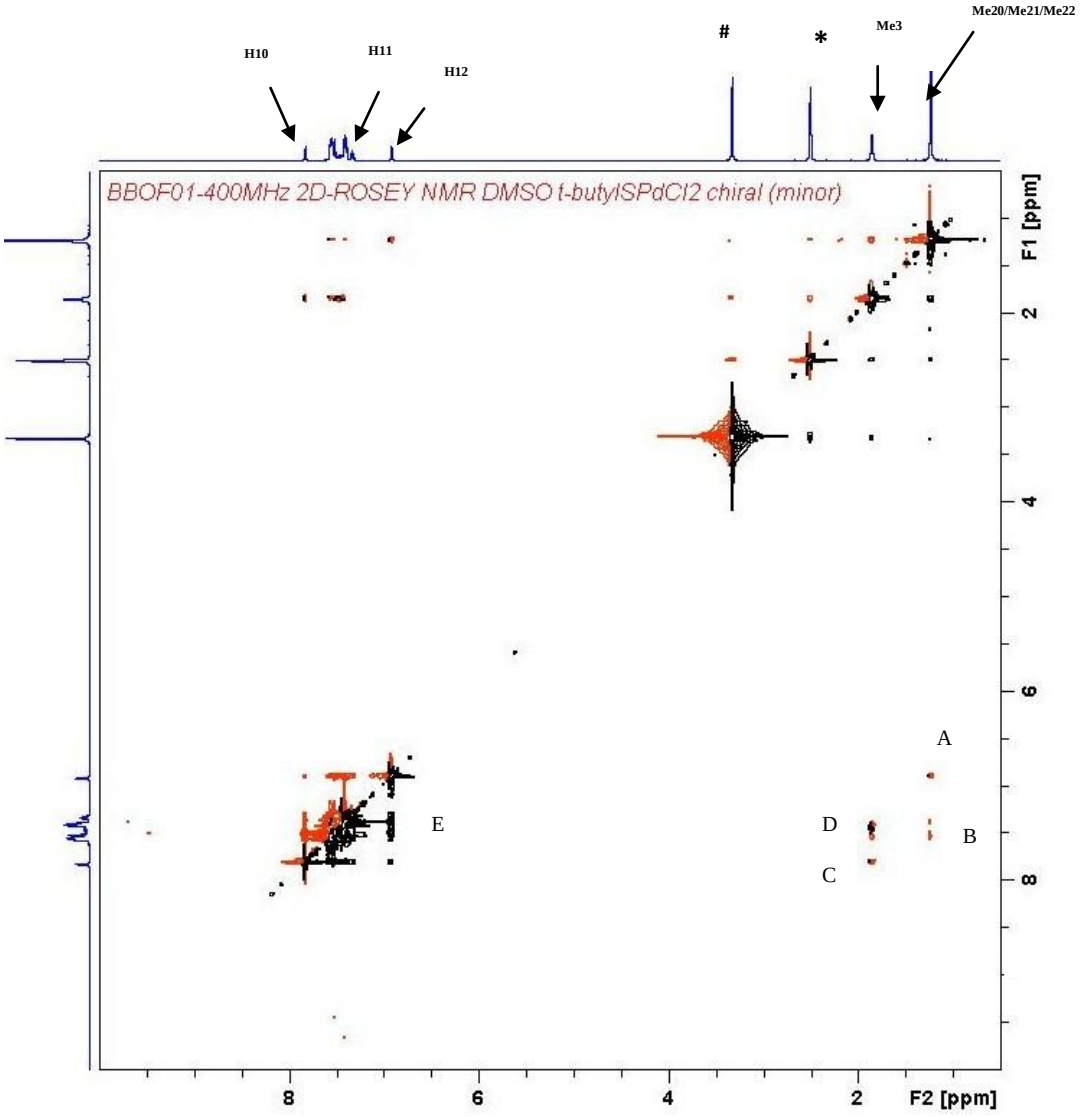


**Figure 3.5** 2D $^{1}$H-$^{1}$H ROSEY NMR spectrum of **($R_S$*,S*,R*)-86** in $(CD_3)_2SO$.

**Selected NOE signals**: **(A)**: Me20/Me21/Me22 – H12; **(B)**: Me20/Me21/Me22 – H11; **(C)**: Me3 – H2; **(D)**: Me3 – H10; **(E)**: H12 – H11; *****$(CD_3)_2SO$ solvent peak; **#**$H_2O$ peak.

Signals (A) & (B) seen in the 2D $^{1}$H-$^{1}$H ROESY NMR, are due to the strong interaction between Me20/Me21/Me22 and H12, H11. The strong NOE signal (E) is due to the interaction between H12 and H11. Therefore in solution the complex **($R_S$*,S*,R*)-86** remains locked in **λ** ring conformation.

**Table 3.3** Selected chemical shifts for **($R_S$*,S*,R*)-86** in $(CD_3)_2SO$.

| Proton | δ (ppm) |
|---|---|
| H10 | 7.82(s) |
| H11 | 7.51(s) |
| H12 | 6.91(s) |
| Me3 | 1.86–1.84(d) |
| Me20/Me21/Me22 | 1.23(s) |

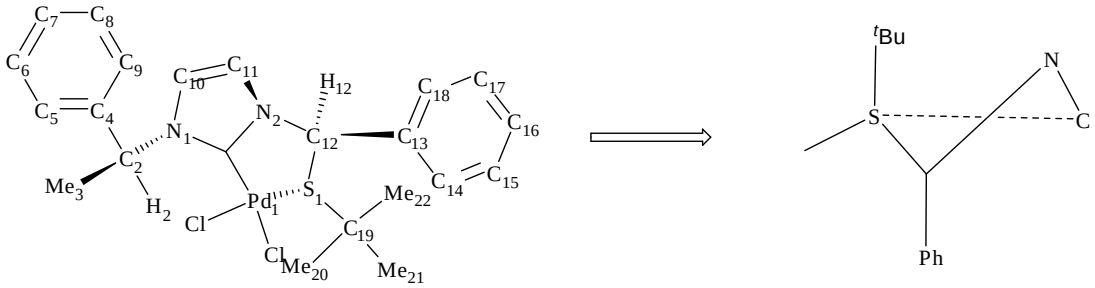


**($R_S$*,S*,R*)-86**

**Figure 3.6** Absolute conformation of the PdCS ring


**(Rs*,S*,R*,λ)-86** **(Ss*,S*,R*,δ)-86**

**Figure 3.7** The staggered orientation of S1and C12 substituents when the PdCS ring adopts the (a) **λ** or (b) **δ** conformation.

If the complex **($R_S$*,S*,R*)-86** is able to undergo ring inversion, the presence of the other conformer with the phenyl group at the equatorial position within PdCS chelate ring should be detected in the 2D $^1$H-$^1$H ROESY NMR. But the 500MHz $^1$H-NMR spectrum of **($R_S$*,S*,R*)-86** in $(CD_3)_2SO$ at room temperature shows the presence of only one signal for each chemically non-equivalent proton which clearly indicates the existence of a single geometrical isomer in solution. Moreover, from the absence of any correlations between the Ph(α) protons with $^t$Bu protons (Me20/Me21/Me22) in the 2D $^1$H-$^1$H ROESY NMR, conclusion can be drawn that the other conformation **(Ss*,S*,R*,δ)-86** does not exist in solution.

#### 3.2.3.3 Solution Structure of complex ($S_S$*,R*,R*)-86

Given that single crystals could not be obtained for the diastereomeric complex **($S_S$*,R*,R*)-86** in an array of solvents, the assignment of the absolute stereochemistry and ring conformation was studied with 2D $^1$H-$^1$H ROESY NMR spectroscopy for the assignment of the absolute stereochemistry and ring conformation. The five-membered palladacycle adopts **δ** conformation when the chiral center has a ***R*** absolute configuration as illustrated in Figure 3.9.

It is well established that in solution state the complex **($S_S$*,R*,R*)-86** exhibits **δ(*R*)** conformation. The phenyl group on the stereogenic carbon invariably takes up the axial position above the PdCS plane. The assignment of proton peaks was obtained from the combination of COSY, HMQC and HMBC NMR spectra. Figure 3.8 presents the 2D $^1$H-$^1$H ROESY NMR spectrum for **($S_S$*,R*,R*)-86** in $(CD_3)_2SO$. Selected chemical shifts of the complex are given in Table 3.4.

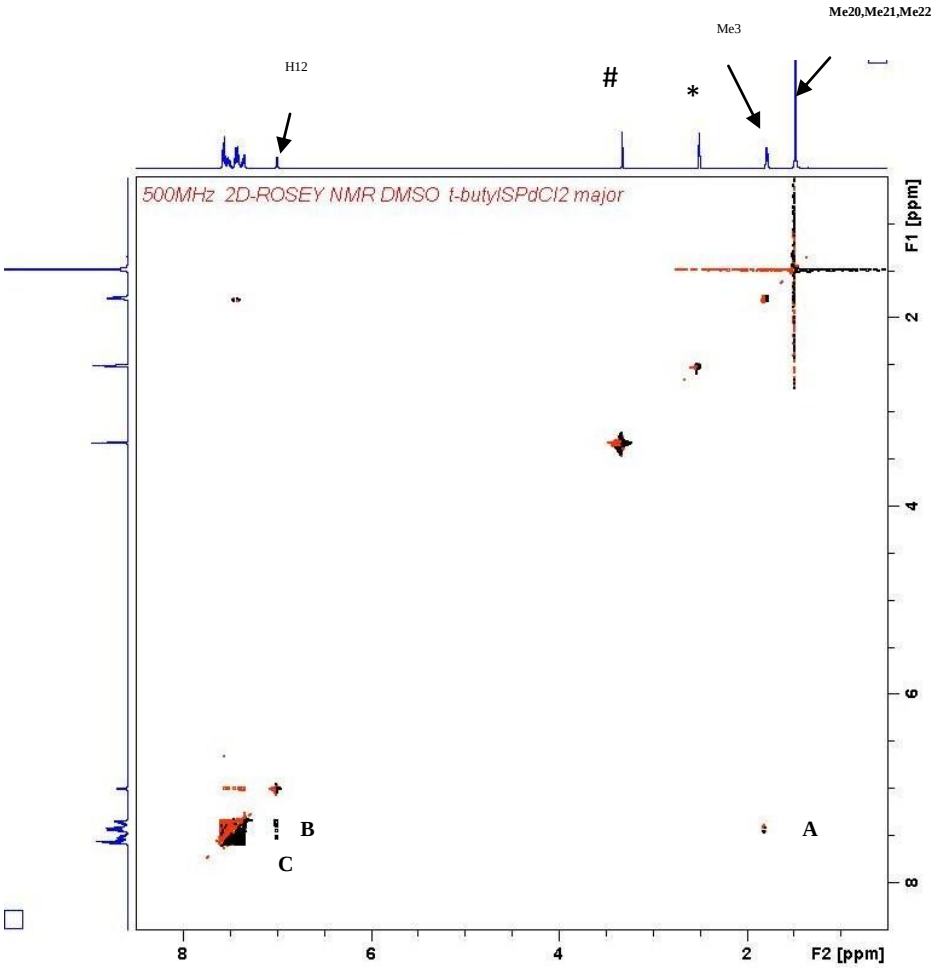


**Figure 3.8** 2D $^{1}$H-$^{1}$H ROSEY NMR spectrum of **($S_S$*,R*,R*)-86** in $(CD_3)_2SO$.

**Selected NOE signals**: **(A)**: Me3 – H2; **(B)**: H12 – H11; **(C)**: H12 – Ph(α); *** -** $(CD_3)_2SO$ solvent peak; **#** - $H_2O$ peak.

Signals (B), (C) seen in the ROESY NMR spectrum, are due to the strong interaction between H12 and H11, Ph(α). The signal (A) is due to the interaction between Me3 and H2. Although the NMR signals of Ph(α) and H11 cannot be assigned conclusively due to overlapping of protons, the absence of signals due to Me20/Me21/Me22 and Ph(α) completely rules out the existence of **λ** conformation in solution.

**Table 3.4** Selected chemical shifts for **($S_S$*,R*,R*)-86** in $(CD_3)_2SO$.

| Proton | δ (ppm) |
|---|---|
| H10 | 7.26-7.27(d) |
| H11 | 6.96-6.97(d) |
| H12 | 6.45(s) |
| Me3 | 1.83–1.82(d) |
| Me20/Me21/Me22 | 1.52(s) |

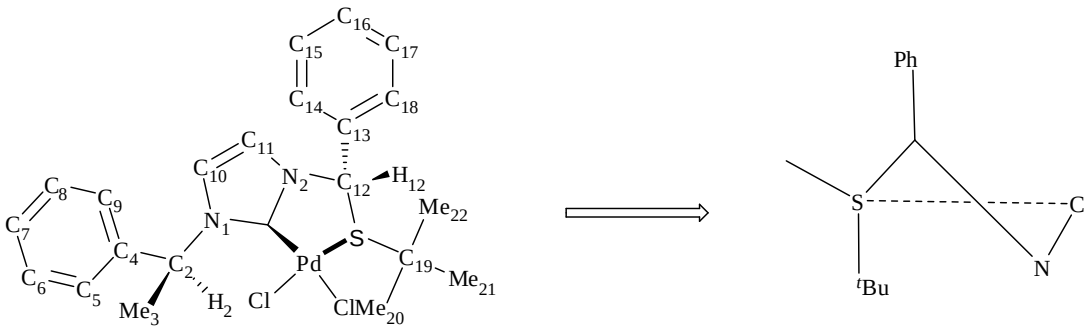


**(Ss*,R*,R*,δ)-86**

**Figure 3.9** Absolute conformation of the PdCS ring.

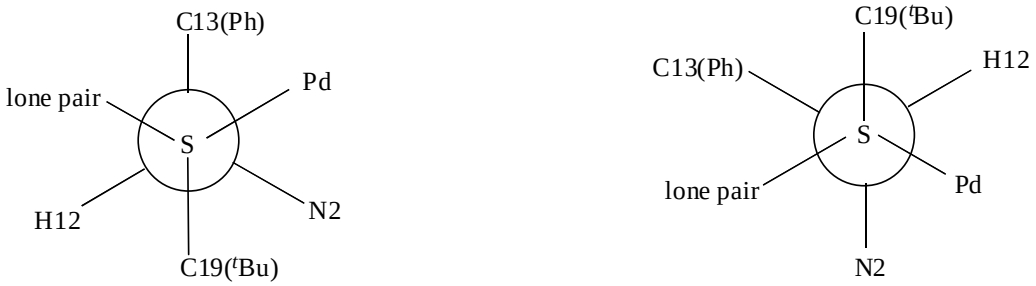


**(Ss*,R*,R*,δ)-86** **(Rs*,R*,R*,λ)-86**

**Figure 3.10** The staggered orientation of S1and C12 substituents when the PdCS ring adopts the (a) **δ** or (b) **λ** conformation.

Hence, in solution the complex **($S_S$*,R*,R*)-86** exists as a soles isomer and therefore remains stereochemically locked in both solid as well as solution state in **δ(*R*)** conformation.

*3.2.3.5 Investigation of the fluxionality of complex ($S_S$*,R*,R*)-86 using VT-NMR techniques*

**Figure 3.10a** and **3.10b** presents the variable-temperature $^1$H-NMR spectra of the complex **($S_S$*,R*,R*)-86** in $CD_3CN$ solution. The $^1$H-NMR spectra of the cyclopalladated complex **($S_S$*,R*,R*)-86** taken at various temperatures shows that they are not fluxional in solution till 243K. Investigation of this fluxionality and solubility of the complex in $CD_3CN$ and extensive precipitation of the complex occurred at lower temperatures. Moreover, from the $^1$H-VT-NMR spectra, the $^t$Bu substituent on sulphur atom and other proton signals remain sharp until 243K.

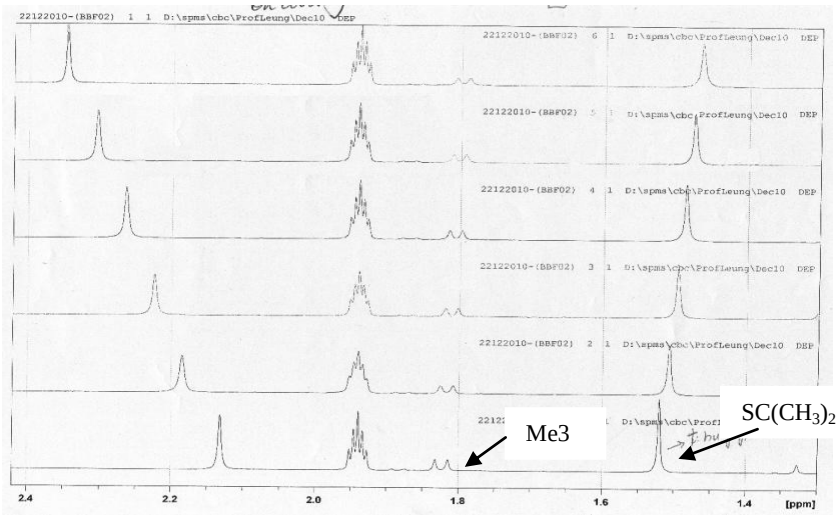


**(a)**

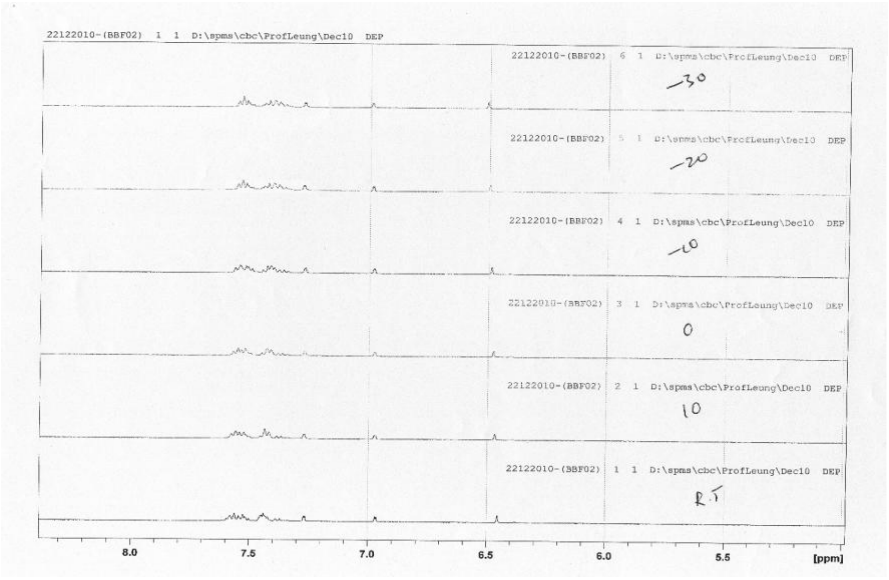


**(b)**

**Figure 3.11(a and b) VT NMR of complex ($S_S$*,R*,R*)-86**

Investigations of the fluxionality of the complex **($S_S$*,R*,R*)-86** at higher temperatures were also undertaken. Figure 3.12 presents the variable-temperature $^1$H-NMR spectra of the complex **($S_S$*,R*,R*)-86** in $CD_3CN$ at higher temperatures. The $^1$H-NMR spectra of the cyclopalladated complex taken at various higher temperatures shown below indicates that they are not fluxional in solution until 348K.

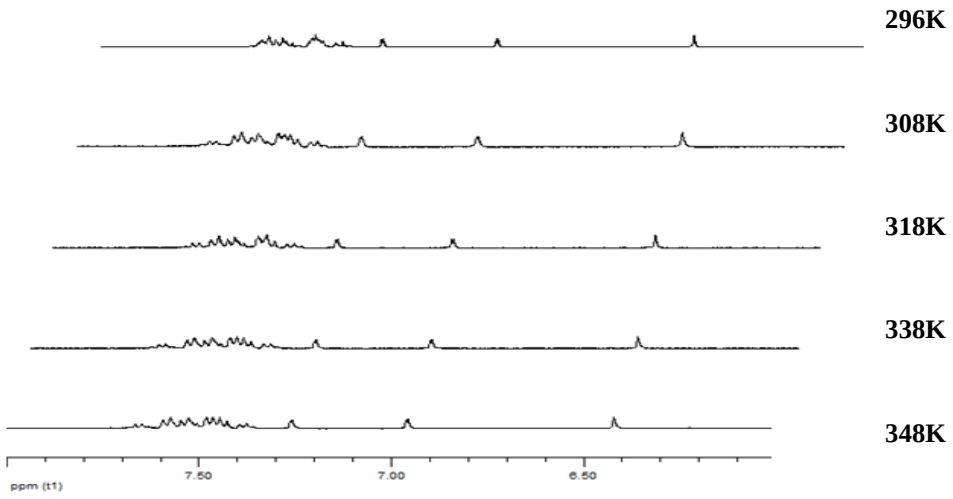


**Figure 3.12 VT NMR of complex ($S_S$*,R*,R*,δ)-86**

Moreover, from the $^{1}$H-VT-NMR spectra, there was no broadening of peaks observed for the $^{t}$Bu substituent on sulphur atom or for the other proton signals and they all remain as sharp peaks upto 348K. Hence, from both the experiments it was concluded that in solution, the process of ring inversion via cleavge of Pd-S bond, followed by the ring inversion and reformation of Pd-S bond with conconmitant inversion of configuration at S to give **(Rs*,R*,R*)-86** with a **λ** ring conformation indicates the absence of pyramidal or ring inversion for complex **($S_S$*,R*,R*,δ)-86**, and as a result sulphur being coordinated to the palladium(II) centre is stereochemically locked with $^{t}$Bu group in axial and the lone pair in equatorial position in solution.

### *3.2.4 Separation of diastereomers palladium complex-87*

The diastereomeric palladium complex **87** contains 4:1 ratio of diastereomers **($R_S$*,S*,R*)-87** and **($S_S$*,R*,R*)-87** respectively. A single crystallization of the diastereomeric mixture from acetonitrile/diethyl ether afforded the less soluble diastereomeric complex **($S_S$*,R*,R*)-87** as yellow crystals in 70% yield and >98% d*e* (according to the $^{1}$H-NMR data) with $[\alpha]_D$ = + **188** (*c* 0.2, $CH_3CN$).

The remaining mother liquor was evaporated to half the volume and seeded with the pure crystals of **($S_S$*,R*,R*)-87** to promote further separation of resolution of remaining compound. After subsequent fractional crystallization, the mother liquor was enriched with diastereomer **($R_S$*,S*,R*)-87** and solvent

was evaporated, and the solid was re-dissolved in minimum amount of analytical grade acetone and recrystallized from acetonitrile/diethylether system. Hence, suitable analytical grade crystals of complex **($R_S$*,S*,R*)-87** were obtained for XRD analysis and according to $^1$H-NMR data, the diastereomer was >95% with $[\alpha]_D$ = **+96** (*c* 0.2, $(CD_3)_2SO$).

The absolute configurations and solid structures of **($R_S$*,S*,R*)-87** and **($S_S$*,R*,R*)-87** were determined by X-ray single crystal diffraction study. It was not possible to assign the ring conformation in solution state as the aromatic protons in $^1$H-NMR spectrum was not well sufficiently well resolved.

### *3.2.4.1 Molecular structure of complex ($R_S$*,S*,R*)-87*

The molecular structure of the chiral complex **($R_S$*,S*,R*)-87** was determined by an X-ray single crystal diffraction study. The yellow coloured crystals with a size of 0.38 x 0.26 x 0.24 $mm^3$ of complex **($R_S$*,S*,R*)-87** were grown by slow diffusion of diethyl ether into an acetonitrile solution of the complex at room temperature. The molecular structure with the numbering scheme is presented in Figure 3.13. Selected bond lengths and bond angles are listed in Table 3.6.

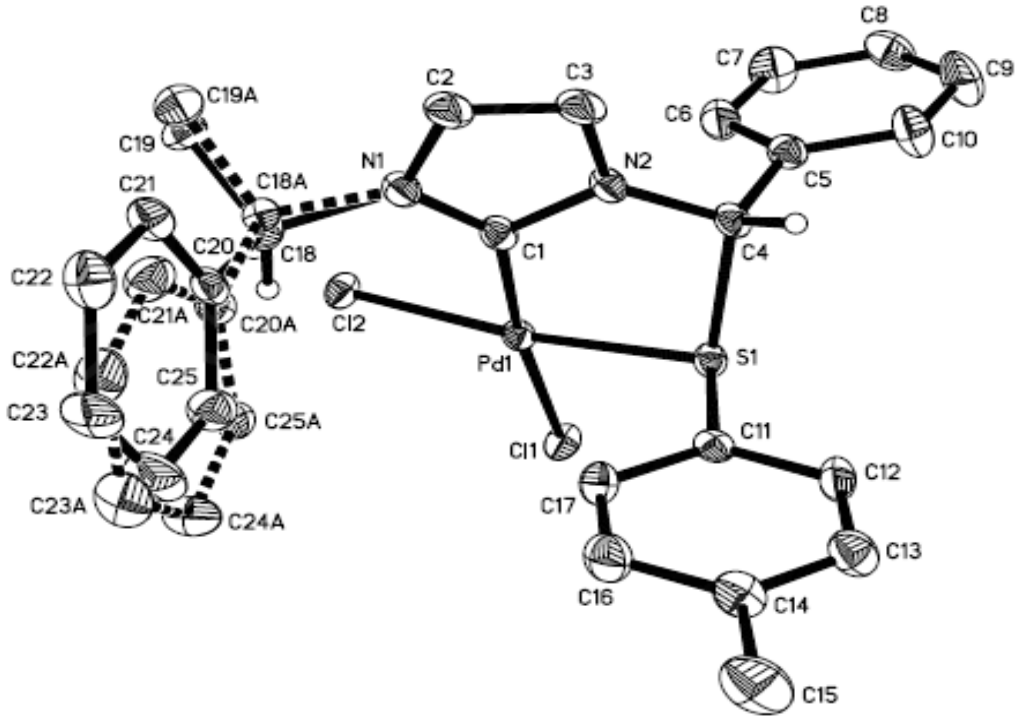


**Figure 3.13** Molecular structure of complex **($R_S$*,S*,R*)-87**; Thermal ellipsoids are drawn at the 50% probability level. Hydrogen atoms except for H **(C4)** andH **(C18)** are omitted for clarity.

There is a slight disorder found on the N1 witig group and the diastereomeric complex **($R_S$*,S*,R*)-87** exhibits a slightly distorted square planar geometry with a bite angle of 83.40°. All the bond lengths and angles are in the normal range as compared to its analogue. The difference in the bond lengths of Pd-Cl(1) [2.352 Å] and Pd-Cl(2) [2.319 Å] elucidates the higher *trans* effect of carbene compared to that of sulphur.

In solid state the complex adopts the **λ** conformation with phenyl at stereogenic centre axially disposed below the coordinating PdCS chelate ring. Upon coordination with palladium, the sulphur atom is stereochemically locked in ***R*** configuration with *p*-tolyl substituent projected almost perpendicularly

above the square plane. This *trans* axial disposition of the phenyl (α) and *p*-tolyl substituent is attributed to the well-defined steric repulsion between the two. It is worth mentioning that the alternate **(Rs,R,R,δ)-87** ring conformation with phenyl substituent on stereogenic carbon in equatorial position suffer a strong repulsion with the (H3) proton on the heterocycle and *p*-tolyl substituent on sulphur atom.

**Table 3.5 Selected bond lengths (Å) and angles (°) of chiral Palladium complex ($R_S$*,S*,R*)-87:**

| | | | |
|---|---|---|---|
| Pd(1)–C(1) | 1.972(5) | C(1)–Pd(1)–S(1) | 83.40(14) |
| Pd(1)–S(1) | 2.274(11) | N(2)–C(4)–C(5) | 116.4(4) |
| Pd(1)–Cl(1) | 2.352(12) | S(1)–C(4)–H(4) | 108.50 |
| Pd(1)–Cl(2) | 2.319(11) | N(2)–C(4)–H(4) | 108.50 |
| C(1)–N(1) | 1.338(6) | C(11)–S(1)–Pd(1) | 111.22(17) |
| C(1)–N(2) | 1.376(6) | C(11)–S(1)–C(4) | 100.0(17) |
| N(1)–C(1)–N(2) | 105.1(4) | Cl(1)–Pd(1)–S(1) | 90.52(4) |
| C(5)–C(4)–S(1) | 108.5(3) | Cl(2)–Pd(1)–S(1) | 172.75(6) |
| N(2)–C(4)–S(1) | 106.1(3) | Cl(1)–Pd(1)–Cl(2) | 91.44(4) |
| N(2)–C(1)–Pd(1) | 117.0 (3) | C(1)–Pd(1)–Cl(1) | 173.47(14) |

*3.2.4.2 Molecular structure of diastereomer ($S_S$*,R*,R*)-87*

The yellow coloured crystals of complex **($S_S$*,R*,R*)-87** with size 0.40 x 0.10 x 0.08 $mm^3$ suitable for single-crystal X-ray diffraction analysis were grown by slow diffusion of diethyl ether into acetonitrile solution of the complex at room temperature. The molecular structure with the numbering scheme is presented in Figure 3.14. Selected bond lengths and bond angles are listed in Table 3.6.

In the solid state, the complex invariably adopts **δ** conformation where both the *p*-tolyl substituent on sulfur and phenyl substituent on α- carbon is placed in axial positions with the former occupying below and the latter on the upper face of the coordinating PdCS ring plane (Figure 3.14). The ***S*** configuration at sulfur is a consequence of the *trans* axial disposition preferred by the phenyl group and the *p*-tolyl on sulfur to minimize steric interactions.

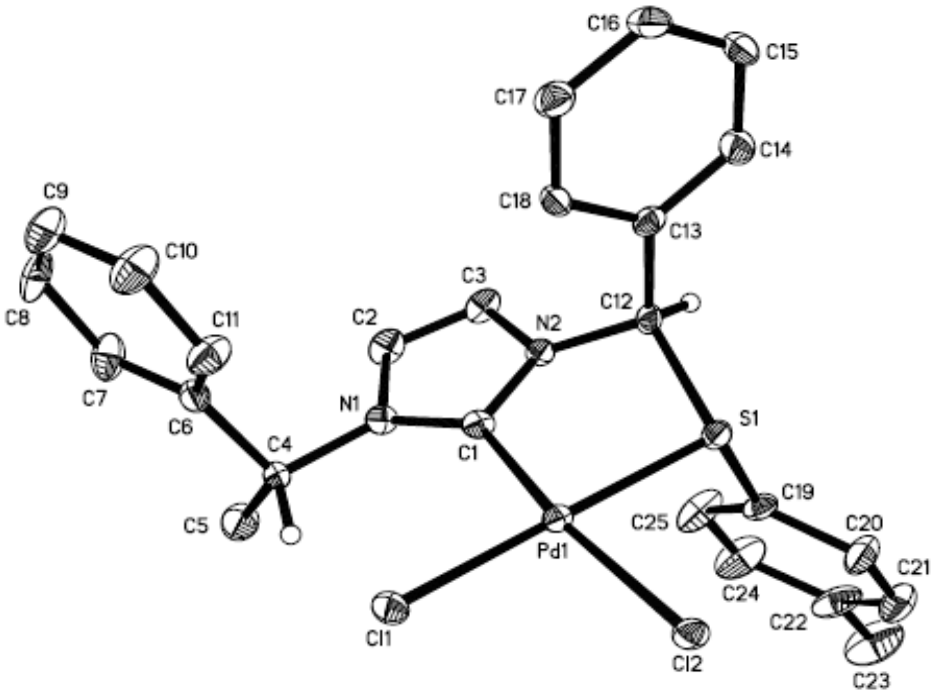


**Figure 3.14** X-ray molecular structure of complex **($S_S$*,R*,R*)-87;** Thermal ellipsoids are drawn at the 50% probability level. . Hydrogen atoms except for H **(C4)** and H **(C12)** are omitted for clarity.

Therefore, the alternative **λ** ring conformation, with the phenyl group in the PdCS coordinating plane placed at equatorial position would be strongly disfavored due to severe steric repulsions between the phenyl group and the (H3) proton/*p*-tolyl substituent on sulphur. As is frequently the case in related systems, the Pd–Cl(2) bond *trans* to the carbene carbon (2.359Å) is longer compared to the Pd–Cl(1) bond *trans* to the sulfur atom (2.327Å) reflecting the

strong *trans* influence effect of the carbene. All the bond lengths and angles are in the normal range and here again the complex exhibited the slight distorted square planar geometry with a bite angle of 84.98$^{o}$.

**Table 3.6 Selected bond lengths (Å) and angles ($^{o}$) of chiral Palladium complex ($S_S$*,R*,R*)-87:**

| | | | |
|---|---|---|---|
| Pd(1)–C(1) | 2.012(4) | C(1)–Pd(1)–S(1) | 84.98(12) |
| Pd(1)–S(1) | 2.259(11) | N(2)–C(12)–S(1) | 106.6(3) |
| Pd(1)–Cl(1) | 2.327(11) | S(1)–C(12)–H(12) | 109.20 |
| Pd(1)–Cl(2) | 2.359(10) | N(2)–C(12)–H(12) | 109.20 |
| C(1)–N(1) | 1.349(5) | C(12)–S(1)–Pd(1) | 99.36(13) |
| C(1)–N(2) | 1.360(6) | C(12)–S(1)–C(19) | 102.98(19) |
| N(1)–C(1)–N(2) | 104.5(3) | C(13)–C(12)–S(1) | 110. 4(3) |
| C(1)–N(2)–C(12) | 123.0(12) | Cl(1)–Pd(1)–S(1) | 174.60(4) |
| C(3)–N(2)–C(12) | 112.2(3) | Cl(1)–Pd(1)–Cl(2) | 170.30(12) |
| N(2)–C(1)–Pd(1) | 117.0 (3) | C(1)–Pd(1)–Cl(1) | 98.82(12) |

### *3.2.5 Separation of diastereomers of platinum complex 88*

In order to compare the ring conformation of the five membered CS ring chelate, a few analogues of platinum(II) were synthesized. The complex exhibits a high degree of solubility in most of the organic solvents compared to palladium(II) complexes. The platinum(II) complexes were prepared using $PtCl_2COD$ as platinum source which can be readily synthesized from $K_2[PtCl_4]$ and *cis* 1,5-cyclooctadiene.

The platinum(II) complex **88** contains 1:1 ratio of two diastereomers **($S_S$*,R*,R*)-88** and **($R_S$*,S*,R*)-88** respectively. A single crystallization of the diastereomeric mixture from acetonitrile/diethyl ether afforded the less soluble diastereomeric complex **($R_S$*,S*,R*)-88** as colourless crystals in 70% yield and >98% d*e* (according to the $^1$H-NMR data) with $[\alpha]_D$ = **+ 100** (*c* 0.2, $CH_3CN$).

The remaining mother liquor was evaporated to half the volume and as usual seeded with the pure crystals of **($R_S$*,S*,R*)-88** to promote further resolution of remaining compound. Successive fraction crystallizations were carried out until the mother liquor was enriched with diastereomer **($S_S$*,R*,R*)-88** and solvent was evaporated. However, the solid failed to crystallize in an array of solvents and according to $^1$H-NMR data, the diastereomeric excess of complex **($S_S$*,R*,R*)-88** was >95% with $[\alpha]_D$ = **+ 190°** (*c* 0.2, $CH_3CN$).

The absolute configuration and solid structure of diastereomeric platinium(II) complexes **($R_S$*,S*,R*)-88** were determined by X-ray single crystal diffractometry. Solution structures of both diastereomers **($S_S$*,R*,R*)-88** & **($R_S$*,S*,R*)-88** were determined by 2D $^1$H-$^1$H ROESY NMR spectroscopic techniques.

*3.2.5.1 Molecular structure of complex ($R_S$*,S*,R*)-88*

Colourless single crystals of size 0.12 x 0.08 x 0.06 mm$^3$ **($R_S$*,S*,R*)-88** were obtained by slow evaporation of a solution in acetone-diethyl ether mixture at room temperature. The molecular structure with the numbering scheme is

presented in Figure 3.15 Selected bond lengths and bond angles are listed in Table 3.7.

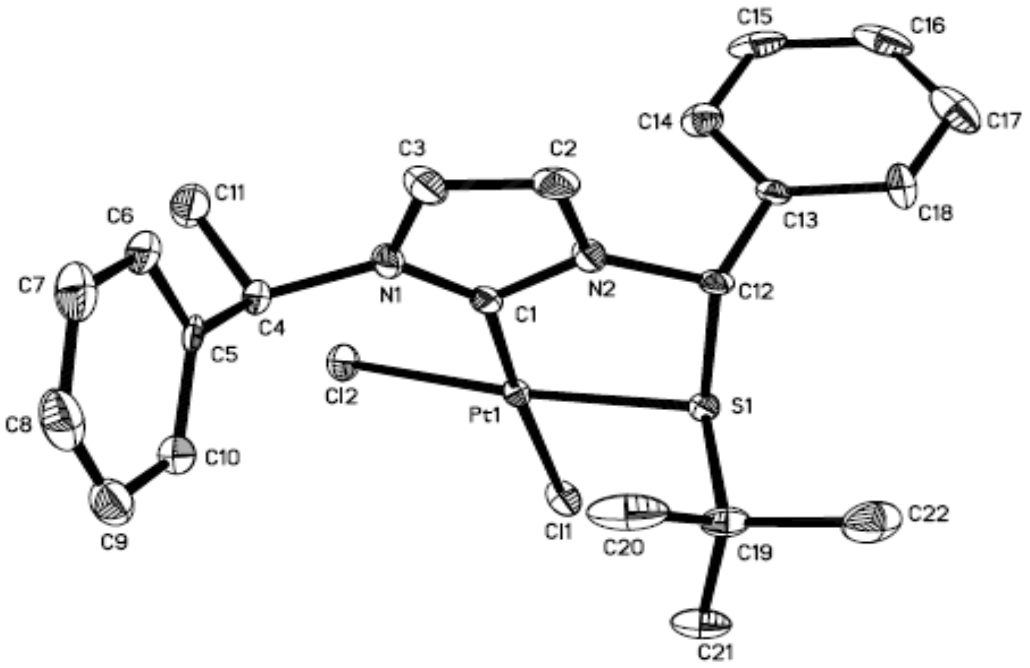


**Figure 3.15** Molecular structure of complex **($R_S$*,S*,R*)-88**; Thermal ellipsoids are drawn at the 50% probability level. Hydrogen atoms are omitted for clarity.

As expected the platinum atom is located in distorted square planar coordination geometry. Similar to **($R_S$*,S*,R*)-88** palladium complex, the organoplatinum five membered ring adopts the **λ** conformation with the sulphur atom pointing above the PtCS coordination plane with comparable bond lengths and angles. Similarly, the phenyl substituent within the CS chelate was also axially disposed below the coordinating plane because of the strong repulsive interaction with H2 proton and $^{t}$Bu substituent, which prevents the free interchange of the former between the axial and equatorial positions. Therefore,

the alternative **δ** ring conformation, with the phenyl group at equatorial position in the PtCS coordinating plane would be highly disfavoured. The chiral sulphur atom has ***R*** configuration and due to higher *trans* effect of carbene to that sulphur is reflected on the longer bond length of Pt–Cl(1)[2.362 Å] compared to Pt–Cl(2)[2.314 Å].

**Table 3.7 Selected bond lengths (Å) and angles (°) of chiral Platinum complex ($R_S$*,S*,R*)-88:**

| | | | |
|---|---|---|---|
| Pt(1)–C(1) | 1.975(5) | C(1)–Pt(1)–S(1) | 85.60(14) |
| Pt(1)–S(1) | 2.245(13) | N(2)–C(12)–S(1) | 106.4(4) |
| Pt(1)–Cl(1) | 2.362(14) | S(1)–C(12)–H(12) | 180.30 |
| Pd(1)–Cl(2) | 2.314(13) | N(2)–C(12)–H(12) | 180.30 |
| C(1)–N(1) | 1.348(6) | C(12)–S(1)–Pt(1) | 99.57(18) |
| C(1)–N(2) | 1.368(7) | C(12)–S(1)–C(19) | 102.3 (3) |
| N(1)–C(1)–N(2) | 104.5(5) | C(13)–C(12)–S(1) | 112.5(4) |
| C(1)–N(2)–C(12) | 124.7(5) | Cl(1)–Pt(1)–S(1) | 89.54(5) |
| N(2)–C(12)–C(13) | 113.0(4) | Cl(1)–Pt(1)–Cl(2) | 89.38(5) |
| N(2)–C(1)–Pt(1) | 116.4(4) | C(1)–Pt(1)–Cl(1) | 174.90(15) |

*3.2.5.2 Solution Structure of diastereomeric complex ($R_S$*,S*,R*)-88*

For the ***S*** absolute configuration at the α-carbon chiral center, the five membered palladacycle adopts **λ** conformation as illustrated in Figure 3.16. The assignment of proton peaks was obtained from the combination of COSY, HMQC and HMBC spectra. Figure 3.15 presents the 2D $^{1}$H-$^{1}$H ROESY NMR spectrum for

**($R_S$*,S*,R*)-88** in $(CD_3)_2SO$. Selected chemical shifts of the complex are given in Table 3.8.

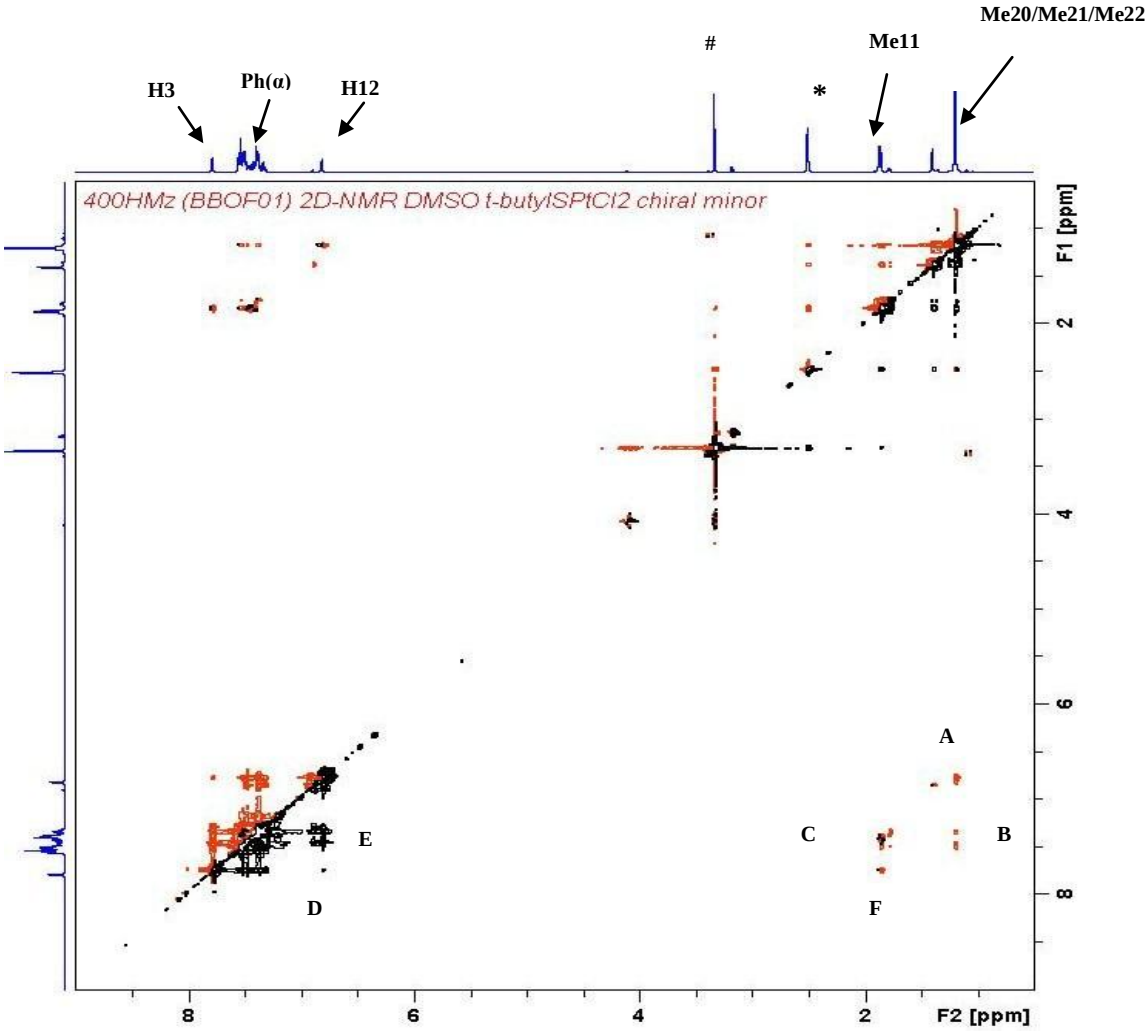


**Figure 3.16** 2D $^1H$-$^1H$ ROSEY NMR spectrum of **($R_S$*,S*,R*)-88** in $(CD_3)_2SO$.

**Selected NOE signals**: *** -** $(CD_3)_2SO$ solvent peak; **#** - $H_2O$ peak; (**A)**: Me20/Me21/Me22 – H12; (**B)**: Me20/Me21/Me21 – H2; (**C)**: Me11 – H4; (**D)**: H12 – H2; (**E)**: H12 – Ph(α); (**F):** Me11-H3.

Signals (A) & (B) seen in the 2D $^1H$-$^1H$ ROESY NMR spectrum, are due to the strong NOE interaction between Me20/Me21/Me22 and H12, H2. The

strong NOE signals (D) & (E) are due to the interaction between H12 and H2, H14/H18(Ph). There is no ring inversion taking place and the complex **($R_S$*,S*,R*)-88** remains locked in **λ** conformation.

**Table 3.8** Selected chemical shifts for **($R_S$*,S*,R*)-88** in $(CD_3)_2SO$.

| **Proton** | **δ(ppm)** |
|---|---|
| Ph(α) | 7.36–7.41(m) |
| H12 | 6.80(s) |
| Me11 | 1.87–1.85(d) |
| Me20/Me21/Me22 | 1.19(s) |

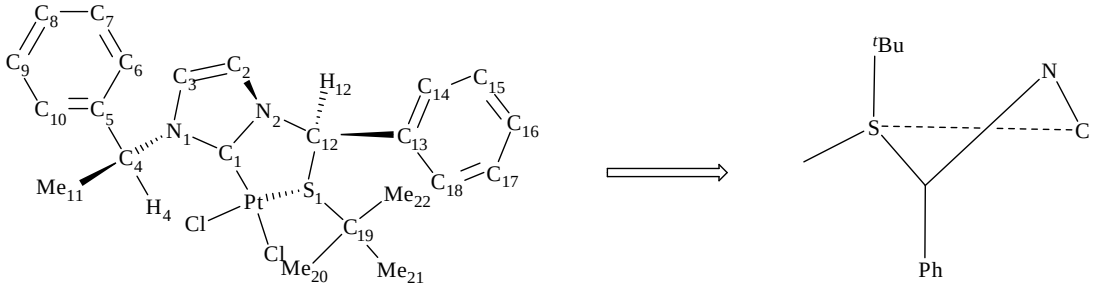


**(Rs*,S*,R*,λ)-88**

**Figure 3.17** Absolute conformation of the PtCS ring.

If the complex **($R_S$*,S*,R*)-88** is able to undergo ring inversion, the presence of the other ring conformer with the phenyl group at the equatorial position within PtCS ring chelate should be detected in the 2D $^1$H-$^1$H ROESY

NMR spectrum. Presence of only one resonance for each chemically non-equivalent proton clearly indicates the existence of a single geometrical isomer in solution. From the absence of any correlations between the Ph(α) protons with $^{t}$Bu protons (Me20/Me21/Me22) in the 2D $^{1}$H-$^{1}$H ROESY NMR, rules out the existence of the other conformer in solution.

Hence, it is clearly pictured that there is no possibility of ring inversion in the five membered chelate of diastereomer **($R_S$*,S*,R*)-88** and the $^{t}$Bu group and lone pair on sulphur are stereochemically locked in axial and equatorial positions in solution.

### *3.2.5.3 Solution Structure of complex* **($S_S$*,R*,R*)-88**

Unfortunately, single crystals for the diastereomeric complex **($S_S$*,R*,R*)-88** suitable for X-ray crystallography could not be obtained froman array of solvents. Nevertheless, the 2D $^{1}$H-$^{1}$H ROESY NMR spectrum was recorded to allow the assignment of the absolute stereochemistry and conformation of the complex. Figure 3.17 presents the 2D $^{1}$H-$^{1}$H ROESY NMR spectrum for **($S_S$*,R*,R*)-88** in $(CD_3)_2SO$.

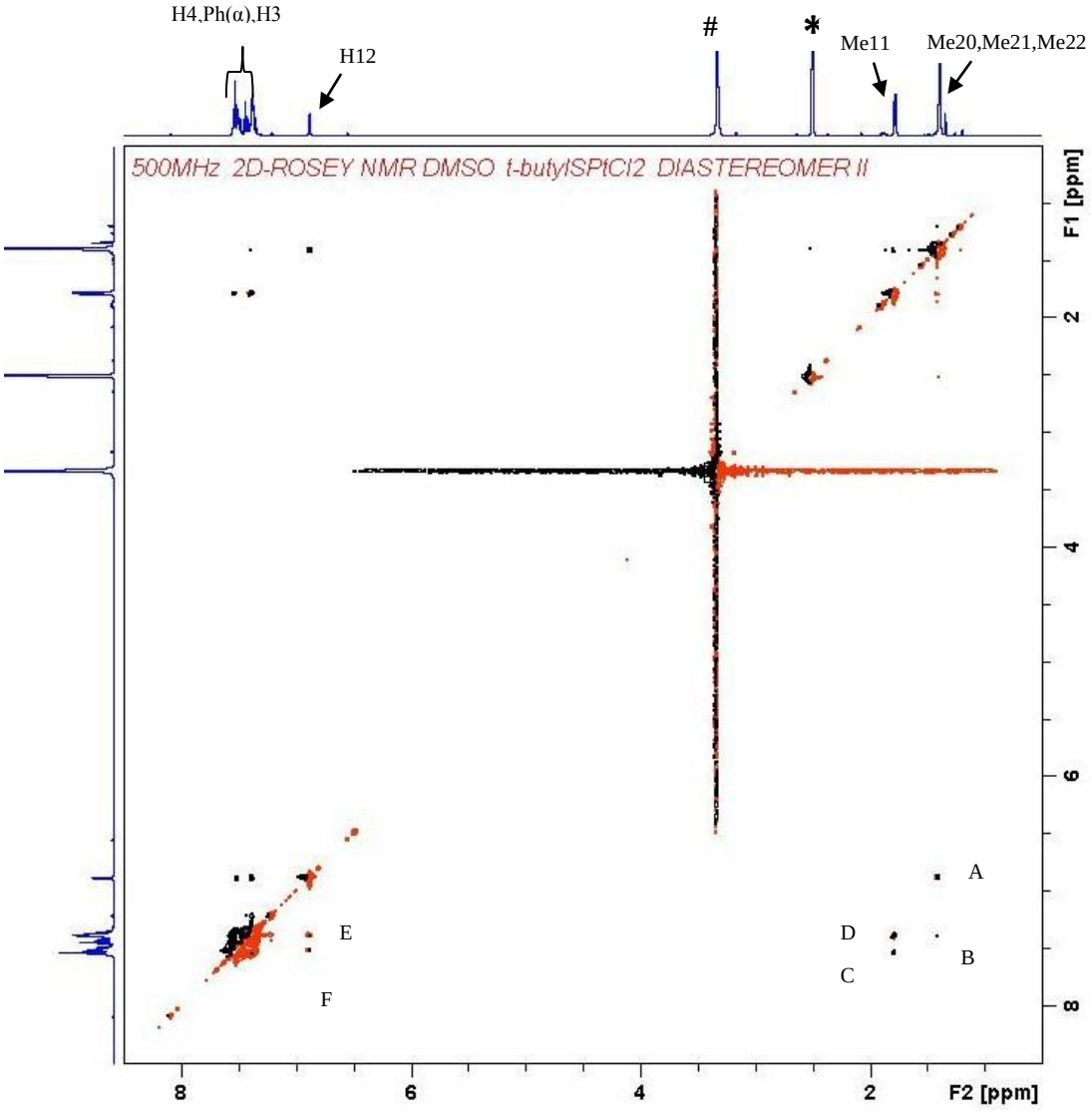


**Figure 3.18** 2D $^{1}$H-$^{1}$H ROSEY NMR spectrum of **($S_S$*,R*,R*)-88** in $(CD_3)_2SO$.

**Selected NOE signals**: **(A)**: Me20/Me21/Me22 – H12; **(B)**: Me11 – H3; **C**: Me11 – H4; **(D)**: Me11 – H3; **(E)**: H12 – Ph(α); **(F)**: H12 – H2; ***** - $(CD_3)_2SO$ solvent peak; **#** - $H_2O$ peak.

**Table 3.9**Selected chemical shifts for **($S_S$*,R*,R*)-88** in $(CD_3)_2SO$.

| **Proton** | **δ (ppm)** |
|---|---|
| Ph(α) | 7.34-7.40(m) |
| H12 | 6.88(s) |
| Me11 | 1.77–1.79(d) |
| Me20/Me21/Me22 | 1.39(s) |

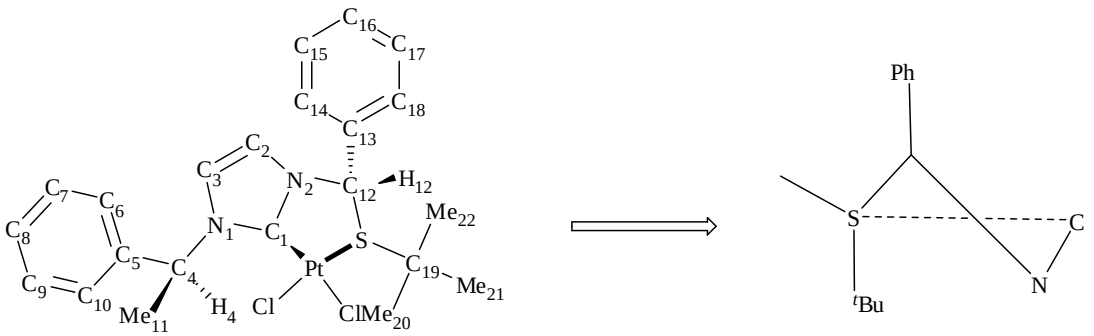


**(Ss*,R*,R*,δ)-88**

**Figure 3.19** Absolute conformation of the PtCS ring.

It is well established that the five-membered palladacycle adopts **δ** conformation when the chiral center has a ***R*** absolute configuration as illustrated in Figure 3.19. The phenyl group on the stereogenic carbon invariably takes up the axial position above the PtCS plane. Signals (A) seen in the ROESY NMR spectrum, are due to the strong interaction between Me20/Me21/Me22and H12. The signals (B), (C) are due to the interaction between Me11 with H4 and H3. The NOE signals of (E), (F) are due to the interaction between H12 with Ph(α) and H2 Moreover, the absence signal due to Me20/Me21/Me22 and Ph(α) completely rules out **λ** conformation in solution. Hence, in solution the complex **($S_S$*,R*,R*)-88** is present as a single isomer and therefore remains stereochemically locked in both solid as well as solution state in **δ(*R*)** conformation.

### *3.2.6 Separation of diastereomers of platinum complex 89*

The ratio of diastereomeric platinum complex **89** were in 4:1 ratio with the mixture of **($R_S$*,S*,R*)-89** and **($S_S$*,R*,R*)-89** respectively. A single crystallization of the diastereomeric mixture from acetonitrile/diethyl ether afforded the less soluble diastereomer **($S_S$*,R*,R*)-89** as colourless crystals in 80% yield and >98% d*e* (according to the $^1$H-NMR data) with $[\alpha]_D$ = **+ 180°** (*c* 0.2, $CH_3CN$).

The remaining mother liquor was subjected to subsequent fraction crystallization with the seeding of pure crystals of **($S_S$*,R*,R*)-89** to promote resolution of remaining compound. However, we failed to obtain suitable analytical grade crystals of complex **($R_S$*,S*,R*)-89** due to their good solubility in an array of solvents and according to $^1$H-NMR data, the diastereomeric excess was >60%.

The absolute configurations and solid structures of **($S_S$*,R*,R*)-89** were determined by X-ray single crystal diffraction. Their ring conformation in solution state was examined with the help of 2D $^1$H-$^1$H ROSEY NMR spectroscopic techniques.

*3.2.6.1Molecular structure of complex ($S_S$*,R*,R*)-89*

Colourless single crystals of size 0.40 x 0.40 x 0.34 mm$^3$ **($S_S$*,R*,R*)-89** were obtained by slow evaporation of a solution in acetone-diethyl ether mixture at room temperature. The molecular structure with the numbering scheme is presented in Figure 3.20 Selected bond lengths and bond angles are listed in

Table 3.9.

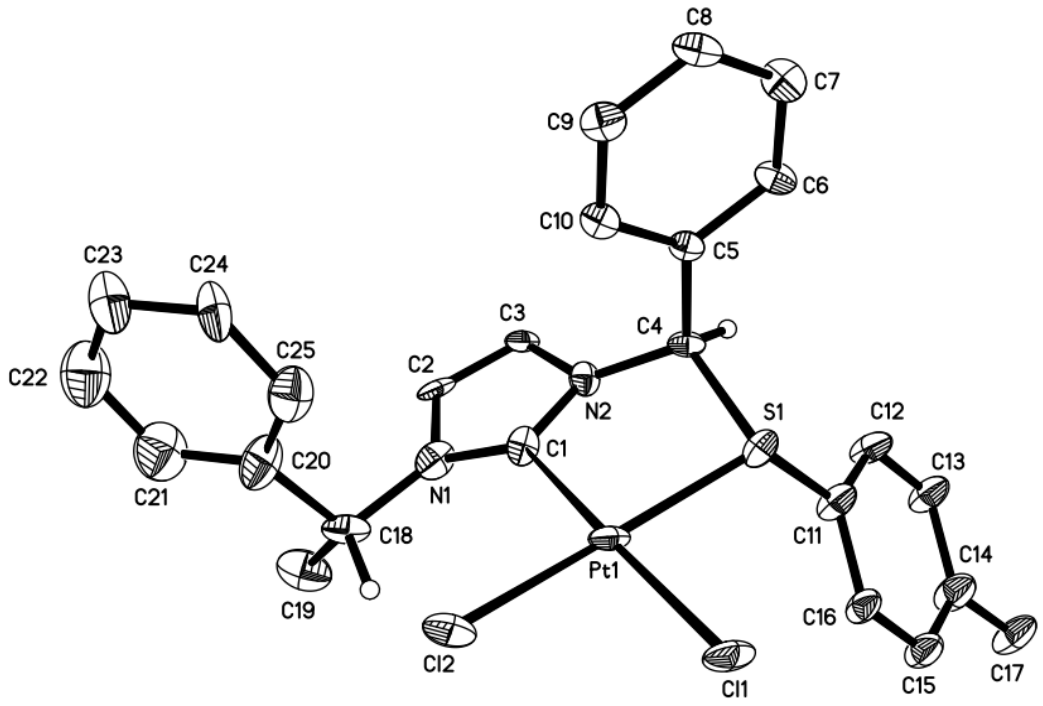


**Figure 3.20** X-ray molecular structure of complex **($S_S$*,R*,R*)-89;** Thermal ellipsoids are drawn at the 50% probability level. Hydrogen atoms except for H **(C4) and** H **(C18)** are omitted for clarity.

Again, in solid state the complex adopts **δ** conformation with *p*-tolyl and phenyl axially *trans* disposed to each other due to steric repulsion between them. The sulphur exhibits the usual ***S*** configuration when coordinated to platinum as a consequence of steric congestion within the coordinating plane. The alternate **λ** ring conformation, with the phenyl group at equatorial position in the PtCS coordinating plane was ruled out due to the invariable repulsive force of H3. The platinum atom is located in a distorted square planar coordination sphere with sulphur in a bidentate manner along with two chloride atoms. The stronger *trans* influence of the NHC donor compared to the sulphur were illustrated by a

Pt(1)–Cl(1) [2.3596 Å] bond longer than Pt(1)–Cl(2) [2.3142 Å] and with C(1)–Pt(1)–S(1) angle of 89.8°.

**Table 3.10 Selected bond lengths (Å) and angles (°) of chiral Platinum complex ($S_S$*,R*,R*)-89:**

| | | | |
|---|---|---|---|
| Pt(1)–C(1) | 1.981(13) | C(1)–Pt(1)–S(1) | 89.8(6) |
| Pt(1)–S(1) | 2.2362(16) | N(2)–C(4)–S(1) | 111.2(13) |
| Pt(1)–Cl(1) | 2.3596(15) | S(1)–C(4)–H(4) | 108.40 |
| Pt(1)–Cl(2) | 2.3142(19) | N(2)–C(4)–H(4) | 108.40 |
| C(1)–N(1) | 1.358(15) | C(11)–S(1)–Pt(1) | 173.45(8) |
| C(1)–N(2) | 1.404(16) | C(4)–S(1)–C(11) | 104.6(9) |
| N(1)–C(1)–N(2) | 104.6(12) | C(5)–C(4)–S(1) | 105.7(13) |
| C(1)–N(2)–C(4) | 119.9(15) | Cl(1)–Pt(1)–S(1) | 88.02(6) |
| C(3)–N(2)–C(4) | 130.0(16) | Cl(1)–Pt(1)–Cl(2) | 88.53(7) |
| N(2)–C(1)–Pt(1) | 114.2(13) | C(1)–Pt(1)–Cl(1) | 177.8(7) |

*3.2.6.2 Solution Structure of complex ($S_S$*,R*,R*)-89*

For the ***R*** absolute configuration at the α-carbon chiral center, the five membered palladacycle can adopt **δ** conformation. Figure 3.21 presents the 2D $^1$H-$^1$H ROESY NMR spectrum for **($S_S$*,R*,R*)-89** in $(CD_3)_2SO$.

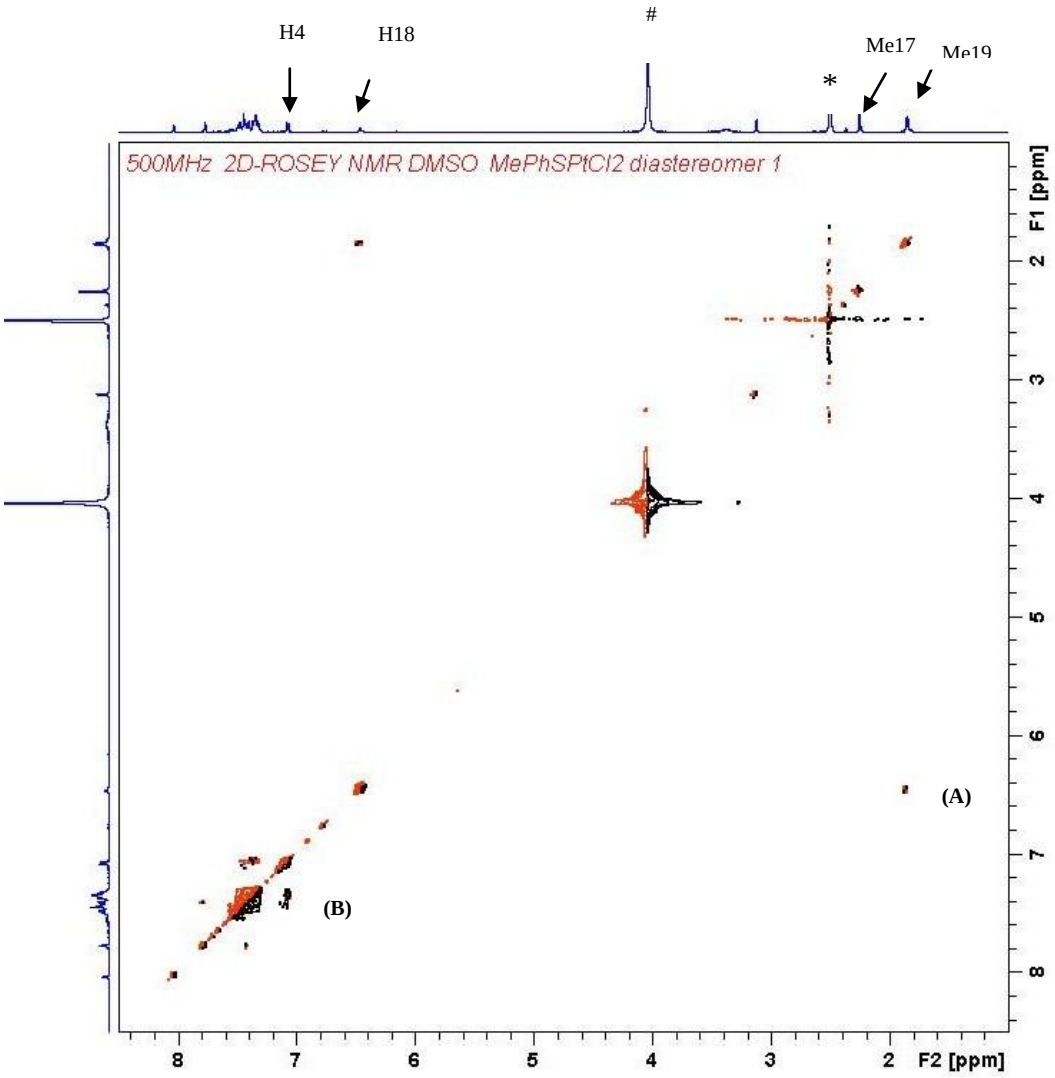


**Figure 3.21** 2D $^{1}$H-$^{1}$H ROSEY NMR spectrum of **($S_S$*,R*,R*)-89** in $(CD_3)_2SO$.

**Selected NOE signals**: **(A)**: Me19 – H18; **(B)**: *p*-tolyl – H4; ***** - $(CD_3)_2SO$ solvent peak; **#** - $H_2O$ peak.

Signal (A) seen in the 2D $^{1}$H-$^{1}$H ROESY NMR, are due to the NOE interaction between Me19 and H18. And a strong NOE signal (B) is due to the interaction between H12/H13(*p*-tolyl) and H4. The absence of a Ph(α) with *p*-tolyl NOE signals completely rules out a **λ** conformation in solution. The Figure 3.22 shows the absolute conformation of the coordinating plane.

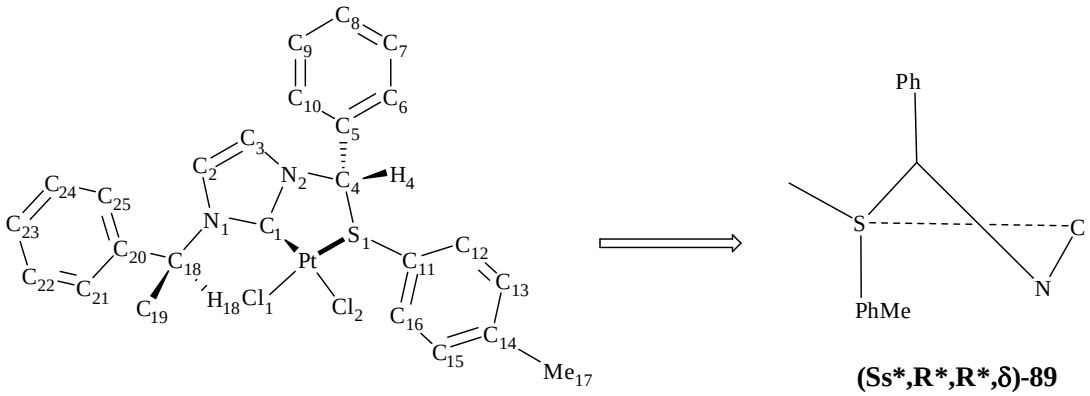


**Figure 3.22** Absolute conformation of the PtCS ring.

Therefore in solution, the process of ring inversion via cleavge of Pd-S bond, followed by the ring inversion and reformation of Pd-S bond with conconmitant inversion of configuration at S to give **(Rs*,R*,R*)-89** with a **λ** ring conformation were absent and hence the complex **($S_S$*,R*,R*)-89** remains locked in **δ** conformation.

## 3.3 Comparison between Metallacycles based on X-ray crystallography data:

In the solid state, the complexes **(Rs*,S*,R*)-86** and **(Rs*,S*,R*)-88** adopts the δ ring conformation, with the phenyl group on the *α* carbon in the axial position below the coordination plane. This can be explained due to repulsive interaction of the $sp^2$ hybridized C and S atoms within the five membered ring (Table 3.11).

**Table 3.11** Comparison between Pd(II) and Pt(II) complexes:

| Complex | Carbene-M/Å | S-M bond/Å | Pd–Cl bond elongation/Å |
|---|---|---|---|
| **(Rs*,S*,R*)-86 (Pd complex)** | 1.982 | 2.2665 | 0.0346 |
| **(Rs*,S*,R*)-88 (Pt complex)** | 1.975 | 2.2451 | 0.0478 |

From X-ray crystallographic data of the above two complexes, the following can be observed.

Firstly, upon changing the metal from Pd(II) to Pt(II) no significant differences was observed in the bond lengths between the carbene carbon to the metal centre. The Carbene–M bond lengths of complexes **(Rs*,S*,R*)-86** and **(Rs*,S*,R*)-88** were all within reported literature values.

Secondly, significant differences were observed on the degree of elongation of the M–Cl bond *trans* to the NHC and we observed M–Cl bond lengths of **(Rs*,S*,R*)-86** is larger compared to **(Rs*,S*,R*)-88.**

And finally, differences were observed on sulphur-metal bond length, with the Pt–S bond distance being shorter compared to Pd–S bond which is in agreement with the stronger coordination of sulphur towards platinum due to the spatial dissimilarity of the 4d and 5d orbitals of the metals.

### 3.4 Catalytic studies on [2,3]-Sigmatropic rearrangement

After obtaining chiral cyclometallated sulphur-NHC complexes and attaining insight into their knowledge about their coordination behaviour on palladium and platinum from our solid state and solution structural studies, their performances in the catalytic [2,3]-sigmatropic rearrangement reaction was investigated.

Recently, Tambar *et al.*[120] reported the first enantioselective [2,3] sigmatropic rearrangement of an amine-*N*-oxide (Scheme 3.9).

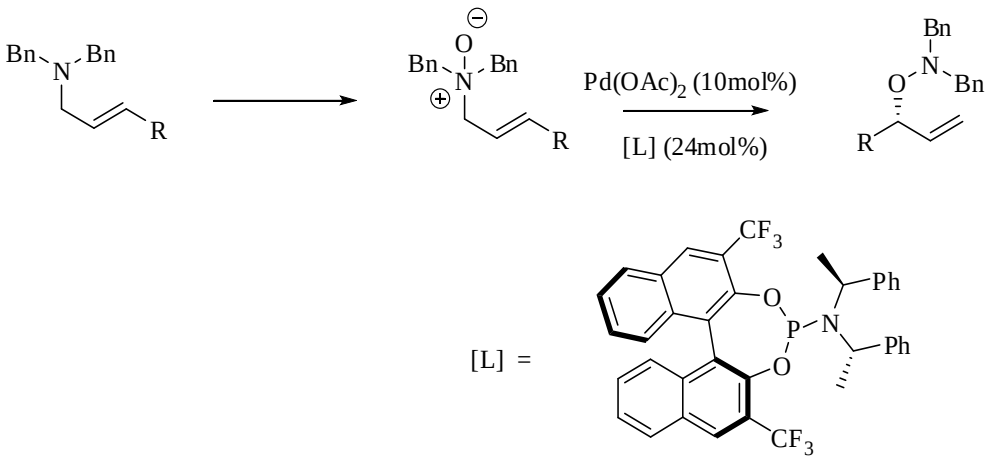


**Scheme 3.9**

Hence, the rearrangement of the amine-N-oxide of *N*,*N*-dibenzylbut-2-en-1-amine was chosen as a model reaction (Scheme 3.10).

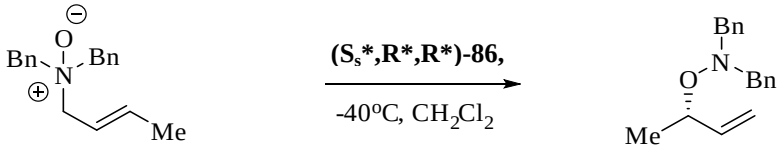


**Scheme 3.10**

The experiment was carried out using 2.5 mol % of **(Ss*,R*,R*)-86** as catalyst, in $CH_2Cl_2$ at –40°C. The reaction proceeded smoothly with full conversion in 5 h but the enantioselectivity was found to be negligible.

It was established from the result obtained for model reaction that the chiral S-NHC cyclopalladated complex was active towards [2,3]-sigmatropic rearrangement furthermore, it was envisaged that enantioselectivity can be achieved by lowering the temperature to –80°C. Therefore, screening of chiral substituted thioether functionalized NHC metal complexes **(Ss*,R*,R*)-86 (Rs*,S*,R*)-86, (Ss*,R*,R*)-87, (Rs*,S*,R*)-87** was initiated and in second series of experiments, the model reaction was attempted with 2.5 mol% of catalyst in $CH_2Cl_2$ at –80°C.

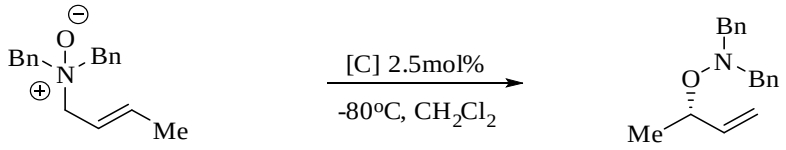


**Scheme 3.11**

**Table 3.12**

| Entry | Catalyst | Time(h) | Conv[a]. | ee%[b] |
|---|---|---|---|---|
| 1 | (Ss*,R*,R*)-86 | 5 | 99 | – |
| 2 | (Rs*,S*,R*)-86 | 5 | 99 | – |
| 3 | (Ss*,R*,R*)-87 | 5 | 99 | – |
| 4 | (Rs*,S*,R*)-87 | 5 | 99 | – |

[a]Determined by 1H-NMR spectra.[b] After the rection time indicated, compounds were worked-up and the ee% were determined by HPLC OD-H, 100% Hx, 0.7 mL/min**.** [c]Reaction conditions: 0.0749mmol of (*E*)-N,N-dibenzylbut-2-en-1-amine, 0.0018mmol of [**C**], at –80°C.

From the results summarized on table 3.12, the reaction proceeded with 100% conversion in 5 h. Conversely, we failed to attain enantioselectivity in a catalytic [2,3]-sigmatropic rearrangement of amine-N-oxide using our chiral S-NHC Pd(II) complexes [**(Rs*,S*,R*,λ)-86, (Ss*,R*,R*,δ)-86** , **(Rs*,S*,R*,λ)-87, (Ss*,R*,R*,δ)-87**] and found that the effect of temperature doesnot improves the enantioselectivity of the reaction.

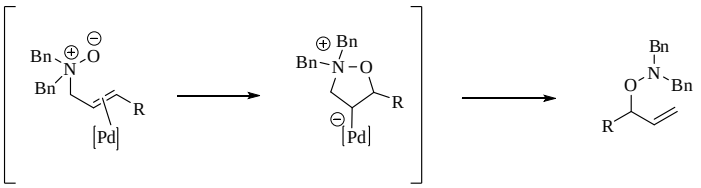


**Scheme 3.12**

The lack of enantioselectivity was suspected to be due to the ineffective nature of catalyst to provide a significant steric influence at the site on the activated olefin which is the rate-determining step to form a product via cyclization-induced mechanism (Scheme 3.12).

## 3.5 Conclusion:

In conclusion, a series of five membered chiral S-NHC metallacycles were synthesized and their ring conformation was determined with the help of X-ray crystallographic and solution phase 2D $^{1}$H-$^{1}$H ROESY NMR studies. From the results obtained it was confirmed that Pd(II) and Pt(II) complexes are structurally rigid and stereochemically locked in chiral ring conformation i.e. either **(Rs*,S*,R*)-λ** or **(Ss*,R*,R*)-δ** in both solid state and solution. Although the catalysts exhibited excellent reactivities in the [2,3]-sigmatropic rearrangement reaction, being complete within 5 h and proceeding in high yields, the enantioselectivities observed for this system were negligible.

Hence, in this thesis an efficient synthetic route has been developed for a series of novel sulphur functionalized NHC based metallacycles. A simple and efficient methodology for allylic amination reaction was also developed with racemic cationic palladium complexes of which complex **(±)-66a** displayed moderate to excellent reactivity for the various substrates as described in chapter two. However, the chiral complexes described in chapter 3 were unable to provide a steric environment to cause any enantioselectivity in the [2,3]-sigmatropic rearrangement of (E)-N,N-dibenzylbut-2-en-1-amine. Since, all our chiral S-NHC cyclopalladated complexes were found to be lack in enantioselectivity, future work in this section will proceed in the direction to attain the required steric environment so as to improve the enantioselectivity of the reaction and this can be presumably obtain by varying the R substituent in sulphur atom of our palladacycles.

# EXPERIMENTAL SECTION

## General Methods

All reactions were carried under an inert atmosphere of Argon using Schlenk line techniques in oven dried glassware. Tetrahydrofuran was distilled from sodium-benzophenone; dichloromethane and acetonitrile were distilled from calcium hydride immediately prior to use. All other solvents and reagents were used as received. $[Pd(\eta^3–C_3H_5)(COD)]^+SbF_6^-$, $PdCl_2(CH_3CN)_2$, were prepared according to the literature procedures. $^1$H-NMR and $^{13}$C-NMR (400 and 100MHz), (500 and 125MHz) spectra were recorded in $CDCl_3$, $CD_3CN$ and $(CH_3)_2SO$ solutions using Bruker Avance 400, 500 NMR spectrometers. Chemical shifts are reported in δ units using $CDCl_3$ (δ 7.26 ppm $^1$H, δ 77.00 ppm $^{13}$C), $CD_3CN$ (δ 1.94 ppm $^1$H, δ 1.32/ 118.26 ppm $^{13}$C) and $(CH_3)_2SO$ (δ 2.50 ppm $^1$H, δ 39.52 ppm $^{13}$C). Coupling constants were recorded in Hz. The following abbreviations for the multiplicity of the peaks are s (singlet), d (doublet), t (triplet), q (quartet), br (broad), m (multiplet). Melting points were obtained using a SRS-Optimelt MPA-100 apparatus and were uncorrected. Mass spectra were obtained on a Finnigan LCQ DECA XP MAX with ESI mode. High resolution mass spectras were obtained using a Water Q-Tof premier also with ESI mode. Optical rotations were measured on the specified solution in 0.1-dm cell at 25°C with a Perkin-Elmer model 341 polarimeter. The Elemental Analysis Laboratory of the Division of Chemistry and Biological Chemistry at the Nanyang Technological University of Singapore performed elemental analyses.

**Synthesis of 1-(2,4,6-trimethylphenyl)-1*H*-imidazole-62a:**

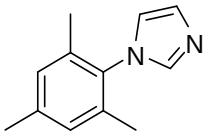

Glacial acetic acid (20 mL), aqueous formaldehyde (6 mL), and aqueous glyoxal (9.2 mL) were stirred in a round bottomed flask and heated at 70ºC. A solution of glacial acetic acid (20 mL), ammonium acetate in water (6.16 g / 4 mL), and mesitylamine (11.2 mL) was added drop-wise to the flask over a period of 30 min. The solution was continuously stirred and heated at 70ºC for 18 h. The reaction mixture was then cooled to room temperature and added drop-wise to a stirred solution of $NaHCO_3$ (60 g) in water (600 mL), resulting in precipitation of the product. The precipitate was isolated and dissolved in ethylacetate, washed with water (3X50 mL), brine and dried over sodium sulphate. On evaporation of organic layer yielded brown-yellow solid. The raw product was re-crystallized using ethyl acetate, to obtain the product 1-(2,4,6-trimethylphenyl)-1*H*-imidazole in a yield of (6 g, 70%). $^{1}$H-NMR (400 MHz, $CDCl_3$): δ 7.43 (s, 1H, NC*H*N), 7.23 (s, 1H, NC*H*=CHN), 6.97 (s, 2H, Ar*H*), 6.89 (s, 1H, NCH=C*H*N), 2.33 (s, 3H, Ar*Me*), 1.99 (s, 6H, Ar*Me*).$^{13}$C-NMR (100MHz, CDCl3): δ 138.8, 137.5, 135.4, 133.4, 129.5, 129.0, 120.0, 21.0, 17.3**.** HRMS: calcd for $C_{12}H_{14}N_2$ $[M + H]^+$ 187.12, found, 187.12.

The data are consistent with that of the literature. [121]

**Synthesis of 1-tert-butyl-1*H*-imidazole-62b:**

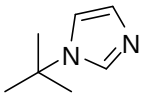

Formaldehyde (20.5 mL, 0.27 mol) was added to the stirred suspension of glyoxal (15.2 mL, 0.27 mol), tert-butylamine (28.8 mL) methanol (200 mL) and distilled water (50 mL) in a round bottomed flask at 70$^{o}$C, followed by dropwise addition of aqueous ammonia (20 mL, 0.27 mol). After 6 h, the reaction mixture was cooled, and volatile impurities were removed using a rotatory evaporator. Dichloromethane (150 mL) was added to the resulting brown oil and extracted with three portions of distilled water. The organic layer was washed with brine and dried over $Na_2SO_4$. On evaporation gave the desired crude product and distillation was carried out at reduced pressure (bp~71$^{o}$C at 1mbar) to obtain colourless 1-tert-butylimidazole (21 g, 62%). $^{1}$H-NMR (400 MHz, $CDCl_3$): δ 7.51 (s, 1H, NC*H*N), 6.94 (s, 1H, NC*H*=CHN), 6.95 (s, 1H, NC*H*=C*H*N), 1.46 (s, 9H, $^{t}$Bu). $^{13}$C-NMR (100 MHz, $CDCl_3$): δ 134.1, 128.8, 116.0, 54.4, 30.3. HRMS: calcd for $C_7H_{12}N_2$ $[M + H]^+$ 125.10, found, 125.11.

**Synthesis of (*R*)-1-(1-phenylethyl)-1*H*-imidazole:**

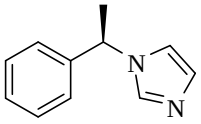

1-(S)-phenylethylamine (25 g, 1 eq) was dissolved in $H_2O$ (210 mL) and phosphoric acid (16 mL) was added till pH 2 was reached. After which, paraformaldehyde (6.2 g) and glyoxal ( 23.8 mL, 40% in $H_2O$) was added to the reaction mixture and was heated to 100$^{o}$C, then saturated ammonium chloride solution ( 11 g, 40 mL $H_2O$) was added dropwise over a period of 1 h. After stirring for another 1 h at 100$^{o}$C, the reaction mixture was cooled to 0$^{o}$C and

sodium hydroxide was added till a pH 12 or higher was observed. The mixture was extracted with methylene chloride (x3, 100 mL), dried over $MgSO_4$ and the solvent was evaporated in vacuum. (viscous transparent oil) was obtained by purification through vacuum distillation. Yield: 18 g (26%), bp: 130°C/7 mbar. $^1$H NMR (500 MHz, $CDCl_3$): δ 7.59 (s, 1H, NC*H*N), 7.33–7.36 (m, 2H, Ar*H*), 7.27–7.31 (m, 1H,Ar*H*), 7.13–7.15 (m, 2H, Ar*H*), 7.08 (s,1H, NC*H*=CHN), 6.93 (s, 1H, NCH=C*H*N), 5.32–5.37 (q, $J_{H-H}$ = 7.0 Hz, 1H, NC*H*$CH_3$), 1.85–1.87 (d, $J_{H-H}$ = 7.5 Hz, 3H, NCHC*H*$_3$). $^{13}$C NMR (100 MHz, $CDCl_3$): δ141.3, 135.8, 129.0, 128.7, 127.9, 125.7, 117.8, 56.3, 21.8. HRMS: calcd for $C_{11}H_{12}N_2[M + H]^+$ 173.10, found, 173.10.

**Synthesis of 3-(bromo(phenyl)methyl)-1-mesityl-1*H*-imidazol-3-ium bromide-63a:**

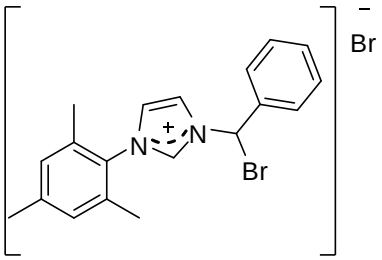


To a stirred 1M solution of $SOBr_2$ (0.826 g, 4.011 mmol), in dicloromethane, 2M solution of 1-(2,4,6-trimethylphenyl)-1H-imidazole (0.75 g, 4.011 mmol) and 2M solution of benzaldehyde (1.062 g, 10.027 mmol) was added simultaneously at –40°C under argon atmosphere. The reaction mixture was slowly warmed to room temperature and allowed to stir for 8 h. On evaporation of the reaction mixture followed by tituration with diethyl ether gave the desired crude product. The crude product was purified by column chromatography on silica using chloroform and methanol as eluent (eluent: chloroform/methanol, 40:1) (1.14 g, 65%). $^1$H-NMR (300 MHz, $CDCl_3$): δ 9.33 (s, 1H, NC*H*N), 8.25 (s, 1H, BrC*H*N), 7.84–7.86 (m, 2H, Ar*H*), 7.75 (s, 1H,

NCH=C*H*N), 7.53–7.58 (m, 3H, Ar*H*), 7.29 (s, 1H, NC*H*=CHN), 7.05 (s, 2H, Ar($Me_3$)*H*), 2.36 (s, 3H, Ar*Me*), 2.04 (s, 6H, Ar*Me*). $^{13}$C-NMR (100 MHz, $CDCl_3$): δ 141.7, 137.7, 134.9, 134.1, 130.8, 130.4, 130.0, 130.0, 129.9, 129.5, 128.2, 124.3, 121.7, 58.4, 21.1, 17.8, 17.7. HRMS: calcd for $C_{19}H_{20}Br_2N_2$[M - Br]$^+$ 355.08, found, 355.08.

**Synthesis of 3-(bromo(phenyl)methyl)-1-tert-butyl-1*H*-imidazol-3-ium bromide-63b:**

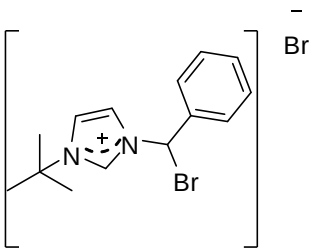


To a stirred 1M solution of $SOBr_2$ (0.826 g, 4.011 mmol) in dichloromethane, 2M solution of 1-tert-butyl-1*H*-imidazole (5 g, 40.326 mmol) and 2M solution of benzaldehyde (4.89 mL, 48.391 mmol) was added simultaneously at –40$^o$C under argon atmosphere. The reaction mixture was slowly warm to room temperature and allowed to stir for 8 h. On evaporation of the reaction mixture followed by tituration with diethyl ether gave the desired pure product (9.75 g, 65%). $^1$H-NMR (400 MHz, $(CD_3)_2SO$): δ 9.79 (s, 1H, NC*H*N), 8.33 (s, 1H, NCH=C*H*N), 8.26 (s, 1H, NC*H*=CHN), 8.12 (s, 1H, Br*H*Ar), 7.72–7.74 (m, 2H, Ar*H*), 7.50–7.54 (m, 3H, Ar*H*), 1.61 (s, 9H, $^t$Bu).$^{13}$C-NMR (100 MHz, $CDCl_3$): δ 136.2, 134.8, 130.4, 129.1, 127.5, 122.0, 121.7, 60.0, 58.3, 28.6. HRMS: calcd for $C_{14}H_{18}Br_2N_2$[M - Br]$^+$ 293.06, found, 293.06.

**Synthesis of 3-mesityl-1-(phenyl(phenylthio)methyl)-1H-imidazol-3-ium bromide-64a:**

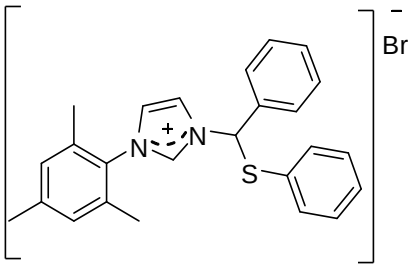


To a stirred solution of 3-(bromo(phenyl)methyl)-1-mesityl-1*H*-imidazol-3-ium bromide (1 g, 2.304 mmol) in dry dichloromethane (50 mL) at – 40$^{o}$C, sodium benzenethiolate (0.304 g, 2.304 mmol) was added. The reaction mixture was warmed to room temperature and allowed to stir for another 4 h. On completion of reaction by TLC, the reaction mixture was filtered and filtrate was evaporated followed by tituration with diethyl ether to yield the desired crude product. The pure product was purified by column chromatography using silica gel and chloroform–methanol as eluent (eluent: chloroform/methanol, 100:3). (0.856 g, 80%). $^{1}$H-NMR(400 MHz, $CDCl_3$): δ 10.69 (s, 1H, NC*H*N), 8.76 (s, 1H, NC*H*S), 7.97–7.98 (d, 2H, Ar*H*), 7.88 (s, 1H, NCH=C*H*N), 7.77–7.90 (d, $J_{H–H}$ = 7.6 Hz, 2H, SAr*H*), 7.44–7.49 (m, 3H, Ar*H*), 7.32–7.36 (t, $J_{H–H}$ = 7.6 Hz, 2H, SAr*H*), 7.27–7.29 (m, 1H, SAr*H*), 6.95 (s, 1H, NC*H*=CHN), 6.91 (s, 1H, Ar($Me_3$)*H*), 6.88 (s, 1H, Ar($Me_3$)*H*), 2.29 (s, 3H, Ar*Me*), 1.93 (s, 3H, Ar*Me*), 1.51 (s, 3H, Ar*Me*).$^{13}$C-NMR (100 MHz, $CDCl_3$): δ 141.4, 137.8, 134.4, 134.1, 133.9, 133.2, 130.3, 130.3, 130.0, 129.8, 129.7, 129.5, 129.1, 127.8, 123.3, 120.2, 66.7, 21.1, 17.6, 17.0. HRMS: calcd for $C_{25}H_{25}N_2SBr$ $[M - Br]^+$ 385.17, found, 385.91.

**Synthesis of 1-tert-butyl-3-(phenyl(phenylthio)methyl)-1*H*-imidazol-3-ium bromide- 64b:**

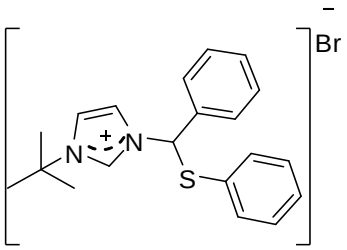


To a stirred solution of 3-(bromo(phenyl)methyl)-1-tert-butyl-1*H*-imidazol-3-ium bromide (1 g, 2.689 mmol) in dry dichloromethane (50 mL) at -40$^{o}$C, sodium benzenethiolate (0.354 g, 2.689 mmol) was added. The reaction mixture was warmed to room temperature and allowed to stir for another 4 h. On completion of reaction by TLC, the reaction mixture was filtered and filtrate was evaporated followed by tituration with diethyl ether to yield the desired crude product. The pure product was purified by column chromatography using silica gel and chloroform–methanol as eluent (eluent: chloroform/methanol, 100:3). (0.886 g, 82%). $^{1}$H-NMR (400 MHz, $CDCl_3$): δ 10.52 (s, 1H, NC*H*N), 8.09 (s, 1H, NC*H*S), 7.89–7.92 (m, 2H, SAr*H*), 7.60–7.64 (m, 2H, Ar*H*), 7.56 (s, 1H, NCH=C*H*N), 7.49 (s, 1H, NC*H*=CHN) 7.42–7.44 (m, 3H, Ar*H*), 7.29–7.33 (m, 3H, SAr*H*), 1.47 (s, 9H, $^{t}$Bu). $^{13}$C-NMR (100 MHz, $CDCl_3$): δ 135.9, 134.0, 133.9, 130.3, 130.1, 129.6, 129.4, 129.3, 128.0, 119.4, 119.3, 67.1, 60.3, 29.8. HRMS: calcd for $C_{20}H_{23}N_2SBr$ $[M - Br]^+$ 323.16, found 323.15.

**Synthesis of 1-tert-butyl-3-(phenyl(*p*-tolylthio)methyl)-1*H*-imidazol-3-ium bromide- 64c:**

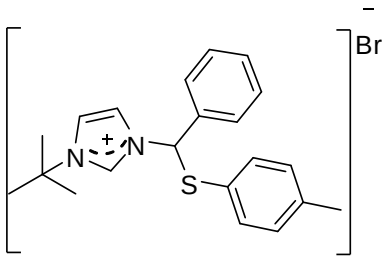


To a stirred solution of 3-(bromo(phenyl)methyl)-1-tert-butyl-1*H*-imidazol-3-ium bromide (1 g, 2.688 mmol) in dry dichloromethane (50 mL) at –40$^{o}$C, sodium 4-methylbenzenethiolate (0.393 g, 2.689 mmol) was added. The reaction mixture was warmed to room temperature and allowed to stir for another 4 h. On completion of reaction by TLC, the reaction mixture was filtered and filtrate was evaporated followed by tituration with diethyl ether to yield the desired crude product. The residue was chromatographed on silica gel with the elution of methanol–chloroform (eluent: chloroform/methanol, 100:3). The fraction of the desired product was collected and concentrated to yield **64c** as white hygroscopic solids. (0.864 g, 80%). $^{1}$H-NMR (400 MHz, $CD_2Cl_2$): δ 10.60 (s, 1H, NC*H*N), 8.06 (s, 1H, NC*H*S), 7.86–7.88 (m, 2H, SAr*H*), 7.52 (s, 1H, NCH=C*H*N), 7.44–7.49 (m, 5H, Ar*H*), 7.15 (s, 1H, SAr*H*), 7.12–7.13 (m, 2H, SAr*H*; NC*H*=CHN), 2.30 (s, 3H, SAr*Me*), 1.44 (s, 9H, $^{t}$Bu).$^{13}$C-NMR (100 MHz, $CD_2Cl_2$): δ 140.0, 136.2, 134.4, 134.2, 130.3, 130.2, 129.3, 127.9, 126.7, 119.3, 119.1, 67.2, 29.6, 20.9. HRMS: calcd for $C_{21}H_{25}N_2SBr$ $[M - Br]^+$ 337.17, found 337.17.

**Synthesis of 1-tert-butyl-3-(tert-butylthio(phenyl)methyl)-1*H*-imidazol-3-ium bromide-64d:**

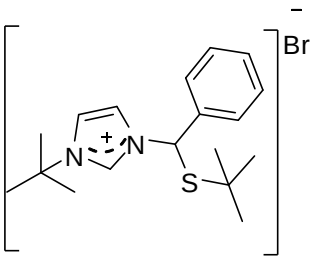


To a stirred solution of 3-(bromo(phenyl)methyl)-1-tert-butyl-1*H*-imidazol-3-ium bromide (1 g, 2.688 mmol) in dry dichloromethane (50 mL) at –40$^{o}$C, sodium 2-methylpropane-2-thiolate (0.3 g, 2.688 mmol) was added. The reaction mixture was warmed to room temperature and allowed to stir for another 4 h. On completion of reaction monitored through TLC, the reaction mixture was filtered and filtrate was evaporated followed by tituration with diethyl ether to yield the desired crude product. The pure product was purified by column chromatography using silica gel and chloroform–methanol as eluent (eluent: chloroform/methanol, 100:3). (0.8 g, 78%). $^{1}$H-NMR (400MHz, $(CD_3)_2SO$): δ 9.86 (s, 1H, NC*H*N), 8.34 (s, 1H, NCH=C*H*N), 8.17 (s, 1H, NC*H*=CHN), 7.38–7.48 (m, 5H, Ar*H*), 7.12 (s, 1H, NC*H*S), 1.61 (s, 9H, S$^{t}$Bu), 1.29 (s, 9H, $^{t}$Bu). $^{13}$C-NMR (100 MHz, $(CD_3)_2SO$): δ 137.5, 133.9, 129.1, 129.0, 126.4, 121.7, 121.3, 64.0, 60.3, 46.5, 30.1, 28.9. HRMS: calcd for $C_{18}H_{27}N_2SBr$ $[M - Br]^+$ 303.19, found 303.19.

**Synthesis of (1-mesityl-3-(phenyl(phenylthio)methyl)-2,3-dihydro-1*H*-imidazol-2-yl) silver(II) bromide-65a:**

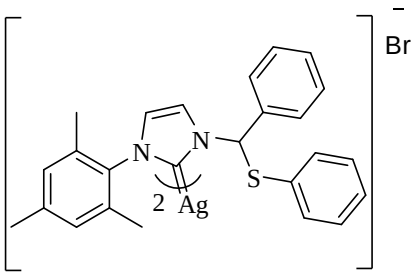


Silver(I)oxide (0.234 g, 1.006 mmol) was added to a solution of 3-mesityl-1-(phenyl(phenylthio)methyl)-1*H*-imidazol-3-ium bromide (0.85 g, 1.831 mmol) in $CH_2Cl_2$ (25 mL), and the suspension was stirred for 4 h at room temperature in dark. The mixture was filtered off through a small celite plug and concentrated to afford crude product.(0.9 g, 89%). $^1$H-NMR (400 MHz, $CDCl_3$):δ 7.87–7.90 (m, 4H, Ar*H*), 7.80–7.82 (m, 2H, NC*H*=CHN), 7.67–7.71 (m, 2H, SAr*H*), 7.58–7.60 (m, 2H, SAr*H*), 7.53–7.56 (m, 4H, Ar*H*), 7.48–7.50 (m, 4H, SAr*H*), 7.44–7.46 (m, 2H, Ar*H*), 7.33–7.34 (m, 1H, NCH=C*H*N), 7.12 (s, 2H, SAr*H*), 6.96 (s, 1H, NCH=C*H*N), 6.85–6.91 (m, 6H, NC*H*S; Ar($Me_3$)*H*), 2.29 (s, 6H, Ar*Me*), 1.90 (s, 3H, Ar*Me*), 1.81 (s, 3H, Ar*Me*), 1.67 (d, 3H, Ar*Me*), 1.62 (d, 3H, Ar*Me*). $^{13}$C-NMR (100 MHz, $CD_3Cl$):δ 139.6, 136.1, 134.5, 134.4, 133.9, 129.9, 129.6, 129.5, 129.4, 129.3, 129.3, 129.2, 126.6, 72.6, 21.0, 17.8, 17.6, 17.5. HRMS: calcd for $C_{50}H_{48}AgN_4S_2$ $[M + H]^+$ 877.25, found 877.24.

**Synthesis of (1-(*tert*-butyl)-3-(phenyl(phenylthio)methyl)-2,3-dihydro-1*H*-imidazol-2-yl)silver(II) bromide-65b:**

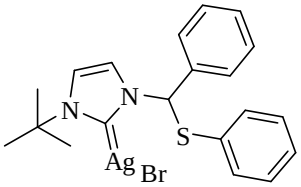

Silver(I)oxide (0.280 g, 1.2 mmol) was added to a solution of 1-tert-butyl-3-(phenyl(phenylthio)methyl)-1*H*-imidazol-3-ium bromide (0.88 g, 2.189 mmol) in $CH_2Cl_2$ (25 mL), and the suspension was stirred for 4 h at room temperature in dark. The mixture was filtered off through a small Celite plug and concentrated to afford crude product (0.958 g, 86%). $^1$H-NMR(400 MHz, $CDCl_3$): δ 7.48–7.51 (m, 2H, Ar*H*; NC*H*=CHN), 7.41–7.43 (m, 3H, Ar*H*), 7.32–7.35 (m, 2H, SAr*H*; Ar*H*), 7.14 (s, 1H, NCH=C*H*N), 6.99 (s, 1H, NC*H*S), 1.56 (s, 9H, $^t$Bu).$^{13}$C-NMR (100 MHz, $CD_3Cl$): δ 136.0, 134.5, 130.7, 129.9, 129.5, 129.4, 129.2, 127.0, 119.8, 117.3, 73.9, 57.8, 31.7, –0.03. HRMS:(calcd) for $C_{20}H_{22}N_2SAgBr$ [M - Br]$^+$ 429.34, found 429.37.

**Synthesis of (1-(tert-butyl)-3-(phenyl(p-tolylthio)methyl)-2,3-dihydro-1H-imidazol-2-yl)silver(II) bromide-65c:**

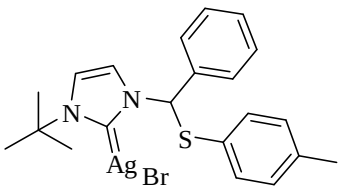

Silver(I)oxide (0.264 g, 1.137 mmol) was added to a solution of 1-tert-butyl-3-(phenyl(*p*-tolylthio)methyl)-1*H*-imidazol-3-ium bromide (0.86 g, 2.067 mmol) in $CH_2Cl_2$ (25 mL) and the suspension was stirred for 4 h at room temperature in dark. The mixture was filtered off through a small Celite plug and

concentrated to afford crude product.(0.92g, 86%). $^{1}$H-NMR(400 MHz, $CDCl_3$): δ 7.47–7.48 (m, 2H, SAr*H*), 7.38–7.43 (m, 3H, Ar*H*), 7.30–7.31 (d, $J_{H–H}$ = 2.0 Hz, 1H, NC*H*=CHN), 7.20–7.22 (m, 2H, Ar*H*), 7.10–7.14 (m, 3H, NCH=C*H*N; SAr*H*), 6.91 (s, 1H, NC*H*S), 2.31 (s, 3H, SAr*Me*), 1.56 (s, 9H, $^{t}$Bu).$^{13}$C-NMR(100 MHz, $CDCl_3$): δ 139.79, 136.04, 134.62, 130.61, 129.42, 129.10, 127.17, 126.97, 119.76, 117.31, 74.10, 57.74, 31.64, 21.21. HRMS:(calcd) for $C_{21}H_{24}N_2SAgBr$ $[M - Br]^+$ 443.07, found 443.07.

**Synthesis of (1-(*tert*-butyl)-3-((*tert*-butylthio)(phenyl)methyl)-2,3-dihydro-1*H*-imidazol-2-yl)silver(II) bromide-65d:**

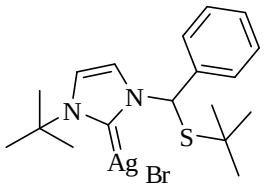


Silver(I)oxide (0.267 g, 1.15 mmol) was added to a solution of 1-(*tert*-butyl)-3-((*tert*-butylthio)(phenyl)methyl)-1*H*-imidazol-3-ium bromide (0.8 g, 2.09 mmol) in $CH_2Cl_2$ (25 mL) and the suspension was stirred for 4 h at room temperature in dark. The mixture was filtered off through a small Celite plug and concentrated to afford crude product. (0.90 g, 88%) $^{1}$H-NMR (400 MHz, $CDCl_3$): δ 7.56–7.57 (d, $J_{H–H}$ = 2 Hz, 1H, NC*H*=CHN), 7.28–7.35 (m, 5H, Ar*H*), 7.23 (d, $J_{H–H}$ = 2.0 Hz, 1H, NCH=C*H*N), 6.91 (s, 1H, NC*H*S), 1.73 (s, 9H, S$^{t}$Bu), 1.33 (s, 9H, $^{t}$Bu).$^{13}$C-NMR(100 MHz, $CDCl_3$): δ 138.5, 129.0, 128.7, 126.5, 119.1, 118.4, 68.5, 58.1, 46.3, 31.8, 31.6, 30.9. HRMS:(calcd) for $C_{18}H_{26}N_2SAgBr$ $[M - Br]^+$ 409.09, found 409.1.

**Synthesis of cationic palladium complex-(±)-66a:**

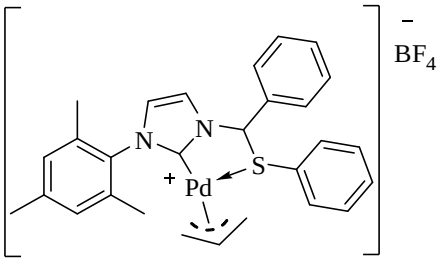


0.9 g (1.58 mmol) of bis(1-mesityl-3-(phenyl(phenylthio)methyl)-2,3-dihydro-1*H*-imidazol-2-yl)silver **65a** and $[Pd(\eta^3–C_3H_5)(COD)]^+BF_4^-$, (0.560 g, 1.58 mmol) in dichloromethane were charged in schlenk tube under argon atmosphere. The mixture was stirred in the dark for 4 h at room temperature, filtered through Celite, concentrated, and the residue was titurated with hexane to afford **66a** (0.87 g, 90%) as a greyish white solid. $^1$H-NMR(400 MHz, $CDCl_3$)**:** δ 7.55–7.57 (m, 1H), 7.52–7.53 (m, 1H), 7.46–7.48 (m, 1H), 7.32–7.44 (m, 7H), 7.27 (m, 1H), 7.22 (m, 1H), 7.08–7.09 (m, 3H), 5.25–5.35 (sep, $J_{H–H}$ = 6.9 Hz, 1H), 4.28–4.30 (m, 1H), 3.12–3.15 (m, 1H), 3.03–3.06 (m, 1H), 2.61–2.69 (dd, $J_{H–H}$ = 12.6 Hz, 1H), 2.42 (s, 3H), 2.12-2.06 (s, 3H), 2.05–1.97 (s, 3H). $^{13}$C-NMR(100 MHz, $CDCl_3$)**:** δ179.9, 140.2, 136.6, 135.6, 135.3, 134.9, 134.5, 133.2, 133.1, 131.3, 130.3, 130.2, 130.1, 130.0, 129.5, 129.4, 129.3, 129.1, 129.0, 128.6, 127.3, 123.9, 123.8, 122.2, 122.1, 119.8, 119.1, 75.0, 69.4, 69.2, 60.6, 60.1, 21.2, 17.7, 17.6, 17.6. HRMS: calcd for $C_{28}H_{29}N_2PdSBF_4$ $[M – BF_4]^+$ 532.13, found 532.12.

**Synthesis of palladium complex (±)-66b:**

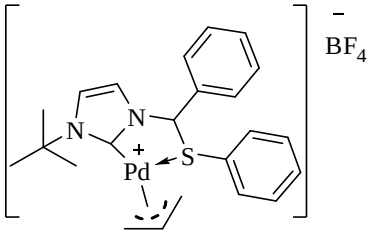

This complex was prepared in a manner analogous to that described for **66a**, using 0.958 g (1.889 mmol) of (1-(*tert*-butyl)-3-(phenyl(phenylthio)methyl)-2,3-dihydro-1*H*-imidazol-2-yl)silver(II) bromide and $[Pd(\eta^3–C_3H_5)(COD)]^+SbF_6^–$, (0.646 g, 1.889 mmol) in dry dichloromethane (20 mL) under argon atmosphere to yield a greyish white powder (0.94 g , 90%). $^1$H-NMR **(**400 MHz, $CD_2Cl_2$**):** δ 7.33–7.51 (m, 18H), 7.28 (b, 2H), 7.13–7.14 (m, 3H), 7.01 (s, 1H, NC*H*S), 6.71–6.74 (m, 2H), 5.58–5.77 (m, 2H), 4.66–4.72 (dd, $J_{H–H}$ = 6.4 Hz, 2H), 4.36–4.38 (d, $J_{H–H}$ = 7.6 Hz, 2H), 3.53–3.65 (dd, $J_{H–H}$ = 13.0 Hz, 2H), 3.17–3.21 (d, $J_{H–H}$ = 13.6 Hz, 2H), 1.81–1.82 (d, $J_{H–H}$ = 4.0 Hz, 18H). $^{13}$C-NMR **(**100 MHz, $CD_2Cl_2$**):** δ131.8, 131.7, 130.4, 130.4, 130.2, 130.1, 129.4, 129.3, 127.3, 126.9, 121.1, 120.8, 119.6, 119.5, 119.3, 68.5, 68.2, 59.3, 59.3, 31.0, 30.9. HRMS: calcd for $C_{23}H_{27}N_2PdSBF_4$ $[M – BF_4]^+$ 469.12, found 469.13.

**Synthesis of palladium complex-(±)-66c:**

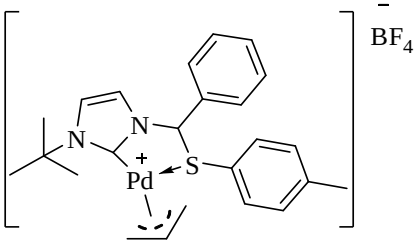

This complex was prepared in a manner analogous to that described for **66a**, using 0.92 g (1.76 mmol) of (1-mesityl-3-(phenyl(*p*-tolylthio)methyl)-2,3-dihydro-1*H*-imidazol-2-yl)silver(II) bromide and (0.602 g, 1.76 mmol) $[Pd(\eta^3–$

$C_3H_5$)(COD)]$^+SbF_6^-$ in dry dichloromethane (20 mL) under argon atmosphere to yield a greyish white powder (0.91 g, 90%). $^1$H-NMR **(**400 MHz, $CD_2Cl_2$)**:** 7.33–7.43 (m, 11H), 7.19–7.28 (m, 7H), 7.12–7.16 (m, 3H), 7.00 (s, 1H, NC*H*S), 6.41–6.60 (m, 2H), 5.59–5.77 (m, 2H), 4.67–4.72 (dd, $J_{H–H}$ = 5.6 Hz, 2H), 4.36–4.37 (d, $J_{H–H}$ = 6.6 Hz, 2H), 3.53–3.64 (dd, $J_{H–H}$ = 12.8 Hz, 2H), 3.16–3.21 (dd, $J_{H–H}$ = 13.0 Hz, 2H), 2.37 (s, 3H, SAr*Me*), 2.35 (s, 3H, SAr*Me*), 1.83–1.84 (d, $J_{H–H}$ = 3.6 Hz, 18H). $^{13}$C-NMR **(**100 MHz, $CD_2Cl_2$)**:** δ177.8, 177.5, 142.9, 142.7, 130.8, 130.8, 130.4, 130.3, 129.4, 129.3, 127.3, 126.9, 121.1, 120.8, 119.5, 119.5, 119.3, 70.7, 70.5, 68.3, 68.1, 59.3, 59.2, 31.0, 30.9, 21.1, 21.0. HRMS: calcd for $C_{24}H_{29}N_2PdSBF_4$ $[M – BF_4]^+$ 482.12, found 482.12.

**Synthesis of palladium complex (±)-66d:**

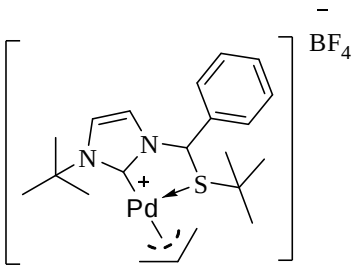


This complex was prepared in a manner analogous to that described for **66a**, using 0.9 g (1.844 mmol) of (1-(*tert*-butyl)-3-((*tert*-butylthio) (phenyl)methyl)-2,3-dihydro-1*H*-imidazol-2-yl)silver(II) bromide and (0.957 g, 1.844 mmol) [Pd($\eta^3$–$C_3H_5$)(COD)]$^+SbF_6^-$, in dry dichloromethane (20 mL) under argon atmosphere to yield a greyish white powder (9.09 g , 92%). $^1$H-NMR **(**500 MHz, $CD_3OD$): δ 8.12–8.12 (d, $J_{H–H}$ = 2.0 Hz, 0.5H), 7.97–7.98 (d, $J_{H–H}$ = 2.5 Hz, 0.5H), 7.65–7.66 (d, $J_{H–H}$ = 2.0 Hz, 1H), 7.47–7.48 (d, $J_{H–H}$ = 2.0 Hz, 1H), 7.45–7.46 (d, $J_{H–H}$ = 2.0 Hz, 0.5H), 7.38–7.43 (m, 6H), 7.34–7.35 (m, 2H), 7.24–7.26 (m, 2H), 7.11–7.12 (m, 2H), 7.06 (s, 0.5H), 6.90 (s, 0.5H), 5.77–5.85 (sep, $J_{H–H}$ = 6.8 Hz, 1H), 5.64–5.72 (sep, $J_{H–H}$ = 6.7 Hz, 1H), 4.80–4.81 (d, $J_{H–H}$ = 7.5 Hz, 1H), 4.63–4.64 (d, $J_{H–H}$ = 7.5 Hz, 1H), 4.48–4.51 (m, 2H), 3.72–3.75 (d, $J_{H–H}$

= 13.0 Hz, 1H), 3.48–3.53 (m, 1H), 3.18–3.21 (d, $J_{H-H}$ = 13.0 Hz, 1H), 1.85 (s, 4H, $^{t}$Bu), 1.83 (s, 9H, $^{t}$Bu), 1.70 (s, 4H, $^{t}$Bu), 1.51 (s, 4H, S$^{t}$Bu), 1.41 (s, 9H, S$^{t}$Bu), 1.37 (s, 9H, S$^{t}$Bu). $^{13}$C-NMR **(**100 MHz, $CDCl_3$)**:** δ 177.8, 177.7, 136.2, 129.6, 129.5, 129.3, 129.2, 129.2, 126.4, 126.3, 126.2, 121.1, 121.0, 120.8, 119.9, 119.6, 119.0, 118.9, 70.8, 67.3, 67.1, 67.1, 65.5, 59.1, 59.0, 55.0, 53.8, 30.9, 30.8, 30.35, 30.3. HRMS: calcd for $C_{21}H_{31}N_2PdSBF_4$ $[M - BF_4]^+$ 448.13, found 448.13.

**Synthesis of palladium complex (±)-67a:**

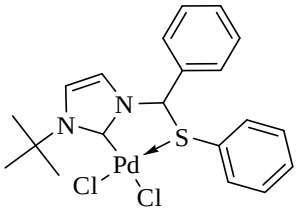


To a stirred solution of (1-(*tert*-butyl)-3-(phenyl(phenylthio)methyl)-2,3-dihydro-1*H*-imidazol-2-yl)silver(II) bromide (0.82 g, 1.611 mmol) in dry acetonitrile (20 mL) was added $PdCl_2(CH_3CN)_2$ (0.415 g, 1.611 mmol) under argon atmosphere. The mixture was stirred in the dark overnight at room temperature, filtered through Celite, concentrated, and the residue was triturated with methanol to afford **67a** (0.451 g, 57%) as a yellow solid. $^{1}$H-NMR: (400 MHz, $CD_3CN$): δ 8.27 (s, 1H, NC*H*S), δ 7.8–7.79 (m, 5H)**,** δ 7.4–7.44 (m, 2H), δ 7.4–7.34 (m, 5H), δ1.97(s, 9H, $^{t}$Bu). $^{13}$C-NMR:(100 MHz, $CD_3CN$): δ 145.21, 139.6, 138.42, 133.68, 130.81, 129.74, 129.69, 129.53, 129.16, 122.43, 121.28, 71.65, 60.65, and 32.12. HRMS: calcd for $C_{20}H_{22}Cl_2N_2SPd[M - 2Cl]^+$ 429.06, found 429.07.

**Synthesis of palladium complex (±)-67b:**

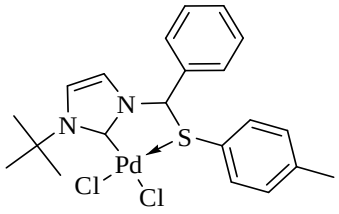


This complex was prepared in a manner analogous to that described for **67a**, using (1-(*tert*-butyl)-3-(phenyl(*p*-tolylthio)methyl)-2,3-dihydro-1*H*-imidazol-2-yl)silver(II) bromide (0.75 g, 1.434 mmol) in dry acetonitrile (20 mL) and 0.370g (1.434 mmol) of $Pd(CH_3CN)_2Cl_2$t o yield a yellow powder (0.4 g, 55%). $^1$H-NMR (500 MHz, $CD_3CN$): δ 8.27 (s, 1H, NC*H*S), 7.69–7.70 (d, $J_{H–H}$ = 2.0 Hz, 1H, SAr*H*), 7.66–7.68 (m, 2H, NC*H*=CHN; SAr*H*), 7.45–7.46 (d, $J_{H–H}$ = 8.0 Hz, 2H, Ar*H*), 7.34–7.39 (m, 4H, SAr*H;* Ar*H*), 7.09–7.11 (m, 2H, NCH=C*H*N; SAr*H*), 2.27 (s, 3H, SAr*Me*), 1.97 (s, 9H, $^t$Bu). $^{13}$C-NMR(100 MHz, $CD_3CN$): δ 145.7, 140.0, 138.8, 133.8, 131.3, 130.2, 130.2, 130.0, 129.6, 122.9, 121.8, 72.1, 61.1, 32.6, 21.6. HRMS: calcd for $C_{21}H_{24}Cl_2N_2SPd[M – 2Cl]^+$ 443.08, found 443.09.

**Synthesis of palladium complex (±)-67c:**

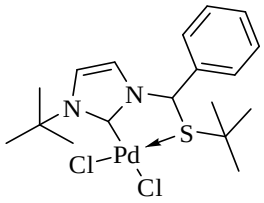


This complex was prepared in a manner analogous to that described for **67a**, using (1-(*tert*-butyl)-3-((*tert*-butylthio)(phenyl)methyl)-2,3-dihydro-1*H*-imidazol-2-yl)silver(II) bromide (0.8 g, 1.656 mmol) in dry acetonitrile (20 mL) and $PdCl_2(CH_3CN)_2$ (0.420 g, 1.656 mmol) under argon atmosphere to yield a

yellow powder. Yield: (0.370 g, 55%). $^{1}$H-NMR(400 MHz, $CD_3CN$): δ7.61–7.63 (m, 2H, Ar*H*), 7.51–7.57 (m, 3H, NCH=C*H*N; Ar*H*), 7.42–7.43 (d, $J_{H–H}$ = 2.0 Hz, 1H, NC*H*=CHN), 7.32–7.34 (m, 1H, Ar*H*), 6.40 (s, 1H, NC*H*S), 1.97 (s, 9H, *t*-Bu), 1.38 (s, 9H, S$^{t}$Bu).$^{13}$C-NMR(100 MHz, $CD_3CN$)**:**δ 131.0, 130.4, 129.9, 128.8, 128.4, 127.9, 123.3, 119.8, 68.1, 62.4, 31.8, 29.7. HRMS: calcd for $C_{18}H_{26}Cl_2N_2PdS[M – 2Cl]^+$ 409.09, found 409.09.

**Synthesis of (*R*)-3-(bromo(phenyl)methyl)-1-(1-phenylethyl)-1*H*-imidazol-3-ium bromide 82:**

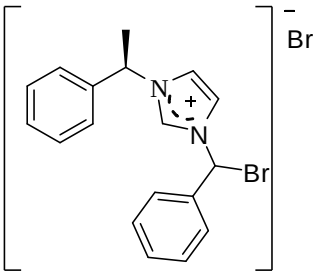


To a stirred 1M solution of $SOBr_2$ (9.57 g, 46.511 mmol), in dicloromethane, 2M solution of (*R*)-1-(1-phenylethyl)-1*H*-imidazole (10 g, 58.139 mmol) and 2M solution of benzaldehyde (12.3 g, 116.28 mmol) was added simultaneously at -40$^{o}$C under argon atmosphere. The reaction mixture was slowly warmed to room temperature and allowed to stir for 8 h. On evaporation of the reaction mixture followed by tituration with diethyl ether gave the desired crude product. The crude product was purified by column chromatography on silica using chloroform and methanol as eluent (eluent: chloroform/methanol, 40:1).Yield: 15.8 g (67%). $^{1}$H-NMR (500 MHz, $(CH_3)_2SO$): δ 11.25 (s, 1H, NC*H*N), 8.56 (s, 1H, NC*H*Br), 7.81–7.83 (m, 2H, NC*H*=C*H*N), 7.47–7.48 (m, 1H, Ar*H*), 7.28–7.44 (m, 9H, BrCHAr*H*, Ar*H*), 5.87–5.90 (q, $J_{H–H}$ = 7.0 Hz, 1H, NC*H*$CH_3$), 2.04–2.06 (d, 3H, NCHC*H*$_3$).$^{13}$C-

NMR (100 MHz, $CDCl_3$):δ 137.0, 136.9, 136.8, 134.8, 134.8, 130.8, 130.8, 129.8, 129.8, 129.7, 129.4, 129.4, 128.1, 128.1, 127.0, 126.9, 121.0, 120.8, 120.7, 61.0, 60.9, 58.5, 21.4, 21.2. HRMS: calcd for $C_{18}H_{18}BrN_2Br[M - Br]^+$ 341.06, found, 341.07.

**Synthesis of (*R*)-3-(phenyl(*p*-tolylthio)methyl)-1-(1-phenylethyl)-1*H*-imidazol-3-ium bromide 83b:** ***[Diastereomer (R,R) and (R,S)-83b in 1:1 ratio].***

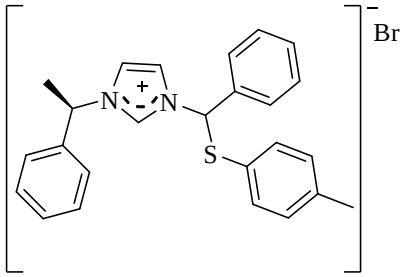


To a stirred solution of (*R*)-3-(bromo(phenyl)methyl)-1-(1-phenylethyl)-1*H*-imidazol-3-ium bromide (2 g, 4.762 mmol) in dry dichloromethane (20 mL) at – 40°C,sodium 4-methylbenzenethiolate (0.695 g, 4.762 mmol) was added. The reaction mixture was warmed to room temperature and allowed to stir for another 4 h. On completion of reaction by TLC, the reaction mixture was filtered and filtrate was evaporated followed by tituration with diethyl ether to yield the desired crude product. The pure product was purified by column chromatography using silica gel and chloroform–methanol as eluent (eluent: chloroform/methanol, 100:3). Diastereomer **(R,R) and (R,S)-83b** in **1:1** ratio. Yield: 1.83 g (83%).$^1$H-NMR (400 MHz, $CDCl_3$): δ 10.93 (s, 1H, NC*H*N), 10.77 (s, 1H, NC*H*N) 7.82–7.88 (m, 5H), 7.75 (s, 1H, NC*H*S), 7.35–7.50 (m, 18H), 7.18–7.20 (d, 2H), 7.08–7.14 (m, 4H), 7.03–7.05 (m, 2H),6.94 (s, 1H, NC*H*=CHN), 6.77 (s, 1H, NC*H*=CHN), 5.61–5.66 (q, $J_{H–H}$ = 7.1 Hz, 1H, NC*H*$CH_3$), 5.44–5.49 (q, $J_{H–H}$ = 6.9 Hz, 1H, NC*H*$CH_3$), 2.36 (s, 3H,

SAr*Me*),2.32 (s, 3H, SAr*Me*), 1.81–1.85 (m, 6H, NCHC$H_3$). $^{13}$C-NMR (100 MHz, $CDCl_3$):δ 137.7, 137.5, 135.7, 135.7, 134.0, 133.9, 133.5, 133.4, 130.2, 129.6, 129.6, 129.3, 129.2, 129.2, 127.6, 127.6, 126.5, 126.4, 121.6, 121.1, 119.9, 119.8, 67.9, 67.6, 59.9, 59.7, 21.4, 20.8. HRMS: calcd for $C_{25}H_{25}N_2SBr$[M - Br]$^+$ 385.17, found, 385.17.

**Synthesis of (*R*)-3-((*tert*-butylthio)(phenyl)methyl)-1-(1-phenylethyl)-1*H*-imidazol-3-ium bromide 83a:** ***[Diastereomer (R,R) and (R,S)-83a in 1:1 ratio]***

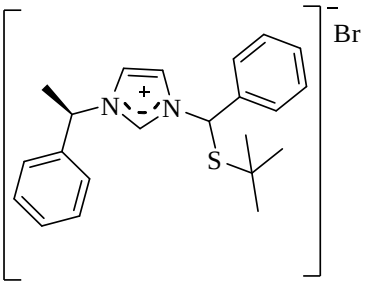


To a stirred solution of (*R*)-3-(bromo(phenyl)methyl)-1-(1-phenylethyl)-1*H*-imidazol-3-ium bromide (2 g, 4.762 mmol) in dry dichloromethane (20 mL) at -40$^o$C, sodium 2-methylpropane-2-thiolate (0.533 g, 4.762 mmol) was added. The reaction mixture was warmed to room temperature and allowed to stir for another 4 h. On completion of reaction monitored through TLC, the reaction mixture was filtered and filtrate was evaporated followed by tituration with diethyl ether to yield the desired crude product. The pure product was purified by column chromatography using silica gel and chloroform-methanol as eluent (eluent: chloroform/methanol, 100:3). Diastereomer **(R,R) and (R,S)-83a** in **1:1** ratio.Yield: 1.63 g (80%)$^1$H-NMR (500 MHz, $(CD_3)_2SO$): δ 11.55 (s, 1H, NC*H*N), 11.48 (s, 1H, NC*H*N) 7.82 (s, 2H), 7.78 (s, 1H, NC*H*S), 7.73 (s, 1H, NC*H*S), 7.57–7.59 (m, 3H), 7.31–7.40 (m, 15H), 7.14–7.15 (m, 2H), 5.78–5.83 (q, $J_{H-H}$ = 7.0 Hz, 1H, NC*H*$CH_3$), 5.69–5.73 (q, $J_{H-H}$ = 6.5 Hz, 1H, NC*H*$CH_3$),

2.05–2.06(d, $J_{H-H}$ = 7.0 Hz, 3H, NCHC$H_3$), 2.02–2.03(d, 3H, $J_{H-H}$ = 7.0 Hz, NCHC$H_3$), 1.41 (s, 9H, SCC$H_3$), 1.40 (s, 9H, SCC$H_3$). $^{13}$C- NMR (100 MHz, $CDCl_3$):δ 137.8, 137.5, 137.5, 135.8, 135.8, 129.5, 129.4, 129.3, 129.3, 129.3, 129.2, 126.8, 126.7, 126.6, 121.4, 121.1, 120.8, 120.7, 64.7, 64.7, 60.4, 60.2, 47.4, 30.9, 30.8, 21.4, 21.3. HRMS: calcd for $C_{22}H_{27}N_2SBr$[M - Br]$^+$ 351.19, found 351.19.

**Synthesis of bis(1-(phenyl(*p*-tolylthio)methyl)-3-((*R*)-1-phenylethyl)-2,3-dihydro-1*H*-imidazol-2-yl)silver(III) bromide 84b:**

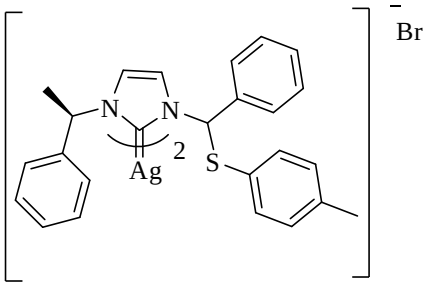


Silver(I)oxide (0.340 g, 1.46 mmol) was added to a solution of (*R*)-3-(phenyl(*p*-tolylthio)methyl)-1-(1-phenylethyl)-1*H*-imidazol-3-ium bromide(1.83 g, 2.087 mmol) in $CH_2Cl_2$ (20 mL) and the suspension was stirred for 4 h at room temperature in dark. The mixture was filtered off through a small Celite plug and concentrated to afford crude product.Yield: 2 g (90%)$^1$H-NMR (400 MHz, $CDCl_3$): δ 7.45–7.50 (m, 4H), 7.37–7.42 (m, 7H), 7.31–7.35 (m, 7H), 7.22–7.24 (d, $J_{H-H}$ = 8.0 Hz, 2H), 7.17–7.19 (d, $J_{H-H}$ = 7.6 Hz, 4H), 7.11–7.13 (d, $J_{H-H}$ = 8.0 Hz, 2H), 7.00–7.05 (m, 4H), 6.93–6.94 (d, $J_{H-H}$ = 1.6 Hz, 1H), 6.87 (s, 1H), 6.80–6.81 (d, $J_{H-H}$ = 3.2 Hz, 2H), 5.50–5.60 (sex, $J_{H-H}$ = 6.6 Hz, 2H, NC*H*$CH_3$), 2.35 (s, 3H, SAr*Me*), 2.32 (s, 3H, SAr*Me*), 1.74–1.75 (d, 3H,$J_{H-H}$ = 6.8 Hz, NCHC$H_3$), 1.70–1.72 (d, 3H,$J_{H-H}$ = 7.2 Hz, NCHC$H_3$).$^{13}$C-NMR (100 MHz, $CDCl_3$): δ 139.8, 139.7, 139.2, 136.1, 134.3, 134.2, 130.6, 129.4, 129.4, 129.1, 129.1, 129.0, 128.8, 128.5, 128.3, 127.3, 127.1, 126.9, 126.6, 126.3, 119.5,

119.4, 73.1, 73.0, 60.6, 60.5, 21.4, 21.3, 21.3, 21.1, –0.1. HRMS: calcd for $C_{50}H_{48}AgN_4S_2Br[M - Br]^+$ 877.25, found, 877.23.

**Synthesis of bis(1-((*tert*-butylthio)(phenyl)methyl)-3-((*R*)-1-phenylethyl)-2,3-dihydro-1*H*-imidazol-2-yl)silver(III) bromide 84a:**

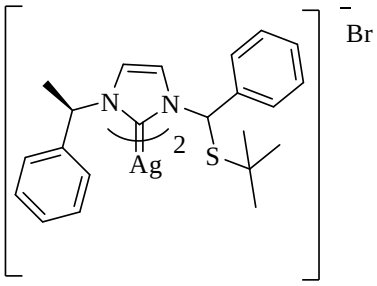


Silver(I)oxide (0.615 g, 2.653 mmol) was added to a solution of (*R*)-3-((*tert*-butylthio)(phenyl)methyl)-1-(1-phenylethyl)-1*H*-imidazol-3-ium bromide (1.63 g, 3.79 mmol) in $CH_2Cl_2$ (20 mL) and the suspension was stirred for 4 h at room temperature in dark. The mixture was filtered off through a small Celite plug and concentrated to afford crude product. Yield: 1.73 g (85%) $^1$H-NMR (500 MHz, $CDCl_3$): δ 7.59–7.60 (m, 2H, NC*H*S), 7.27–7.34 (m, 13H), 7.20–7.24 (m, 5H), 7.01–7.02 (m, 2H), 6.79–6.80 (m, 2H), 5.72–5.75 (t, $J_{H-H}$ = 7.0 Hz,2H, NC*H*$CH_3$), 1.83–1.87(m, 6H, NCHC*H*$_3$), 1.32(s, 9H, SCC*H*$_3$), 1.29 (s, 9H, SCC*H*$_3$). HRMS: calcd for $C_{44}H_{52}AgN_4S_2Br[M - Br]^+$ 807.28, found, 807.30

**Synthesis of palladium complex 86:**

To a stirred solution of silver salt of (*R*)-3-((*tert*-butylthio)(phenyl)methyl)-1-(1-phenylethyl)-1*H*-imidazol-3-ium bromide (0.8 g, 1.074 mmol) in dry acetonitrile (15 mL) $PdCl_2(CH_3CN)_2$ (0.275 g, 1.074 mmol) was added under argon atmosphere. The mixture was stirred in the dark overnight at room temperature, filtered through Celite, concentrated, and the residue was triturated with methanol to afford **(Rs,S,R)-86** & **(Ss,R,R)-86** (0.280

g, 50%) as a yellow solid. The diastereomer were separated from acetonitrile/diethyl ether system.

**Palladium complex (Ss,R,R)-86:**

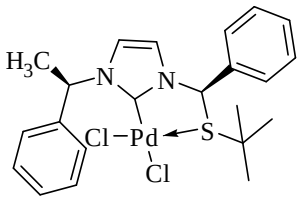

Yellow powder.Yield: 0.170 g with $[\alpha]_D$= +214 (*c* 0.2, $CH_3CN$).m.p: 234–236°C. $^1$H-NMR (400 MHz, $CD_3CN$): δ 7.56–7.59 (m, 3H), 7.54 (s, 1H), 7.51–7.53 (m, 1H), 7.48–7.50 (m, 1H), 7.42–7.46 (m, 4H), 7.35–7.39 (m, 1H), 7.26–7.27 (d, $J_{H-H}$ = 2.4 Hz, 1H, NC*H*=CHN), 6.96–6.97 (d, $J_{H-H}$ = 2.0 Hz,1H, NCH=C*H*N), 6.45 (s, 1H, NC*H*S), 1.82–1.83 (d, $J_{H-H}$ = 6.8 Hz, 3H, NCHC$H_3$), 1.52(s, 9H, SCC$H_3$). $^{13}$C-NMR (100 MHz, $CDCl_3$): δ 157.7, 140.5, 136.0, 130.8, 130.3, 129.3, 128.8, 128.0, 127.0, 122.3, 120.7, 66.6, 57.5, 56.9, 29.9, 21.1. HRMS: calcd for $C_{22}H_{27}Cl_2N_2PdS[M - 2Cl]^+$ 457.09, found, 457.09.

**Palladium complex (Rs,S,R)-86:**

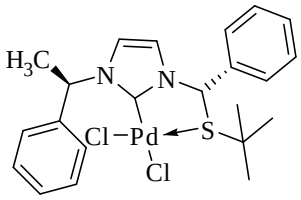

Yellow crystal.Yield 0.10 g with $[\alpha]_D$= (+) 100 (*c* 0.2, $CH_3CN$). m.p: 216–218°C.$^1$H-NMR (400 MHz,$(CD_3)_2SO$): δ 7.82 (s, 1H), 7.51–7.56 (m, 5H) 7.48–7.50 (m, 1H), 7.45–7.46 (m, 1H), 7.39–7.42 (m, 4H), 7.31–7.35 (m, 1H), 6.92 (s, 1H, NC*H*S), 1.84–1.86 (d, $J_{H-H}$ = 6.8 Hz, 3H, NCHC$H_3$), 1.24(s, 9H, SC(C$H_3$)$_3$). $^{13}$C-NMR (100 MHz, $(CD_3)_2SO$): δ 155.8, 141.4, 135.4, 129.7, 129.4,

128.6, 128.1, 126.6, 126.2, 121.3, 120.3, 65.2, 56.8, 55.9, 29.1, 19.4. HRMS: calcd for $C_{22}H_{27}Cl_2N_2PdS[M - 2Cl]^+$ 457.09, found, 457.09.

**Synthesis of palladium complex 87:**

This complex was prepared in a manner analogous to that described for **86**,using bis(1-(phenyl(*p*-tolylthio)methyl)-3-((*R*)-1-phenylethyl)-2,3-dihydro-1*H*-imidazol-2-yl)silver(III) bromide (1 g, 1.140 mmol) in dry acetonitrile (10 mL) and $PdCl_2(CH_3CN)_2$ (0.290 g, 1.140 mmol) under argon atmosphere to yield the **(Rs,S,R)-87** and **(Ss,R,R)-87**, as yellow powder (0.330 g, 52%) as a yellow solid. The diastereomer were separated from acetonitrile/diethyl ether system.

**Palladium complex (Ss,R,R)-87:**

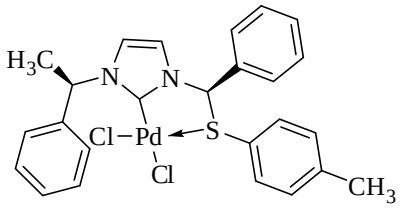


Yellow powder.Yield0.180 g as pure product with $[\alpha]_D$= + 188(*c* 0.2, $CH_3CN$). m.p: 238–240°C. $^1$H-NMR (400 MHz, $CD_3CN$): δ7.83–7.85 (d, $J_{H-H}$ = 8.0 Hz, 1H),7.63–7.68 (m, 1H), 7.55–7.58 (m, 4H), 7.47–7.50 (m, 2H), 7.43–7.45 (m, 2H), 7.37–7.39 (m, 3H),7.09 (s, 1H), 7.01 (s, 1H), 6.91 (s, 1H), 6.48 (s, 1H, NC*H*S), 2.40 (s, 3H, SAr*Me*), 1.88–1.90(d, 3H,$J_{H-H}$ = 7.2 Hz, NCHC$H_3$).$^{13}$C-NMR (100 MHz, $CD_3CN$):δ 143.2, 140.0, 134.2, 133.0, 130.8, 130.7, 129.6, 128.7, 128.4, 128.2, 127.2, 126.8, 125.3, 121.7, 120.8, 75.2, 57.0, 20.4, 20.3.HRMS: calcd for $C_{25}H_{25}Cl_2N_2PdS[M - 2Cl]^+$ 491.08, found, 491.08.

**Palladium complex (Rs,S,R)-87:**

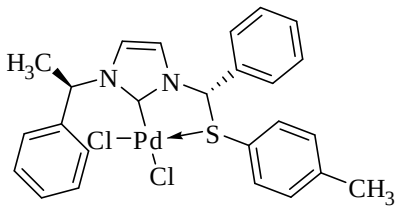

Yellow powder.Yield 0.030 g with $[\alpha]_D$= +96 (*c* 0.2, $(CD_3)_2SO$). m.p: 255–258°C. $^1$H-NMR (400 MHz, $(CD_3)_2SO$): δ7.78 (b, 1H, NC*H*$CH_3$), 7.55–7.59 (m, 8H), 7.41–7.50 (m, 6H), 7.16–7.18 (d, $J_{H-H}$ = 8.0 Hz, 2H), 6.92 (bs, 1H, NC*H*S),2.32 (s, 3H, SAr*Me*), 1.87–1.89(d, 3H,$J_{H-H}$ = 6.8 Hz, NCHC$H_3$). $^{13}$C-NMR due to poor solubility in $CD_3CN$ and $(CD_3)_2SO$ we were not able to perform $^{13}$C experiment. HRMS: calcd for $C_{25}H_{25}Cl_2N_2SPd[M - 2Cl]^+$ 491.08, found, 491.08.

**Synthesis of Platinum complex-88:**

This complex was prepared in a manner analogous to that described for **86**, using silver salt of (*R*)-3-((*tert*-butylthio)(phenyl)methyl)-1-(1-phenylethyl)-1*H*-imidazol-3-ium bromide (0.8 g, 1.074 mmol) in dry DCM (10 mL) and $PtCl_2COD$ (0.4 g, 1.074 mmol) under argon atmosphere to yield a yellow powder. The diastereomer were separated from acetonitrile/diethyl ether system.

**Platinum complex(Ss,R,R)-88:**

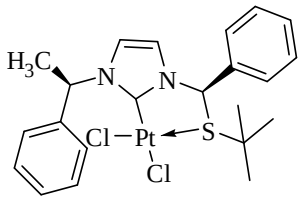

Colourless crystal.Yield 0.230 g with $[\alpha]_D$ = +190(*c* 0.2, $CH_3CN$), m.p: 294–298°C.$^1$H-NMR (500 MHz, $(CD_3)_2SO$): δ 7.53–7.54 (m, 3H), 7.48–7.51 (m, 3H), 7.42–7.52 (m, 2H), 7.37–7.40 (m, 4H), 7.34–7.36 (m, 1H), 6.88 (s, 1H,

NC*H*S), 1.77–1.79 (d, $J_{H-H}$ = 7.0 Hz, 3H, NCHC$H_3$), 1.39(s, 9H, SC(C$H_3$)$_3$). $^{13}$C-NMR (100 MHz, $(CD_3)_2SO$): δ 146.8, 140.3, 135.9, 130.0, 129.9, 129.0, 128.4, 127.5, 126.8, 122.2, 119.7, 65.2, 56.1, 56.0, 28.9, 21.1. HRMS: calcd for $C_{22}H_{27}Cl_2N_2PtS[M-2Cl]^+$ 547.15, found, 547.17.

**Platinum complex (Rs,S,R)-88:**

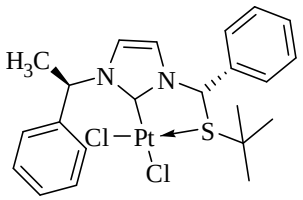


Colourless crystal.Yield 0.180 g with $[\alpha]_D$ = +100(*c* 0.2, $CH_3CN$), m.p: 302–304°C.$^1$H-NMR (400 MHz,$CD_2Cl_2$): δ 7.77–7.78 (d, $J_{H-H}$ = 2.0 Hz, 1H, NC*H*=CHN),, 7.48–7.54 (m, 6H) 7.43–7.46 (m, 1H), 7.36–7.41 (m, 4H), 7.30–7.34 (m, 1H), 6.80 (s, 1H, NC*H*S), 1.85–1.87 (d, $J_{H-H}$ = 6.8 Hz, 3H, NCHC$H_3$), 1.19(s, 9H, SC(C$H_3$)$_3$). $^{13}$C-NMR (100 MHz, $CD_2Cl_2$): δ 149.2, 141.1, 134.8, 130.7, 130.2, 129.4, 128.8, 127.5, 127.0, 121.8, 118.0, 67.0, 57.7, 56.0, 29.4, 20.6. HRMS: calcd for $C_{22}H_{27}Cl_2N_2PtS[M-2Cl]^+$ 547.15, found, 547.17

**Synthesis of Platinum complex – 89:**

This complex was prepared in a manner analogous to that described for **87**, using silver salt of (*R*)-3-((*tert*-butylthio)(phenyl)methyl)-1-(1-phenylethyl)-1*H*-imidazol-3-ium bromide(1 g, 1.140 mmol) in dry DCM (10 mL) and $PtCl_2COD$ (0.425 g, 1.140 mmol) under argon atmosphere to yield a mixture of diastereomer **(Ss,R,R)-89**&**(Rs,S,R)-89**. The diastereomer were separated from acetonitrile/diethyl ether system.

**Platinum complex (Ss,R,R)-89:**

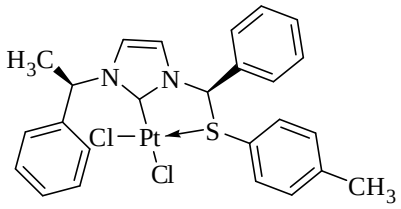


Yellow crystal.Yield 0.635 g with $[\alpha]_D$ = +180(*c* 2.0, $CH_3CN$). m.p: 275–280°C.$^1$H-NMR (500 MHz, $(CD_3)_2SO$): δ 8.03 (d, $J_{H-H}$ = 1.5 Hz, 1H, NC*H*=CHN),7.77 (s, 1H, NC*H*S), 7.47–7.48 (m, 2H), 7.43–7.45 (m, 3H), 7.40 (m, 2H), 7.31–7.37 (m, 6H),7.06–7.08 (d, $J_{H-H}$ = 8.0 Hz, 2H), 6.45–6.47 (m, 1H), 2.25(s, 3H, SAr*Me*), 1.84–1.86(d, 3H, $J_{H-H}$ = 7.5 Hz, NCHC$H_3$).$^{13}$C-NMR (100 MHz, $CD_3CN$): δ 143.2, 140.0, 134.2, 133.0, 130.8, 130.7, 129.6, 128.7, 128.4, 128.2, 127.2, 126.8, 125.3, 121.7, 120.8, 75.2, 57.0, 20.4, 20.3.HRMS: calcd for $C_{25}H_{25}Cl_2N_2PtS[M-2Cl]^+$ 491.08, found, 491.10.

**General procedure for allylic amination:**

The appropriate palladium complex (3.02 mg, 0.005 mmol, 0.02 eq), was added to a dry screw cap reaction tube containing cinnamyl ethyl carbonate (50.0 mg, 0.242 mmol, 1 eq), followed by primary or secondary amines (0.727 mmol, 3 eq) in dry THF (2 mL). The whole reaction tube were heated to 50°C till the reaction reached completion (determined through Thin Layer Chromatography). After the disappearance of starting material, the reaction mixture was cooled to room temperature and the THF was removed under reduced pressure. The residue was then diluted with diethyl ether and filtrated through a pad of silica gel. The ether layer was extracted with water and dried over $MgSO_4$. The layer was concentrated and purified through silica gel column chromatography to give the

desired amination product, determined through $^{1}$H-NMR, $^{13}$C{$^{1}$H}-NMR and High Resolution Mass Spectroscopy.

**Note: For entry 5& 6 in Table 2.7:** 5mol% of catalyst was used in general procedure.

**(E)-N,N-dibenzyl-3-phenylprop-2-en-1-amine:**

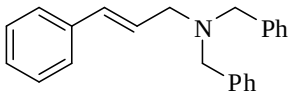


Silica gel column chromatography, eluent: hexane/ethyl acetate, 99:1.Yield: 70.5 mg (93%).$^{1}$H-NMR (400 MHz, $CDCl_3$): δ 7.38–7.40 (m, 4H, $NCH_2Ar$*H*), 7.32–7.36 (m, 3H, $NCH_2Ar$*H*), 7.26–7.31 (m, 5H, $NCH_2Ar$*H*,Ar*H*), 7.24 (s, 1H, Ar*H*), 7.17–7.22 (m, 2H, Ar*H*), 6.50–6.54 (d, $J_{H-H}$ = 15.6 Hz, 1H, C*H*=$CHCH_2$), 6.25–6.33 (sex, $J_{H-H}$ = 6.5 Hz, 1H, CH=C*H*$CH_2$), 3.62 (s, 4H, NC$H_2$Ar), 3.21–3.22 (d, $J_{H-H}$ = 6.4 Hz, 2H, CH=CHC$H_2$). $^{13}$C-NMR (100 MHz, $CDCl_3$):δ139.6, 137.2, 132.4, 128.8, 128.5, 128.2, 127.7, 127.3, 126.8, 126.2, 57.9, 55.7. HRMS: calcd for $C_{23}H_{23}N[M + H]^+$ 314.18, found: 314.19.

**(E)-N,N-diethyl-3-phenylprop-2-en-1-amine:**

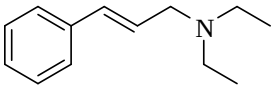


Yield: 37.5 mg (82%).$^{1}$H-NMR (400 MHz, $CDCl_3$): δ 7.36–7.39 (m, 2H, Ar*H*), 7.28–7.32 (m, 2H, Ar*H*), 7.19–7.23 (m, 1H, Ar*H*), 6.49–6.53 (d, $J_{H-H}$ = 16.0 Hz, 1H, C*H*=$CHCH_2$), 6.26–6.33 (sex, $J_{H-H}$ = 6.7 Hz, 1H, CH=C*H*$CH_2$), 3.25–3.27 (d, $J_{H-H}$ = 6.6 Hz, 2H, CH=CHC$H_2$), 2.55–2.61 (q,$J_{H-H}$ = 7.2 Hz, 4H, NC$H_2$), 1.05–1.08 (t, $J_{H-H}$ = 7.0 Hz, 6H, $NCH_2CH_3$). $^{13}$C-NMR (100 MHz, $CDCl_3$):δ137.1, 132.1, 128.5, 127.7, 127.2, 126.2, 55.5, 46.7, 11.7. HRMS: calcd for $C_{13}H_{19}N[M + H]^+$ 190.15, found: 190.16.

**1-cinnamylpiperidine:**

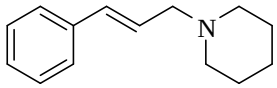

Yield: 47.8 mg (98%).$^{1}$H-NMR (400 MHz, $CDCl_3$): δ 7.36–7.38 (m, 2H, Ar*H*), 7.28–7.31 (m, 2H, Ar*H*), 7.19–7.23 (m, 1H, Ar*H*),6.47–6.51 (d, $J_{H–H}$ = 16.0 Hz, 1H, C*H*=CHCH$_2$), 6.27–6.34 (sex, $J_{H–H}$ = 6.8 Hz, 1H, CH=C*H*CH$_2$), 3.11–3.13 (d, $J_{H–H}$ = 6.8 Hz, 2H, CH=CHC*H*$_2$), 2.43 (s, 4H, NC*H*$_2$), 1.58–1.63 (p, $J_{H–H}$ = 5.6 Hz, 4H, NCH$_2$C*H*$_2$), 1.43–1.46 (t, $J_{H–H}$ = 5.4 Hz, 2H, NCH$_2$CH$_2$C*H*$_2$). $^{13}$C-NMR (100 MHz, $CDCl_3$):δ137.1, 132.6, 128.5, 127.3, 127.2, 126.2, 61.9, 54.6, 26.0, 24.3. HRMS: calcd for $C_{14}H_{19}N[M + H]^+$ 202.15, found: 202.16.

**4-cinnamylmorpholine:**

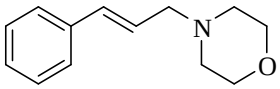

Yield: 48.7 mg (98%).$^{1}$H-NMR (400 MHz, $CDCl_3$): δ 7.36–7.38 (m, 2H, Ar*H*), 7.28–7.32 (m, 2H, Ar*H*), 7.21–7.26 (m, 1H, Ar*H*), 6.51–6.55 (d, $J_{H–H}$ = 16.0 Hz, 1H, C*H*=CHCH$_2$), 6.22–6.29 (sex, $J_{H–H}$ = 6.8 Hz, 1H, CH=C*H*CH$_2$), 3.72–3.74 (t, $J_{H–H}$ = 4.6 Hz, 4H, OC*H*$_2$), 3.14–3.16 (d, $J_{H–H}$ = 6.8 Hz, 2H, CH=CHC*H*$_2$), 2.50 (s, 4H, NC*H*$_2$). $^{13}$C-NMR (100 MHz, $CDCl_3$):δ136.8, 133.3, 128.5, 127.5, 126.3, 126.0, 66.9, 61.4, 53.6. HRMS: calcd for $C_{13}H_{17}NO[M + H]^+$ 204.13, found: 204.14.

**(E)-N-benzyl-N-ethyl-3-phenylprop-2-en-1-amine:**

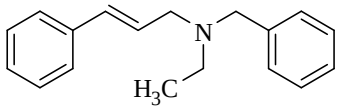

Silica gel column chromatography, eluent: hexane/ethyl acetate, 19:1. Yield: 55.8 mg (92%).$^{1}$H-NMR (400 MHz, $CDCl_3$): δ 7.35–7.35 (m, 4H,

$NHCH_2ArH$), 7.28–7.33 (m, 4H, $NHCH_2ArH$, Ar*H*), 7.20–7.26 (m, 2H, Ar*H*), 6.50–6.54 (d, $J_{H–H}$ = 16.0 Hz, 1H, C*H*=$CHCH_2$), 6.25–6.33 (sex, $J_{H–H}$ = 6.7 Hz, 1H, CH=C*H*$CH_2$), 3.64 (s, 2H, $NCH_2Ar$), 3.25–3.27 (d, $J_{H–H}$ = 6.6 Hz, 2H, $CH=CHCH_2$), 2.56–2.62 (q, $J_{H–H}$ = 7.1 Hz, 2H, $NCH_2CH_3$), 1.08–1.11 (t, $J_{H–H}$ = 7.2 Hz, 3H, $NCH_2CH_3$). $^{13}$C-NMR (100 MHz, $CDCl_3$): δ 139.2, 137.1, 132.5, 129.0, 128.5, 128.2, 127.4, 127.3, 126.9, 126.3, 57.6, 55.6, 47.1, 11.7. HRMS: calcd for $C_{18}H_{21}N[M + H]^+$ 252.17, found: 252.18.

**(E)-N-benzyl-N-methyl-3-phenylprop-2-en-1-amine:**

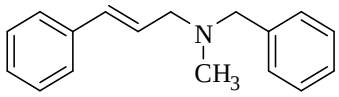


Silica gel column chromatography, eluent: hexane/ethyl acetate, 19:1. Yield: 45.8 mg (80%).$^1$H-NMR (400 MHz, $CDCl_3$): δ 7.37–7.39 (m, 2H, $NHCH_2ArH$), 7.32–7.35 (m, 4H, $NHCH_2ArH$, Ar*H*), 7.28–7.30 (m, 2H, Ar*H*), 7.25–7.27 (m, 1H, Ar*H*), 7.20–7.23 (m, 1H, Ar*H*), 6.52–6.55 (d, $J_{H–H}$ = 15.6 Hz, 1H, C*H*=$CHCH_2$), 6.28–6.35 (sex, $J_{H–H}$ = 6.6 Hz, 1H, CH=C*H*$CH_2$), 3.55 (s, 2H, $NCH_2Ar$), 3.19–3.20 (d, $J_{H–H}$ = 6.2 Hz, 2H, $CH=CHCH_2$), 2.24 (s, 3H, $NCH_3$). $^{13}$C-NMR (100 MHz, $CDCl_3$): δ 138.8, 137.1, 132.6, 129.1, 128.5, 128.2, 127.4, 127.4, 127.0, 126.3, 61.8, 59.8, 42.1. HRMS: calcd for $C_{17}H_{19}N[M + H]^+$ 238.15, found: 238.16.

**(E)-3-phenyl-N-(1-phenylethyl)prop-2-en-1-amine:**

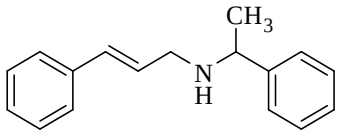


Silica gel column chromatography, eluent: hexane/ethyl acetate, 4:1. Yield: 50.7 mg (88%). $^1$H-NMR (400 MHz, $CDCl_3$): δ 7.33–7.34 (m, 6H, NHCHAr*H*, Ar*H*), 7.27–7.30 (m, 2H, Ar*H*), 7.23–7.26 (m, 1H, Ar*H*), 7.18–7.22

(m, 1H, Ar*H*), 6.42–6.46 (d, $J_{H-H}$= 16.0 Hz, 1H, C*H*=CHCH$_2$), 6.23–6.30 (sex, $J_{H-H}$= 6.3 Hz, 1H, CH=C*H*CH$_2$), 3.84–3.89 (q, $J_{H-H}$ = 6.7 Hz, 1H, NHC*H*), 3.41 (s, 1H, N*H*), 3.24–3.27 (t, $J_{H-H}$ = 4.8 Hz, 2H, CH=CHC*H*$_2$), 1.39–1.41 (d, $J_{H-H}$ = 6.8 Hz, 3H, NHCHC*H*$_3$). $^{13}$C-NMR (100 MHz, CDCl$_3$):δ144.7, 137.0, 131.6, 128.5, 128.5, 127.8, 127.3, 127.1, 126.7, 126.2, 57.5, 49.4, 23.8.HRMS: calcd for $C_{17}H_{19}N[M + H]^+$ 238.15, found: 238.16.

**(E)-N-cinnamyl-3-phenyl-N-(1-phenylethyl)prop-2-en-1-amine:**

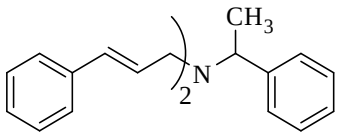


Silica gel column chromatography, eluent: hexane/ethyl acetate, 49:1. Yield: 4.2 mg (7%).$^1$H-NMR (400 MHz, CDCl$_3$): δ 7.40–7.42 (m, 1H, NCHAr*H*), 7.36–7.38 (m, 4H, NCHAr*H*), 7.30–7.34 (m, 6H, Ar*H*), 7.28 (s, 1H, Ar*H*), 7.20–7.24 (m, 3H, Ar*H*), 6.49–6.53 (d, $J_{H-H}$ = 16.0 Hz, 2H, C*H*=CHCH$_2$), 6.24–6.31 (p, $J_{H-H}$ = 6.4 Hz, 2H, CH=C*H*CH$_2$), 3.97–4.02 (m, 1H, NC*H*), 3.26–3.39 (m, 4H, CH=CHC*H*$_2$), 1.43–1.45 (d, $J_{H-H}$ = 7.2 Hz, 3H, NHCHC*H*$_3$). $^{13}$C-NMR (100 MHz, CDCl$_3$): NMR not obtained due to insufficient sample. HRMS: calcd for $C_{26}H_{27}N[M + H]^+$ 354.21, found: 354.22.

**(E)-N-(1-(naphthalen-2-yl)ethyl)-3-phenylprop-2-en-1-amine:**

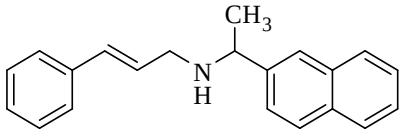


Silica gel column chromatography, eluent: hexane/ethyl acetate, 4:1. Yield: 47.9 mg (69%).$^1$H-NMR (400 MHz, CDCl$_3$): δ 7.81–7.85 (m, 3H, Np*H*), 7.75 (s, 1H, Np*H*), 7.42–7.50 (m, 3H, Np*H*), 7.32–7.34 (m, 2H, Ar*H*), 7.26–7.30 (m, 2H, Ar*H*), 7.18–7.23 (m, 1H, Ar*H*), 6.42–6.46 (d, $J_{H-H}$ = 15.6 Hz, 1H,

C*H*=CHCH$_2$), 6.24–6.32 (sex, $J_{H–H}$ = 6.4 Hz, 1H, CH=C*H*CH$_2$), 4.01–4.06 (q, $J_{H–H}$ = 6.5 Hz, 1H, NHC*H*), 3.27–3.29 (m, 2H, CH=CHC*H*$_2$), 3.00 (s, 1H, N*H*), 1.46–1.48 (d, $J_{H–H}$ = 6.4 Hz, 3H, NHCHC*H*$_3$). $^{13}$C-NMR (100 MHz, CDCl$_3$):δ142.3, 137.0, 133.4,132.8, 131.6, 128.5, 128.3, 128.0, 127.7, 127.6, 127.3, 126.2, 126.0, 125.5, 125.5, 124.8, 57.6, 49.5, 24.0.HRMS: calcd for $C_{21}H_{21}N[M + H]^+$ 288.17, found: 288.18.

**(E)-N-cinnamyl-N-(1-(naphthalen-2-yl)ethyl)-3-phenylprop-2-en-1-amine:**

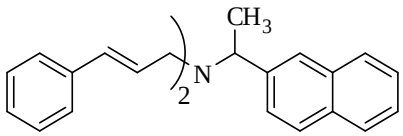


Silica gel column chromatography, eluent: hexane/ethyl acetate, 49:1. Yield: 3.7 mg (5%).$^1$H-NMR (400 MHz, CDCl$_3$): δ 7.79–7.84 (m, 4H, Np*H*), 7.62–7.64 (m, 1H, Np*H*), 7.43–7.49 (m, 2H, Np*H*), 7.28–7.38 (m, 8H, Ar*H*), 7.20–7.24 (m, 2H, Ar*H*), 6.50–6.54 (d, $J_{H–H}$ = 16.0 Hz, 2H, C*H*=CHCH$_2$), 6.27–6.34 (sex, $J_{H–H}$ = 6.6 Hz, 2H, CH=C*H*CH$_2$), 4.21–4.26 (m, 1H, NC*H*), 3.28–3.40 (m, 4H, CH=CHC*H*$_2$), 1.53–1.54 (d, $J_{H–H}$ = 5.2 Hz, 3H, NCHC*H*$_3$). $^{13}$C NMR (100 MHz, CDCl$_3$): NMR not obtained due to insufficient sample. HRMS: calcd for $C_{30}H_{29}N[M + H]^+$ 404.23, found: 404.24.

**(E)-N-(naphthalen-1-ylmethyl)-3-phenylprop-2-en-1-amine:**

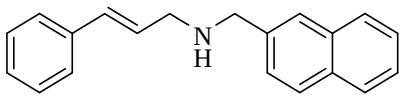


Silica gel column chromatography, eluent: hexane/ethyl acetate, 4:1. Yield: 33.4 mg (50%).$^1$H-NMR (400 MHz, CDCl$_3$): δ 8.12–8.14 (d, $J_{H–H}$ = 8.4 Hz, 1H, Np*H*), 7.84–7.87 (d, $J_{H–H}$ = 8.2 Hz, 1H, Np*H*), 7.76–7.78(d, $J_{H–H}$ = 8.0 Hz, 1H, Np*H*), 7.52–7.54 (m,1H, Np*H*), 7.48–7.51 (m, 2H, Np*H*), 7.40–7.46 (m, 1H, Np*H*), 7.36–7.39 (m, 2H, Ar*H*), 7.28–7.32 (m, 2H, Ar*H*), 7.20–7.23 (m, 1H,

Ar*H*), 6.55–6.59 (d, $J_{H-H}$ = 16.0 Hz, 1H, C*H*=CHCH$_2$),6.32–6.39 (sex, $J_{H-H}$ = 6.3 Hz, 1H, CH=C*H*CH$_2$), 4.27 (s, 2H, NC*H*$_2$), 3.52–3.54 (d, $J_{H-H}$ = 6.0 Hz, 2H, CH=CHC*H*$_2$).$^{13}$C-NMR (100 MHz, $CDCl_3$):δ137.1, 135.7, 133.9, 131.8, 131.6, 128.7, 128.5, 128.3, 127.8, 127.4, 126.3, 126.1, 125.6, 125.4, 123.6, 51.6, 50.8. HRMS: calcd for $C_{20}H_{19}N[M + H]^+$ 274.15, found: 274.16.

**(E)-N-benzyl-3-phenylprop-2-en-1-amine:**

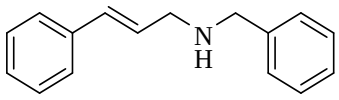


Silica gel column chromatography, eluent: hexane/ethyl acetate, 3:1. Yield: 22.5 mg (42%).$^1$H-NMR (400 MHz, $CDCl_3$): δ 7.36–7.37 (m, 2H, NHCH$_2$Ar*H*), 7.33–7.34 (m, 3H, NHCH$_2$Ar*H*), 7.28–7.32 (m, 3H, Ar*H*), 7.20–7.27 (m, 2H, Ar*H*), 6.52–6.56 (d, $J_{H-H}$ = 16.0 Hz, 1H, C*H*=CHCH$_2$), 6.28–6.35 (sex, $J_{H-H}$ = 6.3 Hz, 1H, CH=C*H*CH$_2$), 3.84 (s, 2H, NHC*H*$_2$), 3.43–3.45 (d, $J_{H-H}$ = 6.0 Hz, 2H, CH=CHC*H*$_2$), 2.17–2.33 (s, 1H, N*H*). $^{13}$C-NMR (100 MHz, $CDCl_3$):δ 139.9, 137.1, 131.6, 128.5, 128.4, 128.2, 128.1, 127.4, 127.0, 126.3, 53.2, 51.1. HRMS: calcd for $C_{16}H_{17}N[M + H]^+$ 224.14, found, 224.14 .

**(E)-N-benzyl-N-cinnamyl-3-phenylprop-2-en-1-amine:**

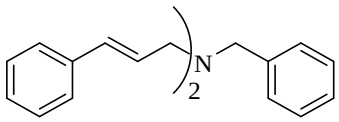


Silica gel column chromatography, eluent: hexane/ethyl acetate, 49:1. Yield: 15.0 mg (28%).$^1$H-NMR (400 MHz, $CDCl_3$): δ 7.37–7.39 (m, 6H, NCH$_2$Ar*H*, Ar*H*), 7.27–7.35 (m, 7H, Ar*H*), 7.20–7.25 (m, 2H, Ar*H*), 6.53–6.57 (d, $J_{H-H}$ = 16.0 Hz, 2H, C*H*=CHCH$_2$), 6.28–6.35 (sex, $J_{H-H}$ = 6.6 Hz, 2H, CH=C*H*CH$_2$), 3.69 (s, 2H, NC*H*$_2$), 3.30–3.32 (d, $J_{H-H}$ = 6.4 Hz, 4H, CH=CHC*H*$_2$). HRMS: calcd for $C_{25}H_{25}N[M + H]^+$ 340.20, found: 340.21.

**4-allylmorpholine:**

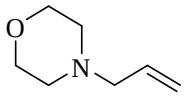

Yield: (98%). $^{1}$H-NMR (400 MHz, $CDCl_3$): δ5.9–5.8(m, 1H, C*H*CH=CH), 5.19–5.1(t, 2H, C*H*=C*H*), 3.7–3.6 (t, $J_{H-H}$ = 4.4 Hz, 4H, OC$H_2$), 2.42–2.4 (t, $J_{H-H}$ = 4.4 Hz, 4H, NC$H_2$), 2.96–2.94 (d, $J_{H-H}$ = 8.8 Hz, 2H) $^{13}$C-NMR (100 MHz, $CDCl_3$): δ 134.4, 118.2, 67.9, 66.8, 53.4. HRMS: calcd for $C_7H_{15}NO[M + H]^+$ 128.1, found:128.12.

**(E)-4-(but-2-en-1-yl)morpholine:**

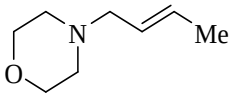

Silica gel column chromatography, eluent: $CHCl_3$/MeOH, 95:5.Yield: 48.5mg (98%). $^{1}$H-NMR (400 MHz, $CDCl_3$): δ 5.59–5.70 (m, 1H, MeC*H*=CH), 5.45–5.52 (m, 1H, MeCH=C*H*), 3.71–3.73(t, $J_{H-H}$ = 4.6 Hz, 4H, OC$H_2$), 2.94–2.96 (d, $J_{H-H}$ = 6.7 Hz, 2H, CH=CHC$H_2$), 2.47 (s, 4H, NC$H_2$), 1.67–1.70 (d, $J_{H-H}$ = 6.3 Hz, 3H,Me*H*). $^{13}$C-NMR (100 MHz, $CDCl_3$):δ 130.1, 126.4, 66.7, 61.0, 53.3, 17.8. HRMS: calcd for $C_8H_{15}NO[M + H]^+$ 142.12, found: 142.13.

**4-cinnamylmorpholine:**

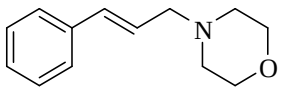

Yield: 48.7 mg (98%).$^{1}$H-NMR (400 MHz, $CDCl_3$): δ 7.36–7.38 (m, 2H, Ar*H*), 7.28–7.32 (m, 2H, Ar*H*), 7.21–7.26 (m, 1H, Ar*H*), 6.51–6.55 (d, $J_{H-H}$ = 16.0 Hz, 1H, C*H*=CHCH$_2$), 6.22–6.29 (sex, $J_{H-H}$ = 6.8 Hz, 1H, CH=C*H*CH$_2$), 3.72–3.74 (t, $J_{H-H}$ = 4.6 Hz, 4H, OC$H_2$), 3.14–3.16 (d, $J_{H-H}$ = 6.8 Hz, 2H, CH=CHC$H_2$), 2.50 (s, 4H, NC$H_2$). $^{13}$C-NMR (100 MHz, $CDCl_3$): δ 136.8, 133.3,

128.5, 127.5, 126.3, 126.0, 66.9, 61.4, 53.6. HRMS: calcd for $C_{13}H_{17}NO[M + H]^+$ 204.13, found: 204.14.

**Mixture of compounds (Table2.11;Entry 4 )**

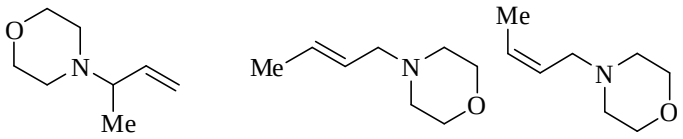


Yield: 44.2 mg (90%). $^1$H-NMR (500 MHz, $CDCl_3$): δ 5.73–5.66 (m, 0.5H), δ5.59–5.52 (m, 1.1H cis/trans linear product), 5.45–5.39 (m, 1H, cis/trans linear product), 5.06–5.05 (d, 0.5H), 5.03 (s, 0.5H), 4.19–4.11 (m, 0.5H), 3.66–3.65 (t, $J_{H–H}$ = 8.5 Hz, 6H, OC$H_2$) cis/trans linear product), 2.97–2.95 (d, 0.5H), 2.87–2.85 (d, 2H), 2.38 (m, 6H, NC$H_2$, cis/trans linear product), 1.63–1.62 (d, $J_{H–H}$ = 6.5 Hz, 3H,Me*H*, trans isomer), 1.59–1.6 (d, $J_{H–H}$ = 6.5 Hz, 0.7H,Me*H*, cis isomer), 1.1–1.09 (d, $J_{H–H}$ = 6.5 Hz, 1.5H,Me*H*,Me branched isomer). HRMS: calcd for $C_8H_{15}NO[M + H]^+$141.12, found:141.12.

**Mixture of compounds ( Table2.11; Entry 5 )**

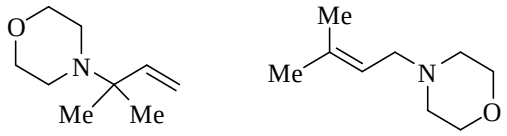


Yield: 33.3 mg (68%). $^1$H-NMR (500 MHz, $CDCl_3$): δ 5.85–5.80 (dd, $J_{H–H}$ = 11 Hz, 10.5Hz 0.5H), 5.25–5.24 (m, 1H, linear isomer), 5.07–5.02 (m, 1H, branched isomer), 3.72–3.70 (t, $J_{H–H}$ = 9 Hz, 5H, branched & linear isomer), 2.95–2.94 (d, $J_{H–H}$ = 7 Hz, 4H, linear isomer), 2.54–2.52 (t, $J_{H–H}$ = 9.5Hz, 2H, linear isomer), 2.44 (b, 3H, linear isomer), 1.73 (s, 6H, linear isomer), 1.65 (s, 3H, branched isomer). HRMS: calcd for $C_9H_{17}NO[M + H]^+$156.13, found: 156.13.

**(E)-4-(3,7-dimethylocta-2,6-dienyl)morpholine**

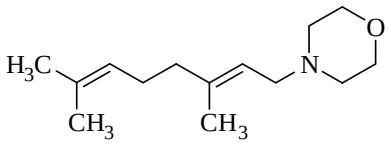

Yield: 25.0 mg (50%). $^{1}$H-NMR (500 MHz, $CDCl_3$): δ 5.26-5.25 (m, 1H, C*H*=$CH_2$N ), 5.08–5.05 (m, 1H, $(CH_3)_2$C=C*H*), 3.73–3.71 (t, $J_{H-H}$ = 9.5 Hz, 4H, OC$H_2$ ), 2.97–2.96 (d, $J_{H-H}$ = 7 Hz, 2H, CH=C$H_2$N), 2.44 (bs, 4H, NC$H_2$), 2.10–2.02 (m, 4H), 1.66 (s, 3H, Me), 1.64 (s, 3H, Me), 1.59 (s, 3H, Me). $^{13}$C-NMR (100 MHz, $CDCl_3$): δ 139.0, 131.3, 123.9, 120.1, 66.8, 56.2, 53.4, 39.6, 26.2, 25.5, 17.5, 16.2. HRMS: calcd for $C_{14}H_{26}NO[M + H]^{+}$224.19, found: 224.19.

**(E)-4-(1,3-diphenylallyl)morpholine**

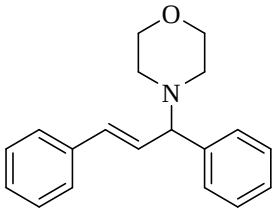

Yield: 48.0 mg (98%).$^{1}$H-NMR (500 MHz, $CDCl_3$): δ 8.05 (s, 1H Ar*H*), 7.44–7.43 (m, 2H, Ar*H*), 7.39–7.38(m, 3H, Ar*H*), 7.32–7.29 (m, 3H, Ar*H*), 7.24–7.22 (m, 1H, Ar*H*), 6.70–6.67 (d, $J_{H-H}$ = 16.0 Hz, 1H, ArC*H*=CH), 6.41–6.37 (dd, $J_{H-H}$ = 6.5 Hz, 6.5Hz, 1H, ArCH=C*H*), 5.39–5.38 (d, $J_{H-H}$ = 6.5 Hz, 1H), 3.67–3.52 (t, $J_{H-H}$ = 10 Hz, 4H, OC$H_2$), 2.90–2.88 (t, $J_{H-H}$ = 10 Hz, 24H, NC$H_2$). HRMS: calcd for $C_{19}H_{22}NO[M + H]^{+}$ 280.17, found: 280.16.

**N,N-dibenzyl-O-(but-3-en-2-yl)hydroxylamine**

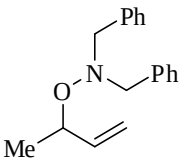


Yield: 48.1 mg (98%). $^{1}$H-NMR (500 MHz, $CDCl_3$): δ 7.36–7.35 (m, 4H, Ar*H*), 7.32–7.24 (m, 6H, Ar*H*), 5.59–5.52 (m, 1H, C*H*=$CH_2$ ), 5.02–4.98 (dd, *J* = 17Hz, 1Hz , 2H, CH=C$H_2$), 3.89–3.856 (m, 3H), 3.78–3.76 (d, $J_{H-H}$ = 12.5 Hz, 2H), 0.95 (d, *J* = 6.5 Hz, 3H ); 13C-NMR (125 MHz, $CDCl_3$) δ 140.2,138.0, 130.0, 128.5, 127.4, 115.6, 79.6, 62.9, 19.4 HRMS: calcd for $C_{18}H_{22}NO$ [M + H]$^{+}$]+): 268.17, found 268.17.

## REFERENCES


1. Wanzlick, H. W.; Schikora, E. Angew. Chem. 1960, 72, 494; (b) Wanzlick, H. W,; Kleiner, H. J. Angew . Chem. 1961, 73, 493; (c) Wanzlick, H. W. Angew. Chem. Int. Ed. Engl. 1962,1 ,75; (d) Ofele, K. J. Organomet. Chem. 1968, 12, 42.
2. Arduengo, A. J,; Harlow, R. L,; Kline, M. J. Am. Chem. Soc. 1991, 113, 361.
3. Hahn, F. E,; Jahnke, M. C. Angew. Chem. Int. Ed. 2008, 47, 3122; (b) Diez-Gonzalez, S,; Marion, N,; Nolan, S. P. Chem. Rev. 2009, 109, 3612.
4. Weskamp, T,; Bohm, V. P. W,; Hermann, W. A. J. Organomet. Chem. 2000, 600, 12; (b) Nolan, S. P. N-Heterocyclic Carbenes in Synthesis, Wiley-VCH, Weinheim, Germany, 2006.
5. Herrmann, W. A. Angew. Chem. Int. Ed. 2002, 41, 1290.
6. Herrmann, W. A,; Goossen, L. J.; Artusher, G. R. J,; Köcher, C. Organometallics 1997, 16, 2472.
7. Lee, S .W,; Hartwig, J. F. J. Org. Chem. 2001, 66, 3402.
8. Seiders, T. J,; Ward, D. W,; Grubbs, R. H. Org. Lett. 2001, 3, 3225.
9. Powell, M. T,; Hou, D. R,; Perry, M. C,; Cui, X. H,; Burgess, K. J. Am. Chem. Soc. 2001, 123, 8878.
10. Merzouk, M,; Moore, T,; Williams, N. A. Tetrahedron, 2007, 48, 8914.
11. Herrmann, W. A.; Schütz, J,; Frey, G. D,; Herdtweck, E. Organometallics 2006, 25, 2437; (b) Leuthäuβer, S,; Schwarz, P,; Plenio, H. Chem. Eur. J. 2007, 13, 7195; (c) Gusev, D. M. Organometallics 2009, 28, 6458.
12. Hillier, A. C,; Sommer, W. H,; Yong, B. S,; Petersen, J. L,; Cavallo, L,; Nolan, S. P. Organometallics 2003, 22, 4322.
13. Süssner, M,; Plenio, H. Chem. Commun. 2005, 43, 5417; (b) Mercs, L,; Labat, G,; Neels, A,; Ehlers, A,; Albrecht, M. Organometallics 2006, 25, 5648.
14. Huynh, H. V,; Han, Y,; Jothibasu, R,; Yang, J. A. Organometallics 2009, 28, 5395.

15. Magill, M. A,; Cavell, K. J,; Yates, B. J. Am. Chem. Soc. 2004, 126, 8717.
16. Hillier, A. C,; Sommer, W. J,; Yong, B. S,; Petersen, J. L,; Cavallo, L,; Nolan, S. P. Organometallics 2003, 22, 4322.
17. Clavier, H,; Nolan, S. P. Chem. Comm. 2010, 46, 841.
18. McGuinness, D. S,; Green, M. J,; Cavell, K. J,; Skelton, B. W,; White, A. H. J. Organomet. Chem. 1998, 565, 165.
19. McGuinness, D. S,; Green, M. J,; Cavell, K. J,; Skelton, B. W,; White, A. H. J. Organomet. Chem. 1998, 565, 165; (b) McGuinness, D. S,; Cavell, K. J,; Skelton, B. W,; White, A. H. Organometallics 1999, 18, 1596; (c) McGuinness, D. S,; Cavell, K. J,; Yates, B. F,; Skelton, B. W,; White, A. H. J. Am. Chem. Soc. 2001, 123, 8317; (d) Caddick, S,; Cloke, F. G. N,; Hitchcock, P. B,; Leonard, J,; Lewis, A. K,; McKerrecher, D,; Titcomb, L. R. Organometallics 2002, 21, 431; (e) McGuinness, D. S,; Mueller, W,; Wasserscheid, P,; Cavell, K. J,; Skelton, B. W,; White, A. H,; Englert, U. Organometallics 2002, 21, 175.
20. McGuinness, D. S,; Saendig, N,; Yates, B. F,; Cavell, K. J. J. Am.Chem. Soc. 2001, 123, 4029.
21. Normand, A.T,; Cavell, K. J. Eur. J. Inorg. Chem. 2008, 2781.
22. Braunstein, P,; Naud, F. Angew. Chem. Int. Ed. 2001, 40, 680.
23. Lee, C. C,; Ke, W. C,; Chan, K. T,; Lai, C. L,; Hu, C. H,; Lee, H. M. Chem. Eur. J. 2007, 13, 582; (b) Hahn, F. E,; Jahnke, M. C,; Pape, T. Organometallics 2006, 25, 5927; (c) Yang, C. L,; Lee, H. M,; Nolan, S. P. Org. Lett. 2001, 3, 1511.
24. Danopoulos, A. A,; Tsoureas, N,; Macgregor, S. A,; Smith, C. Organometallics 2007, 26, 253; (b) Mas-Marza, E,; Sanau, M,; Peris, E. J. Organomet. Chem. 2005, 690, 5576; (c) Mas-Marza, E,; Sanau, M,; Peris, E. Inorg. Chem. 2005, 44, 9961.
25. Gade, L. H,; Bellemin-Laponnaz, S. Coord. Chem. Rev. 2007, 251, 718.
26. Liao, C. Y,; Chan, K. T,; Zeng, J. Y,; Hu, C. H,; Tu, C,; Lee, H. M. Organometallics 2007, 26, 1692; (b) Spencer, L. P,; Winston, S,; Fryzuk,

M. D. Organometallics 2004, 23, 3372; (c) Arnold, P. L.; Liddle, S. T. Chem. Commun. 2006, 3959.

27. Herrmann, W. A,; Goossen, L. J,; Spiegler, M. J. Organomet. Chem. 1997, 547, 357.
28. Wang, A. E,; Xie, J. H,; Wang, L. X,; Zhou, Q. L. Tetrahedron, 2005, 61, 259.
29. Christmann, U,; Vilar, R. Angew. Chem. Int. Ed., 2005, 44, 366; (b) Hillier, A. C,; Grasa, G. A,; Viciu, M. S,; Lee, H. M,; Yang, C,; Nolan, S. P. J. Organomet. Chem. 2002, 653, 69.
30. Albert, K,; Gisdakis, P,; Rösch, N. Organometallics 1998, 17, 1608.
31. Herrmann, W. A,; Köcher, C,; Goossen, L. J,; Artus, G. R. J. Chem. Eur. J. 1996, 2, 1627.
32. Seo, H.; Park, H.–J.; Kim, B. Y.; Lee, J. H.; Son, S. U.; Chung, Y. K. Organometallics, 2003, 22, 618.
33. Tsoureas, N,; Danopoulos, A. A,; Tulloch, A. A. D,; Light, M. E. Organometallics 2003, 22, 4750.
34. Lee, H. M,; Chiu, P. L,; Zeng, J. Y. Inorg. Chim. Acta, 2004, 357, 4313.
35. Wang, A. E,; Zhong, J,; Xie, J. H,; Li, K,; Zhou, Q. L. Adv. Synth. Catal. 2004, 346, 595.
36. Zhong, J,; Xie, J. H,; Wang, A. E,; Zhang, W,; Zhou, Q. L. Synlett. 2006, 8, 1193.
37. Field, L. D,; Messerle, B. A,; Vuong, K. Q,; Turner, P. Organometallics 2005, 24, 4241.
38. Seo, H,; Park, H. J,; Kim, B. Y,; Lee, J. H,; Son, S. U,; Chung, Y. K. Organometallics 2003, 22, 618.
39. Bappert, E,; Helmchen, G. Synlett, 2004, 10, 1789.
40. Becht, J. M,; Bappert, E,; Helmchen, G. Adv. Synth. Catal. 2005, 347, 1495.
41. Hahn, F. E,; Jahnke, M. C,; Pape, T. Organometallics 2006, 25, 5927.
42. Gischig, S,; Togni, A. Organometallics 2004, 23, 2479; (b) Gischig, S,; Togni, A. Eur. J. Inorg. Chem. 2005, 4745.

43. Lee, H. M,; Zeng, J. Y,; Hu, C. H,; Lee, M. T. Inorg. Chem. 2004, 43, 6822.
44. Chiu, P. L,; Lee, H. M. Organometallics 2005, 24, 1692.
45. Zeng, J. Y,; Hsieh, M. H,; Lee, H. M. J. Organomet. Chem. 2005, 690, 5662.
46. Lee, C. C,;. Ke, W. C,; Chan, K. T,; Lai, C. L,; Hu, C. H,; Lee, H. M. Chem.-Eur. J. 2007, 13, 582.
47. Herrmann, W. A,; Goossen, L. J,; Spiegler, M. Organometallics 1998, 17, 2162.
48. Powell, M. T,; Hou, D. R,; Perry, M. C,; Cui, X. H,; Burgess, K. J. Am. Chem. Soc. 2001, 123, 8878.
49. Sprinz, J,; Helmchen, G. Tetrahedron Lett. 1993, 34, 1769; (b) Review: Pfaltz, A,; Blankenstein, J,; Hilgraf, R,; Hörmann, E,; McIntyre, S,; Menges, F,; Schönleber, M,; Smidt, S.P,; Wüstenberg, B,; Zimmermann, N. Adv. Synth. Catal. 2003, 345, 33.
50. C´esar, V,; Bellemin-Laponnaz, S,; Wadepohl, H,; Gade, L. H. Chem. Eur. J. 2005, 11, 2862.
51. Poyatos, M,; Maisse-Francois, A,; Bellemin-Laponnaz, S,; Gade, L. H. Organometallics 2006, 25, 2634.
52. Yuan, Y,; Raabe, G,; Bolm, C. J. Organomet. Chem. 2005, 690, 5747.
53. Ren, L,; Chen, A.C,; Decken, A,; Crudden, C.M,; Can. J. Chem. 2004, 82, 1781.
54. Bolm, C,; Focken, T,; Raabe, G. Tetrahedron Asymm. 2003,14,1733.
55. Schneider, N,; C´esar, V,; Bellemin-Laponnaz, S,; Gade, L. H. Organometallics 2005, 24, 4886.
56. Tulloch, A. A. D,; Danopoulos, A. A,; Tooze, R.P,; Cafferkey, S. M,; Kleinhenz, S,; Hursthouse, M. B. Chem. Commun. 2000, 14, 1247.
57. Winston, S,; Stylianides, N,; Tulloch, A.A.D,; Wright, J.A,; Danopoulos, A.A. Poly. 2004, 23, 2813.
58. Chianese, A. R,; Bremer, P. T,; Wang, C,; Reynes, R. J. Organometallics 2009, 28, 5244.

59. Gründemann, S,; Albrecht, M,; Loch, J. A,; Faller, J. W., Crabtree, R. H. Organometallics 2001, 20, 5485; (b) Loch, J. A,; Albrecht, M,; Peris, E,; Mata, J,; Faller, J. W,; Crabtree, R. H. Organometallics 2002, 21, 700.
60. Hahn, F. E,; Jahnke, M. C,; Gomez-Benitez, V,; Morales-Morales, P,; Pape, T. Organometallics 2005, 24, 6458.
61. Sellmann, D,; Prechtel, W,; Knoch, F,; Moll, M. Organometallics 1992, 11, 2346.
62. Huynh, H. V,; Chew, Y. X. Inorg. Chim. Acta. 2010, 363, 1979.
63. (a). Huynh, H. V,; Yeo, C. H,; Chew, Y. X. Organometallics 2010, 29, 1479; (b). Huynh, H. V,; Yeo, C. H,; Tan, G.K. Chem. Commun. 2006, 3833.
64. Ros, A,; Monge, D,; Alcarazo, M,; Alvarez, E,; Lassaletta, J.M,; Fernandez, R. Organometallics 2006, 25, 6039.
65. Roseblade, S. J,; Ros, A,; Monge, D,; Alcarazo, M,; Alvarez, E,; Lassaletta, J. M,; Fernandez, R. Organometallics 2007, 26, 2570.
66. Huynh, H. V,; Yuan, D,; Han, Y. Dalton Trans. 2010, 363, 1979.
67. Hiraki, K,; Fuchita, Y,; Takechi, K. Inorg. Chem. 1981, 20, 4316.
68. Takahashi, Y,; Tokuda, A,; Sakai, S,; Ishii, Y. J. Organomet. Chem. 1972, 35, 415.
69. Hirake, K,; Fuchita, Y,; Maruta, T. Inorg. Chim. Acta 1980, 45, L205; (b) Fuchita, Y,; Hirake, K,; Yamaguchi, T,; Maruta, T. J. Chem. Soc. Dalton Trans. 1981, 2405; (c) Siedle, A. R. J. Organomet. Chem.1981, 20, 115.
70. Dupont, J,; Beydoun, N,; Pfeffer, M. J. Chem. Soc. Dalton Trans. 1989, 1715.
71. Abel, E. W,; Booth, M,; Orrell, K. G. J. Chem. Soc., Dalton Trans. 1980, 1582; Cross, R. J,; Dalgleish, I. G,; Smith, G. J,; Wardle, R. Ibid. 1972, 992; Yoshida, G,; Urosawa, H,; Okawara, R. J. Organomet. Chem. 1976, 113, 85.
72. van Koten, G,; Jastrzebski, J. T. B. H,; Noltes, J. G,; Pontenagel, W. M. G. F,; Kroon, J. Spek, A. L. J. Am. Chem. Soc., 1978,100, 5021; van Koten, G,; Noltes, J. G. Ibid. 1979, 101, 6593; Van Koten, G,;

Jastrzebski, J. T. B. H,; Noltes, J. G,; Verhoeckx, G. J,; Spek, A. L,; Kroon, J. J. Chem. Soc., Dalton Trans. 1980, 1352; Arlen, C,; Pfeffer, M,; Bars, O,; Le Borgne, G. Ibid. 1986, 359.

73. Dupont, J.; Pfeffer, M. J. Chem. Soc. Dalton Trans. 1990, 3193.
74. Dupont, J,; Gruber, A. S,; Fonseca, G. S,; Monteiro, A. L,; Ebling, H. Organometallics 2001, 20, 171.
75. Alper, H. J. Organomet. Chem. 1974, 80, C29.
76. Trost, B. M,; Merlic, C. A. J. Am. Chem. Soc.1990, 112, 9590; Ward, Y. ,; Villanueva, L. A,; Allred, G. D,; Liebeskind, L. S. J. Am. Chem. Soc. 1996, 118, 897; (b) Malkov, A. V,; Langer, V,; Lloyd-Jones, G. C,; Spoor, P,; Kocˇovsky´, P. Organometallics 2001, 20, 673.
77. Tsuji, J,; Minami, I,; Shimizi, I. Tetrahedron Lett. 1984, 25, 5157, (b).Minami, I.; Shimizu, I.; Tsuji, J. J. Organomet. Chem. 1985,296, 269.
78. Mora, G,; Piechaczyk, O,; Le Goff, X. F,; Le Floch, P. Organometallics 2007, 26, 1846.
79. Trost, B. M,; Toste, F.D. J. Am. Chem. Soc. 1998, 121, 4545.
80. Ozawa, F,; Okamoto, H,; Kawagishi, S,; Yamamoto, S,; Minami, T,; Yoshifuji, M. J. Am. Chem. Soc. 2002, 124, 10968.
81. Kinoshita, H,; Shinokubo, H,; Oshima, K. Org. Lett. 2004, 6, 4085.
82. Yang, S. C. Tetrahedron Lett. 2006, 62, 3949.
83. Mora, G,; Deschamps, B,; van Zutphen, S,; Xavier, S,; Ricard, L,;. Le Floch, P. Organometallics 2007, 26, 1846.
84. Flahaut, A.; Roland, S.; Mangeney, P. J. Orgnomet. Chem. 2007, 692, 5754; (b) Roland, S,; Cotet, W,; Mangeney, P. Eur. J. Inorg. Chem. 2009, 13, 1796.
85. Chianese, A. R,; Bremer, P. T,; Wong, C,; Reynes, R. J. Organometallics 2009, 28, 5244.
86. Herrmann, W. A,; Böhm, V. P. W,; Gstöttmayr, G. W. K,; Grosche, M,; Resinger, C. P,; Weskamp, T. J. Organomet. Chem. 2001, 617, 616; (b) Grasa, G. A,; Nolan, S. P. Org. Lett. 2001, 3, 119

87. Herrmann, W. A,; Elison, M,; Fischer, J,; Köcher, C,; Artus, G. R. J. Angew. Chem. Int. Ed. 1995, 34, 2371
88. Herrman, W. A,; Reisinger, C. P,; Spiegler, M. J. Organomet. Chem. 1998, 557, 93.
89. Wang, W. F,; Zhang, T,; Shi, M. Organometallics 2009, 28, 2640.
90. Zhou, J. R,; Fu, G. C. J. Am. Chem. Soc. 2003, 125, 12527; (b) Hadei, N,; Kantchev, E. A. B,; O'Brien, C. J,; Organ, M. G. Org. Lett. 2005, 7, 3805; (c) Hadei, N,; Kantchev, E. A. B,; O'Brien, C. J,; Organ, M. G. J. Org. Chem. 2005, 70, 8503; (d) Organ, M. G,; Arola, S. Dubovyk, I,; Hadei, N,; Kantchev, E. A. B,; O'Brien, C. J,; Valente, C. Chem. Eur. J. 2006, 12, 4749.
91. Huang, J,; Nolan, S. P. J. Am. Chem. Soc. 1999, 121, 9889; (b) Frisch, A. C,; Rataboul, F,; Zapf, A,; Beller, M. J. Organomet. Chem. 2003, 687, 403.
92. Herrman, W. A,; Reisinger, C. P,; Spiegler, M. J. Organomet. Chem. 1998, 557, 93; (b) Caddick, S,; Cloke, F. G. N,; Clentsmith, G. K. B,; Hitchcock, P. B,; McKerrecher, D,; Titcomb, L. R,; Wiliams, M. R. V. J. Organomet. Chem. 2001, 617-618, 635.
93. Anders, E,; Tropsch, J. G,; Katritzky, A. R,; Rasala, D. J. Org. Chem. 1989, 54, 4808.
94. Wang, H. M. J,; Lin, I. J. B. Organometallics 1998, 17, 972.
95. Faller, J. W,; Wilt, J. C. Organometallics 2005, 24, 5076; (b) Faller, J. W. Adv. Organomet. Chem. 1977, 16, 211; (c) Breutel, C,; Pregosin, P. S,; Salzmann, R,; Togni, A. J. Am.Chem. Soc. 1994, 116, 4067; (d) Herrmann, J,; Pregosin, P. S,; Salzmann, R,; Albinati, A. Organometallics 1995, 14, 3311; (e) Pregosin, P. S,; Salzmann, R. Coord. Chem. Rev. 1996, 155, 35; (f) Evans, D. A,; Michael, F. E,; Tedrow, J. S,; Campos, K. R. J. Am. Chem. Soc. 2003, 125, 3534; (g) Faller, J. W,; Sarantopoulos, N. Organometallics 2004, 23, 2179; (h) Filipuzzi, S,; Pregosin, P,; Albinati, A,; Rizzato, S. Organometallics 2006, 25, 5955; (i) Filipuzzi, S,; Pregosin, P. S,; Albinati, A,; Rizzato, S. Organometallics 2008, 27, 437;

(j) Filipuzzi, S.; Pregosin, P. S.; Calhorda, M. J.; Costa, P. J. Organometallics 2008, 27, 2949.

96. Zhang, T,; Shi, M. Chem. Eur. J. 2008, 14, 3759.
97. Hiskey, R. G,; Adams, J. B. J. Org. Chem. 1966, 31, 2178.
98. Chianese, A.R,; Bremer, P.T,; Wong, C,; Reynes, R.J. Organometallics 2009, 28, 5244.
99. Hayashi, T.; Kishi, K.; Yamamoto, A.; Ito, Y. Tetrahedron Lett. 1990, 31, 1743.
100. Faller, J. W,; Wilt, J. C. Organometallics 2005, 24, 5076; (b) Prètốt, R,; Pfaltz, A. Angew. Chem. Int. Ed. 1998, 37, 323; (c) van Haaren, R. J,; Druijven, C. J. M,; van Strijdonck, G. P. F,; Oevering, H,; Reek, J. N. H,; Kamer, P. C. J,; van Leeuwen, P. W. N. M. J. Chem. Soc. Dalton Trans. 2000, 10, 1549; (d) You, S. L,; Zhu, X. Z,; Luo, Y. M,; Hou, X. L,; Dai, L. X. J.Am. Chem. Soc. 2001, 123, 7471.
101. Godleski, S. A. In Comprehensive Organic Synthesis, 1st ed., Semmelhack, M. F., Ed., Pergamon Press, NewYork, 1991, 4, 58.
102. Helmchem, G,; Kazmaier, U,; Forster, S. In Catalytic Asymmetric Synthesis, 3rd ed., Ojima, I., Ed.; John Wiley & Sons, Inc. New Jersey, 2010; 497.
103. Marckwald, W,; McKenzie, A. Ber. Dtsch. Chem. Ges. 1899, 32, 2130.
104. Pope, W. J,; Peachey, S. J. J. Chem. Soc. Trans. 1899, 75, 1066.
105. Rouhi, A. M. Chemical and Engineering News, 2003, 45.
106. Kim, K. S,; Sack, J. S,; Tokarski, J. S,; Qian, L,; Chao, S. T,; Leith, L,; Kelly, Y. F,; Misra, R. N,; Hunt, J. T,; Kimball, S. D,; Humphreys, W. G,; Wautlet, B. S,; Mulheron, J. G,; Webster, K. R. J. Med. Chem., 2000, 43, 4126.
107. Sakurai, R,; Sakai, K. Tetrahedron Asymm. 2003, 14, 411.
108. Sakurai, R,; Sakai, K,; Yuzawa, A,; Hirayama, N. Tetrahedron Asymm. 2003, 14, 3713.
109. B´alint, J,; Hell, Z,; Markovits, I,; P´ark´anyi, L,; Fogassy, E. Tetrahedron Asymm. 2000, 11, 1323.

110. B´alint, J,; Egri, G,; Fogassy, E.; B¨ocskei, Z. S,; Simon, K,; Gaj´ary, A,; Friesz, A. Tetrahedron Asymm. 1999, 10, 1079.
111. Chan, C,; Durand, V,; Fasquelle, F,; F´eru, R,; Gilbertsen, H,; Jacobelli, A,; Kebsi, E,; Lallier, J,; Maignel, B,; Martin, S,; Milano, M,; Ouaguaed, Y,; Pascal, M. P,; Pruniaux, J,; Puaud, M. N,; Rocher, C,; Terrasse, R,; Doherty, A. J. Med. Chem. 2000, 43, 4850.
112. Ma, S,; Wu, S. Chem. Commun. 2001, 441.
113. Haynes, R. K,; Au-Yeung, T. L,; Chan, W.K,; Lam, W. L,; Li, Z. Y,; Yeung, L. L,; Chan, A. S. C,; Li, P,; Koen, M,; Mitchell, C. R,; Vonwiller, S. Eur. J. Org. Chem. 2000, 3205.
114. Chuard, T,; Cowling, S. J,; Fernandez-Ciurleo, M,; Jauslin, I,; Goodby, J. W,; Deschenaux, R. Chem. Commun. 2000, 2109.
115. Seki, M,; Yamada, S,; Kuroda, T,; Imashiro, R,; Shimizu, T. Synthesis 2000, 12, 1677.
116. Nöteberg, D.; Branalt, J,; Kvarnström, I,; Linschoten, M,; Musil, D,; Nyström, J. E,; Zuccarello, G,; Samuelsson, B. J. Med. Chem. 2000, 43, 1705.
117. Yoneda, A,; Hakushi, T. Organometallics 1994, 13, 4912; (b) Spencer, J,; Maassarani, F,; Pfeffer, M,; DeCian, A,; Fischer, J. Tetrahedron Asymm. 1994, 5, 321; (c) Spencer, J,; Pfeffer, M. Tetrahedron Asymm. 1995, 6, 419; (d) Wu, W. J,; Cui, X. L,; Du, C.X,; Wang, W.L,; Guo, R.Y,; Chen, R. F. Dal. Trans. 1998, 3727; (e) Dinina, V.V,; Razmyslova, E.,; Kuz'mina, L.G,; Churakov, A.V,; Rubina, M.Y,; Grishin, Y.K. Tetrahedron Asymm. 1999, 10, 3147; (f) Dunina, V.V,; Gorunova, O. N,; Kuz'mina, L. G,; Kataeva, N.A,; Grishin, Y. K. Tetrahedron Asymm. 1999, 10, 3951; (g) Dunina, V. V,; Gorunova, O.N,; Livantsov, M.V,; Grishin, Y. K,; Kuz'mina, L. G,; Kataeva, N. A,; Churakov, A.V. Tetrahedron Asymm. 2000, 11, 3967; (h) Li, Y. X,; Selvaratnam, S,; Vittal, J. J,; Leung, P. H. Inorg. Chem. 2003, 42, 3229; (i) Ding, Y,; Li, Y. X,; Zhang, Y,; Pullarkat, S. A,; Leung, P. H. Eur. J. Inorg. Chem. 2008, 11, 1880; (j) Ding, Y,; Li, Y. X,; Pullarkat, S. A,; Yap, S. L,;

Leung, P. H. Eur. J. Inorg. Chem. 2009, 2, 267; (k) Ding, Y,; Chiang, M. Y,; Pullarkat, S. A,; Li, Y. X,; Leung, P. H. Organometallics 2009, 28, 4358.

118. Abdellah, I,; Debono, N,; Canac, Y,; Duhayon, C,; Chauvin, R. Dal. Trans. 2009, 7196.
119. Chiang, M,; Li, Y,; Krishnan, D,; Sumod, P,; Ng, K. H,; Leung, P. H. Eur. J. Inorg. Chem. 2010, 9, 1413.
120. Tambar, U. K,; Bao, H,; Qi, X. J. Am. Chem. Soc. 2011, 133, 1206.
121. Arduengo, A. J,; Gentry, F. P,; Taverkere, Jr.; P. K,; Simmons, H. E. (E. I. Du Pont de Nemours & Co.) U.S. Patent 6, 2001, 77, 575.

# APPENDICES

**Table A1** Crystal data for compound **(Rs*,S*)-66a**

| | | |
|---|---|---|
| Empirical formula | C28 H29 B F4 N2 Pd S | |
| Formula weight | 618.80 | |
| Temperature | 103(2) K | |
| Wavelength | 0.71073 Å | |
| Crystal system | Orthorhombic | |
| Space group | P2(1)2(1)2(1) | |
| Unit cell dimensions | a = 8.3349(12) Å | α= 90°. |
| | b = 17.001(2) Å | β= 90°. |
| | c = 18.996(3) Å | γ = 90°. |
| Volume | 2691.8(7) $Å^3$ | |
| Z | 4 | |
| Density (calculated) | 1.527 $Mg/m^3$ | |
| Absorption coefficient | 0.815 $mm^{-1}$ | |
| F(000) | 1256 | |
| Crystal size | 0.30 x 0.08 x 0.02 $mm^3$ | |
| Theta range for data collection | 1.61 to 25.71°. | |
| Index ranges | -10<=h<=10, -20<=k<=18, -22<=l<=23 | |
| Reflections collected | 27367 | |
| Independent reflections | 5066 [R(int) = 0.1033] | |
| Completeness to theta = 25.71° | 98.9 % | |
| Absorption correction | Semi-empirical from equivalents | |
| Max. and min. transmission | 0.9839 and 0.7921 | |
| Refinement method | Full-matrix least-squares on $F^2$ | |
| Data / restraints / parameters | 5066 / 12 / 337 | |
| Goodness-of-fit on $F^2$ | 1.137 | |
| Final R indices [I>2sigma(I)] | R1 = 0.0611, wR2 = 0.1490 | |
| R indices (all data) | R1 = 0.0866, wR2 = 0.1691 | |
| Absolute structure parameter | 0.00(6) | |
| Largest diff. peak and hole | 1.835 and -2.317 $e.Å^{-3}$ | |

**Table A2** Crystal data for compound (**Ss*,R*)-67b**

| | | |
|---|---|---|
| Empirical formula | C21 H24 Cl2 N2 Pd S | |
| Formula weight | 513.78 | |
| Temperature | 103(2) K | |
| Wavelength | 0.71073 Å | |
| Crystal system | Orthorhombic | |
| Space group | Pna2(1) | |
| Unit cell dimensions | a = 16.1758(13) Å | α= 90°. |
| | b = 8.9069(7) Å | β= 90°. |
| | c = 14.5998(9) Å | γ= 90°. |
| Volume | 2103.5(3) $Å^3$ | |
| Z | 4 | |
| Density (calculated) | 1.622 $Mg/m^3$ | |
| Absorption coefficient | 1.244 $mm^{-1}$ | |
| F(000) | 1040 | |
| Crystal size | 0.18 x 0.10 x 0.10 $mm^3$ | |
| Theta range for data collection | 2.61 to 32.16°. | |
| Index ranges | -24<=h<=23, -13<=k<=13, -12<=l<=21 | |
| Reflections collected | 15140 | |
| Independent reflections | 6121 [R(int) = 0.0692] | |
| Completeness to theta = 32.16° | 98.0 % | |
| Absorption correction | Semi-empirical from equivalents | |
| Max. and min. transmission | 0.8857 and 0.8070 | |
| Refinement method | Full-matrix least-squares on $F^2$ | |
| Data / restraints / parameters | 6121 / 1 / 248 | |
| Goodness-of-fit on $F^2$ | 1.007 | |
| Final R indices [I>2sigma(I)] | R1 = 0.0431, wR2 = 0.0846 | |
| R indices (all data) | R1 = 0.0606, wR2 = 0.0928 | |
| Absolute structure parameter | 0.04(3) | |
| Largest diff. peak and hole | 0.829 and -0.825 $e.Å^{-3}$ | |

**Table A3** Crystal data compound for **(±)-67c**

| | |
|---|---|
| Empirical formula | C18 H26 Cl2 N2 Pd S |
| Formula weight | 479.77 |
| Temperature | 296(2) K |
| Wavelength | 0.71073 Å |
| Crystal system | Monoclinic |
| Space group | P2(1)/c |
| Unit cell dimensions | a = 9.7207(2) Å α= 90°.<br>b = 16.0338(2) Å β= 108.3230(10)°.<br>c = 13.8366(2) Å γ = 90°. |
| Volume | 2047.23(6) $Å^3$ |
| Z | 4 |
| Density (calculated) | 1.557 $Mg/m^3$ |
| Absorption coefficient | 1.272 $mm^{-1}$ |
| F(000) | 976 |
| Crystal size | 0.36 x 0.34 x 0.12 $mm^3$ |
| Theta range for data collection | 2.00 to 32.50°. |
| Index ranges | -14<=h<=14, -18<=k<=24, -20<=l<=20 |
| Reflections collected | 46969 |
| Independent reflections | 7411 [R(int) = 0.0259] |
| Completeness to theta = 32.50° | 100.0 % |
| Absorption correction | Semi-empirical from equivalents |
| Max. and min. transmission | 0.8623 and 0.6574 |
| Refinement method | Full-matrix least-squares on $F^2$ |
| Data / restraints / parameters | 7411 / 0 / 223 |
| Goodness-of-fit on $F^2$ | 1.297 |
| Final R indices [I>2sigma(I)] | R1 = 0.0207, wR2 = 0.0649 |
| R indices (all data) | R1 = 0.0244, wR2 = 0.0746 |
| Largest diff. peak and hole | 1.289 and -1.198 $e.Å^{-3}$ |

**Table A4** Crystal data for compound **(±) 82**

| | | |
|---|---|---|
| Empirical formula | C39 H39 Cl2 N2 P Pd S | |
| Formula weight | 776.05 | |
| Temperature | 103(2) K | |
| Wavelength | 0.71073 Å | |
| Crystal system | Monoclinic | |
| Space group | P2(1)/n | |
| Unit cell dimensions | a = 15.2842(3) Å | α= 90°. |
| | b = 13.5565(2) Å | β= 109.3280(10)°. |
| | c = 18.5542(3) Å | γ= 90°. |
| Volume | 3627.76(11) $Å^3$ | |
| Z | 4 | |
| Density (calculated) | 1.421 $Mg/m^3$ | |
| Absorption coefficient | 0.791 $mm^{-1}$ | |
| F(000) | 1592 | |
| Crystal size | 0.36 x 0.30 x 0.20 $mm^3$ | |
| Theta range for data collection | 1.90 to 27.50°. | |
| Index ranges | -19<=h<=19, -17<=k<=15, -23<=l<=24 | |
| Reflections collected | 43311 | |
| Independent reflections | 8320 [R(int) = 0.0351] | |
| Completeness to theta = 27.50° | 99.8 % | |
| Absorption correction | Semi-empirical from equivalents | |
| Max. and min. transmission | 0.8579 and 0.7639 | |
| Refinement method | Full-matrix least-squares on $F^2$ | |
| Data / restraints / parameters | 8320 / 0 / 419 | |
| Goodness-of-fit on $F^2$ | 1.137 | |
| Final R indices [I>2sigma(I)] | R1 = 0.0374, wR2 = 0.1118 | |
| R indices (all data) | R1 = 0.0479, wR2 = 0.1300 | |
| Largest diff. peak and hole | 2.346 and -1.087 $e.Å^{-3}$ | |

**Table A5** Crystal data for compound **(Rs*,S*,R*)-86**

| | | |
|---|---|---|
| Empirical formula | C22 H26 Cl2 N2 Pd S | |
| Formula weight | 527.81 | |
| Temperature | 103(2) K | |
| Wavelength | 0.71073 Å | |
| Crystal system | Orthorhombic | |
| Space group | P2(1)2(1)2(1) | |
| Unit cell dimensions | a = 10.4613(3) Å | α= 90°. |
| | b = 11.5237(3) Å | β= 90°. |
| | c = 18.8138(5) Å | γ= 90°. |
| Volume | 2268.06(11) $Å^3$ | |
| Z | 4 | |
| Density (calculated) | 1.546 $Mg/m^3$ | |
| Absorption coefficient | 1.156 $mm^{-1}$ | |
| F(000) | 1072 | |
| Crystal size | 0.38 x 0.26 x 0.24 $mm^3$ | |
| Theta range for data collection | 2.07 to 40.47°. | |
| Index ranges | -19<=h<=17, -17<=k<=20, -31<=l<=34 | |
| Reflections collected | 57020 | |
| Independent reflections | 14052 [R(int) = 0.0333] | |
| Completeness to theta = 40.47° | 99.6 % | |
| Absorption correction | Semi-empirical from equivalents | |
| Max. and min. transmission | 0.7688 and 0.6677 | |
| Refinement method | Full-matrix least-squares on $F^2$ | |
| Data / restraints / parameters | 14052 / 0 / 257 | |
| Goodness-of-fit on $F^2$ | 1.061 | |
| Final R indices [I>2sigma(I)] | R1 = 0.0286, wR2 = 0.0614 | |
| R indices (all data) | R1 = 0.0358, wR2 = 0.0719 | |
| Absolute structure parameter | 0.001(13) | |
| Largest diff. peak and hole | 0.708 and -0.880 $e.Å^{-3}$ | |

**Table A6** Crystal data compound for **(Rs*,S*,R*)-87**

| | | |
|---|---|---|
| Empirical formula | C25 H24 Cl2 N2 Pd S | |
| Formula weight | 561.82 | |
| Temperature | 103(2) K | |
| Wavelength | 0.71073 Å | |
| Crystal system | Monoclinic | |
| Space group | P2(1) | |
| Unit cell dimensions | a = 8.3912(6) Å | α= 90°. |
| | b = 16.8888(11) Å | β= 111.410(3)°. |
| | c = 9.1081(6) Å | γ= 90°. |
| Volume | 1201.70(14) $Å^3$ | |
| Z | 2 | |
| Density (calculated) | 1.553 $Mg/m^3$ | |
| Absorption coefficient | 1.097 $mm^{-1}$ | |
| F(000) | 568 | |
| Crystal size | 0.10 x 0.08 x 0.04 $mm^3$ | |
| Theta range for data collection | 2.40 to 28.50°. | |
| Index ranges | -11<=h<=11, -14<=k<=22, -12<=l<=12 | |
| Reflections collected | 14030 | |
| Independent reflections | 5341 [R(int) = 0.0480] | |
| Completeness to theta = 28.50° | 99.8 % | |
| Absorption correction | Semi-empirical from equivalents | |
| Max. and min. transmission | 0.9574 and 0.8982 | |
| Refinement method | Full-matrix least-squares on $F^2$ | |
| Data / restraints / parameters | 5341 / 229 / 332 | |
| Goodness-of-fit on $F^2$ | 1.094 | |
| Final R indices [I>2sigma(I)] | R1 = 0.0358, wR2 = 0.0821 | |
| R indices (all data) | R1 = 0.0479, wR2 = 0.1055 | |
| Absolute structure parameter | -0.03(3) | |
| Largest diff. peak and hole | 0.654 and -0.839 $e.Å^{-3}$ | |

**Table A7** Crystal data compound for **(Ss*,R*,R*)-87**

| | | |
|---|---|---|
| Empirical formula | C25 H24 Cl2 N2 Pd S | |
| Formula weight | 561.82 | |
| Temperature | 103(2) K | |
| Wavelength | 0.71073 Å | |
| Crystal system | Orthorhombic | |
| Space group | P2(1)2(1)2(1) | |
| Unit cell dimensions | a = 8.8787(17) Å | α= 90°. |
| | b = 16.224(3) Å | β= 90°. |
| | c = 16.602(3) Å | γ= 90°. |
| Volume | 2391.4(8) $Å^3$ | |
| Z | 4 | |
| Density (calculated) | 1.560 $Mg/m^3$ | |
| Absorption coefficient | 1.102 $mm^{-1}$ | |
| F(000) | 1136 | |
| Crystal size | 0.40 x 0.10 x 0.08 $mm^3$ | |
| Theta range for data collection | 2.51 to 30.51°. | |
| Index ranges | -12<=h<=12, -22<=k<=23, -23<=l<=23 | |
| Reflections collected | 7910 | |
| Independent reflections | 7922 [R(int) = 0.0000] | |
| Completeness to theta = 25.00° | 99.6 % | |
| Absorption correction | Semi-empirical from equivalents | |
| Max. and min. transmission | 0.9170 and 0.6669 | |
| Refinement method | Full-matrix least-squares on $F^2$ | |
| Data / restraints / parameters | 7922 / 0 / 283 | |
| Goodness-of-fit on $F^2$ | 1.061 | |
| Final R indices [I>2sigma(I)] | R1 = 0.0389, wR2 = 0.0982 | |
| R indices (all data) | R1 = 0.0464, wR2 = 0.1027 | |
| Absolute structure parameter | -0.02(4) | |
| Largest diff. peak and hole | 0.647 and -0.705 $e.Å^{-3}$ | |

**Table A8** Crystal data compound for **(Rs*,S*,R*)-88**

| | | |
|---|---|---|
| Empirical formula | C22 H26 Cl2 N2 Pt S | |
| Formula weight | 616.50 | |
| Temperature | 103(2) K | |
| Wavelength | 0.71073 Å | |
| Crystal system | Orthorhombic | |
| Space group | P2(1)2(1)2(1) | |
| Unit cell dimensions | a = 10.4741(2) Å | α= 90°. |
| | b = 11.5386(2) Å | β= 90°. |
| | c = 18.7933(3) Å | γ= 90°. |
| Volume | 2271.29(7) $Å^3$ | |
| Z | 4 | |
| Density (calculated) | 1.803 $Mg/m^3$ | |
| Absorption coefficient | 6.515 $mm^{-1}$ | |
| F(000) | 1200 | |
| Crystal size | 0.12 x 0.08 x 0.06 $mm^3$ | |
| Theta range for data collection | 2.07 to 30.66°. | |
| Index ranges | -8<=h<=14, -16<=k<=9, -26<=l<=23 | |
| Reflections collected | 15190 | |
| Independent reflections | 6936 [R(int) = 0.0256] | |
| Completeness to theta = 30.66° | 99.5 % | |
| Absorption correction | Semi-empirical from equivalents | |
| Max. and min. transmission | 0.6959 and 0.5086 | |
| Refinement method | Full-matrix least-squares on $F^2$ | |
| Data / restraints / parameters | 6936 / 0 / 258 | |
| Goodness-of-fit on $F^2$ | 1.142 | |
| Final R indices [I>2sigma(I)] | R1 = 0.0267, wR2 = 0.0633 | |
| R indices (all data) | R1 = 0.0302, wR2 = 0.0867 | |
| Absolute structure parameter | -0.001(8) | |
| Extinction coefficient | 0.0055(2) | |
| Largest diff. peak and hole | 2.153 and -1.218 $e.Å^{-3}$ | |

**Table A9** Crystal data compound for **(Ss*,R*,R*)-89**

| | | |
|---|---|---|
| Empirical formula | C25 H24 Cl2 N2 Pt S | |
| Formula weight | 650.51 | |
| Temperature | 103(2) K | |
| Wavelength | 0.71073 Å | |
| Crystal system | Orthorhombic | |
| Space group | P2(1)2(1)2(1) | |
| Unit cell dimensions | a = 16.1669(7) Å | a= 90°. |
| | b = 16.5609(7) Å | b= 90°. |
| | c = 8.8953(4) Å | g = 90°. |
| Volume | 2381.61(18) $Å^3$ | |
| Z | 4 | |
| Density (calculated) | 1.814 $Mg/m^3$ | |
| Absorption coefficient | 6.219 $mm^{-1}$ | |
| F(000) | 1264 | |
| Crystal size | 0.40 x 0.40 x 0.34 $mm^3$ | |
| Theta range for data collection | 1.76 to 30.60°. | |
| Index ranges | -22<=h<=23, -23<=k<=23, -12<=l<=12 | |
| Reflections collected | 51133 | |
| Independent reflections | 7273 [R(int) = 0.0588] | |
| Completeness to theta = 30.60° | 99.6 % | |
| Absorption correction | Semi-empirical from equivalents | |
| Max. and min. transmission | 0.2263 and 0.1899 | |
| Refinement method | Full-matrix least-squares on $F^2$ | |
| Data / restraints / parameters | 7273 / 1105 / 547 | |
| Goodness-of-fit on $F^2$ | 1.195 | |
| Final R indices [I>2sigma(I)] | R1 = 0.0392, wR2 = 0.0902 | |
| R indices (all data) | R1 = 0.0438, wR2 = 0.0919 | |
| Absolute structure parameter | 0.035(9) | |
| Largest diff. peak and hole | 1.476 and -3.248 $e.Å^{-3}$ | |